

AD-A063 935

COASTAL ENGINEERING RESEARCH CENTER FORT BELVOIR VA
AN EVALUATION OF TWO GREAT LAKES WAVE MODELS.(U)

F/G 8/8

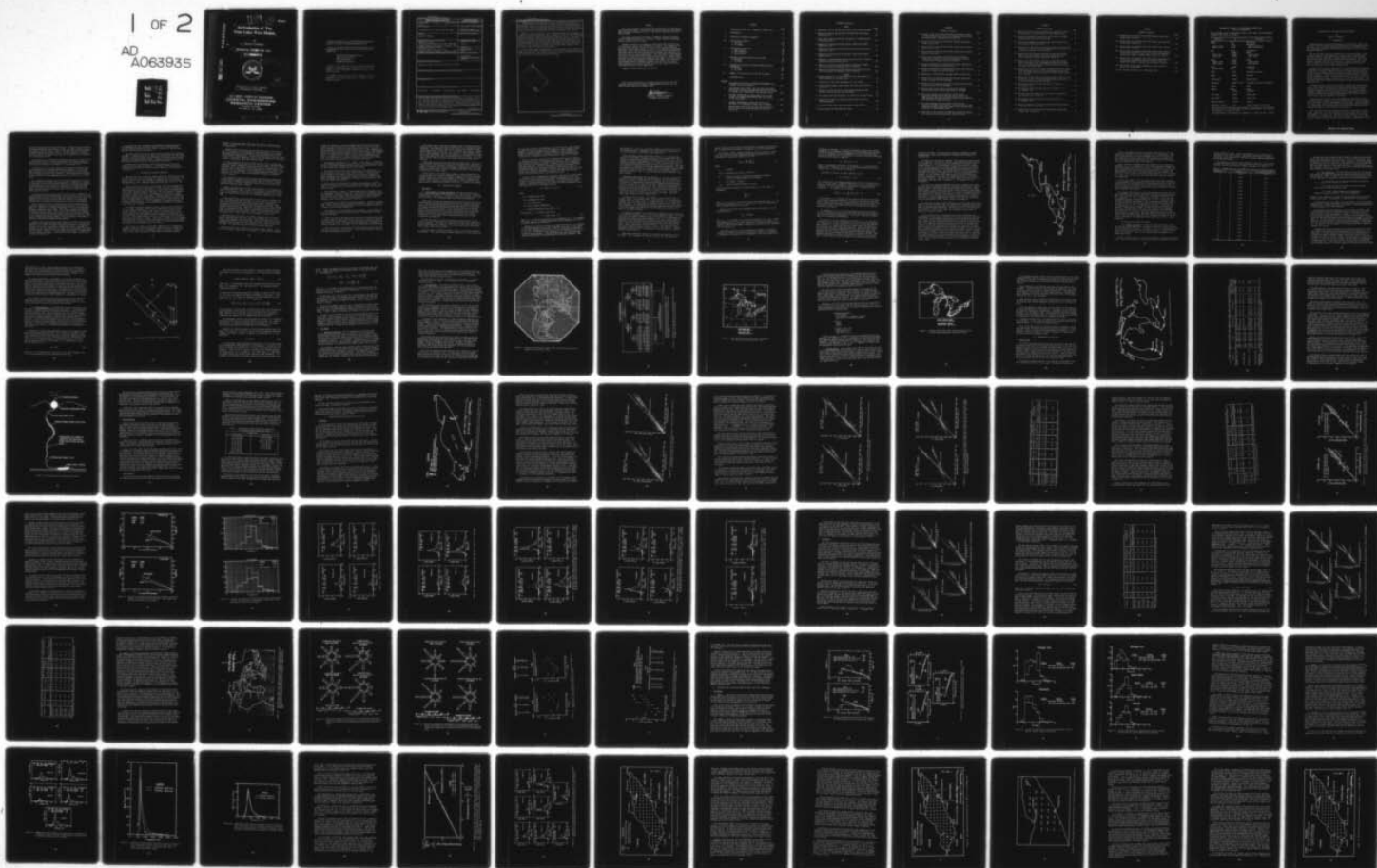
UNCLASSIFIED

OCT 78 E F THOMPSON
CERC-TR-78-1

NL

1 OF 2

AD
A063935



AD A063935

DDC FILE COPY

LEVEL

12

TR 78-1

6
**An Evaluation of Two
Great Lakes Wave Models.**

by

10 Edward F. Thompson

7
TECHNICAL REPORT NO. 78-1

11 ~~OCTOBER~~ 1978



DDC
RECEIVED
JAN 30 1979
C

12 178p.

Approved for public release;
distribution unlimited.

**U.S. ARMY, CORPS OF ENGINEERS
COASTAL ENGINEERING
RESEARCH CENTER**

Kingman Building
Fort Belvoir, Va. 22060

037 050 +
79 01 29 052

Reprint or republication of any of this material shall give appropriate credit to the U.S. Army Coastal Engineering Research Center.

Limited free distribution within the United States of single copies of this publication has been made by this Center. Additional copies are available from:

*National Technical Information Service
ATTN: Operations Division
5285 Port Royal Road
Springfield, Virginia 22151*

Contents of this report are not to be used for advertising, publication, or promotional purposes. Citation of trade names does not constitute an official endorsement or approval of the use of such commercial products.

The findings in this report are not to be construed as an official Department of the Army position unless so designated by other authorized documents.

UNCLASSIFIED

SECURITY CLASSIFICATION OF THIS PAGE (When Data Entered)

REPORT DOCUMENTATION PAGE		READ INSTRUCTIONS BEFORE COMPLETING FORM
1. REPORT NUMBER TR 78-1	2. GOVT ACCESSION NO.	3. RECIPIENT'S CATALOG NUMBER
4. TITLE (and Subtitle) AN EVALUATION OF TWO GREAT LAKES WAVE MODELS		5. TYPE OF REPORT & PERIOD COVERED Technical Report
		6. PERFORMING ORG. REPORT NUMBER
7. AUTHOR(s) Edward F. Thompson		8. CONTRACT OR GRANT NUMBER(s)
9. PERFORMING ORGANIZATION NAME AND ADDRESS Department of Army Coastal Engineering Research Center (CERRE-CO) Kingman Building, Fort Belvoir, Virginia 22060		10. PROGRAM ELEMENT, PROJECT, TASK AREA & WORK UNIT NUMBERS A31464
11. CONTROLLING OFFICE NAME AND ADDRESS Department of Army Coastal Engineering Research Center Kingman Building, Fort Belvoir, Virginia 22060		12. REPORT DATE October 1978
		13. NUMBER OF PAGES 174
14. MONITORING AGENCY NAME & ADDRESS (if different from Controlling Office)		15. SECURITY CLASS. (of this report) UNCLASSIFIED
		15a. DECLASSIFICATION/DOWNGRADING SCHEDULE
16. DISTRIBUTION STATEMENT (of this Report) Approved for public release; distribution unlimited.		
17. DISTRIBUTION STATEMENT (of the abstract entered in Block 20, if different from Report)		
18. SUPPLEMENTARY NOTES		
19. KEY WORDS (Continue on reverse side if necessary and identify by block number) Great Lakes Wave heights Wave hindcasts Wave models Wave periods		
20. ABSTRACT (Continue on reverse side if necessary and identify by block number) <p>Two operational numerical Great Lakes wave models are described in detail and evaluated. One model is a modern spectral wave model developed at the U.S. Army Engineer Waterways Experiment Station (WES) for hindcasting extreme historic wave conditions in the Great Lakes. The other model is a relatively simple, significant wave model developed at the Techniques Development Laboratory (TDL) of the National Weather Service (NWS) for providing predictions to aid local forecasters in Great Lakes areas.</p> <p style="text-align: right;">(continued)</p>		

(cont)

UNCLASSIFIED

SECURITY CLASSIFICATION OF THIS PAGE(When Data Entered)

The evaluation of the WES model consists of comparing wave hindcasts for nine storms in Lake Erie during fall 1975, with Waverider accelerometer buoy measurements taken near Cleveland, Ohio, and Erie, Pennsylvania. Evaluation of the TDL model consists of comparing forecasts during fall 1975 and fall 1976 with Waverider buoy measurements at the Lake Erie sites and three Lake Michigan sites, near Holland and South Haven, Michigan, and Michigan City, Indiana.

When all the data gathered in this study are combined, the WES hindcast significant heights for specific times are generally within 0.5 meter (1.6 feet) of gage significant heights, but occasional differences of over 1 meter (3.3 feet) are observed. The WES peak spectral periods for high wave conditions have a small tendency to be shorter than gage peak spectral periods. The WES hindcasts, especially hindcast spectral shapes, tend to be more accurate for situations where fetches are reasonably well defined than for situations where fetches are poorly defined and highly variable with slight changes in wind direction. The differences may be systematic.

TDL forecast significant heights have a strong tendency to be higher than gage significant heights, although there may be a reverse tendency during very high wave conditions. TDL forecast significant periods are relatively unbiased but less variable than gage peak spectral periods.

Form with fields for:

- WES hindcast
- TDL forecast
- Wave Direction
- Wind Direction
- Wind Speed
- Wave Period
- Wave Height
- Wave Shape
- Wave Direction
- Wave Period
- Wave Height
- Wave Shape

Handwritten signature: R

PREFACE

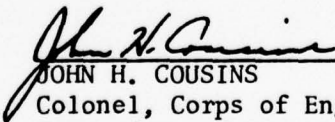
This report presents a description and evaluation of two operational Great Lakes wave models. The work was carried out under the wave measurement and analysis program of the U.S. Army Coastal Engineering Research Center (CERC).

The report was prepared by Edward F. Thompson, Hydraulic Engineer, under the supervision of Dr. D. Lee Harris, Chief, Coastal Oceanography Branch, Research Division, CERC.

Valuable assistance in planning the field wave data collection and in preparing the report was provided by Dr. Harris. The cooperation of Drs. D.T. Resio and C.L. Vincent of the U.S. Army Engineer Waterways Experiment Station (WES) and Mr. N.A. Pore of the Techniques Development Laboratory (TDL), National Weather Service, in providing information for the model descriptions and providing wave estimates for comparison with field wave data is greatly appreciated. Able assistance in implementing the field wave data collection program was provided by T. Miloser, CERC. Assistance in deploying and retrieving the wave buoys was provided by the National Oceanic and Atmospheric Administration (NOAA), the Great Lakes Environmental Research Laboratory (GLERL), and the U.S. Coast Guard. GLERL cooperation in permitting CERC to record the signal from one of the GLERL wave buoys is also appreciated.

Comments on this publication are invited.

Approved for publication in accordance with Public Law 166, 79th Congress, approved 31 July 1945, as supplemented by Public Law 172, 88th Congress, approved 7 November 1963.


JOHN H. COUSINS
Colonel, Corps of Engineers
Commander and Director

CONTENTS

	Page
CONVERSION FACTORS, U.S. CUSTOMARY TO METRIC (SI)	9
I INTRODUCTION	11
II DISCUSSION OF PHYSICAL PROCESSES	13
III DESCRIPTION OF MODELS.	16
1. WES Model	16
2. TDL Model	29
IV DESCRIPTION OF GAGE DATA	36
1. Gage Systems.	36
2. Data Recording.	41
3. Data Analysis	41
V COMPARISON BETWEEN HINDCASTS AND GAGE DATA	43
1. WES Model	43
2. TDL Model	62
VI DISCUSSION AND EVALUATION BASED ON MODEL-GAGE DATA COMPARISONS.	75
1. WES Model	75
2. TDL Model	105
VII SUMMARY OF THE EVALUATION OF WES AND TDL MODELS.	112
LITERATURE CITED	113
APPENDIX	
A WES METHOD FOR ADJUSTING ANEMOMETER MEASUREMENTS TO A STANDARD SITE AND ELEVATION.	117
B TIME-HISTORY PLOTS OF WES, TDL, AND GAGE SIGNIFICANT WAVE HEIGHT, PERIOD, AND DIRECTION FOR FALL 1975 STORMS AT PRESQUE ISLE, PENNSYLVANIA, AND CLEVELAND, OHIO	119
C SPECTRAL COMPARISONS OF LESSER QUALITY DUE TO POOR MATCHING OF HINDCAST-GAGE RECORD TIMES OR TO NOISE IN THE GAGE RECORD	138
D SPECTRAL COMPARISONS IN WHICH MOST OF THE GAGE SPECTRUM IS AT FREQUENCIES HIGHER THAN 0.23 HERTZ.	150
E TIME-HISTORY PLOTS OF TDL AND GAGE SIGNIFICANT WAVE HEIGHT, PERIOD, AND DIRECTION FOR FALL 1975 AND FALL 1976.	157

CONTENTS--Continued

TABLES

	Page
1 Frequencies used in the WES Great Lakes wave hindcasting model. .	24
2 Details of location and operation of Great Lakes wave gages during 1974-76	38
3 Great Lakes storms selected for evaluation of hindcasting and forecasting models	42
4 Comparison of measured and WES hindcast significant heights during fall 1975	50
5 Comparison of measured and WES hindcast peak spectral periods during fall 1975	52
6 Comparison of measured and TDL forecast significant heights during 1975-76	65
7 Comparison of measured peak spectral periods and TDL forecast significant periods during 1975-76	68
8 Comparison of measured and WES hindcast significant heights for well-defined and ambiguous fetch situations.	100
9 Comparison of measured and WES hindcast peak spectral periods for well-defined and ambiguous fetch situations.	100

FIGURES

1 Segment demarcations in Lake Erie used in the WES analysis of wind estimation in the Great Lakes	22
2 Illustration of WES model propagation of wave energy.	27
3 National Meteorological Center (NMC) 1977 point grid used for computation.	31
4 Schematic illustration of the relationship between the NMC PE model and the TDL wind and wave models.	32
5 TDL surface wind forecast points (12 areas) for the Great Lakes .	33
6 Standard Great Lakes wave forecast points used in the TDL forecasting model.	35
7 Location of CERC Great Lakes wave gages during 1974-76.	37
8 Mooring system for CERC Waverider buoys	40

CONTENTS

FIGURES--Continued

	Page
9 Location of WES wave hindcasting model grid points nearest to CERC Waverider buoy sites, and anemometer wind stations providing input to the WES model in Lake Erie	44
10 Scatter plots of measured versus WES hindcast significant height in Lake Erie	46
11 Scatter plots of measured versus WES hindcast peak spectral period in Lake Erie	48
12 Scatter plots of measured versus WES hindcast peak spectral period in Lake Erie	49
13 Scatter plots of measured versus WES hindcast maximum significant height for selected storms during fall 1975 in Lake Erie at Presque Isle and Cleveland.	53
14 Overall distributions of measured and hindcast significant heights at Presque Isle and Cleveland	55
15 Overall distributions of measured and hindcast peak spectral periods at Presque Isle and Cleveland	56
16 Comparisons of WES hindcast and gage spectra in Lake Erie. . . .	57
17 Scatter plots of measured versus TDL forecast significant heights in Lakes Erie and Michigan.	63
18 Scatter plots of measured versus TDL forecast peak spectral period in Lakes Erie and Michigan	67
19 Thirteen major Great Lakes areas for which shipboard observational data have been published in the SSMO.	70
20 Wave roses showing the distribution of TDL forecast significant height versus forecast wind direction and SSMO shipboard observed significant height versus observed wind direction at Lake Erie sites	71
21 Wave roses showing the distribution of TDL forecast significant height versus forecast wind direction and SSMO shipboard observed significant height versus observed wind direction at Lake Michigan sites.	72
22 Comparison of TDL forecast and SSMO mean significant height as a function of wind direction at Lake Erie sites.	73

CONTENTS

FIGURES--Continued

	Page
23 Comparison of TDL forecast and SSMO mean significant height as a function of wind direction at Lake Michigan sites.	74
24 Overall distributions of measured, TDL forecast, and SSMO shipboard observed significant height	76
25 Overall distributions of measured peak spectral period and TDL forecast significant period	78
26 Comparisons of WES hindcast and gage spectra in Lake Erie for situations in which the wind was approximately perpendicular to shore and fetches are well defined	82
27 Comparison of WES hindcast spectrum and spectrum obtained from a Canadian Waverider buoy record taken near Point Pelee, Lake Erie, during a storm on 7 April 1973.	83
28 Comparison of WES hindcast spectrum and spectrum obtained from a NOAA Great Lakes Environmental Research Laboratory gage on an offshore tower near Muskegon, Michigan, during a storm on 29 October 1965.	84
29 Comparison of the rate of change of dimensionless wave height with dimensionless fetch in the WES numerical model with rates of change observed by Mitsuyasu (1968) and Hasselmann, et al. (1973)	86
30 Comparisons of WES hindcast and gage spectra in Lake Erie for situations in which the wind was approximately parallel to shore and fetches are poorly defined.	87
31 WES hindcast wind field over Lake Erie at 1900 e.s.t., 18 October 1975	88
32 WES hindcast wind field over Lake Erie at 1900 e.s.t., 21 November 1975.	91
33 WES wave model grid points in the vicinity of Long Point and Presque Isle in Lake Erie	92
34 WES hindcast wind field over Lake Erie at 1600 e.s.t., 10 November 1975.	95
35 Definition sketch for sectors around Cleveland and Presque Isle gage sites in Lake Erie.	96
36 Scatter plots of measured versus WES hindcast significant height near Presque Isle.	97

CONTENTS

FIGURES--Continued

	Page
37 Scatter plots of measured versus WES hindcast significant height near Cleveland	98
38 Scatter plots of measured versus WES hindcast peak spectral period near Presque Isle.	101
39 Scatter plots of measured versus WES hindcast peak spectral period near Cleveland	102
40 Scatter plots of measured versus WES hindcast peak spectral period near Presque Isle for cases in which the measured significant height is greater than or equal to 1 meter.	103
41 Scatter plots of measured versus WES hindcast peak spectral period near Cleveland for cases in which the measured significant height is greater than or equal to 1 meter.	104
42 Plot of mean surface water temperature versus month for Lakes Erie and Michigan	107
43 Weather map for 0700 e.s.t., 29 October 1975	110

CONVERSION FACTORS, U.S. CUSTOMARY TO METRIC (SI)
UNITS OF MEASUREMENT

U.S. customary units of measurement used in this report can be converted to metric (SI) units as follows:

Multiply	by	To obtain
inches	25.4	millimeters
	2.54	centimeters
square inches	6.452	square centimeters
cubic inches	16.39	cubic centimeters
feet	30.48	centimeters
	0.3048	meters
square feet	0.0929	square meters
cubic feet	0.0283	cubic meters
yards	0.9144	meters
square yards	0.836	square meters
cubic yards	0.7646	cubic meters
miles	1.6093	kilometers
square miles	259.0	hectares
knots	1.852	kilometers per hour
acres	0.4047	hectares
foot-pounds	1.3558	newton meters
millibars	1.0197×10^{-3}	kilograms per square centimeter
ounces	28.35	grams
pounds	453.6	grams
	0.4536	kilograms
ton, long	1.0160	metric tons
ton, short	0.9072	metric tons
degrees (angle)	0.01745	radians
Fahrenheit degrees	5/9	Celsius degrees or Kelvins ¹

¹To obtain Celsius (C) temperature readings from Fahrenheit (F) readings, use formula: $C = (5/9) (F - 32)$.

To obtain Kelvin (K) readings, use formula: $K = (5/9) (F - 32) + 273.15$.

AN EVALUATION OF TWO GREAT LAKES WAVE MODELS

by
Edward F. Thompson

I. INTRODUCTION

People working in and near large bodies of water such as lakes, seas, and oceans have long appreciated the awesome power of wind-generated waves. Large waves can sink ships, damage harbors and coastal structures, and move considerable quantities of bottom sediment which can alter or block navigation channels.

Ancient mariners could have developed an intuitive knowledge of wave conditions based on their experiences. However, their intuition must have been woefully inadequate in assessing the severity and recurrence intervals of storms more severe than any they had observed. Also, these mariners probably had little or no ability to predict extremely large waves in advance of their arrival, a serious handicap in the days of small sailing ships with no radio communications.

During the 20th century, engineers have continually faced the problem of designing and constructing facilities in remote, unfamiliar coastal and ocean areas. Recent oil company activities in Alaska and the North Sea, and the iron ore shipping activity along the northwest coast of Australia are good examples. The cost of even relatively small failures, delays, or mishaps can be quite large. Major failures, such as collapse of a North Sea oil platform or sinking of a ship, can cost millions of dollars. Thus, engineers often need a quantitative knowledge of wave climate and extreme wave conditions.

The most pervasive source of wave data is observations taken aboard ships. The shipboard observations have been computerized and archived at the National Oceanic and Atmospheric Administration's (NOAA) National Climatic Data Center, Asheville, North Carolina. This system permits a meaningful summarization of observations in broad geographical areas. It could be considered an automated approximation to the ancient mariners' intuition but with poor geographic resolution.

During the last 35 years, two other methods for obtaining wave data have been refined enough to become useful and practical in many situations. The first method is direct measurement with wave gages. Gage measurements with modern data collection and analysis procedures provide more reliable wave information at the measurement site than any other method, and are especially useful at sites near high-cost projects.

The use of wave gages for detailed coverage of large areas is impractical. Generally, it is also impractical to obtain many years of wave measurements at a single site. Because of these limitations with gages, the ability to synthesize wave data from wind data is very useful. Wind data are readily available at many coastal locations, particularly in the

United States and other developed countries. At many sites the wind data have been recorded for long periods of time, providing extensive historical records of severe storms. Thus, if the wind data are representative of winds causing wave generation and if suitable methods for relating winds to waves are available, wave data can be synthesized, or "hindcast," for a long period of time.

Since World War II, hindcasting techniques have been available in the form of empirical curves relating significant wave height and period to windspeed, wind duration, and overwater fetch. The hindcasting curves can be used to estimate wave conditions at a particular site.

In about the last 10 years, numerical wave hindcasting models have been developed for use on high-speed digital computers. Most of these models hindcast wave conditions at every intersection of a grid which covers the body of water being considered. The models provide estimates of wave conditions at many geographical points as easily as at a single point.

The strengths and weaknesses of wave hindcasting models are related to their ability to simulate, either explicitly or implicitly, the physical processes involved in wave growth and decay. (The physical processes are discussed in the next section.) Numerical wave hindcasting models usually incorporate some details of the wind-field structure and the physics of wave generation and decay which cannot be considered in the simple empirical curves.

Wave hindcasts from any model always contain errors introduced by the limited quality and representativeness of the wind data as well as by the approximations involved in transforming the wind data into wave data. The cumulative effect of the errors on the wave hindcasts can be properly assessed only by comparing the hindcasts with field wave measurements.

Recent concern by the U.S. Army Engineer Division, North Central, about the inadequacy of available design wave data has led to the development of a numerical wave hindcasting model at the U.S. Army Engineer Waterways Experiment Station (WES). The model, developed and reported by Resio and Vincent (1976c, 1976d, 1977a, 1977b, 1978a), was designed to hindcast waves during the most severe storms over a 69-year interval. It is a sophisticated spectral wave model which operates only on a large-capacity, high-speed digital computer. The wind input to the model is obtained from nearshore anemometer measurements.

Another operational numerical wave model for the Great Lakes has been developed by the Techniques Development Laboratory (TDL) of the National Weather Service (NWS). The model is presently used only for making predictions to aid local forecasters in Great Lakes areas. The model is a significant wave type, designed for trouble-free and extremely fast operation on a digital computer. The wind input to the model is obtained from the NWS computer wind model. Both the WES and TDL models are described in detail in Section III.

In conjunction with development of the WES wave hindcasting model, wave gage data used for evaluating the model were collected by the Coastal Engineering Research Center (CERC) in Lakes Erie and Michigan. The data are discussed in Section IV.

Gage data from nine storms in Lake Erie were selected for evaluating the model. Hindcasts from the WES model were obtained for the same storms. Forecasts from the TDL model were obtained for the entire period of gage operation, including the nine storms. Comparisons of gage data with the WES hindcasts and TDL forecasts are presented in Section V.

Similarities and differences between measurements and hindcasts-forecasts are discussed in Section VI. The major conclusions of the evaluation of the hindcasts-forecasts against gage data are summarized in Section VII.

II. DISCUSSION OF PHYSICAL PROCESSES

When air flows over a solid or liquid medium, the velocity of the air and the velocity of the other medium are identical at the interface. For example, when air flows over asphalt or compacted dirt, the velocity at the interface is zero. When air flows over water, the velocity at the interface is equal to the surface velocity of the water.

Above, but near the solid or liquid medium, the airspeed depends on the airspeed far from the interface, viscosity of the air, and the turbulence characteristics of the airflow. Viscous effects predominate for a very small distance above the interface, but this distance is usually less than 0.1 meter (0.3 foot). At distances on the order of 1 meter (3.3 feet) or more from the interface, turbulent exchange of momentum is much more important than viscous effects in determining the velocity profile. The predominance of turbulent exchange leads to the familiar logarithmic airspeed profile. In the atmosphere, the logarithmic profile is valid up to an elevation of perhaps 20 meters (66 feet), according to Kraus (1972, pp. 135-136).

The extent of vertical turbulent mixing, and hence the airspeed profile, is highly dependent on the relative temperatures of the air and the other medium. For example, when cool air is flowing over a warm surface, the air near the surface is heated, then rises and gains horizontal momentum from the higher velocity surroundings to which the air has risen. The airspeed profile for this situation would have relatively strong gradients near the surface. When warm air flows over a cool medium, the air near the surface is cooled and acquires a stable vertical temperature profile which decreases vertical mixing. The airspeed profile would have relatively weak gradients near the surface.

The airflow, or winds, in the earth's atmosphere are a response to atmospheric pressure gradients which are usually caused by differential heating and cooling of air in different parts of the globe. There is always a level above the earth's surface where the pressure gradient

becomes a significant factor affecting the airflow. This level is usually less than 100 meters (328 feet) from the air-earth interface at midlatitudes.

Another level occurs above the interface where the acceleration of the air in response to the atmospheric pressure gradient is in approximate equilibrium with the acceleration resulting from rotation of the earth (Coriolis acceleration). At this level and higher, the wind, which is free of any effects emanating directly from the presence of the earth's surface, is sometimes called the "free-air" wind.

In some situations the wind velocity near the earth's surface has little relationship to the free-air wind velocity; e.g., when atmospheric conditions cause a temperature inversion near the earth's surface. Other situations where the surface and free-air winds are unrelated may arise when the wind is channeled by local topography such as high cliffs, large mountains, or tall buildings; or when large temperature differences are caused by, for example, snow-covered mountains adjacent to temperate waters or deserts.

The concept of a free-air wind velocity representing an equilibrium between pressure gradients and acceleration due to the earth's rotation is very useful, although the free-air wind velocity is never precisely constant in space or time. Additional spatial variability enters the wind field near the earth's surface.

Another pertinent aspect of the wind field which is not reflected in most published wind velocity values is the gustiness of the wind. Gustiness, or the amount of the variation in windspeed and direction about the mean, can significantly affect the wave-generating capability of a given wind.

Other complications arise when the wind blows over an irregular surface. When wind blows past buildings in a city, the flow acquires characteristics resulting from stagnation against upwind obstructions, increased speed of flow channeled around obstructions, boundary layer development for flow past obstructions, and sheltering and eddy shedding downwind from obstructions. Generally, distortions to the wind are quite small at horizontal distances from the obstruction greater than seven times the height of the obstruction. Thus, even the tallest buildings would have little effect on the wind 3 kilometers (2 miles) away.

When wind blows over water, the surface irregularities are usually smaller than buildings (but often cover a much larger area), are more regular, and propagate, grow, and decay. The surface water waves create corresponding waves in the air very near the water. These low-altitude atmospheric waves, which were first measured in the field by Elder and Soo (1967), are important factors in water-wave growth and decay.

When wind blows over a smooth water surface, ripples appear. If the wind is more than a light breeze, the ripples grow with time and downwind

distance to form waves. Since wind-generated waves are nearly irrotational, the primary mechanism for energy transfer from wind to water can be deduced to be pressure rather than viscous forces. The rate of energy transfer from wind to water depends heavily on the windspeed profile within about 5 meters (15 feet) of the water surface. The windspeed profile is significantly dependent on the air-water temperature difference, as discussed earlier. Thus, for cool winds blowing over warm water, wave generation is relatively effective; for warm winds blowing over cool water, wave generation is relatively ineffective.

According to Hasselmann, et al. (1973), little energy is transferred to low-frequency waves directly from the wind. The wind energy is transferred to the higher frequency waves which in turn transfer their energy to lower frequencies through nonlinear interactions.

Pollutants in water can significantly affect wave generation. Oil has historically been used to calm troubled waters. In the extreme, a thick surface film of highly viscous oil can severely attenuate the higher frequency waves and prevent further wave growth. Massive warm water discharges from a powerplant can enhance wave generation by modifying the surface wind profile.

Objects in the water sometimes affect wave generation. Extensive stands of seaweed can effectively attenuate high-frequency waves. Ice inhibits wave generation by decreasing the water surface area on which waves can grow.

Wave generation in nature is often complicated by irregularities in the boundaries of the water body over which the wind is blowing. Common complications are tortuous shorelines, peninsulas or shoals extending out into the water, islands, and limited fetch width, where fetch is defined as the overwater trajectory of the wind.

Wave energy is dissipated by several mechanisms. Viscosity converts wave energy into heat, but the resulting temperature change is infinitesimal. The viscosity of water and hence its rate of energy dissipation increase with decreasing temperature.

Wave energy is also dissipated by wave breaking. Wave breaking can occur in deep water during strong winds and in shallow water as waves approach the beach.

Another dissipative mechanism which operates in shallow water (where "shallow" water is usually considered to be water in which the depth is less than half the wavelength) is friction between the bottom and water motion near the bottom. Dissipation by this mechanism is thought to be significant and varies with depth, bottom composition, and bottom slope.

Some wave energy is reflected back toward deep water when waves are traveling shoreward in shallow water. This mechanism tends to decrease the wave energy approaching shore.

Wave energy can be affected by changes in wave direction induced by shallow water. When a wave enters shallow water, its propagation speed decreases. The propagation speed often varies along a particular wave crest because parts of the crest are in different water depths. Differential forward speeds along the crest result in a reorientation of the crest. This phenomenon, called wave refraction, can intensify or reduce wave energy density per unit area depending on the situation. Very near shore, shortly before breaking, wave heights usually increase due to shoaling.

Refraction is usually most significant very near shore, but it can have important implications even in relatively deep water. According to Pierson (1972), the accidental sinking of a trawler in the North Sea in depths of 90 meters (300 feet) was probably a consequence of "very high confused pyramidal seas" created by crossing wave trains resulting from refraction over a nearby shoal.

Surface waves can be affected by currents. Waves propagating into a current which has a velocity component in opposition to the direction of wave advance will increase in height and decrease in speed and wavelength. Waves entering a current which has a velocity component with the waves will experience the opposite effects. In either case, differential speeds created along the wave crest will give rise to refraction.

III. DESCRIPTION OF MODELS

1. WES Model.

a. Description of the WES Wind Model. The WES wave hindcasting model (Resio and Vincent, 1976c, 1976d, 1977a, 1977b, 1978a) is actually a combination of two models: a model for the wind field and a model for the wave field. These component models are described separately.

Discussion is focused on the particular wind and wave models used in generating the hindcasts for this evaluation study. However, this study is also intended to provide perspective on the reliability of WES hindcasts used to prepare design wave estimates for each of the Great Lakes. The design wave estimates were derived from WES hindcasts of extreme waves during a 69-year interval. Since a few aspects of the wind model used in this study differ from the wind model used for the design wave estimates, differences and similarities are noted in this section. Further detail on the model used in preparing design wave estimates is provided in Appendix A.

The WES wind model is based on theoretical representations of the physical processes affecting winds over land and over water. Empiricism is used sparingly. This model is identical to the WES wind model used in generating extreme wave hindcasts in the Great Lakes (Resio and Vincent, 1976a, 1976b, 1976d, 1977b, 1978a).

The wind input to the WES wind model consists of overland anemometer measurements. Data from selected stations along the U.S. coast were used

for Lakes Erie, Ontario, and Michigan. Data from both U.S. and Canadian stations were used for Lakes Huron and Superior. Since anemometer measurements are highly dependent on the anemometer elevation above the ground, the WES wind model is designed to adjust input anemometer wind velocities to a standard elevation (chosen to be 6 meters or 20 feet).

Since the wind data used in this evaluation study were all taken at the standard elevation, no adjustment was necessary. However, during the 69-year interval covered by the WES extreme wave hindcasts, anemometers were located at various elevations. Anemometers were also occasionally relocated spatially. The WES technique for adjusting windspeeds to the standard elevation and location was empirical (discussed in App. A). The need for empirical adjustment of much of the wind data used to obtain design wave estimates introduced a potential for error which did not exist in the wind data used in this evaluation study.

The next step in estimating the overwater wind field in the WES model is to convert each overland wind, adjusted to standard elevation and location, to an equivalent overwater wind. The overwater wind is specified at a standard elevation of 19.5 meters (64 feet) above the water surface. The equation relating overland and overwater windspeeds in the WES model used for this evaluation study is

$$U_w = R(U_L, T_a - T_w) U_L \quad (1)$$

where

U_w = windspeed over water

U_L = windspeed over land

T_a = air temperature

T_w = water surface temperature

R = function depending on U_L and $T_a - T_w$.

The function R is further specified as

$$R = \psi(U_L) \phi_n(T_a - T_w) \quad (2)$$

where ψ is a function accounting for the dependence of R on windspeed over land, and ϕ_n a function accounting for the dependence of R on air-water temperature difference.

Equation (2) can be visualized as an expression for R as a function of overland windspeed with a small adjustment to account for the effect of air-water temperature difference. The two dimensionless functions, ψ and ϕ_n , are formulated in a general way and applied directly to all locations and situations. These functions were calculated from theoretical considerations and substantiated by empirical evidence. The

derivations of ψ and ϕ_n are given in Resio and Vincent (1976c) and are summarized below. Remarkably, this approach which requires very little site-specific calibration, works quite well.

When referring to Resio and Vincent (1976c), it is cautioned that some of the wind model refinements discussed in that report were not included in the operational hindcasting model used in this study. The refinements include an adjustment to R in equation (2) for short fetches over which the wind profile is adjusting to its overwater form, and a relationship between the difference in wind direction over water and land as a function of windspeed and air-lake temperature difference. The curve representing the function ψ in equation (2) also differs slightly from the curve in Resio and Vincent (1976d), but the difference is due to drafting inaccuracy. The ψ curve in Resio and Vincent (1976d) is the more accurate.

Theoretical expressions for the functions ψ and ϕ_n were derived using a three-layer concept of winds over water. In the top layer, or free air, the wind is considered to be unaffected by friction and to be determined by an approximate equilibrium between the acceleration produced by the rotation of the earth and the atmospheric pressure gradient. A useful estimate of the wind in this layer, called the "geostrophic" wind, is based on the assumption that lines of constant pressure in the atmosphere are straight and unmoving. The middle and bottom layers both include the effect of friction with the earth's surface. The middle layer also includes the effect of rotation of the earth. These two layers make up the planetary boundary layer.

The WES planetary boundary layer model is very similar to that of Cardone (1969). In the lower layer, or Prandtl layer, of the planetary boundary layer the shear stress is assumed constant. In the upper layer, or Ekman layer, the shear stress is assumed to decrease with elevation above the earth. An expression for windspeed and direction in the planetary boundary layer was obtained by deriving equations for wind velocity in both the Prandtl and Ekman layers and by forcing the velocities to match at the common boundary.

An important parameter in the theoretical expression for wind velocity in the planetary boundary layer is the surface roughness height. For winds over land, the surface roughness height was assumed to be independent of windspeed and constant for each anemometer site. Land surface roughness height was estimated empirically at each site from the relationship between geostrophic windspeed (estimated from weather maps) and anemometer winds. The estimated land surface roughness heights were typically between 1 and 15 centimeters (0.03 and 0.5 foot). For winds over water, the surface roughness height changes as the sea state changes. Surface roughness height over water was expressed in the WES model as a function of the friction velocity.

Temperature differences between air and land were neglected in the WES model. This assumption of neutral stability near the ground may

have no effect on the accuracy of the hindcasts for high wind conditions, but it could affect the accuracy of hindcasts for low wind conditions.

The constant surface roughness height and neutral stability assumptions over land led to the assumption that the windspeed profile is described by a logarithmic equation as follows:

$$U_L(Z) = \frac{U_*}{K} \ln\left(\frac{Z}{Z_{OL}}\right) \quad (3)$$

where

Z = elevation

$U_L(Z)$ = windspeed over land at elevation Z

U_* = friction velocity (a function of measured windspeed, elevation of measurements, and latitude)

K = von Karman's constant

Z_{OL} = surface roughness height over land.

It was estimated with empirical evidence that over a wide range of windspeeds,

$$\frac{U_*}{U_g} \approx C_1 \quad (4)$$

where U_* is the friction velocity derived from measured wind, U_g the geostrophic windspeed, and C_1 a constant for a specified anemometer level, roughness height, and latitude.

Equations (3) and (4) were combined, and the elevation $Z = Z_m$ was specified to give

$$U_g = C_2 U_L(Z_m) \quad (5)$$

where C_2 is a constant for a specified anemometer level (Z_m), roughness height, and latitude. Thus, with $Z_m = 6$ meters (20 feet) and Z_{OL} estimated empirically, a simple, approximate relationship between windspeed over land and geostrophic windspeed is provided for each anemometer site by equation (5).

The equations used to relate windspeed over water to geostrophic windspeed are rather involved because surface roughness is permitted to increase with windspeed and the dependence on air-water temperature

difference is included. A set of four equations relating wind profile parameters in the planetary boundary layer to geostrophic wind velocity is solved iteratively for each anemometer site and calculation time. The set of equations can be visualized as a system in which the following functional relationship is applied:

$$U_w = F(U_g, f, \theta_\alpha - \theta_s) \quad (6)$$

where F represents a functional relationship; θ_α is the potential temperature at anemometer level, θ_s the potential temperature at sea surface, and f the Coriolis acceleration.

Equations (5) and (6) are then combined to give

$$U_w = F(U_L, f, \theta_\alpha - \theta_s) . \quad (7)$$

This completes the link between windspeed over land and windspeed over water in the WES model. Comparing equations (1) and (7) and noting that potential temperature difference is equivalent to actual temperature difference, it is evident that the function R in equation (1) is related to F in equation (7) as follows:

$$R(U_L, T_\alpha - T_w) = \frac{1}{U_L} F(U_L, f, \theta_\alpha - \theta_s) . \quad (8)$$

The function ψ in equation (2) was derived from theory by setting the air-water temperature difference in equation (8) equal to zero and using a single latitude of 45° as representative for all the Great Lakes. Thus, the functional dependence between overland wind and the ratio, R , of overwater wind at 19.5-meter elevation to overland wind at 6-meter elevation was obtained.

The dependence of R on overland windspeed for neutral stability was also investigated empirically by WES using shipboard observations of lake winds and airport measurements of land winds. Empirical evidence supports the theoretical formulation.

The effect of air-lake temperature difference on R is treated as independent of the effect of windspeed on R , as indicated in equation (2). Because theoretical evaluation of the effect of air-lake temperature difference is complex and requires climatological data which are not available, WES used an empirical approach. Shipboard observations of lake winds and airport measurements of land winds were used. The shipboard observations were taken by anemometer-equipped ships participating in the Great Lakes Marine Observations Program of the NWS. The shipboard anemometers, mounted at elevations of about 20 to 21 meters (65 to 70 feet) above the water surface, were checked periodically for

accuracy by the NWS. The observations represent windspeeds visually averaged over 1 minute and corrected to eliminate the influence of ship velocity.

The lakes were divided into segments. The segments in Lake Erie are shown in Figure 1. For each 3° air-lake temperature difference interval in a segment, the stability factor was computed as the ratio of the average value of R for observations in the interval and in a particular 2.6 meters per second (5 knots) windspeed interval to the average R for all observations in the windspeed interval, regardless of air-lake temperature difference. By segregating the data into windspeed intervals, the effect of windspeed on R (which is incorporated in the function ψ) was reduced. WES found that the stability factor was actually independent of windspeed for speeds greater than 3.1 meters per second (6 knots). Thus, for each lake segment the stability factor for moderate and high winds, designated ϕ_n in equation (2), was determined.

This model for relating windspeed over land to windspeed over water was also used in preparing design wave estimates for Lakes Erie, Ontario, Michigan, Huron, and Superior (Resio and Vincent, 1976a, 1976b, 1976d, 1977a, 1978a). Resio and Vincent (1976a, 1976b) described a more empirically based wind model and stated that it was used in preparing the design wave estimates for Lakes Erie and Ontario. However, the more empirical wind model was not actually used to produce the design wave estimates (D.T. Resio, personal communication, 8 March 1978) and the description in Resio and Vincent (1976a, 1976b) should be disregarded.

To check the validity of using equation (2) and overland wind measurements to estimate overlake winds, WES computed the root-mean-square (rms) error of estimated overlake winds in comparison to shipboard wind measurements in Lakes Michigan and Huron. The rms error was 2.1 meters per second (4 knots) or less in both lakes for windspeeds greater than 6.2 meters per second (12 knots).

To use equation (2) in conjunction with historic overland wind measurements, climatological estimates of air-lake temperature difference in each lake were assumed to depend only on wind direction and time of year. Mean air-lake temperature difference was computed from available observations for 10° wind direction arcs and each of the 12 months of the year. The component of the rms error due to the use of climatological estimates of air-lake temperature difference was estimated to be less than 2.1 meters per second for most conditions in Lakes Erie and Ontario. Thus, operational windspeed estimates by the WES model in Lakes Erie and Ontario can be expected to have an overall rms error of about 2.9 meters per second (5.7 knots) (based on 2.1 meters per second due to climatological specification of air-lake temperature difference and 2.1 meters per second due to other uncertainties in the model as compared to observations). Both of these errors are present in the data being evaluated in this study.

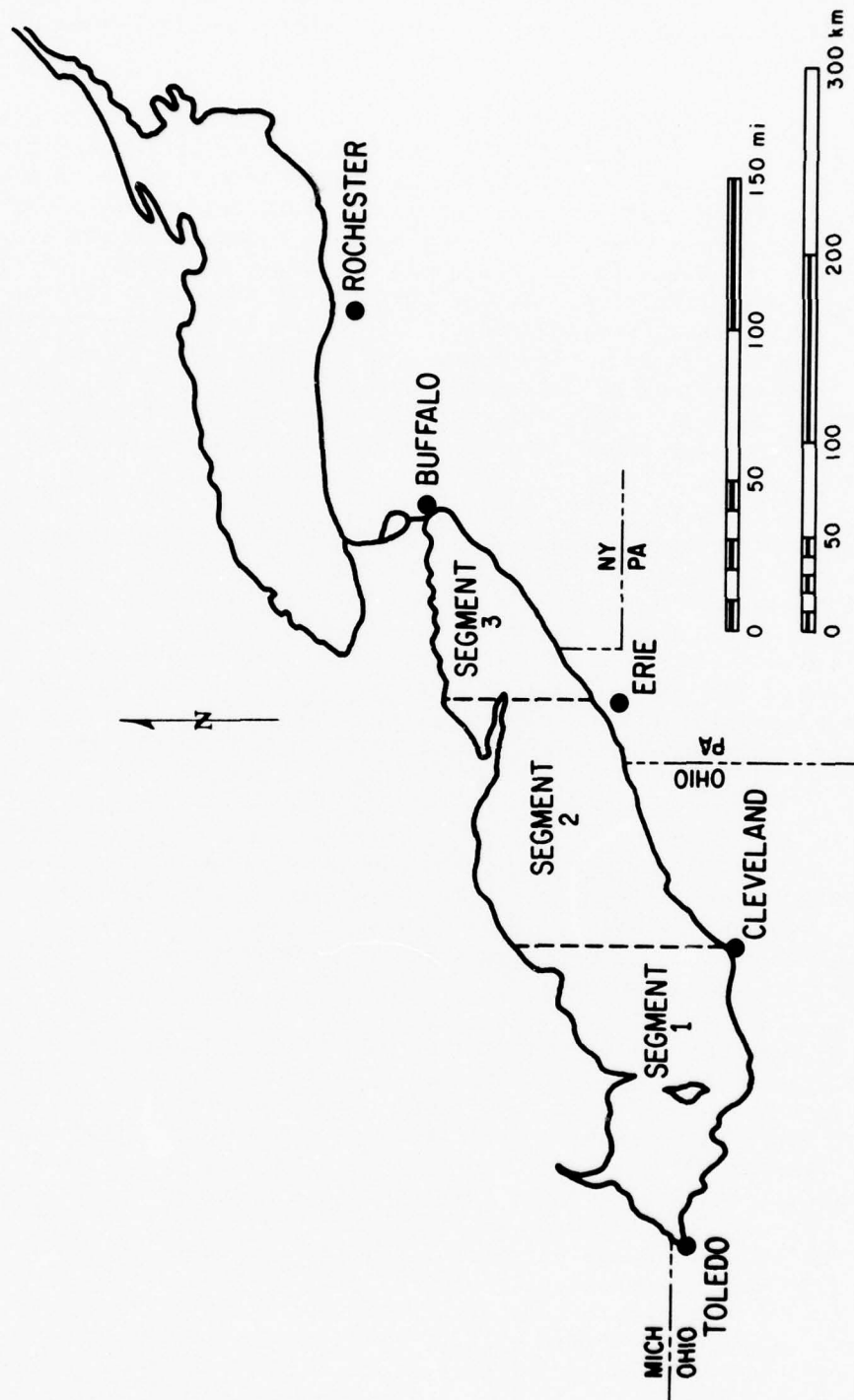


Figure 1. Segment demarcations in Lake Erie used in the WES analysis of wind estimation in the Great Lakes (from Resio and Vincent, 1976c).

Similar procedures were used to estimate climatological air-lake temperature differences in Lakes Michigan, Huron, and Superior. Additional contributions to the rms windspeed error would be expected in the design wave hindcasts because of shortcomings in available wind data, particularly data taken during the first 43 years of the 69-year interval considered (see App. A for details).

After overwater windspeeds have been computed for each overland anemometer site, it is necessary to use them to estimate windspeed and direction at many grid points in the lake. Windspeeds in the WES model were estimated at every overwater grid intersection of a square grid superimposed on each lake. The grid squares were 16 kilometers (10 miles) on a side in Lake Erie for this study, and were also 16 kilometers on a side in all of the Great Lakes when the WES design wave estimates were generated.

The WES wind model in this evaluation study used hourly anemometer wind measurements to provide hourly wind velocity estimates at each grid intersection. The WES model used to generate design wave estimates for the Great Lakes also provided hourly wind velocity estimates, but some of the estimates were based on hourly wind input interpolated from three hourly anemometer measurements.

To estimate wind velocity at any grid intersection in the lake, overlake windspeeds and directions derived from overland anemometer measurements were separated into east-west (U) components and north-south (V) components. U and V components at any point in the lake were estimated by taking a weighted average of U and V components from available anemometer measurements. The weighting factors were based on the distance between the point of interest and the measurement sites. Estimates of the U and V components at the point of interest were then recombined to give estimates of wind direction at the point of interest. Windspeed was estimated as the average of the windspeeds measured at the two nearest sites when the measured wind directions were within 90° of each other, which was usually the case for strong winds generating large waves. When wind directions measured at the two nearest sites differed by more than 90° , windspeed at the point of interest was estimated as the magnitude of the vector sum of the U and V components.

b. Description of the WES Wave Model.

(1) General Procedure. The WES wave model developed by Resio and Vincent provides spectra as a function of direction at each overwater grid intersection in the model. The model sets up a two-dimensional array at each grid intersection to store spectral energy as a function of frequency and direction. Values in the energy array are updated in 15-minute time steps.

Energy is lumped into 30° sectors, resulting in 12 possible wave directions. The wind is assumed to be blowing along the centerline of the 30°

sector in which it falls. Since wind directions in the model can be specified to the nearest degree, considerable directional resolution is sacrificed in the wave model to maintain tractable computer memory and processing requirements.

Wave energy is specified at 20 different frequencies. The frequency spacings are varied to give a more uniform wave period resolution than would be obtained with constant frequency spacings (see Table 1).

Table 1. Frequencies used in the WES Great Lakes wave hindcasting model.

Sequential No.	Frequency (Hz)	Corresponding period (s)
1	0.056	17.9
2	0.061	16.4
3	0.067	14.9
4	0.073	13.7
5	0.078	12.8
6	0.084	11.9
7	0.089	11.2
8	0.095	10.5
9	0.100	10.0
10	0.106	9.4
11	0.111	9.0
12	0.117	8.5
13	0.123	8.1
14	0.128	7.8
15	0.139	7.2
16	0.150	6.7
17	0.161	6.2
18	0.178	5.6
19	0.195	5.1
20	0.230	4.3

Hindcasting with the WES wave model amounts to adding or subtracting energy from the energy stored in the 12 by 20 direction-frequency array during each time step at each grid point. Energy at a grid point changes in response to two basic processes: wave generation and wave propagation. These two processes as treated in the WES model are discussed below. The WES wave model contains no calibration constants. The wave model used in this study is identical to the wave model used in preparing the WES design wave estimates in the Great Lakes.

(2) Wave Generation. The WES model procedures for incrementing wave energy at a grid point during wave generation conditions were developed by Barnett (1966). Energy in the 12 by 20 direction-frequency array at each grid point is adjusted to account for the following processes:

(a) Energy gain due to turbulent pressure fluctuations in the atmosphere (Phillips mechanism);

(b) energy gain due to resonant interaction between waves and wind (Miles mechanism); and

(c) energy transfer between wave components of different frequency (wave-wave interaction mechanism).

Energy is also adjusted to account for wave propagation toward and away from the grid point. This process is considered in a later section.

The WES model does not compute the actual details of the above mechanisms because detailed computations would require an inordinate amount of computer time. Instead, the model uses Barnett's (1966) parameterization of the mechanisms for routine operation.

The parameterized wave-generation terms (Phillips and Miles mechanisms) contain a directional spreading factor to account for the fact that some wave energy can propagate at angles to the wind direction. The directional spreading factor is a function of the n th power of the cosine of the angle between wind direction and wave propagation direction, where n varies between about one for the highest frequency energy and four near the spectral peak. The directional spreading is rather large. Even for the most sharply focused directional distribution in the model ($n = 4$), over one-half the energy in the primary direction is spread to adjacent 30° sectors.

Although the WES model spectrum has reasonable provision for including energy at the lowest wind wave frequencies to be expected in the Great Lakes, the model spectrum obviously does not have provisions for including the higher frequency energy (wave periods shorter than 4.3 seconds; see Table 1) which is common in the Great Lakes as discussed in Section V. Since wave energy at periods shorter than 4.3 seconds can be a significant part of the total energy, even for high wave conditions, the WES model has a simple provision for including the contribution of high-frequency energy to the total energy and the significant wave height.

The procedure is to add a single energy value which is the product of the energy that would be present at periods shorter than 4.3 seconds if that part of the spectrum were fully developed times a scaling factor. The scaling factor is never less than zero or greater than one. It is computed as a function of the local friction velocity.

Wave energy dissipation is considered in the WES model adjacent to major land boundaries. Some consideration is also given to Pelee Island and the other islands near the west end of Lake Erie in that several grid points in the area are considered as land rather than water. The small amount of dissipation which occurs in nature away from the boundaries of Lake Erie because of viscous effects in the water and friction with the bottom is not considered in the model. Dissipation due to bottom friction would be most important for the highest and longest waves, for which most of Lake Erie would not be considered deep water. The neglect of dissipation may give the WES model a small tendency to overestimate wave energy.

Thus, for each grid point and each time step during wave generation, energy is added to various direction-frequency bands on the basis of local winds and energy is transferred between frequency bands in a particular direction to account for wave-wave interactions.

(3) Wave Propagation. The other basic process considered in the WES model is propagation of energy between grid points. The propagation procedure is based on temporal and spatial gradients of energy for each direction-frequency band. Spatial gradients are estimated by assuming that the energy in each direction-frequency band varies linearly between grid points. Temporal gradients are estimated by assuming that the energy in each direction-frequency band at a grid point varies linearly with time. In any particular computational time step, the assumption of temporal linearity of energy gradients extends only to the two preceding time steps. The basis for the propagation procedure is discussed in Resio and Vincent (1977a). A simplified description of the procedure is given below.

In Figure 2, consider energy propagating across a grid square to grid point (2,2) moving toward the south. For a given wave frequency, point "a" is located upstream (north) from (2,2), a distance equal to the distance traveled by a wave of that frequency during one computational time step; i.e., a wave with the given frequency would arrive at grid point (2,2) exactly at computation time if it had been at point "a" at the previous computation time. The distance, L_a , between point "a" and the grid point (2,2) is

$$L_a = C_g \Delta t \quad (10)$$

where C_g is the group velocity of waves with the given frequency, and Δt the time represented by one computational time step.

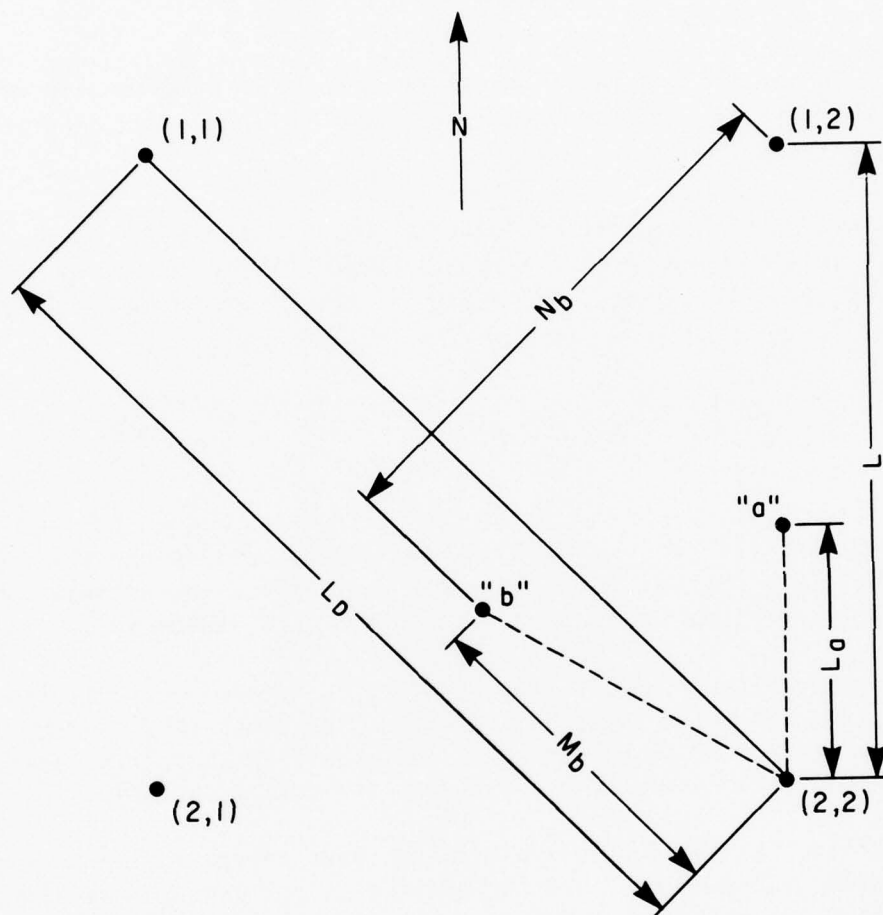


Figure 2. Illustration of WES model propagation of wave energy.

The spatial gradient of wave energy at the given frequency between grid points (1,2) and (2,2) during the $(n + 1)^{\text{th}}$ time step is estimated as

$$\text{spatial gradient} = (E_{2,2}^n - E_{1,2}^n) \frac{1}{L} \quad (11)$$

where $E_{i,j}^n$ is the energy at the given frequency and direction at grid point i,j during the n th time step, and L the distance between adjacent grid points.

To account for the temporal gradient of energy, the model at time step $(n + 1)$ uses an average of the spatial gradients at time step n and time step $(n - 1)$. Hence, the energy at the given frequency at grid point (2,2) and time step $(n + 1)$ is computed as

$$E_{2,2}^{n+1} = E_{2,2}^n - (E_{2,2}^n - E_{1,2}^n + E_{2,2}^{n-1} - E_{1,2}^{n-1}) \frac{L_\alpha}{2L} \quad (12)$$

The equivalent of equation (12) in the WES model would contain additional terms representing the influence of wave energy sources and sinks on $E_{2,2}^{n+1}$. However, the source-sink terms do not affect the propagation scheme and, for simplicity, are omitted from this discussion.

The propagation equation (12) would apply to energy at all frequencies arriving at grid point (2,2) moving toward the south (Fig. 2). However, the value of L_α would be different for each frequency. The energy values would also generally be different for each frequency.

Equation (12) would also apply to the wave energy moving toward the north, east, and west in Figure 2, and the energy propagating along grid diagonals (northeast, southeast, southwest, and northwest) if L were replaced by

$$L_D = \sqrt{2} L \quad (13)$$

A slightly more complex propagation procedure is used for waves which are not propagating along gridlines or grid diagonals. Consider the estimation of energy at grid point (2,2) in Figure 2 moving toward the east-southeast. Point "b" in the figure is located so the distance between "b" and grid point (2,2) is equal to $C_G \Delta t$ where again C_G represents the group velocity for the particular frequency being considered. It is assumed in the WES model that energy gradients over the grid square are

linear. Hence, the energy arriving at grid point (2,2) during time step $(n + 1)$, which conceptually was located at point "b" during time step n , is estimated as

$$E_{2,2}^{n+1} = E_{2,2}^n - (E_{2,2}^n - E_{1,1}^n + E_{2,2}^{n-1} - E_{1,1}^{n-1}) \frac{M_b}{L_D} + (E_{2,1}^n - E_{1,2}^n) \left(\frac{N_b}{L_D} - \frac{1}{2} \right) \quad (14)$$

where M_b is the length of the projection of a line between point "b" and grid point (2,2) on the diagonal through point (2,2), and N_b the distance as defined in Figure 2.

If grid point (2,1) were on land (e.g., representing a spit projecting out into the lake), the propagation scheme is exactly the same, but zero energy is assumed at the land grid point. However, this can lead to situations in which the assumption of small lateral variations in energy is invalid.

In the above examples, one time step is considered at one grid point. In routine use, the model performs similar calculations at every grid point for every direction-frequency combination for which there is wave energy. Further, these calculations are repeated at 15-minute time steps.

The grid in the WES model is set up to cover the deeper parts of the Great Lakes. The grid points nearest shore in each lake are about 8 kilometers (5 miles) lakeward of the coastline. No wave energy is introduced from outside the grid; however, energy generated by winds blowing offshore is partly accounted for at nearshore grid points by the simple parametric representation of energy at periods shorter than 4.3 seconds (discussed earlier). Energy which propagates outside the grid is lost.

2. TDL Model.

a. General Description. TDL has developed a Great Lakes wave-forecasting model which operates in conjunction with the National Meteorological Center (NMC) Primitive Equation (PE) atmospheric model. (Several distinct numerical models are used by NWS for weather analysis and prediction; however the PE model most nearly duplicates the actual hydrodynamic equations.) The TDL model is designed for quick, economical real-time operation on a large-capacity computer to produce reasonably accurate forecasts of significant wave height, period, and direction.

The forecasts, which are made available within several hours to NWS forecasting offices in Great Lakes areas, need to be accurate enough to let local forecasters anticipate the arrival and magnitude of hazardous wave conditions with reasonable assurance. The accuracy needed to satisfy this requirement is probably less than the accuracy desired for engineering use. However, because of the good quality meteorological

data used, the TDL model or some adaptation of the TDL model might provide wave estimates which are accurate enough for engineering use. The model would certainly provide more reliable estimates if hindcast, rather than forecast, winds were used.

The TDL model is actually a combination of two models: a surface wind model and a wave model. These component models are described separately below.

b. TDL Wind Model. The NMC PE atmospheric model, which produces twice daily forecasts at many geographical grid points (Fig. 3), provides the basic input to the TDL surface wind model. The relationship between the PE model and the TDL wind and wave models is schematically illustrated in Figure 4. The PE model origin times are 0000 and 1200 hours, Greenwich mean time (G.m.t.). PE model forecasts include elevations of constant pressure surfaces, temperatures and wind velocities estimated at standard pressure levels, windspeed estimated in the surface boundary layer, and surface pressure estimates. The parameters provided by the PE model are referred to as "predictors" because they are the basis for the TDL surface wind forecasts.

The rationale of the TDL surface wind model is to use the PE model predictors as independent variables in linear equations to predict surface windspeed components and net surface windspeed at ship anemometer height (about 18 meters or 60 feet) above the water surface. With the equations established, surface wind forecasts are easily derived from PE model output as depicted in Figure 4. Details of the TDL surface wind model, as given by Feit and Barrientos (1974), are summarized below.

To establish linear equations for surface windspeed components and net windspeed, a large set of meteorological observations was obtained aboard commercial vessels as part of the cooperative Marine Observation Program. Each observation represents approximately a 1-minute average wind estimated aboard an anemometer-equipped vessel situated at least 8 kilometers from shore. The anemometers are usually located on the roof of the pilots' house at a height of about 18 meters; however, the actual height can vary by 3 meters (10 feet) between ships and with loading differences.

The observations were divided into 12 groups according to the geographical sector in which they were taken (Fig. 5). The observations were further subdivided by the time of year in which they were taken: "summer" (April to September) and "winter" (October to December). Because ice greatly decreases the activity of commercial vessels on the Great Lakes during January through March, the few observations taken during these months were not used.

More than one shipboard observation was often reported in a particular sector at a particular time. In these cases, only the highest reported wind was retained as the most representative of the peak wind that occurred at the center of the sector. This procedure enables NWS to conservatively estimate the most hazardous conditions in the lakes.

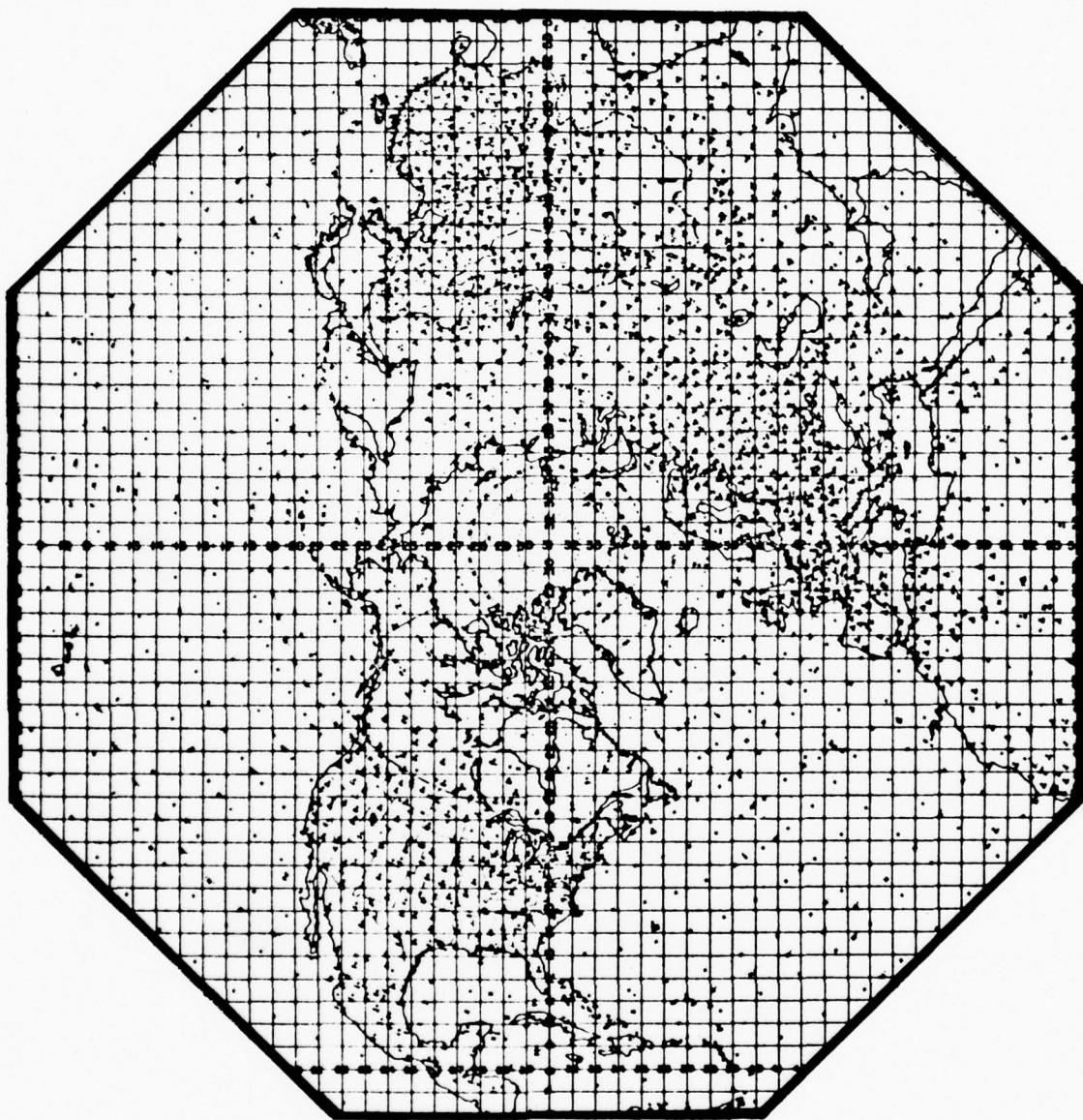


Figure 3. National Meteorological Center (NMC) 1977 point grid used for computation (from Pore, 1976).

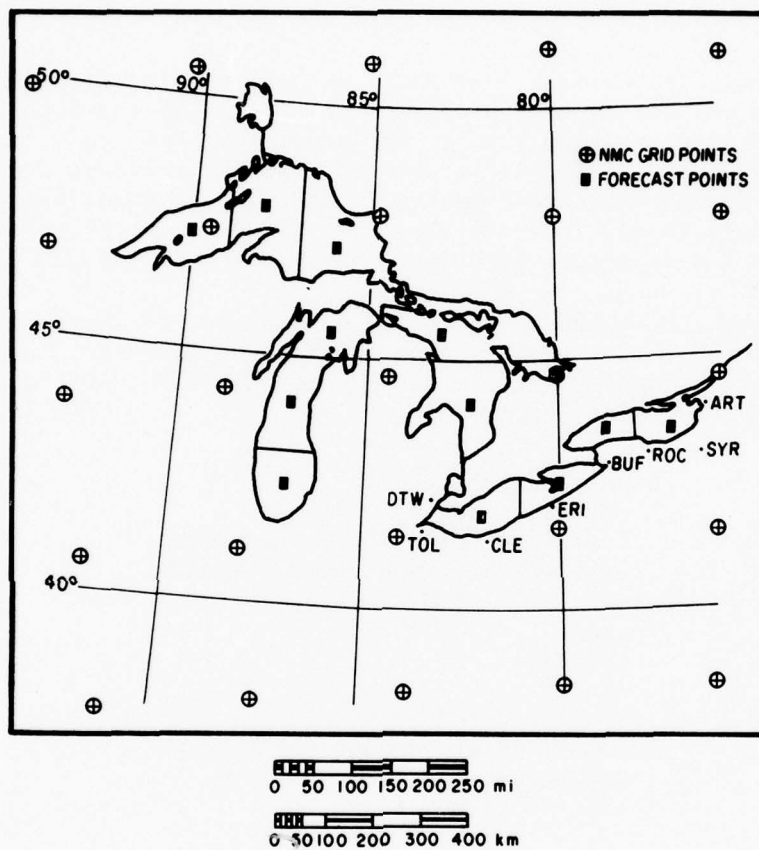


Figure 5. TDL surface wind forecast points (12 areas) for the Great Lakes (from Pore, 1976).

To develop forecasting equations, each shipboard observation was paired with PE model predictors interpolated to TDL forecast points (Fig. 5). The PE model predictors are segregated by the model origin time (0000 and 1200 hours G.m.t.) because of expected diurnal effects. Data pairs from all sectors were then recombined in one large sample for each PE model origin time. Although this approach tends to obscure local effects, the benefits of a large data sample and fewer prediction equations are expected to outweigh any negative effects.

The actual form of each forecasting equation is developed on the basis of the ability of each predictor to reduce the variance between observed and forecast windspeeds. The predictors are ranked in terms of their effectiveness, and coefficients in a linear regression equation to be used for forecasting are computed. Although the same forecasting equations apply to all lake sectors, the values of the PE model predictors used in the equations depend on the sector considered.

Ultimately, there are 12 forecasting equations for each forecasting time (see Fig. 4). For example, for the +6-hour forecast, there is a forecasting equation for each of the 12 possible combinations of elements selected from the following groups:

- windspeed parameter:
 - net windspeed
 - north-south (U) windspeed component
 - east-west (V) windspeed component
- season:
 - summer
 - winter
- PE model origin time:
 - 0000 hours G.m.t.
 - 1200 hours G.m.t.

Surface windspeed is estimated with the net windspeed forecasting equation. The combined U and V components are not used to estimate net windspeed because such an estimate tends to be lower than the true windspeed. Surface wind direction is estimated as the direction indicated by vector addition of the U and V components estimated from the appropriate forecasting equations.

c. TDL Wave Model. Since January 1975, NWS has been using the surface wind forecasts discussed previously to forecast surface wave significant height and period at 64 Great Lakes regular forecast points (Fig. 6) and at several other points where CERC has obtained wave records. Significant wave forecasts are derived from estimates of windspeed, fetch length and duration time using an automated version of the Bretschneider (1970) equations. Details of the TDL wave model, given by Pore (1977), are summarized below.

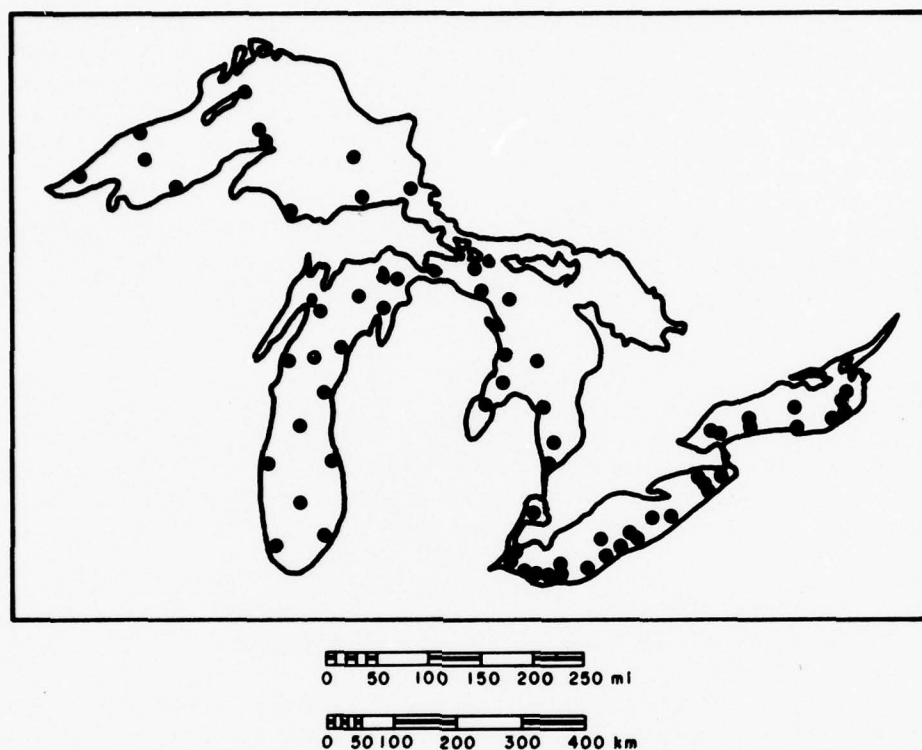


Figure 6. Standard Great Lakes wave forecast points used in the TDL forecasting model (from Pore, 1976).

The windspeed estimate used in the wave forecast model is the surface windspeed forecast for the center of the lake sector where the wave forecast point is located. This windspeed estimate is used even when the fetch extends outside the sector in which the wave forecast point is located.

Fetch lengths are tabulated for each wave forecast point at 15° intervals. In some cases, the fetch lengths are reduced by the method of Saville (1954) to account for limited fetch width. The appropriate fetch length is chosen from the fetch-length table for each forecast point according to the wind direction at forecast time. Fetch-length reduction by ice is not considered.

Wind duration time is estimated as the length of time during which the wind has been blowing within 45° of the direction at forecast time. The duration time is then estimated as either 3, 9, 15, 21, 27, or 33 hours.

Since the duration is based only on wind direction, the windspeed can vary considerably over the duration. To account for the variations, an "effective" windspeed is determined by computing a weighted average windspeed over the duration time. The equation for effective windspeed is linear, with the winds closest to forecast time weighted the heaviest. The windspeed at the forecast time is weighted 50 percent.

A duration-limited fetch is calculated from the duration and effective windspeed. If the duration-limited fetch is shorter than the geographical fetch, it is used as the effective fetch.

Using the derived effective fetch and effective windspeed, significant wave height and period are calculated with Bretschneider's (1970) equations. There is evidence that Bretschneider's equations can overestimate significant height by as much as 20 percent in short fetch situations (Resio and Hiipakka, 1976).

IV. DESCRIPTION OF GAGE DATA

1. Gage Systems.

To evaluate estimates obtained from the wave models, CERC operated wave gages in Lakes Erie and Michigan during the fall of 1975 and 1976. During fall 1975, CERC also recorded the signal from a wave gage in Lake Michigan operated by the Great Lakes Environmental Research Laboratory (GLERL) of NOAA. Gage locations are shown in Figure 7; location coordinates and dates of operation are listed in Table 2. Some preliminary measurements taken during fall 1974 were analyzed and transmitted to WES for use in calibrating and testing the Lake Erie hindcasting model. These measurements are not used in this evaluation study.

Two basic wave gages were used: the Waverider accelerometer buoy, and a submerged pressure-sensitive gage. The Waverider buoys were

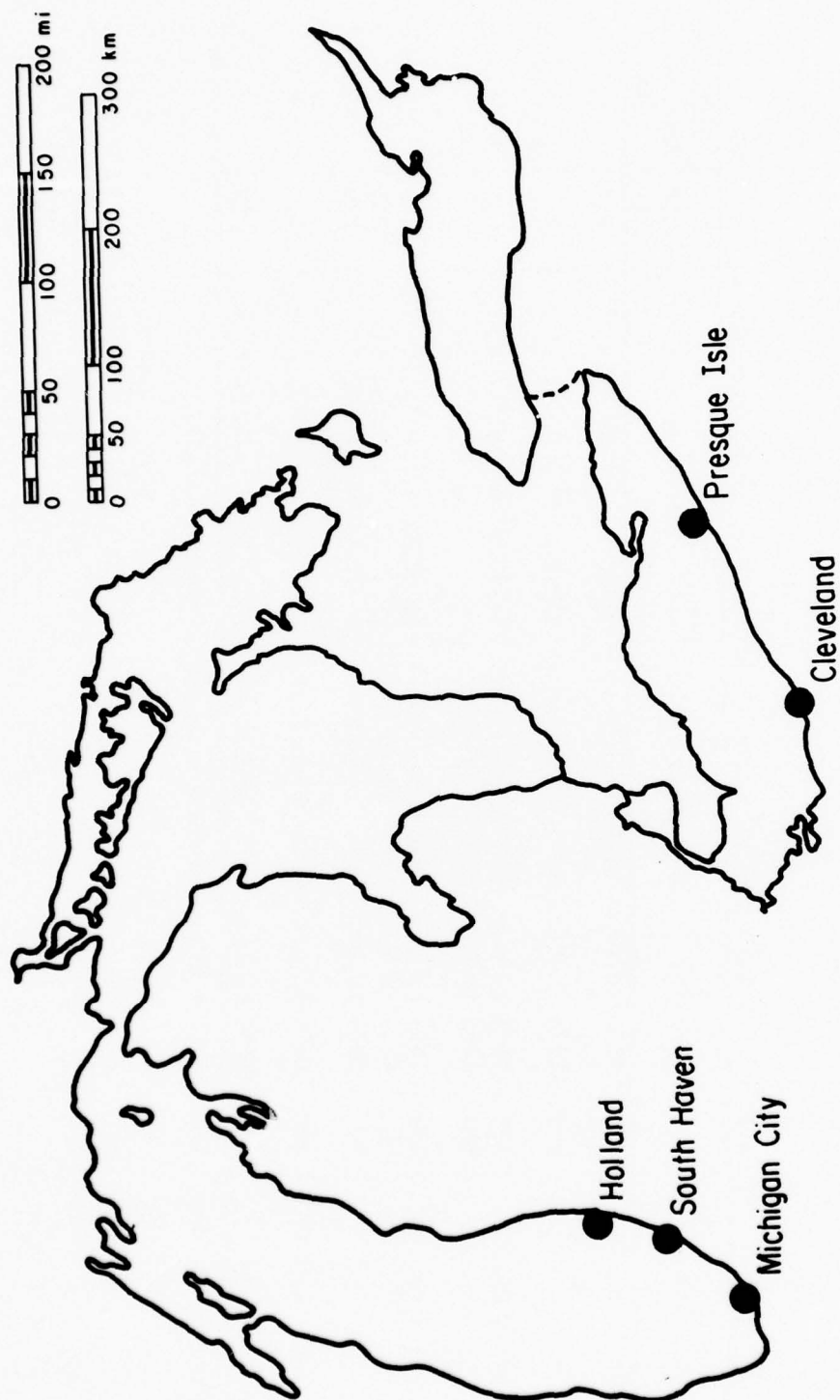


Figure 7. Location of CERC Great Lakes wave gages during 1974-76.

Table 2. Details of location and operation of Great Lakes wave gages during 1974-76.

Location	Date	Gage type	Coordinates	Water depth (m)	Distance from shore (km)
Presque Isle, Pa.	Oct. 1974 to Feb. 1975	Waverider	42°13.5' N., 80°07.0' W.	19.0	6.4
	Sept. 1975 to Dec. 1975				
	Sept. 1975 to Dec. 1976	Pressure	42°10.2' N., 80°07.1' W.	4.6	0.3
Cleveland, Ohio	Oct. 1974 to Jan. 1975	Waverider	41°35.0' N., 81°46.0' W.	16.0	10.5
	Sept. 1975 to Dec. 1975				
Michigan City, Ind.	Sept. 1974 to Nov. 1974	Waverider ¹	41°47.5' N., 87°03.5' W.	24.0	12.9
	Sept. 1975 to Nov. 1975	Waverider ¹	41°45.4' N., 86°59.0' W.	18.3	6.4
	Oct. 1974 to Dec. 1976	Pressure	41°42.0' N., 86°59.5' W.	7.0	0.4
South Haven, Mich.	Sept. 1976 to Dec. 1976	Waverider	42°27.5' N., 86°21.0' W.	34.0	8.0
Holland, Mich.	Sept. 1976 to Dec. 1976	Waverider	42°47.5' N., 86°18.0' W.	47.0	7.2

¹Operated by NOAA's Great Lakes Environmental Research Laboratory (GLERL).

moored in relatively deep water; the pressure gages were located in relatively shallow water. Gage type, water depth, and distance from shore for each gage location are given in Table 2. Since neither the hindcasting nor the forecasting model considers shallow-water effects, only data from the Waverider buoys were used in this study.

The CERC Waverider buoys were moored as shown in Figure 8. Each buoy senses vertical acceleration and electronically integrates the acceleration signal twice. The buoy then transmits the double-integrated signal, which represents surface displacement, to an onshore receiver. The receiver was a standard radio receiver tied into a CERC signal conditioning unit which converted the signal to a frequency-modulated signal suitable for telephone line transmission.

The buoy systems operated reasonably well during fall 1974. The system at Cleveland, Ohio, provided good quality digital records for 73 percent of the six hourly observations while it was deployed. The system at Presque Isle, Pennsylvania, provided good quality digital records for 65 percent of the observations.

The operation of the buoy systems during fall 1975 was only marginally satisfactory. The main source of trouble appeared to be locally generated signals which interfered with the signal transmitted from the buoys. At least one of these interfering signals did not exist the previous year. The transmitting frequency was changed once in the Presque Isle buoy during fall 1975, but the transmitted signal continued to be noisy. The Cleveland system had a tendency to lose the signal when the buoy was in a wave trough during high wave conditions, perhaps because of the relatively low elevation of the receiving antenna (about 15 meters (50 feet) above the water). Records were occasionally lost from both sites because of telephone line noise and recorder problems at CERC. During fall 1975, good quality digital records were obtained for 52 percent of the six hourly observations at Cleveland and 33 percent at Presque Isle.

Because of the problems encountered during fall 1975, several additional precautions were taken in fall 1976. More time was spent on selecting onshore receiver sites which were relatively free from interference signals. The omnidirectional receiving antennas used in fall 1975 were replaced with directional antennas which blocked out all signals originating landward of the receiver. Other important considerations were a high support at each site on which the antenna could be mounted, a secure place for the receiver electronics, and placement of the buoys close to shore but not in water shallower than about 30 meters (100 feet).

Accelerometer buoy wave measurements were taken during fall 1976 at South Haven and Holland, Michigan. The buoy system at South Haven operated reasonably well, providing good quality digital records for 69 percent of the six hourly observations. Eight percent of the missing observations at South Haven resulted from the delay between failure and replacement of an electronic component in the receiver.

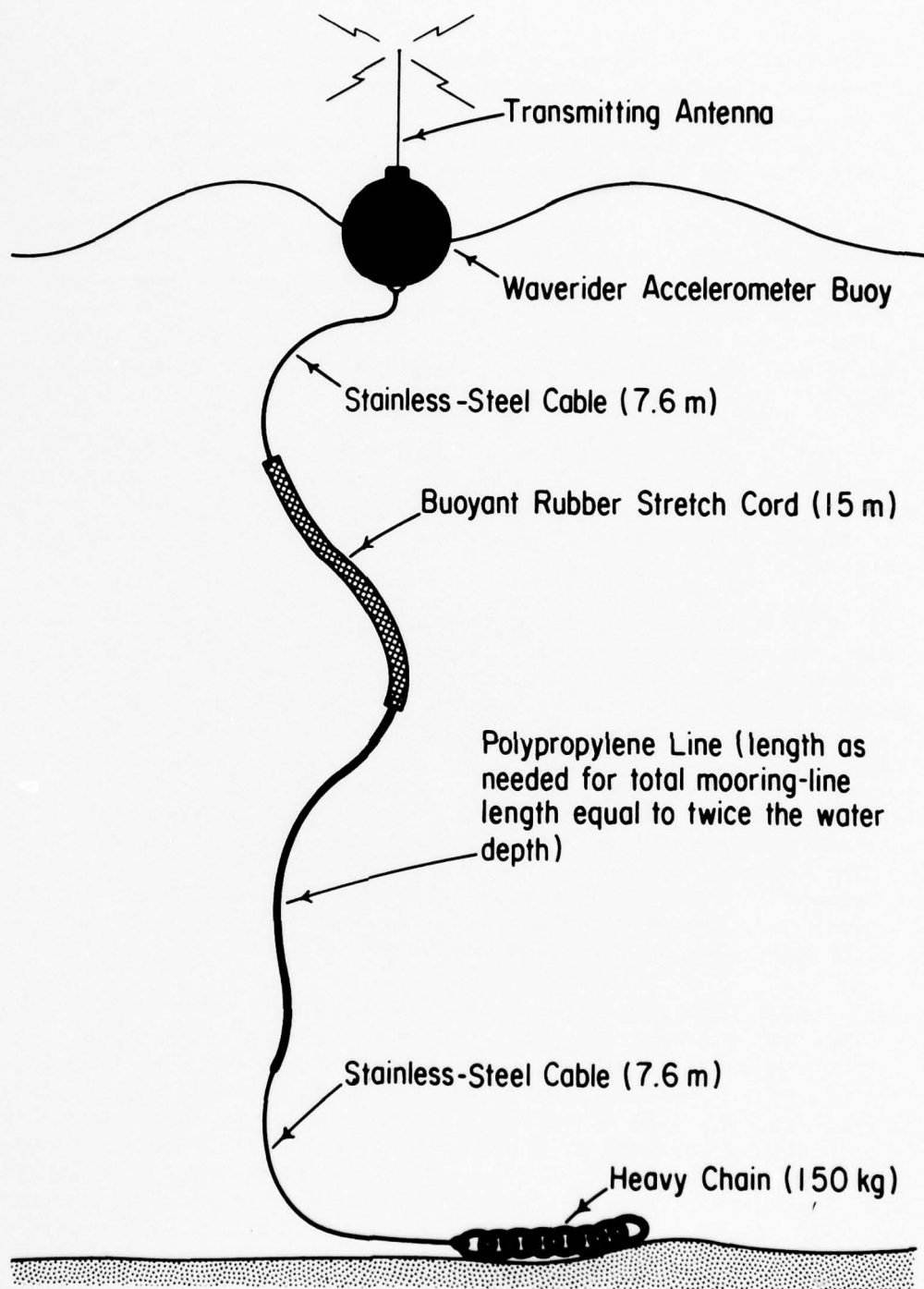


Figure 8. Mooring system for CERC Waverider buoys.

The buoy system at Holland operated poorly during fall 1976, providing good digital records for only 39 percent of the observations. A major problem at Holland was large electronic drift in the signal level in response to local temperature fluctuations. A small heater was installed to help stabilize the temperature of the receiver, but it was not sufficient. If the building housing the receiver had been well heated or if the receiver circuitry had been designed to compensate for temperature, this problem may have been avoided.

In addition to the temperature drift, the signal from the Holland buoy system was often noisy. The noise was partially due to radio transmissions from ships approaching and departing Holland Harbor. The signal from Holland further deteriorated in early December 1976 when one of the receiving antenna guy wires was cut by vandals. The antenna was then bent and damaged by wind forces.

2. Data Recording.

Signals from both the Waverider buoys and the pressure gages were transmitted by telephone line in real time to the CERC laboratory. At CERC, the signals were digitized and recorded on computer-compatible magnetic tape, and also recorded directly with a pen-and-ink strip-chart recorder. Since the recording procedures used in fall 1975 differed significantly from the procedures used in fall 1976, they are discussed separately below. The discussion concerns recording procedures for the Waverider buoy data; however, procedures for the pressure-gage data were comparable.

During fall 1975, a 20-minute digital record was obtained every 2 hours from each gage. The procedures are discussed in detail by Peacock (1974). Auxiliary 4.5-minute pen-and-ink strip-chart records were recorded once every 6 hours from each gage.

During fall 1976, three digital recording procedures were used. From 21 September to 1 November, 20-minute digital records from the Waverider buoy gages were obtained continuously by the procedures discussed in Peacock (1974). For several weeks before 21 September, digital records were taken at the rate of two per 2 hours for Holland and three per 2 hours for South Haven by similar procedures. After 1 November the digital data recording was controlled by a Data Acquisition System (DAS) which collected two successive 20-minute records every 6 hours from each gage under normal wave conditions. Whenever the significant wave height exceeded 1.8 meters (6.0 feet), digital records were automatically taken twice per hour until the significant height dropped below 1.8 meters. Auxiliary 4.5-minute pen-and-ink strip-chart records were taken six times per 6 hours during most of fall 1976.

3. Data Analysis.

The initial step in the data analysis for fall 1975 was to analyze one digital record every 6 hours from each gage with the standard CERC

spectral analysis program (Thompson, 1974, 1977). This initial analysis procedure was also followed for the fall 1976 data taken on or before 1 November. For the fall 1976 data taken after 1 November the initial procedure was to analyze every available digital record.

Since the Waverider buoy records often contained signal noise, the next analysis step for both the fall 1975 and fall 1976 data was to analyze one pen-and-ink record every 6 hours from each Waverider buoy with the standard CERC pen-and-ink record analysis method (Thompson, 1977). The pen-and-ink record analyses were possible only when the records contained little or no noise; therefore, they served as a good check on the digital analyses.

The initial digital and pen-and-ink record analyses were reviewed to identify days during which the waves were relatively high and the Waverider buoy gages were operating reasonably well. The results of the review were summarized in terms of storms for which data useful in evaluating hindcasting and forecasting models had been collected. Ten storms were selected during fall 1975, and seven storms during fall 1976 (Table 3).

Table 3. Great Lakes storms selected for evaluation of hindcasting and forecasting models.

Storm dates	
Fall 1975	Fall 1976
11 to 15 Sept.	20 to 24 Sept.
20 to 25 Sept.	21 to 23 Oct.
17 to 19 Oct.	28 Oct. to 10 Nov.
25 to 26 Oct.	17 to 19 Nov.
29 to 30 Oct.	21 to 23 Nov.
1 to 2 Nov.	9 to 18 Dec.
10 to 16 Nov.	20 to 24 Dec.
20 to 22 Nov.	
26 to 28 Nov.	
30 Nov. to 1 Dec.	

All available digital records from Great Lakes gages during the storm days of fall 1975 listed in Table 3 were then analyzed. Under optimum conditions, digital analyses were obtained at 2-hour intervals. No additional digital analyses were done for the fall 1976 data. Thus, for the 1976 storm days before 2 November (except for 20 September), there is an additional five unanalyzed digital records for every analyzed digital record. Since the part of this evaluation study dealing with storm data is focused on the fall of 1975 (discussed in the next section), additional digital analyses for the fall of 1976 did not seem warranted.

Since most of the storms for fall 1976 occurred after 1 November, digital records were available at only 6-hour intervals for the early and late stages of the storms, during which the significant height was

less than 1.8 meters, as discussed previously. To supplement the digital analyses, all available pen-and-ink records were analyzed for the storm days of fall 1976, providing a maximum of six analyses every 6 hours for each gage.

For both fall 1975 and fall 1976, pen-and-ink record analyses were used to fill gaps in the digital analyses.

Significant heights and periods for each of the storms were tabulated and, for the fall 1975 data, put on computer punchcards for use in evaluating Great Lakes wave models. Wave energy spectra obtained from the digital analyses were stored on magnetic tape.

V. COMPARISON BETWEEN HINDCASTS AND GAGE DATA

1. WES Model.

To obtain hindcasts suitable for evaluation, the WES model developed by Resio and Vincent was run for the selected fall 1975 storms in Lakes Erie and Michigan. The computer run for Lake Michigan was faulty and was not repeated because of the expense of running the WES model. Only the Lake Erie data were used for evaluation. The model was not run for the 1 and 2 November 1975 storm, so this storm was omitted from the evaluation. Additional comparisons of WES hindcasts with wave measurements are provided in Resio and Vincent (1978b) for Lakes Erie, Ontario, and Superior.

The WES model was not run for any of the fall 1976 storms. Because no major storms occurred during fall 1976 and the Waverider operation was intermittent, it was decided that running the WES model for these storms was not worth the cost.

WES hindcasts for fall 1975 storms in Lake Erie were generated at 15-minute time steps using hourly wind data. Hindcast data were provided to CERC for 2-hour intervals at standard grid points bracketing the Cleveland Waverider buoy site, and at one standard grid point near the Presque Isle Waverider buoy site (Fig. 9). The WES model used wind input from four anemometer stations (Toledo and Cleveland, Ohio, Erie, Pennsylvania, and Buffalo, New York), two of which were located near the gage sites. Neither WES nor TDL had access to any of the gage data until after the hindcasts were completed.

Significant wave height, peak spectral period, and energy as a function of frequency and direction are available from the WES wave hindcasting model. Only significant height, peak period, and one-dimensional spectrum can be used for comparison with Waverider buoy measurements, where the one-dimensional hindcast spectrum for this study was obtained by computing the total energy at each frequency, regardless of direction. These parameters differ slightly from the parameters produced for the published design wave estimates in that the published estimates were based only on wave energy with an onshore component of motion.

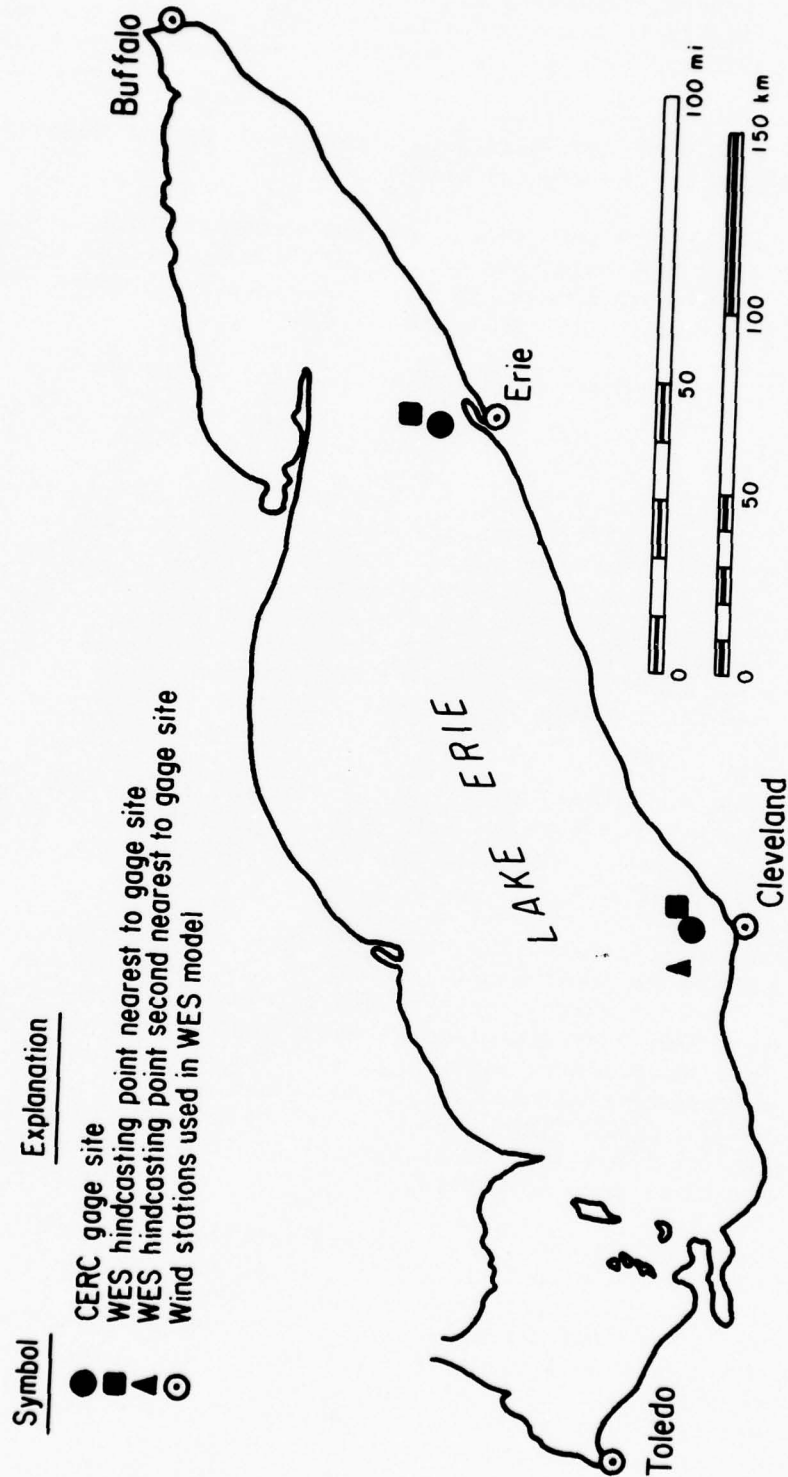


Figure 9. Location of WES wave hindcasting model grid points nearest to CERC Waverider buoy sites, and anemometer wind stations providing input to the WES model in Lake Erie.

Time-history plots of significant wave height and peak spectral period for both gage and hindcast data (App. B) show that the hindcasts have considerable skill in reproducing storm histories. In these plots, hindcast data are shown only for the WES grid point nearest the gage. Hindcast significant heights at grid points bracketing the Cleveland gage were usually within 0.1 meter of each other. They rarely differed by more than 0.2 meter (0.7 foot).

For some storms (e.g., the 17, 18, and 19 October storm) the differences between hindcasts and measurements during most phases of the storm at both Presque Isle and Cleveland are remarkably small. The differences during most of the 10 to 15 November storm are also surprisingly small. However, for some storms the differences are as great as 1 meter. For example, on 24 September at Cleveland, the WES model underestimated the rate at which significant height was growing so that when the gage measured peak wave conditions, the model was still in the early stages of wave generation. On 10 November at Presque Isle, the model overestimated the highest significant height by more than 1 meter.

If only the effectiveness of the hindcasting model in estimating the magnitude of peak storm conditions is considered, the WES model fares well in the Cleveland, 24 September example, being within 0.2 meter of the highest gage estimate. However, on 10 November at Presque Isle, the WES estimate of the highest wave conditions appears to be too high.

Peak spectral period from the WES hindcasting model is generally within 1 second of the peak spectral period from gage records. The discrepancies are smaller for high than for low wave conditions. In many cases, discrepancies at short periods are due to the lack of consideration of periods shorter than 4.3 seconds in the WES model. Aside from effects of the WES short period cutoff, there is no obvious bias in the hindcast peak spectral periods.

Scatter plots of measured versus hindcast significant heights for Presque Isle and Cleveland are shown in Figure 10. The plotted gage heights represent only digital analyses of records taken within 20 minutes of the corresponding hindcasts. All of the paired heights are from the nine selected storms during fall 1975. Each plot includes a 45° line, a straight dashline about which the average squared error between hindcast and measurement is a minimum (two-parameter regression line), and a straight line through the origin about which the average squared error is a minimum (one-parameter regression line). Each plot also includes bands showing the 95-percent confidence intervals around the one-parameter regression line. The confidence bands are straight lines passing through the origin with slopes differing from the slope, b , of the one-parameter regression line by \pm (standard error of b) \times (Student's t for 95-percent confidence).

At Presque Isle, no clear bias is apparent in the hindcasts corresponding to measured significant heights less than 2 meters (6.6 feet). However, there is evidence of a tendency for the Presque Isle hindcasts

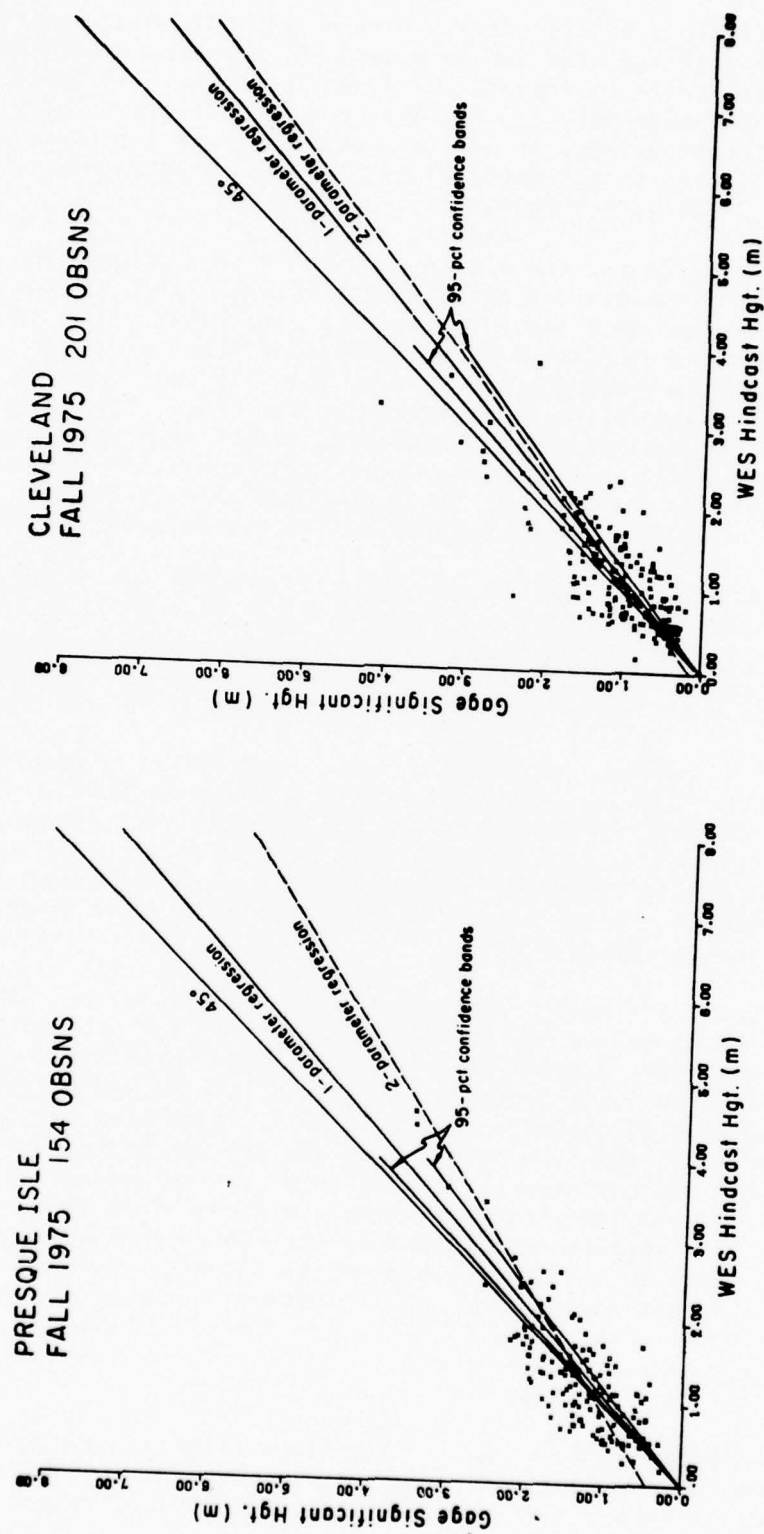


Figure 10. Scatter plots of measured versus WES hindcast significant height in Lake Erie. Only digital analyses are considered.

to be high for measured heights greater than 2 meters. At Cleveland the hindcasts appear to have a small tendency to be high for measured significant heights less than 2 meters. For measured significant heights above 2 meters, the Cleveland hindcasts have no clear bias.

Scatter plots of measured versus hindcast peak spectral period are shown in Figure 11 for Presque Isle and Cleveland. The gage periods are grouped into intervals. The inward pointing tick marks on the vertical axes indicate the midpoint of each gage period interval. The inward pointing tick marks on the horizontal axes indicate the discrete period values provided by the WES model in the range of 4 to 10 seconds (see Table 1). Each plot includes a 45° line, a two-parameter linear regression line, and a one-parameter linear regression dashline. Each plot also includes bands showing the 95-percent confidence intervals around the two-parameter regression line. For each value along the x-axis (horizontal), the confidence bands differ from the two-parameter regression line by \pm (standard error of y predicted by two-parameter regression line) \times (Student's t for 95-percent confidence). The confidence bands are curved because there is uncertainty about both the slope and the intercept of the two-parameter regression line.

The plots indicate that for measured periods longer than about 5.5 seconds the hindcast periods tend to be too short; for measured periods shorter than about 4 seconds the hindcast periods tend to be too long. However, this tendency results from formulation of the hindcasting model so as not to permit peak periods shorter than 4.3 seconds.

Because the WES model is not designed to adequately handle the shorter wave periods, and this shortcoming clouds the comparison in Figure 11, another set of wave period scatter plots which omits cases where the measured significant height was less than 1 meter was generated (Figure 12). The plots indicate small tendencies for the hindcast periods to be too long when the measured periods are relatively short, and too short when the measured periods are relatively long.

The correlation between measured and hindcast significant heights is 0.80 at Presque Isle and 0.79 at Cleveland (Table 4). If cases in which the measured significant height is less than 1 meter are ignored, the correlation is about the same at Presque Isle, but drops to 0.68 at Cleveland.

The agreement between predicted and observed mean significant height at Presque Isle is excellent; the agreement at Cleveland is very good. The mean hindcast height at Cleveland is 0.14 meter higher than the measurements. If the lower waves are ignored, the difference between means is further reduced at both locations.

The variances of the hindcast significant heights are higher than the variances of the measurements at both locations, particularly at Presque Isle. The rms error between hindcasts and measurements is 0.44 meter (1.4 feet) at both sites. The rms error for the higher waves only is

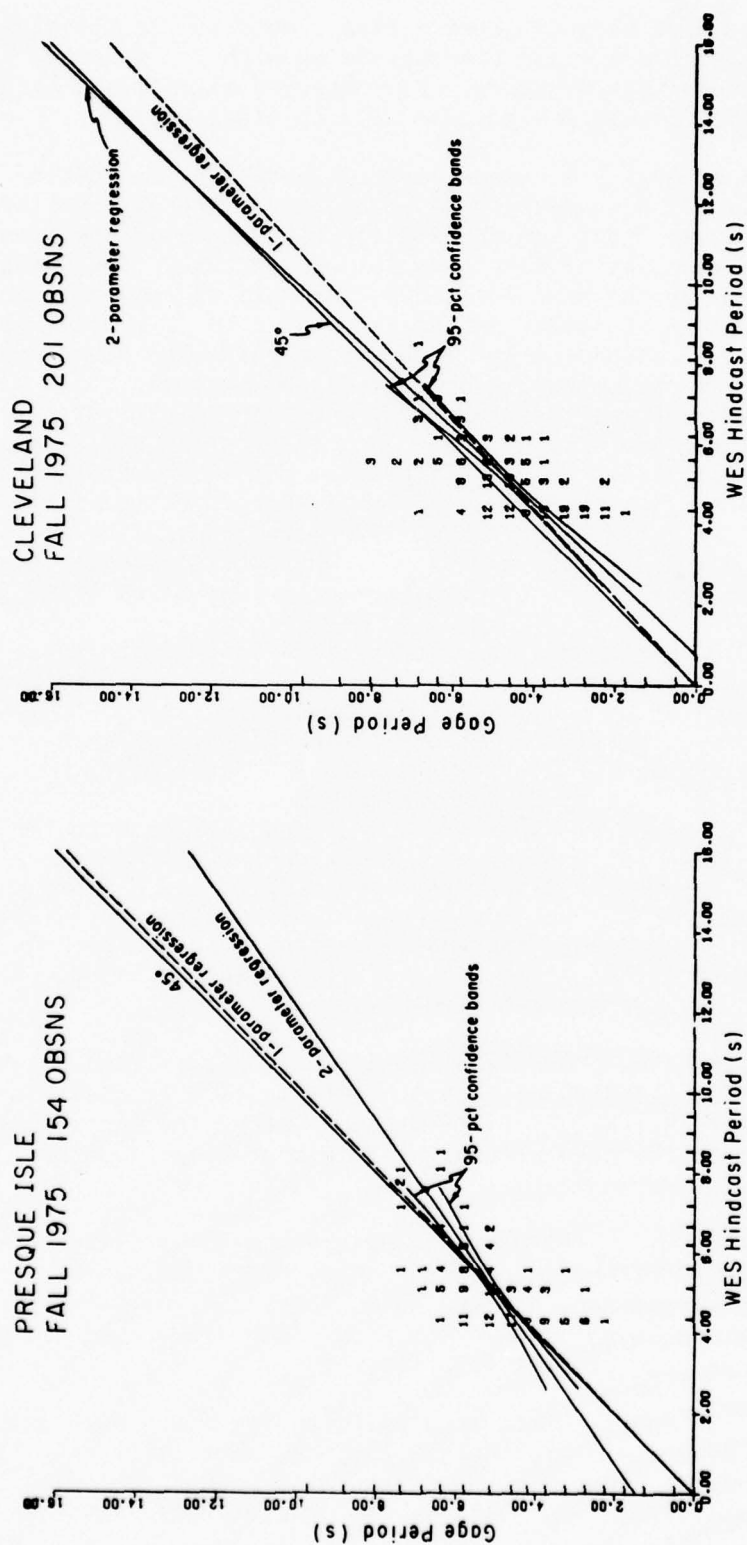


Figure 11. Scatter plots of measured versus WES hindcast peak spectral period in Lake Erie.
Only digital analyses are considered.

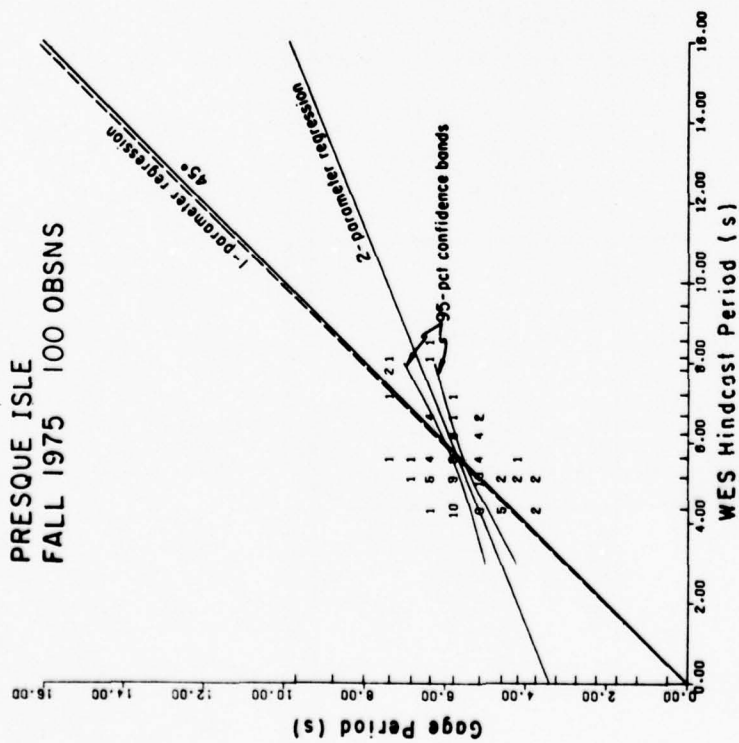
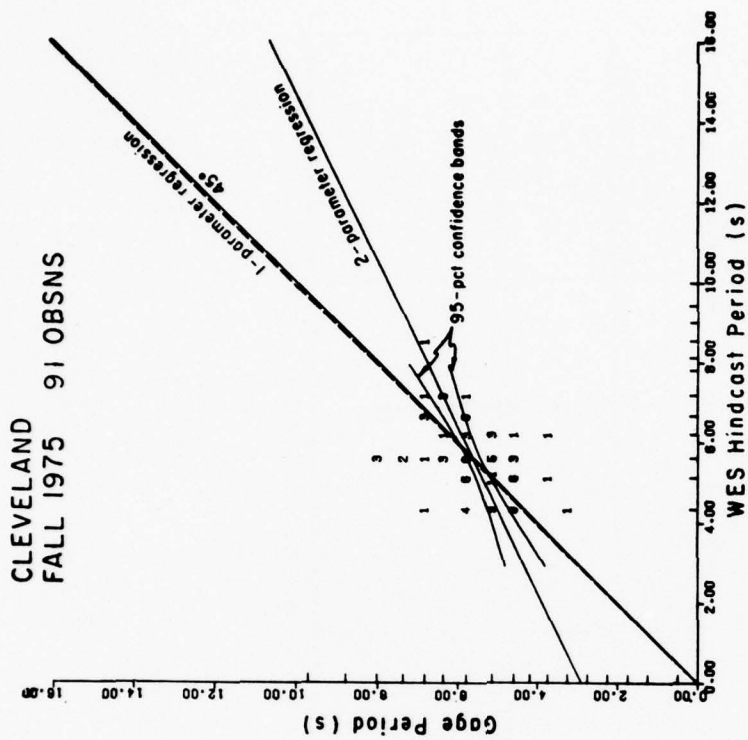


Figure 12. Scatter plots of measured versus WES hindcast peak spectral period in Lake Erie (cases where the measured significant height is less than 1 meter are omitted). Only digital analyses are considered.

Table 4. Comparison of measured and WES hindcast significant heights during fall 1975.

Location	Obsns. No.	Correlation	$H_G = A H_{WES}^1$	Mean significant hgt. (m)		Variance of significant hgt. (m ²)		Rms error in significant hgt. (m)	
				WES	Gage	WES	Gage	Gage vs. hindcast	Gage vs. corrected hindcast
Presque Isle	154	0.80	0.90	1.31	1.27	0.53	0.33	0.44	0.41
Cleveland	201	0.79	0.85	1.17	1.03	0.42	0.39	0.44	0.39
Presque Isle (only where $H_G \geq 1m$)	100	0.78	0.91	1.59	1.59	0.52	0.21	0.46	0.44
Cleveland (only where $H_G \geq 1m$)	91	0.68	0.91	1.60	1.54	0.42	0.31	0.49	0.47

¹ H_G = significant height from Waverider buoy gage; H_{WES} = significant height from WES wave hindcast.

slightly greater. When the hindcasts are scaled by the one-parameter regression coefficient ("A" in Table 4), the rms error is reduced to about 0.4 meter (1.3 feet) at both locations.

The correlation between observed and hindcast peak spectral periods is 0.59 at Presque Isle and 0.63 at Cleveland (Table 5). The correlation between periods during the higher wave conditions is lower at both locations. The mean peak periods at Presque Isle are virtually identical; at Cleveland the mean hindcast peak period is half a second longer than the mean measured peak period. If only the higher wave conditions are considered, the mean hindcast period is shorter than the mean measured period at both locations.

The variances of hindcast periods are considerably smaller than the variances of measured periods at both locations. This difference in variance is clearly evident in the scatter plots in Figure 11. However, if only the higher wave conditions are considered, the variance of hindcast periods and the variance of measurements are comparable at Cleveland, and the variance of hindcast period exceeds the variance of measurements at Presque Isle. The rms error between hindcast and measured peak spectral periods is about 0.9 second at Presque Isle and 1.1 seconds at Cleveland. When the linear regression equation is used to adjust the hindcast peak periods, the rms errors in comparison to measurements are reduced by only about 0.1 second. When linear regression equations are used to adjust hindcast periods for the higher waves only, the rms error is about 0.7 second at Presque Isle and 0.8 second at Cleveland.

Since the WES hindcasting model is designed primarily for large storms, its capability of estimating the maximum significant height for each storm is considered. Plots of maximum significant height from gage versus hindcast for each of the fall 1975 storms are shown in Figure 13. The plots include 11 data points for 9 storms because the 20 to 25 September and 10 to 16 November storms were each considered as 2 storms (20, 21, and 22 September and 23, 24, and 25 September; 10, 11, and 12 November and 13 to 16 November) for this display.

Since gage coverage during a storm was seldom reliable, Figure 13 contains a special symbol to indicate when gage coverage was "good"; good coverage means a usable gage analysis within 2 hours of the highest hindcast significant height and reasonably complete gage coverage of the growth or decay of significant height during the storm. Storms for which the gage coverage did not meet these criteria are designated as having "poor gage coverage." The time-history plots in Appendix B show the full extent of gage coverage for each storm. Both digital and pen-and-ink record analyses were considered in obtaining maximum significant heights from the gage. One-parameter regression lines for the WES hindcasts with good gage coverage and for the TDL forecasts are also shown in Figure 13.

Figure 13 indicates a small tendency for the WES model to overestimate maximum significant heights for the storms considered in this

Table 5. Comparison of measured and WES hindcast peak spectral periods during fall 1975.

Location	Obsns. (No.)	Correlation	$T_G = A + B T_{WES}^1$		Mean period (s)		Variance of period (s ²)		Rms error in period (s)	
			A (s)	B	WES	Gage	WES	Gage	Gage vs. hindcast	Gage vs. corrected hindcast
Presque Isle	154	0.59	1.48	0.70	5.11	5.07	0.85	1.20	0.93	0.88
Cleveland	201	0.63	-0.81	1.06	4.99	4.50	0.62	1.76	1.14	1.03
Presque Isle (only where $H_G \geq 1m$) ²	100	0.49	3.41	0.40	5.46	5.62	0.91	0.61	0.91	0.68
Cleveland (only where $H_G \geq 1m$) ²	91	0.48	2.90	0.48	5.42	5.52	0.77	0.79	0.92	0.79

¹ T_G = peak spectral period from Waverider buoy gage; T_{WES} = peak spectral period from WES wave hindcast.

² H_G = significant height from Waverider buoy gage.

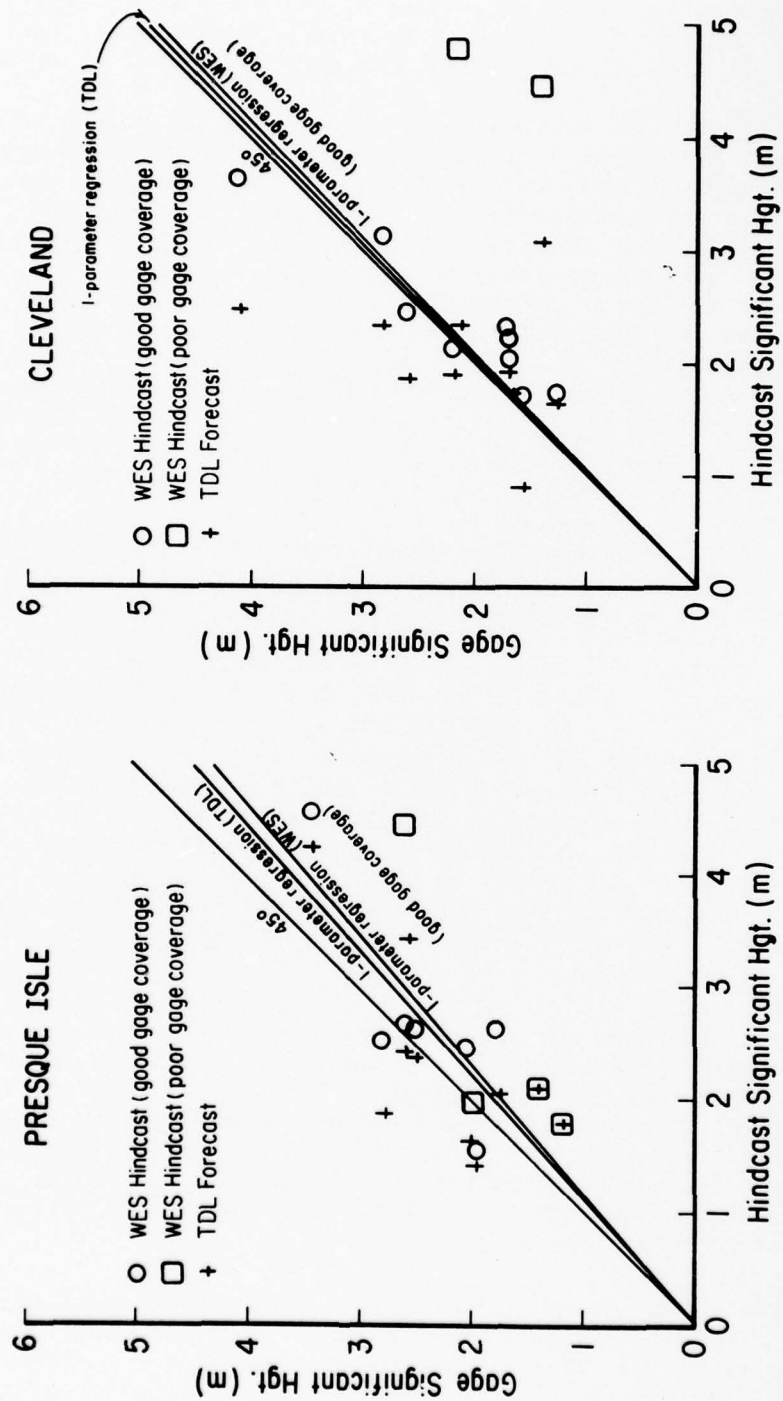


Figure 13. Scatter plots of measured versus WES hindcast maximum significant height for selected storms during fall 1975 in Lake Erie at Presque Isle and Cleveland. Both digital and pen-and-ink analyses are considered.

study. Part of the observed tendency may be due to missing gage records near the peaks of the storms. However, this effect is expected to be small for the circular symbols. Maximum hindcast significant heights deviate less from measurements at Cleveland than at Presque Isle.

Although the WES hindcasts cover only selected storms in fall 1975, the overall distribution of significant heights can be compared with gage data during the storms to give an indication of how well the hindcasts estimate wave climate. The overall distributions of hindcast and measured significant heights (including both digital and pen-and-ink record analyses) are plotted in Figure 14. At Presque Isle the distributions are similar for about the lower 70 percent of the significant heights, but the distribution of hindcasts is clearly higher for the upper 20 percent of the cases. Part of the difference at higher significant heights may be due to intermittent gage operation. However, at Cleveland where the gage operation was more consistent, the distribution of hindcast significant heights shows a slightly greater tendency to exceed the distribution of measured significant heights.

The overall distributions of peak spectral periods are shown in Figure 15. As discussed earlier, the distribution of hindcasts cannot extend to periods shorter than 4.3 seconds, so the high concentration of hindcast periods in the 4-to-5-second range in the figure is expected. The concentration of hindcast periods and the concentration of measured periods are quite similar for wave periods longer than 6 seconds.

Variance, or energy, spectra from Presque Isle and Cleveland are plotted in Figure 16 for 18 cases. Hindcast spectra for the two grid points which bracket the gage location are both shown with each Cleveland gage spectrum. The \times symbols in the Cleveland spectral plots represent hindcasts for the grid point closest to the gage (see Fig. 9). In general, the hindcast and gage spectra are similar. Many of the hindcast spectral peaks are quite close in both magnitude and frequency to gage spectral peaks.

In several cases the gage spectra have more than one prominent peak. The Cleveland spectra at 1420, 24 September, and 2020, 18 October, are two good examples. In both examples the hindcast spectrum has only one peak, and it fairly well matches one of the gage peaks. However, the hindcast spectra have no indication of an energy concentration at the frequency of the lowest frequency gage spectral peak. This observation--that the hindcasting model can miss low-frequency spectral peaks--is discussed in the following section.

An additional group of 43 spectral plots is provided in Appendix C. The plots in this appendix are considered to be of lesser quality than the comparisons in Figure 16 because of either poor matching between the times of the hindcast and the gage record or noise in the gage record. Several spectra for which the gage records were excessively noisy have been deleted from Appendix C.

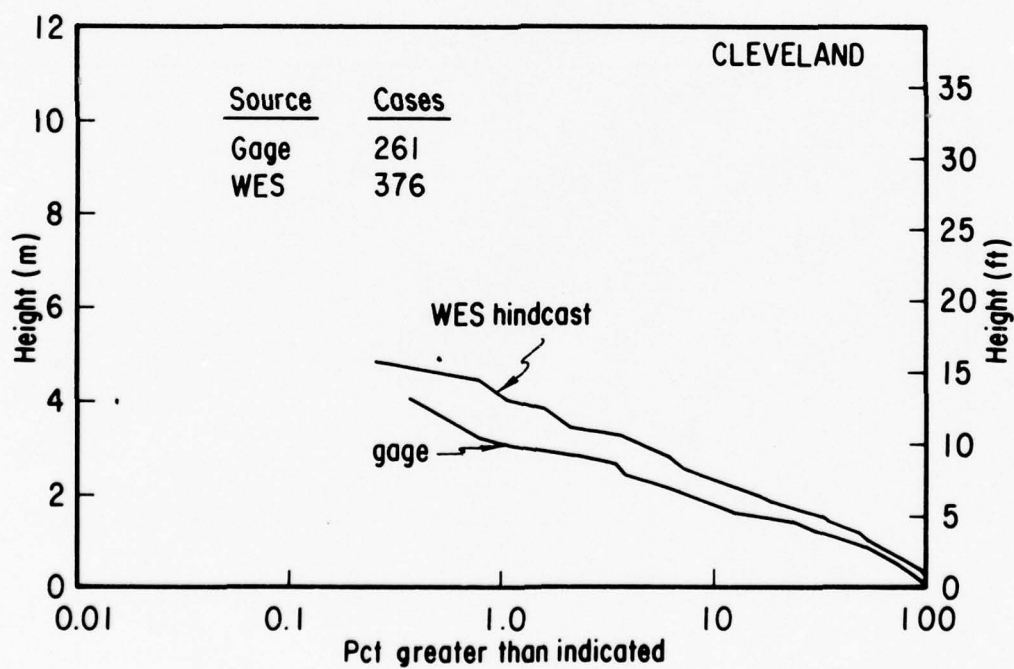
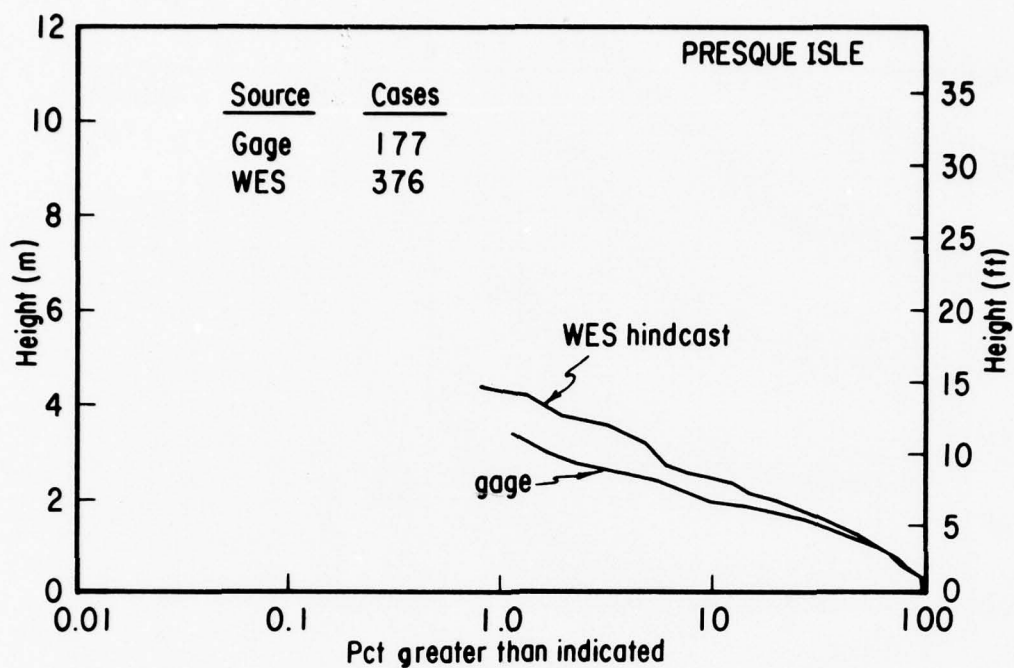


Figure 14. Overall distributions of measured and hindcast significant heights at Presque Isle and Cleveland. Both digital and pen-and-ink analyses are included.

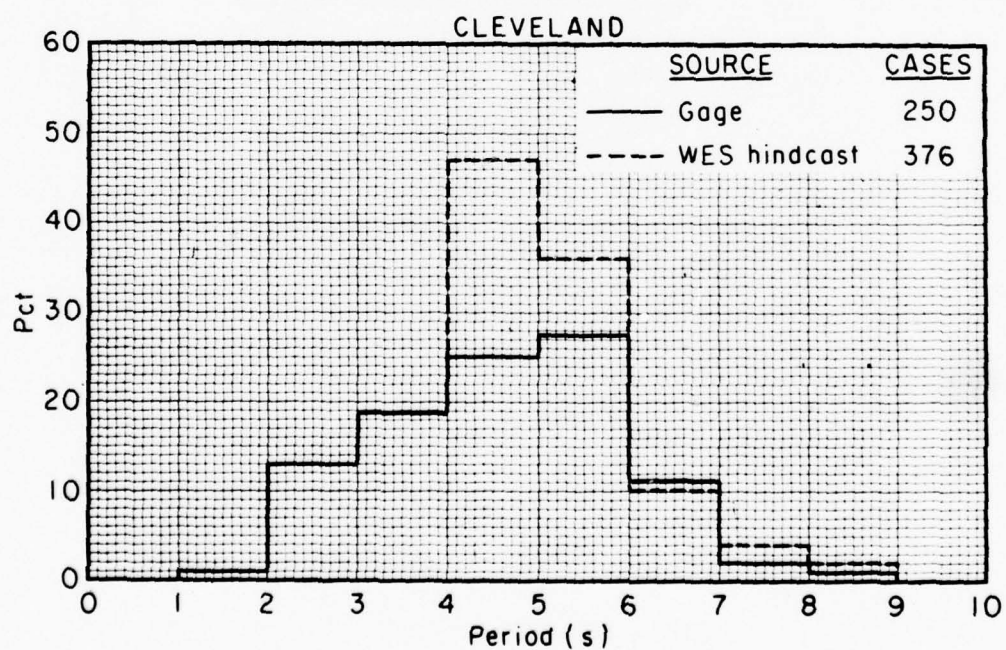
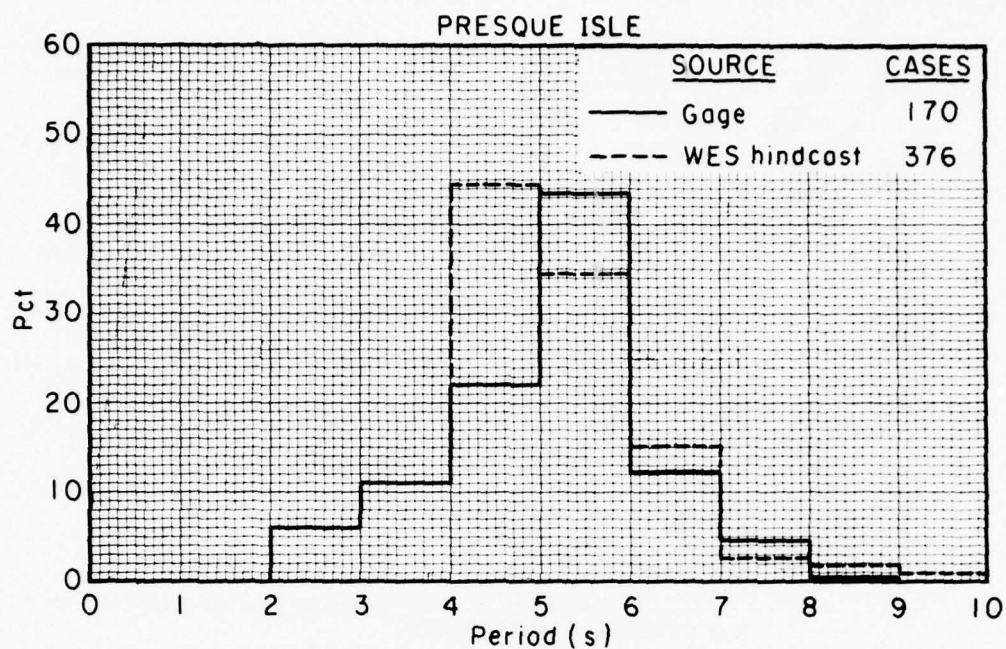


Figure 15. Overall distributions of measured and hindcast peak spectral periods at Presque Isle and Cleveland. Both digital and pen-and-ink analyses are included.

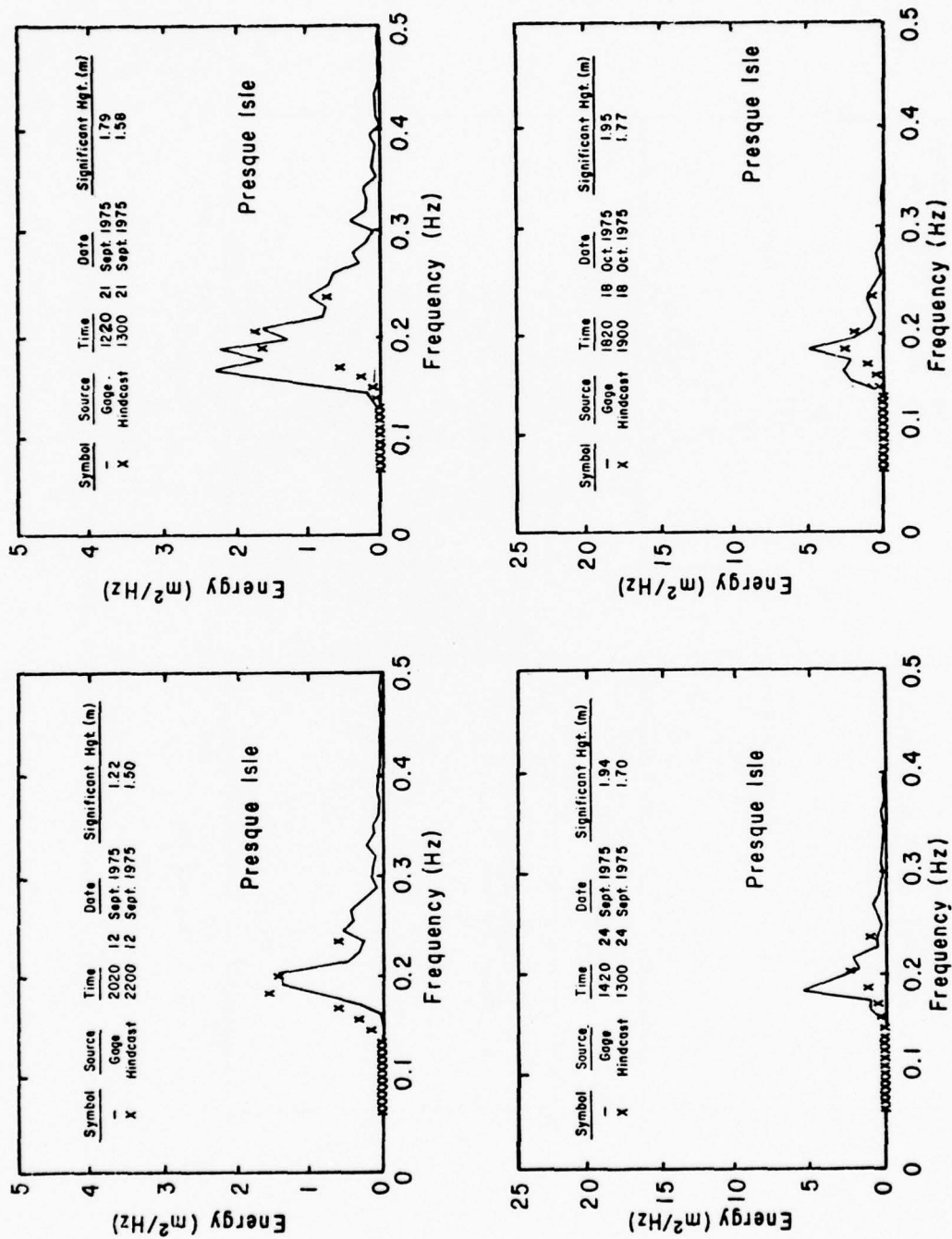


Figure 16. Comparisons of WES hindcast and gage spectra in Lake Erie.

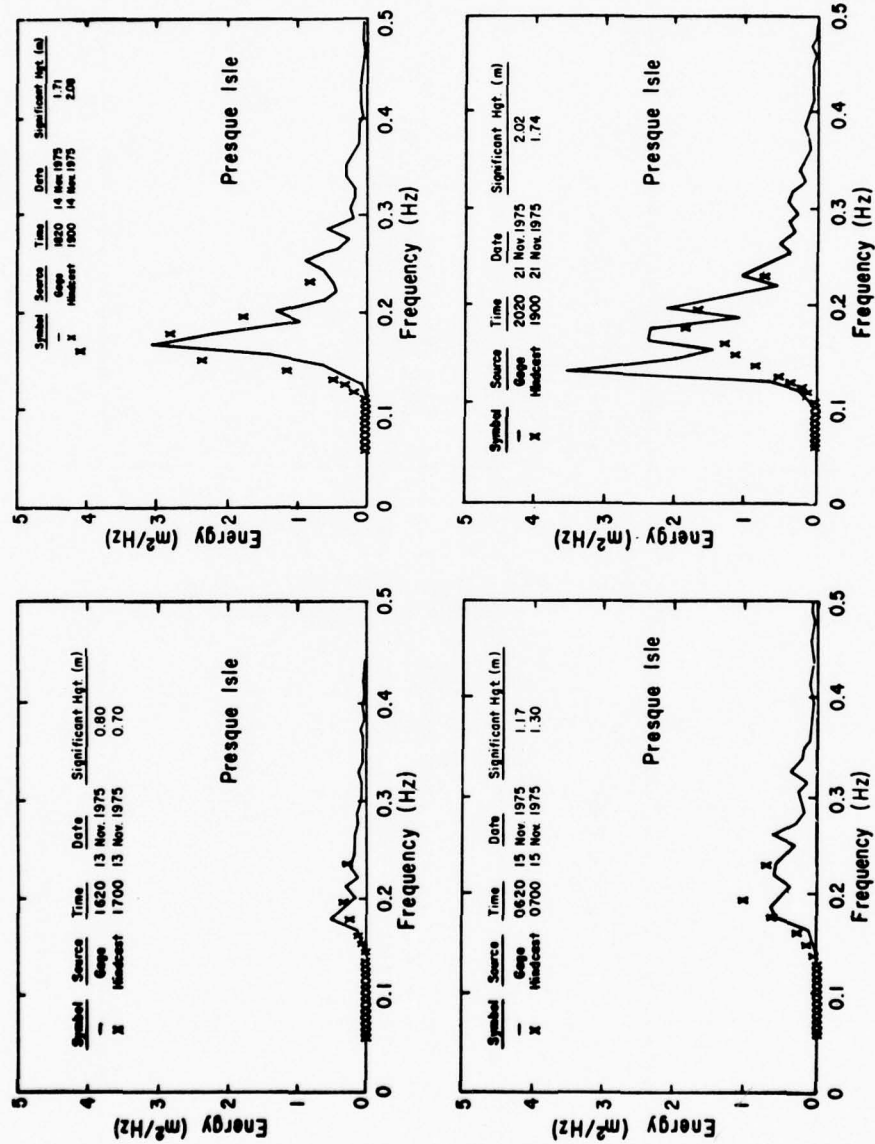


Figure 16. Comparisons of WES hindcast and gage spectra in Lake Erie.--Continued

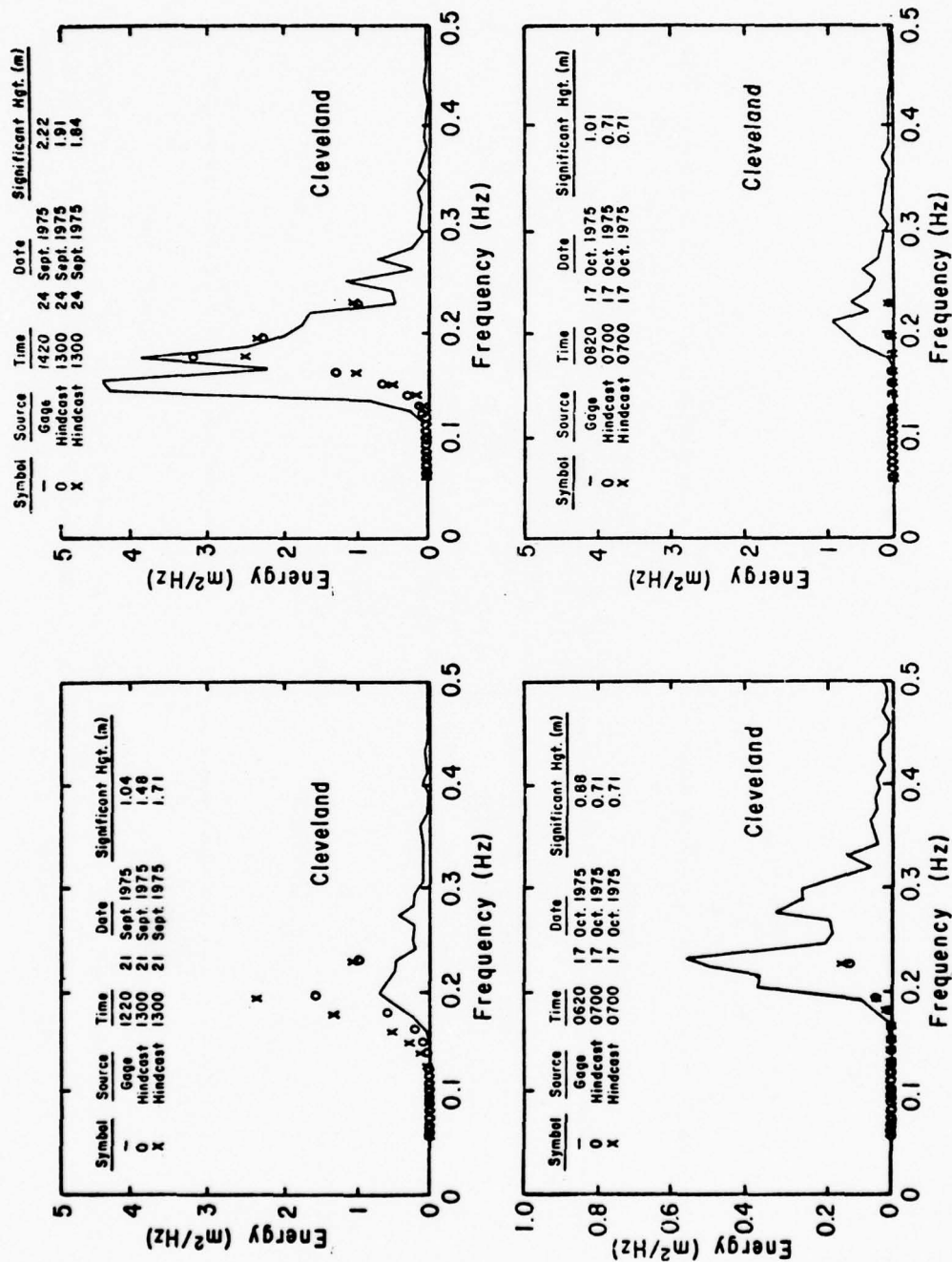


Figure 16. Comparisons of WES hindcast and gage spectra in Lake Erie. Hindcast spectra for two grid points bracketing the gage site are shown, with the x symbols designating spectra from the grid point closest to the gage site.--Continued

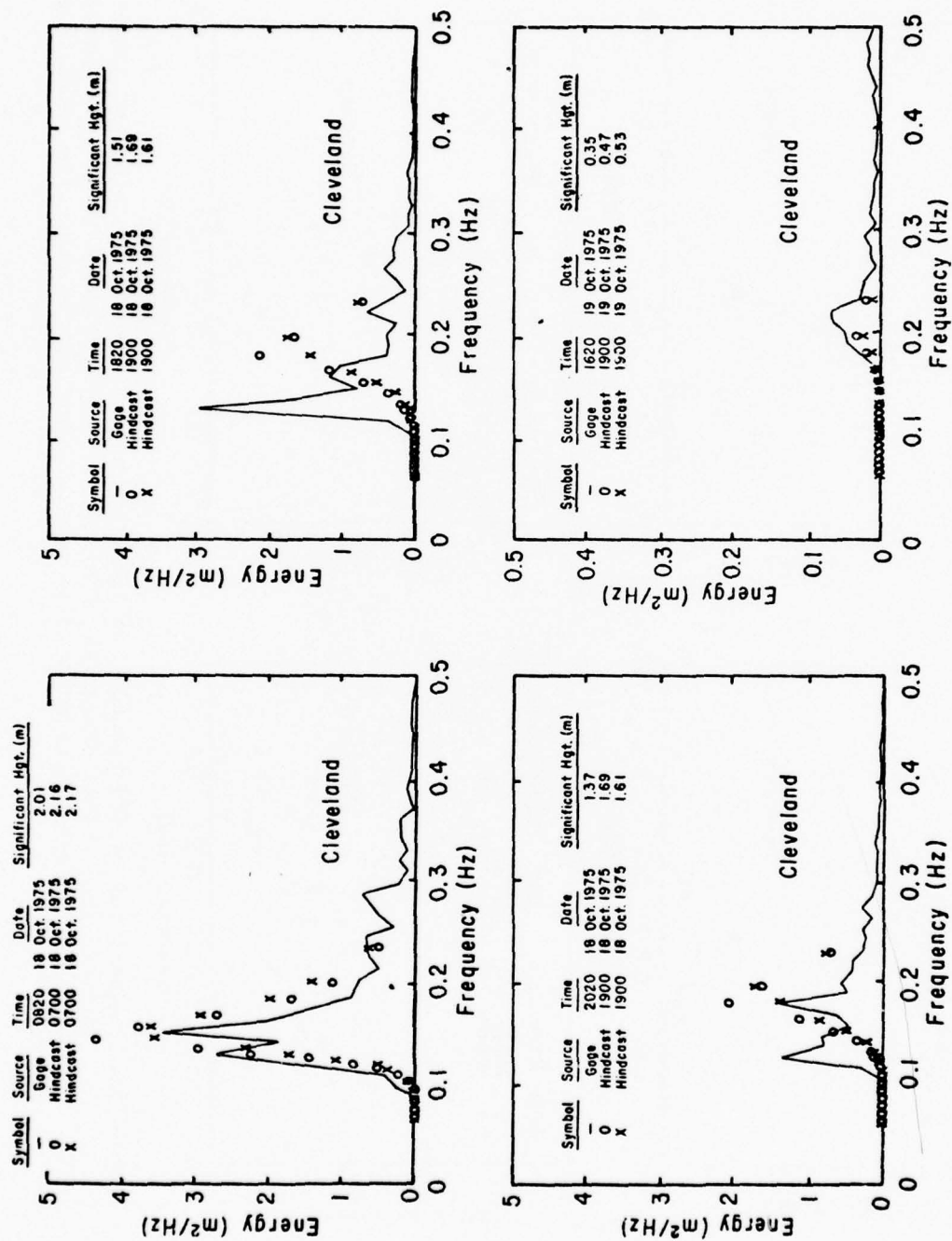


Figure 16. Comparisons of WES hindcast and gage spectra in Lake Erie. Hindcast spectra for two grid points bracketing the gage site are shown, with the x symbols designating spectra from the grid point closest to the gage site.--Continued

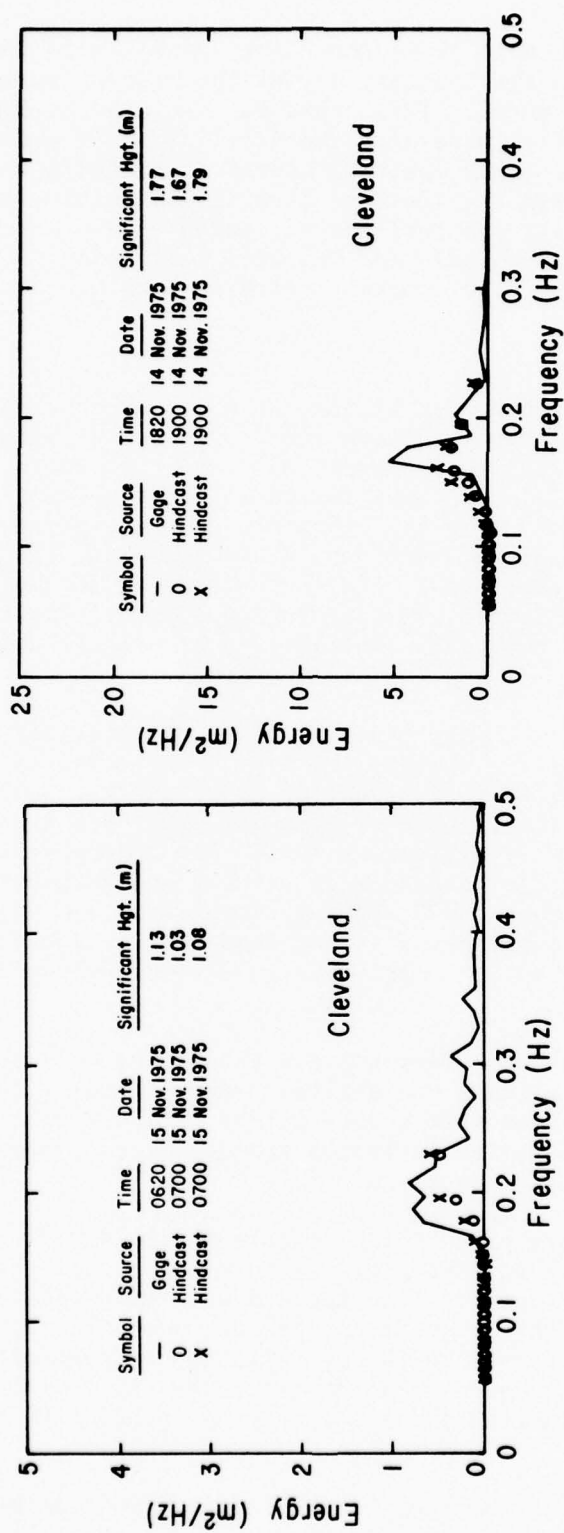


Figure 16. Comparisons of WES hindcast and gage spectra in Lake Erie. Hindcast spectra for two grid points bracketing the gage site are shown, with the x symbols designating spectra from the grid point closest to the gage site.--Continued

A third group of spectral plots represents cases where most of the gage spectrum is at high frequencies, beyond the high-frequency cutoff (0.23 hertz) of the WES model. These spectra, included in Appendix D, are probably most useful in assessing the skill of WES's empirical technique for estimating the total spectral energy at frequencies above 0.23 hertz. Comparing hindcast and measured significant heights for cases where the plotted hindcast spectral points indicate zero energy (e.g., 1900, 14 September at Cleveland), the WES empirical technique has no clear bias and appears to be accurate to within about 0.2 meter.

2. TDL Model.

The three parameters provided by the TDL wave forecasting model are significant wave height, significant period, and wind direction (which is assumed to coincide with wave direction). The parameters were provided at 6-hour intervals at special forecast points which coincide with Waverider buoy locations. Time-history plots of these parameters for the 0- and 6-hour forecasts at Michigan City, Cleveland, and Presque Isle during September to November 1975, and at South Haven and Holland during September to December 1976 are provided in Appendix E. The time-history plots include available buoy gage measurements of significant height and peak spectral period.

The plots in Appendix E show that the TDL model provides forecasts which are clearly useful for NWS applications. The model is generally effective in forecasting the occurrence of high and low, increasing and decreasing, wave conditions. However, the TDL model has a noticeable tendency to overestimate significant height. The tendency is especially evident for the data at Cleveland during October and November 1975, at Michigan City during October 1975, and at South Haven and Holland during November 1976. There is perhaps a slight tendency to underestimate significant height for the very highest wave conditions measured by the gage.

The TDL model appears to underestimate the longer wave periods and possibly tends to overestimate the shortest wave periods. In several storms, such as the Presque Isle and Cleveland data during 10 to 15 September 1975, the TDL period estimates are quite good, generally within 1 second of the gage estimate.

Detailed time-history plots for Lake Erie storms during fall 1975 are provided in Appendix B. The plots contain additional gage data and significant heights and periods from the WES wave hindcasting model as well as significant height, significant period, and direction from the TDL model. The WES hindcasts in the comparisons are generally closer than the TDL forecasts to gage data; however, the TDL estimates are surprisingly good considering the simplicity and predictive nature of the TDL model.

General tendencies are evident in the scatter plots of measured versus forecast significant height in Figure 17. A straight line

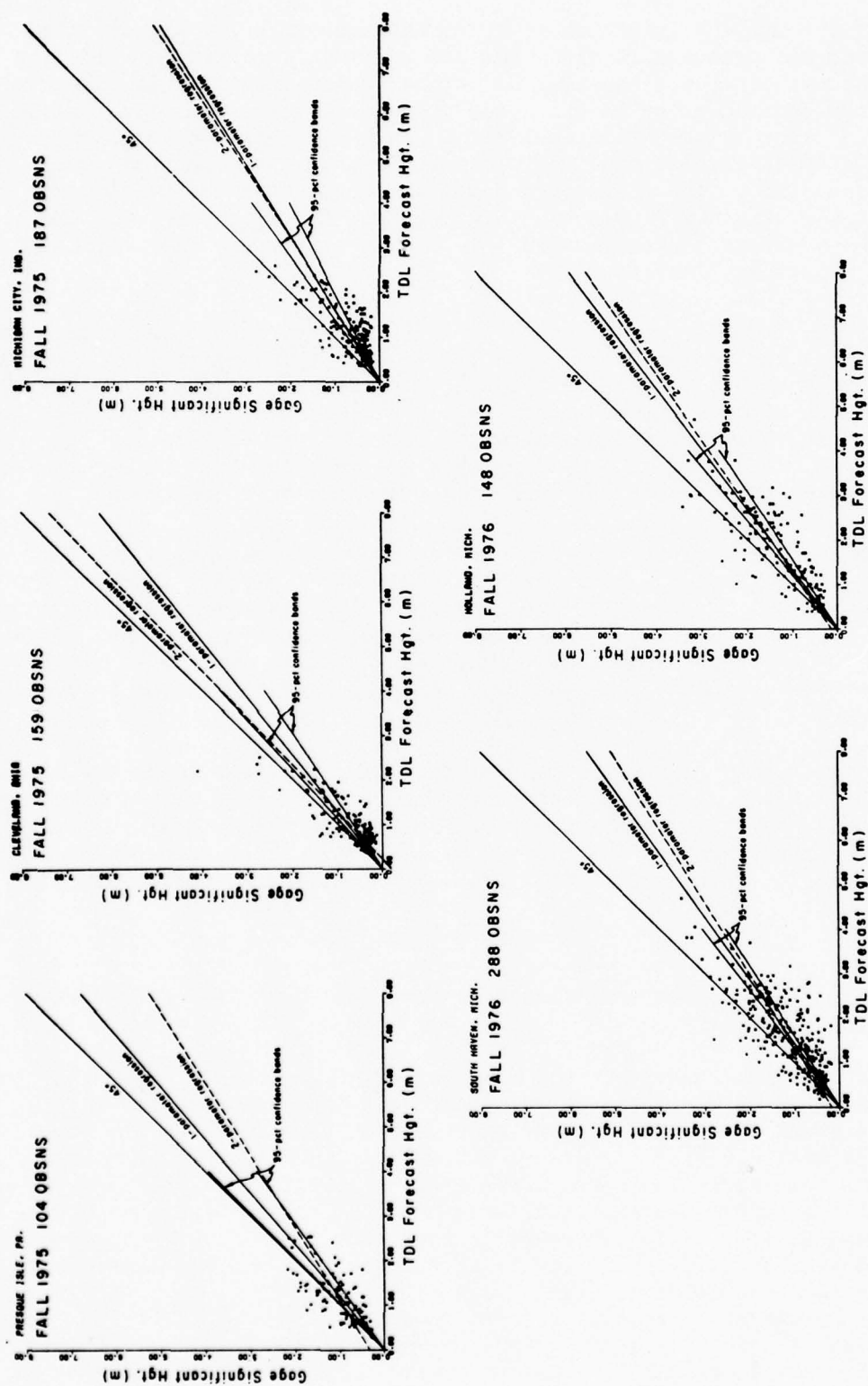


Figure 17. Scatter plots of measured versus TDL forecast significant heights in Lakes Erie and Michigan.

passing through the origin about which the squared error between forecasts and measurements is minimized (one-parameter regression line); a straight dashline, not constrained to pass through the origin, about which the squared error is minimized (two-parameter regression line); and a 45° line are shown in each plot. Each plot also includes bands showing the 95-percent confidence intervals around the one-parameter regression line. The confidence bands are straight lines passing through the origin with slopes differing from the slope, b , of the one-parameter regression line by \pm (standard error of b) \times (Student's t for 95-percent confidence).

The TDL forecast heights show a clear tendency to be higher than gage heights for gage heights less than 1 meter. The TDL heights are generally less than the gage heights for gage heights above 2 meters at Cleveland and Michigan City. This tendency is not evident at Presque Isle, possibly because there are no gage heights greater than 2.2 meters. The TDL heights at South Haven and Holland show a strong tendency to exceed the gage heights for the entire range of wave conditions represented.

The scatter is markedly less for the Cleveland data than for the other data. Cleveland generally has the shortest maximum fetch of the five locations. In general, the largest deviations from gage data (more than 1 meter in numerous cases) appear in the Lake Michigan data (Michigan City, South Haven, and Holland). The Lake Michigan sites have considerably longer maximum fetches than the Lake Erie sites (Presque Isle and Cleveland).

Correlations, regression parameters, means, and variances are summarized in Table 6. Correlations range from 0.66 to 0.79 with the Holland data having the highest correlation. Regression parameters are reasonably consistent between locations. By averaging the regression parameters, the following representative regression equation is obtained:

$$H_G = 0.74 H_{TDL} \quad (15)$$

where H_G is the gage significant height, and H_{TDL} the TDL forecast significant height.

For all five locations, the mean forecast height is greater than the mean measured height. The differences again indicate that the forecasts tend to overestimate significant wave height. The difference between means is smallest at Presque Isle (12 percent) and largest at Michigan City (66 percent). Variances of forecast significant heights are considerably greater than variances of gage significant heights at South Haven and Holland. The variances of forecasts are also slightly greater than the variances of measurements at Presque Isle and Michigan City. At Cleveland the forecast significant heights appear to be less variable than measurements; however, the difference in variances is at least partially due to one very high significant height (4 meters or 13 feet) measured in November 1975. The rms errors between forecasts and

Table 6. Comparison of measured and TDL forecast significant heights during 1975-76.

Location	Obsns. (No.)	Correlation	$H_G = B H_{TDL}$	Mean significant hgt. (m)		Variance of significant hgt. (m ²)		Rms error in significant hgt. (m)	
				TDL	Gage	TDL	Gage	Gage vs. forecast	Gage vs. corrected forecast
Presque Isle (fall 1975)	104	0.67	0.85	1.19	1.05	0.29	0.25	0.44	0.40
Cleveland (fall 1975)	159	0.77	0.78	0.99	0.73	0.23	0.35	0.46	0.39
Michigan City (fall 1975)	187	0.66	0.61	1.11	0.67	0.26	0.24	0.60	0.37
South Haven (fall 1976)	288	0.74	0.70	1.65	1.19	0.68	0.47	0.73	0.47
Holland (fall 1976)	148	0.79	0.74	1.82	1.37	0.77	0.57	0.71	0.47

H_G = significant height from Waverider buoy gage; H_{TDL} = significant height from TDL forecast.

measurements are larger at the Lake Michigan sites (0.6 to 0.7 meter or 2.0 to 2.3 feet) than at the Lake Erie sites (0.4 to 0.5 meter or 1.3 to 1.6 feet).

Figure 18 shows computed peak spectral period from gage records versus significant period forecast by TDL. Each plot includes a 45° line, a two-parameter regression line, and a one-parameter regression dashline. Each plot also includes bands showing the 95-percent confidence intervals around the two-parameter regression line. For each value along the x-axis (horizontal), the confidence bands differ from the two-parameter regression line by \pm (standard error of y predicted by two-parameter regression line) \times (Student's t for 95-percent confidence). The confidence bands are curved because there is uncertainty about both the slope and the intercept of the two-parameter regression line.

Although there is considerable scatter, the forecast periods show less variability than the gage periods, especially at Presque Isle, Cleveland, and Michigan City. The data from Presque Isle show a clear tendency for the forecast periods to be shorter than the measured periods. Data from the other locations do not clearly favor either long or short periods. Differences between forecasts and measurements are generally less than 2 seconds; however, differences of more than 2 seconds appear in all five plots. Several unusually long measured periods plotted for South Haven occurred during very low wave conditions and are probably of little practical interest in this study.

The correlation between forecast and gage periods ranges from 0.39 to 0.67 (Table 7). The highest correlation is for the Holland data. The lowest correlation is for the South Haven data although the few unusually long gage periods contribute heavily to the low correlation. Regression parameters in Table 7 indicate a curious consistency between Michigan City and Cleveland and between Presque Isle and Holland. A representative regression equation obtained by averaging the parameters from all sites except South Haven (which is distorted by a few long gage periods) is:

$$T_G = 1.25 + 0.77 T_{TDL}. \quad (16)$$

Mean forecast period estimates at Presque Isle are 0.75 second shorter than mean gage estimates (Table 7). At Cleveland, Holland, and South Haven the differences between means are less but still indicate shorter forecast periods in the mean. At Michigan City the mean forecast period is slightly greater than the mean gage period. The variance for forecast periods is less than for gage periods at all locations except Holland. The difference is over 50 percent at Cleveland and Michigan City. The variances show that TDL forecast periods are generally less variable than measured periods. Rms errors between forecasts and measurements ranged from about 1.0 to 1.6 seconds.

Plots of maximum significant wave height from gage versus TDL forecast and WES hindcast for each of the fall 1975 Lake Erie storms were

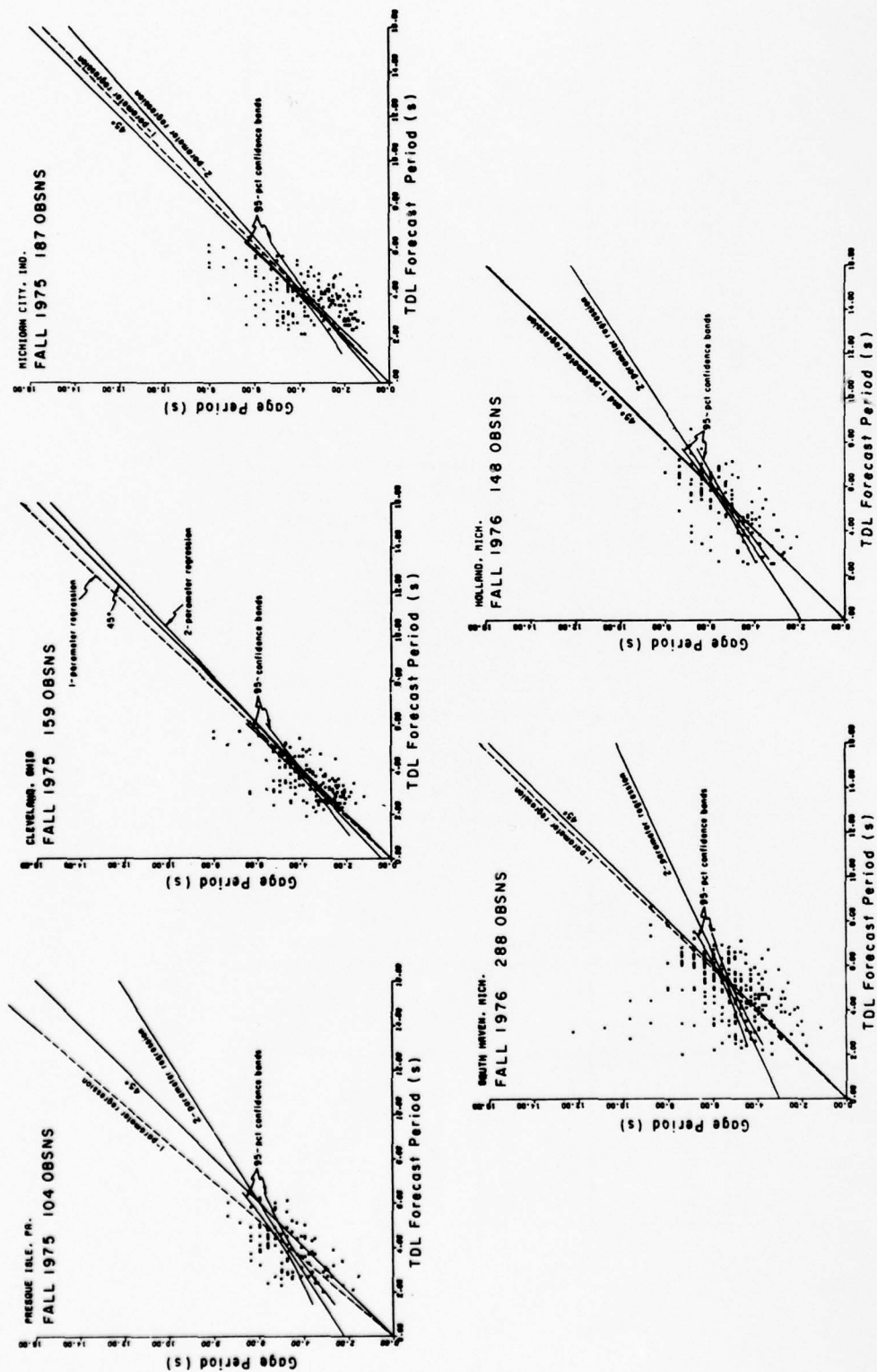


Figure 18. Scatter plots of measured versus TDL forecast peak spectral period in Lakes Erie and Michigan.

Table 7. Comparison of measured peak spectral periods and TDL forecast significant periods during 1975-76.

Location	Obsns. (No.)	Correlation	$T_G = A + B T_{TDL}$		Mean period (s)		Variance of period (s ²)		Rms error in period (s)	
			A (s)	B	TDL	Gage	TDL	Gage	Gage vs. forecast	Gage vs. corrected forecast
Presque Isle (fall 1975)	104	0.56	2.22	0.63	3.95	4.70	1.09	1.36	1.29	0.97
Cleveland (fall 1975)	159	0.66	0.43	0.94	3.55	3.75	0.91	1.84	1.05	1.03
Michigan City (fall 1975)	187	0.50	0.40	0.86	3.84	3.72	0.90	2.66	1.43	1.42
South Haven (fall 1976)	288	0.39	3.03	0.45	4.94	5.27	1.78	2.37	1.63	1.42
Holland (fall 1976)	148	0.67	1.96	0.64	5.20	5.31	1.84	1.69	1.08	0.96

¹ T_G = peak spectral period from Waverider buoy gage; T_{TDL} = significant period from TDL forecast.

presented in Figure 13. The TDL model has a clear tendency to estimate a lower maximum significant height than the WES model, although part of this apparent tendency may be due to the 6-hour interval between TDL estimates as compared to a 2-hour display interval between WES estimates. In comparison to measured maximum significant heights for the storms in which the gage data coverage was reasonably good, the TDL estimates at Cleveland are clearly inferior to the WES estimates. At Presque Isle, neither model produces estimates which are clearly superior.

The Summary of Synoptic Meteorological Observations (SSMO) (National Oceanic and Atmospheric Administration, 1975) provides shipboard observational data on the distribution of significant wave heights as a function of wind direction for the areas shown in Figure 19. These data can be compared to summaries of the TDL forecasts. Wave roses showing the distribution of significant heights in each of eight directions from both SSMO and forecast data are shown in Figure 20 for the Lake Erie sites and in Figure 21 for the Lake Michigan sites. The roses represent wave conditions during the fall months only. Spring and summer were omitted because wave conditions in the Great Lakes are generally more severe during the fall than during spring and summer. Winter was omitted because few ship observations are available during winter and because ice formation, which can significantly reduce fetch lengths, is not taken into account in the TDL model. The fall months actually summarized are September to November in Lake Erie and September to December in Lake Michigan. December was omitted from the Lake Erie summaries because the number of shipboard observations was significantly lower than in September, October, and November. In Lake Michigan, the number of observations in December was comparable to the number of observations in the other 3 months.

The distribution of significant wave heights in each direction compiled from TDL forecasts compares favorably with the SSMO height distribution (Figs. 20 and 21). The similarities are not surprising since TDL used shipboard observations in developing its forecasting equations. The TDL distributions show some systematic differences from the SSMO distributions which would be expected since the TDL forecast sites are nearshore while the centroid of the areas over which the shipboard observations have been summarized is relatively far from shore. The systematic differences are particularly evident in the Lake Michigan roses where waves from the east and southeast are noticeably lower in the forecasts than in the SSMO.

A comparison of the mean forecast significant height in each direction at each site with the corresponding mean significant height computed from the SSMO is given in Figure 22 for Lake Erie and in Figure 23 for Lake Michigan. The mean forecast heights tend to be lower than the mean shipboard observed heights for directions in which the fetch to the forecast site is shorter than the fetch to the centroid of the SSMO area. Conversely, the mean forecast heights tend to be higher for directions in which the forecasting fetch is longer than the fetch to the centroid

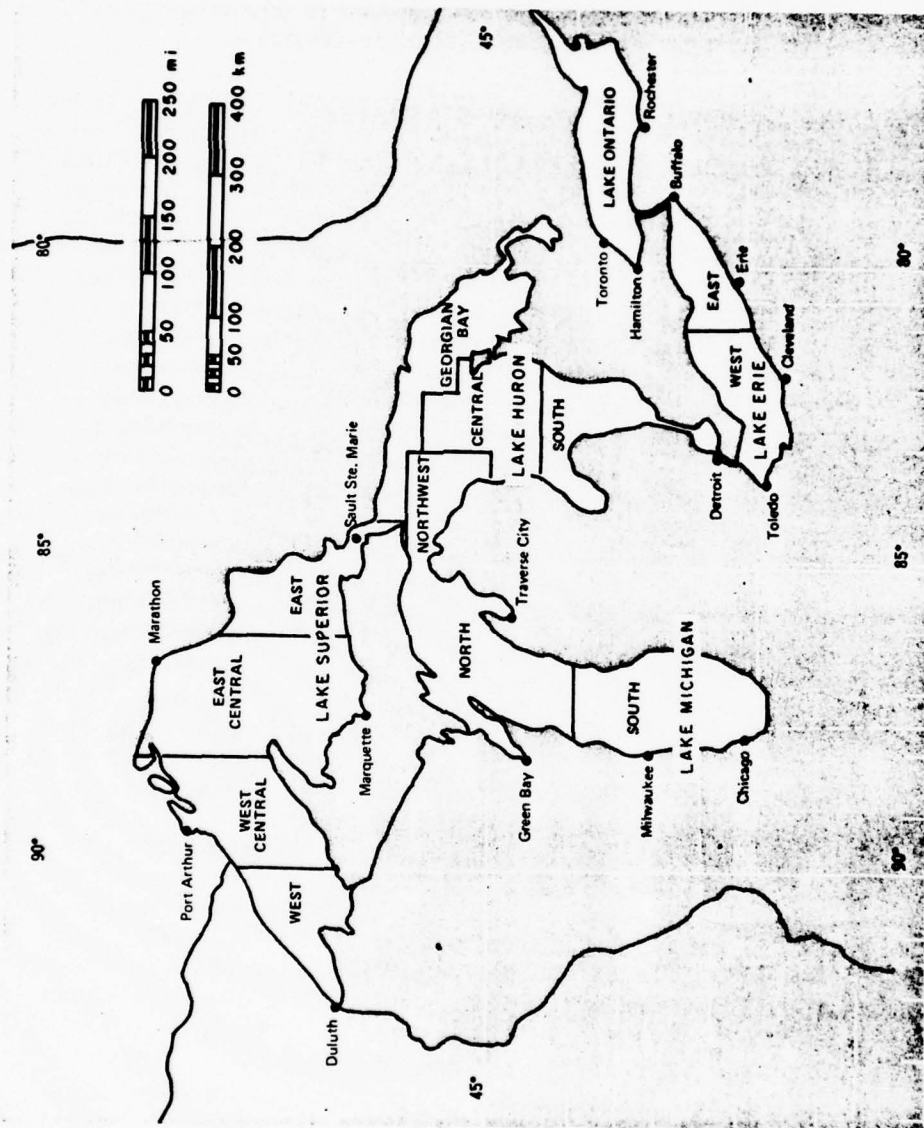


Figure 19. Thirteen major Great Lakes areas for which shipboard observational data have been published in the SSMO (Summary of Synoptic Meteorological Observations) (from National Oceanic and Atmospheric Administration, 1975).

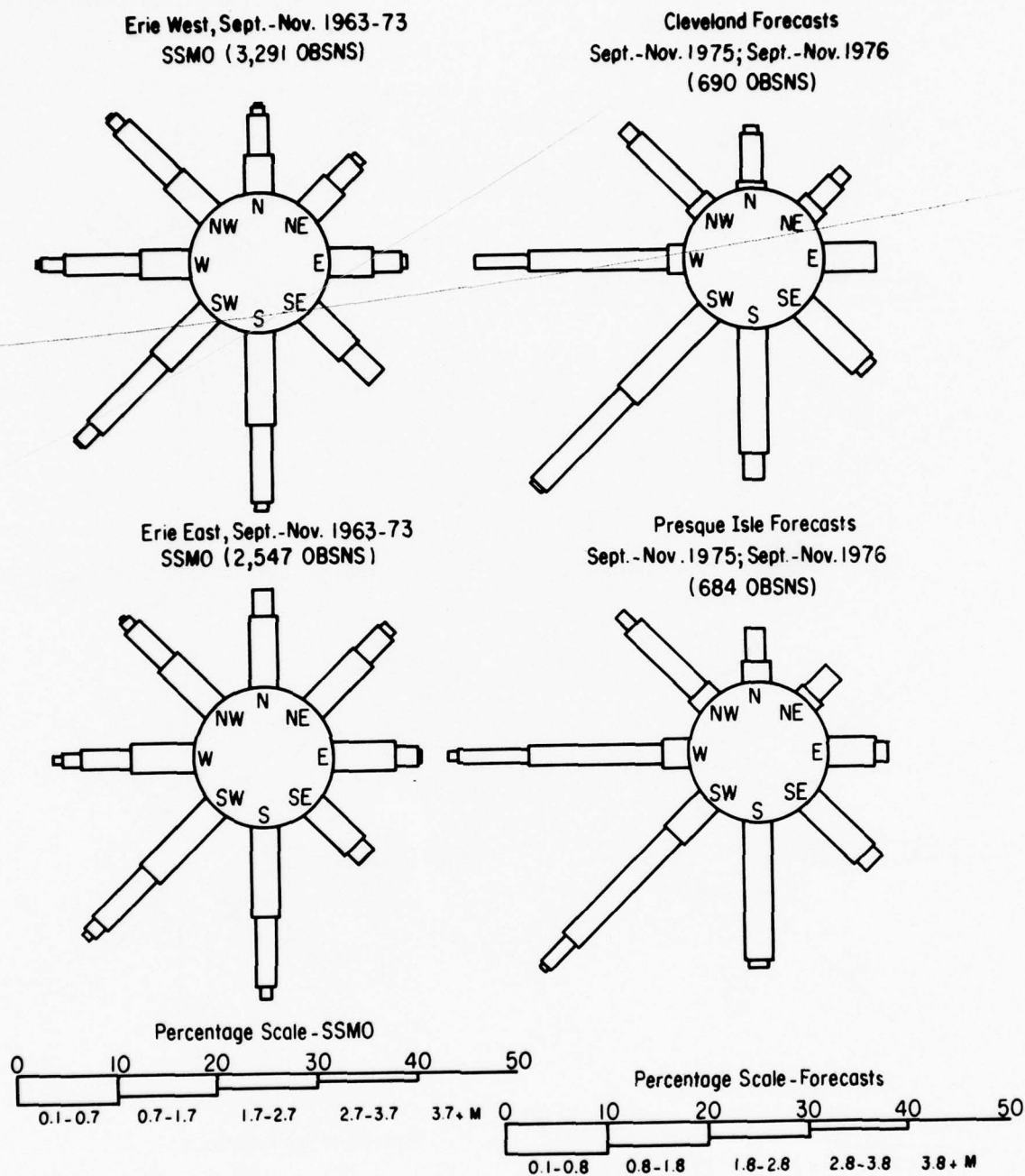
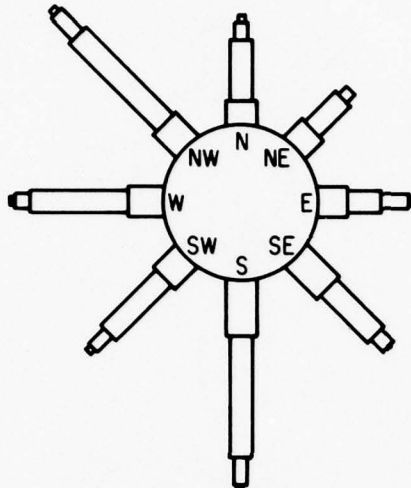
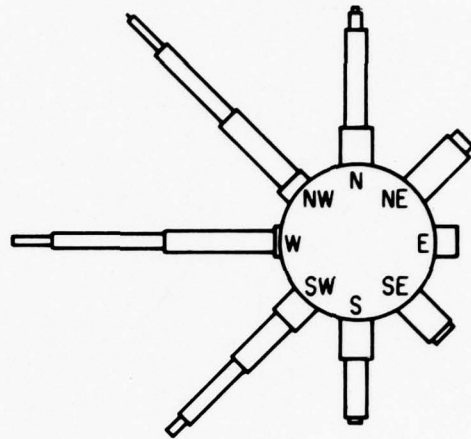


Figure 20. Wave roses showing the distribution of TDL forecast significant height versus forecast wind direction and SSMO shipboard observed significant height versus observed wind direction at Lake Erie sites.

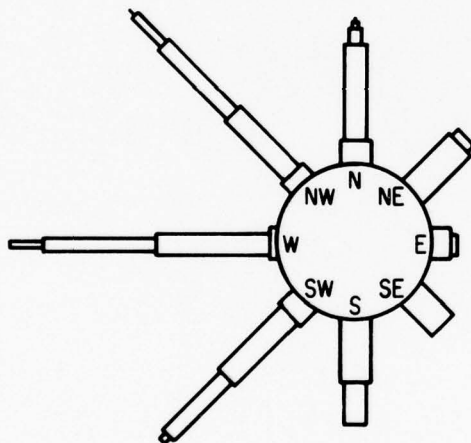
Michigan South, Sept.-Dec. 1963-73
SSMO (4,587 OBSNS)



Holland Forecasts, Sept.-Dec. 1976
(460 OBSNS)



South Haven Forecasts, Sept.-Dec. 1976
(471 OBSNS)



Michigan City Forecasts, Sept.-Dec. 1976
(933 OBSNS)

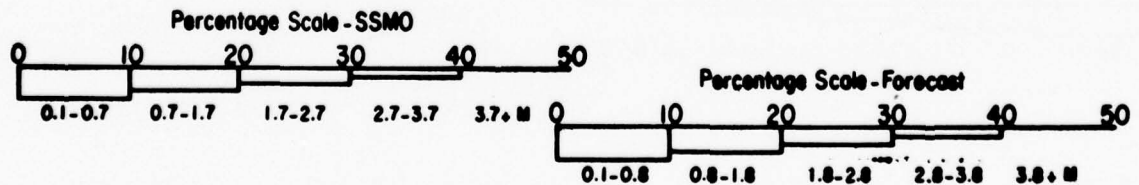
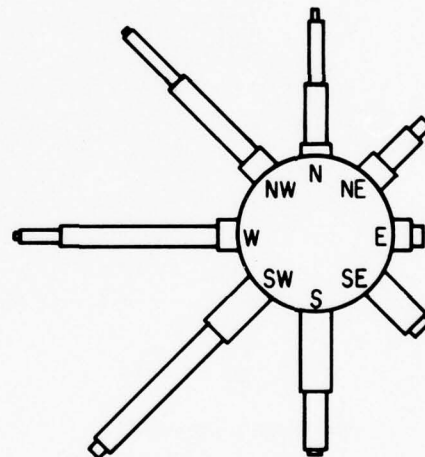


Figure 21. Wave roses showing the distribution of TDL forecast significant height versus forecast wind direction and SSMO shipboard observed significant height versus observed wind direction at Lake Michigan sites.

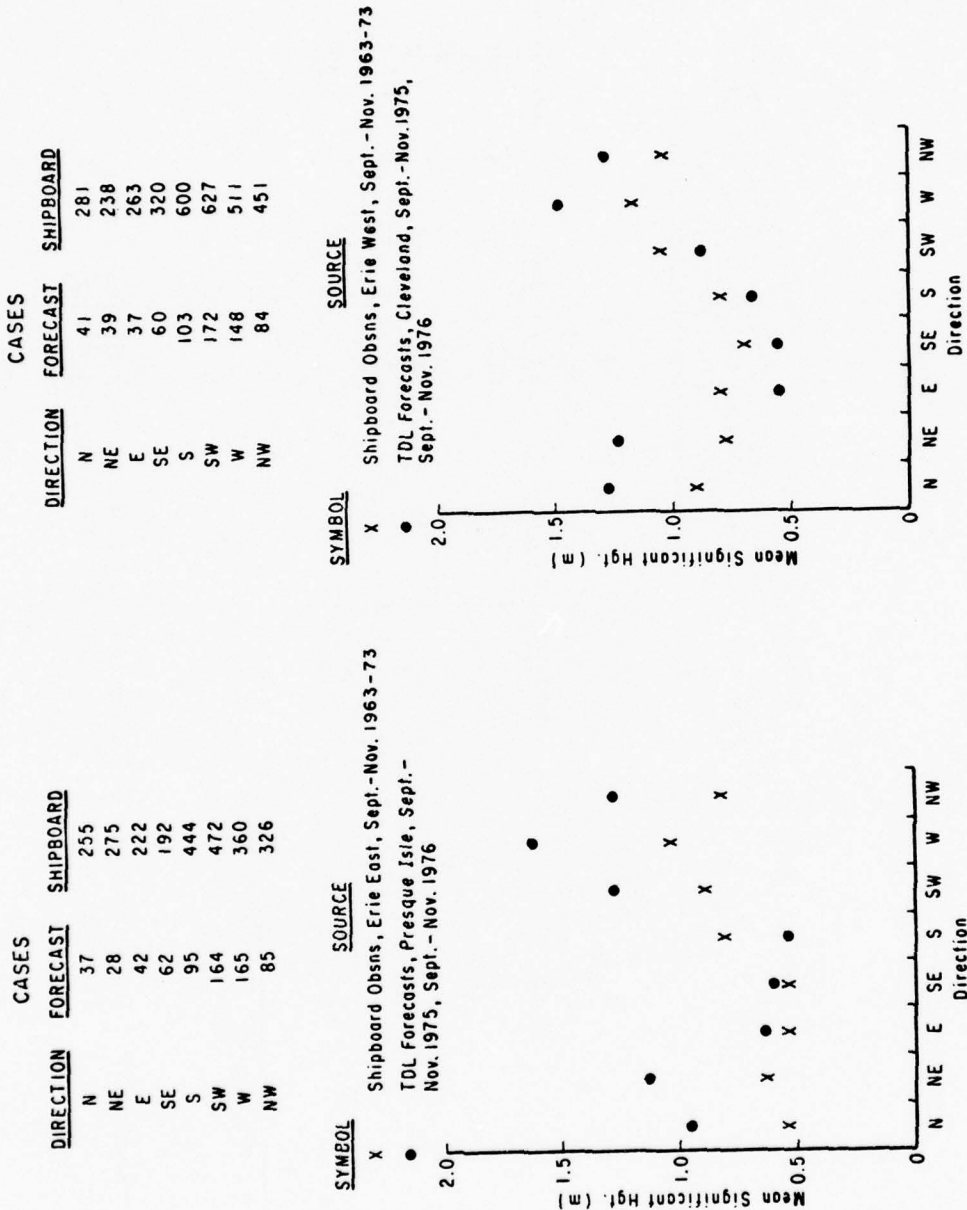


Figure 22. Comparison of TDL forecast and SSMO mean significant height as a function of wind direction at Lake Erie sites.

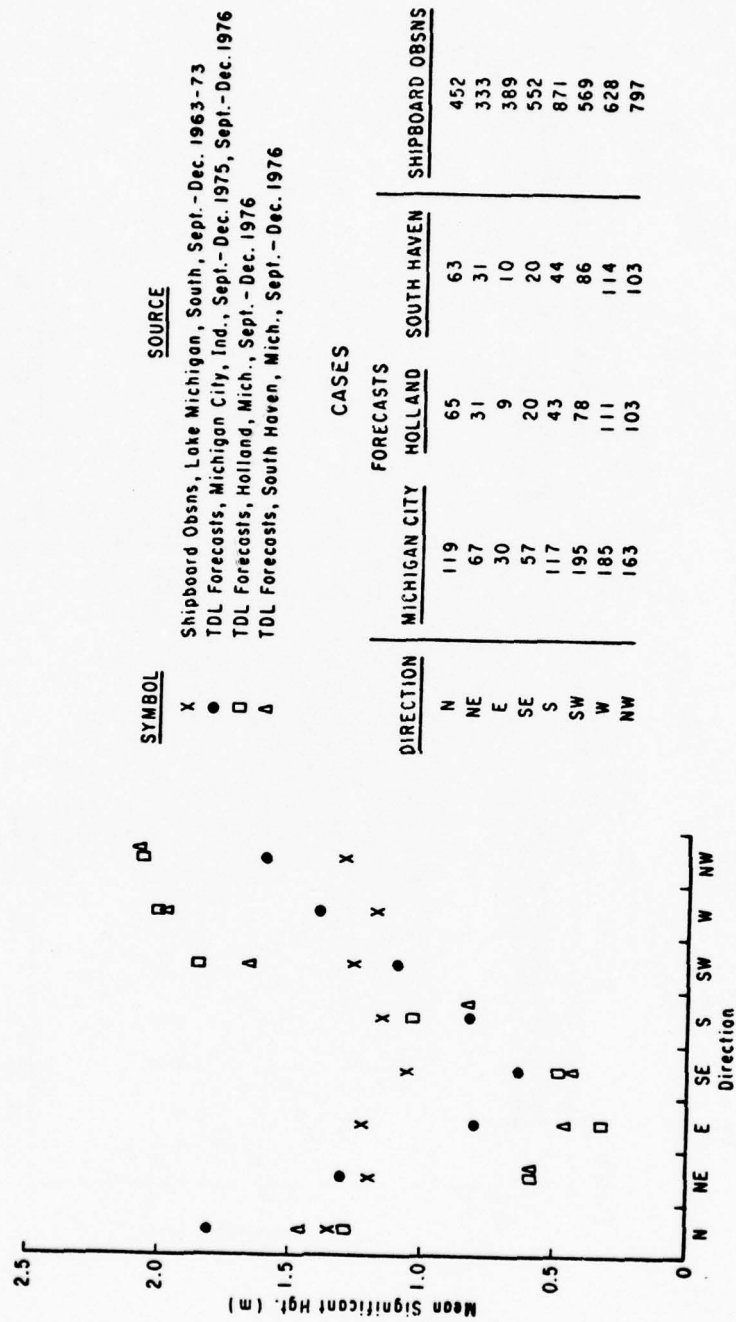


Figure 23. Comparison of TDL forecast and SSMO mean significant height as a function of wind direction at Lake Michigan sites.

of the SSMO area. The consistent explainable differences between TDL forecasts and shipboard observations indicate a measure of skill in the TDL forecasts.

Overall distributions of significant height from gage, TDL forecast, and SSMO are plotted in Figure 24. The TDL curves fall above the gage curves, indicating higher waves, in every case except for the lowest 80 percent of the significant heights at Presque Isle and the highest 3 percent of the significant heights at Cleveland. The TDL curve is higher than the SSMO curve at Presque Isle, South Haven, and Holland, and virtually identical to the SSMO curve for the lower 90 percent of the significant heights at Cleveland and Michigan City. The TDL curves at all sites show a small tendency to be lower relative to the SSMO curves for high significant heights than for low significant heights.

Overall distributions of significant wave period from gage and TDL forecast are plotted as histograms (Fig. 25). In most cases the TDL distributions indicate a shortage of periods in the ends of the distribution (periods shorter than 2 seconds and longer than 7 seconds). The highest peak of the distribution of TDL periods falls in an interval adjacent to the interval in which the gage periods are most concentrated in every case except at Presque Isle. At Presque Isle, the TDL periods show a general tendency to be shorter than gage periods. At the other sites there is no clear bias.

VI. DISCUSSION AND EVALUATION BASED ON MODEL-GAGE DATA COMPARISONS

1. WES Model.

a. Winds. A qualitative discussion of similarities and differences between the true wind fields over Lake Erie and the wind fields estimated by the WES model is presented in this section. How wave estimates from the WES model are affected by ambiguities in the fetch and by schemes for wave generation and propagation is also discussed.

Most of the storms considered in this evaluation study were associated with the passage of weather fronts over the lakes. Because of the poor areal coverage of wind data used as input to the WES model and finite temporal resolution, the sudden changes in windspeed and direction associated with fronts cannot be represented in detail. Storms associated with fronts aligned parallel to the long axis of Lake Erie are particularly difficult to represent properly.

For example, consider the half-meter increase in significant height at both Cleveland and Presque Isle near midnight on 11 September. The Daily Weather Maps published by NOAA indicated a cold front was passing over Lake Erie moving toward the southeast at about that time. The front was aligned nearly parallel with the long axis of the lake. Thus, wind stations along the U.S. shore of the lake would not be expected to register the abrupt wind shifts associated with the front until the front had actually passed over the lake. As shown in Appendix B, the hindcasts

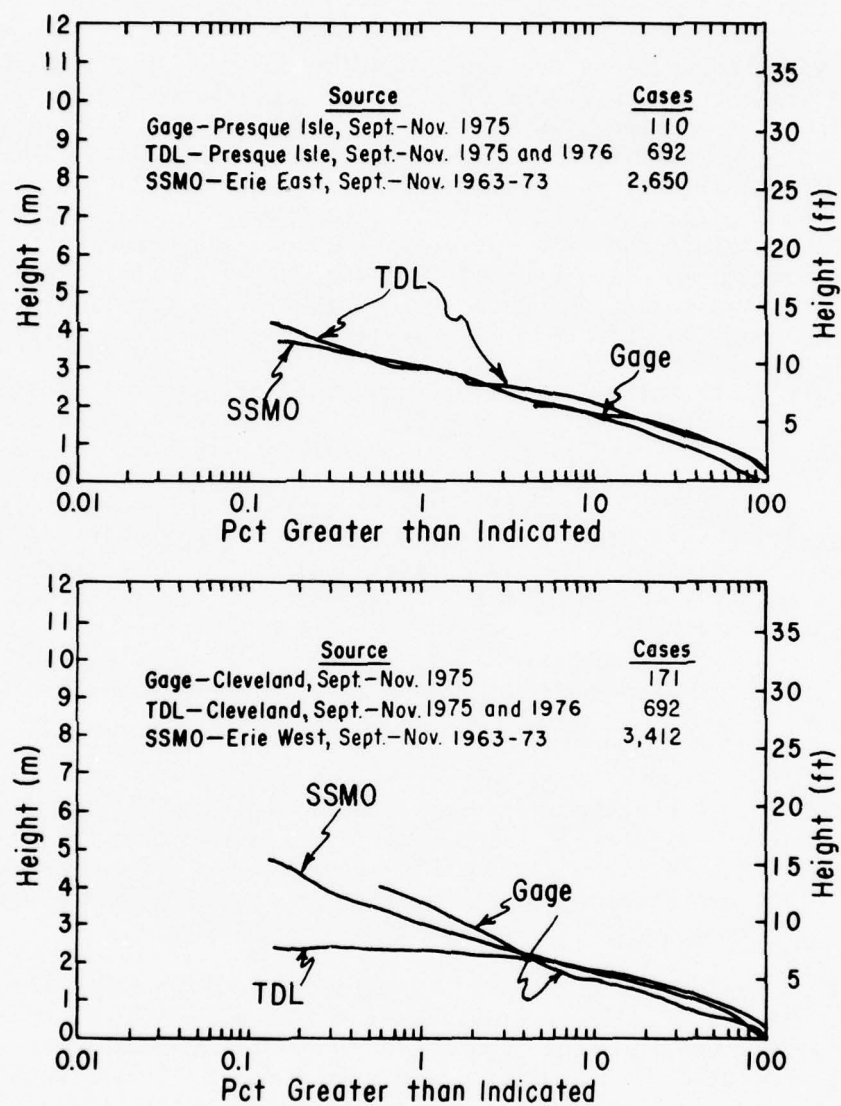


Figure 24. Overall distributions of measured, TDL forecast, and SSMO shipboard observed significant height.

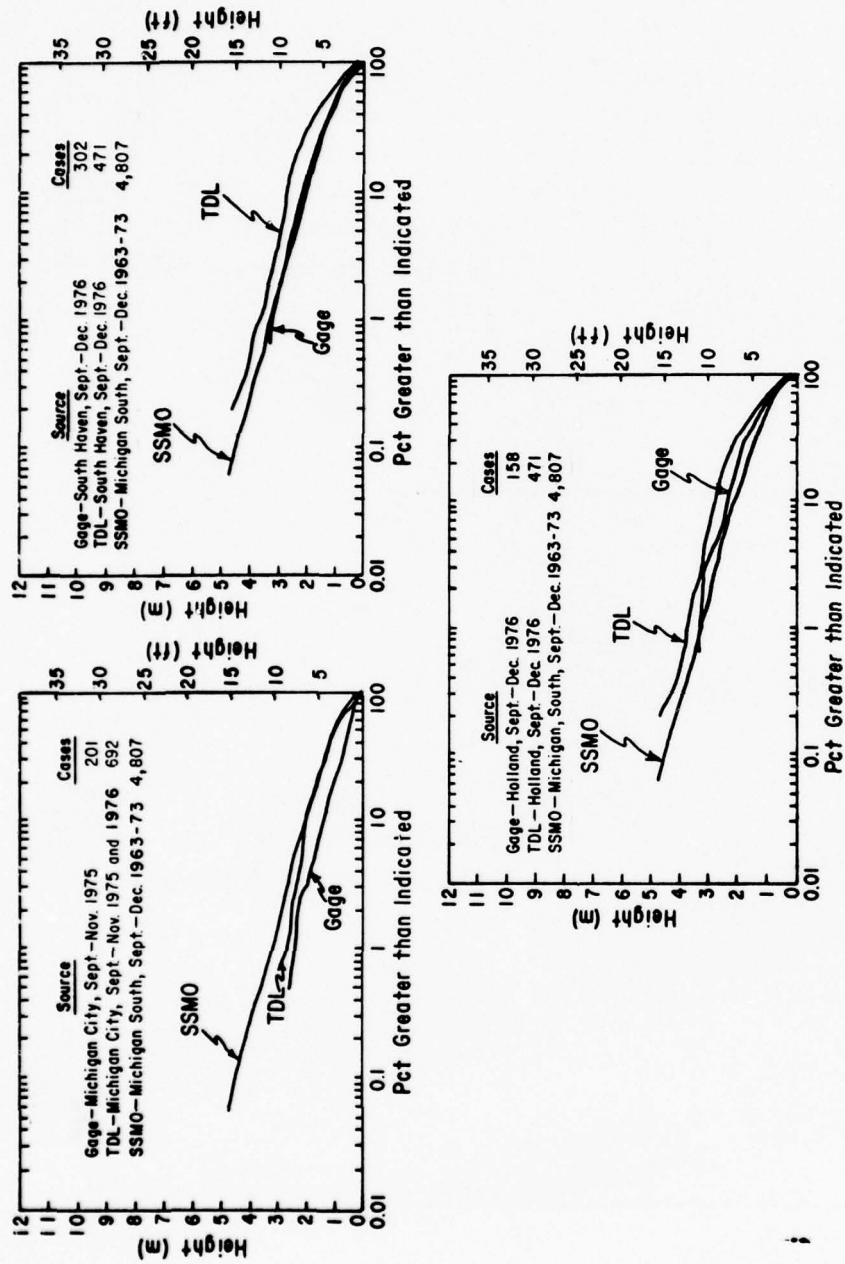
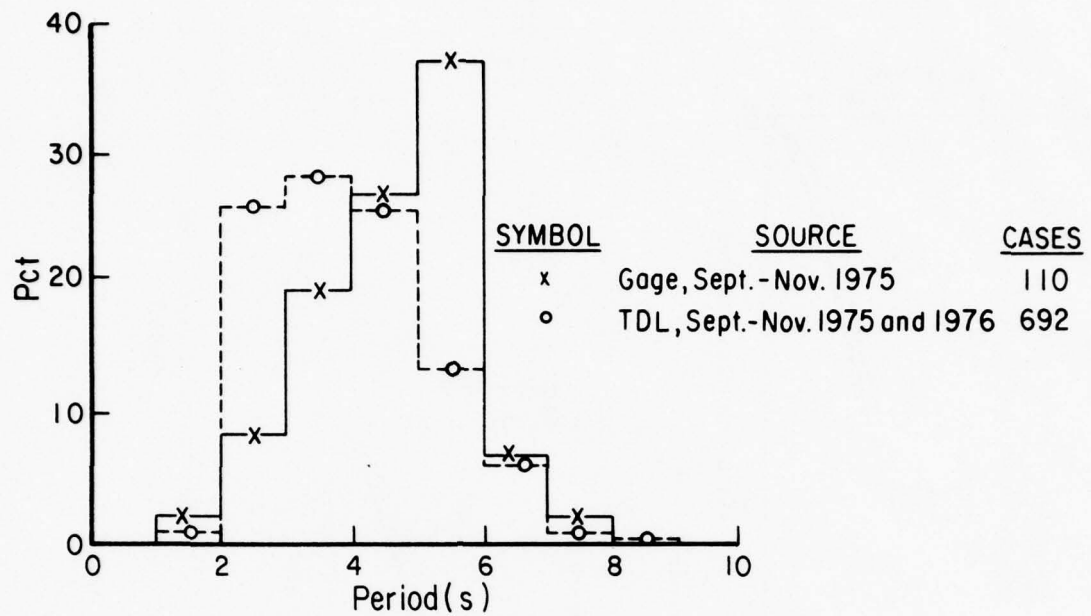


Figure 24. Overall distributions of measured, TDL forecast, and SSMO shipboard observed significant height.--Continued

Presque Isle



Cleveland

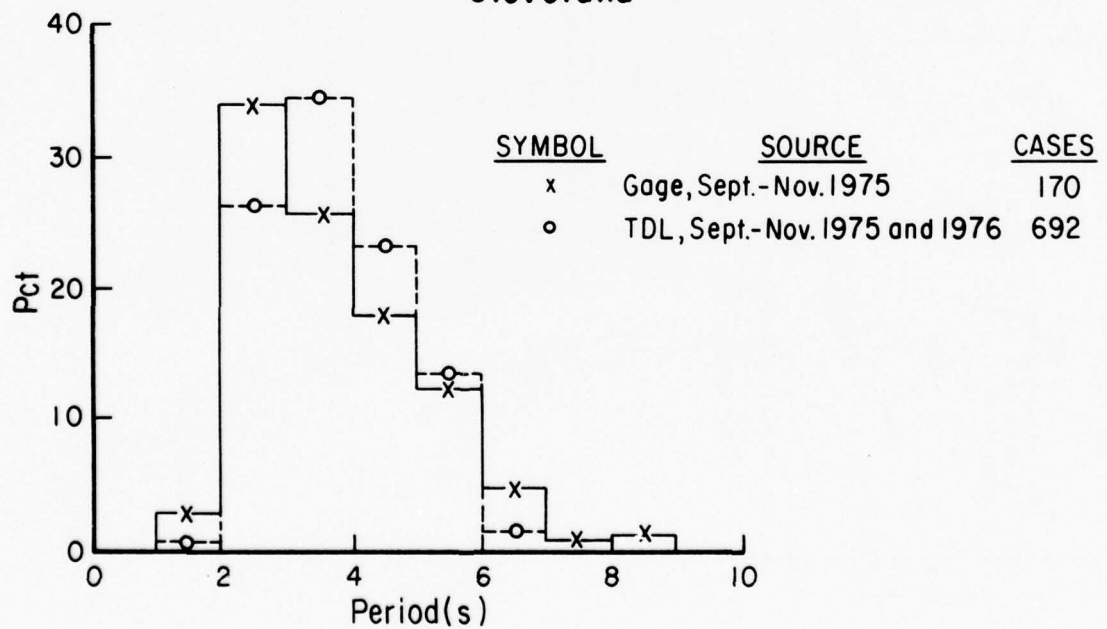


Figure 25. Overall distributions of measured peak spectral period and TDL forecast significant period.

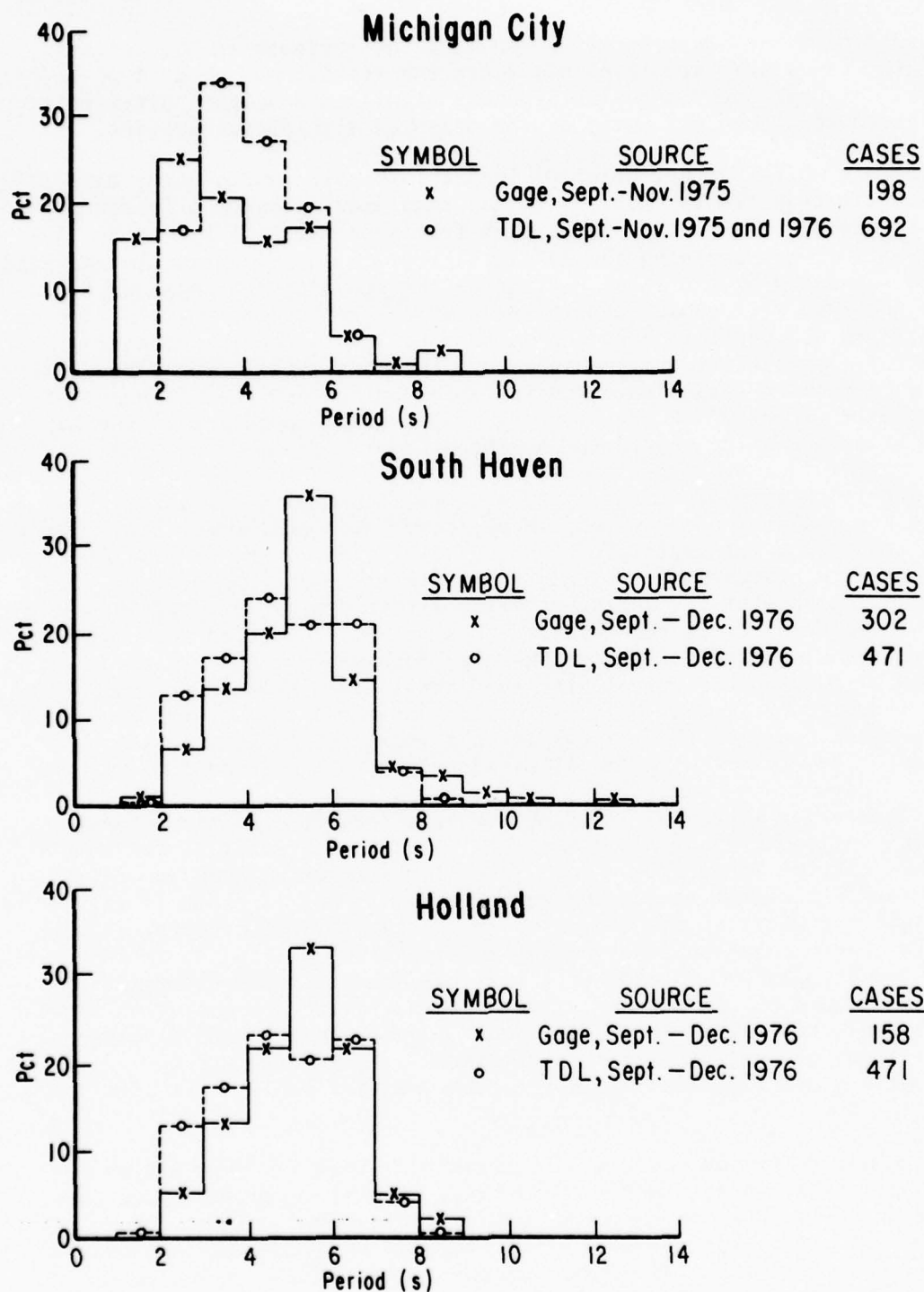


Figure 25. Overall distributions of measured peak spectral period and TDL forecast significant period.--Continued

lagged behind the measurements in showing the increase in significant heights, especially at Cleveland, where the timelag was about 4 to 6 hours. At both locations, the hindcast significant heights ultimately increased to within 0.2 meter of the measured significant heights.

Fronts which are not parallel to the lake axis (which occur more frequently than fronts parallel to the lake axis) present a lesser problem to the WES hindcasting model than fronts parallel to the axis. However, all fronts crossing the lake give rise to uncertainties in the wind field generated by the model. Although the presence of a weather front over the lake will cause deterioration of the results of any hindcasting model, the WES model is expected to be superior to the TDL model in treating fronts aligned perpendicular to the long axis of the lake. The TDL model, which uses wind estimates observed in the lake, is expected to be more effective at identifying a front aligned parallel to the long lake axis and moving toward the southeast.

The importance of representing weather fronts properly is expected to be diminished when only very large storms are considered; i.e., storms with recurrence intervals of 1 year or more. The 13 and 14 November storm, which generated the highest significant height measured in Lake Erie during this study, and to a lesser extent the 17, 18, and 19 October storm, are examples of the type of storm which is expected to be responsible for climatological extreme waves. Both storms involved circulation around a low-pressure system with no frontal passage over the lake. The WES hindcast significant heights for both of these storms were generally better than for the other storms in this study. This is precisely the type of storm that the WES model was designed to handle best.

Any weather situation in which the windspeed or direction changes significantly over short distances will present difficulties for both the WES and the TDL models. Such situations can occur even in well-organized storms not associated with weather fronts if there is significant curvature of the isobars over the lake. If the curvature were sufficient to cause a difference of more than 90° in wind direction measured at adjacent anemometer sites, the WES windspeed estimates in the lake would be computed by a vectorial averaging process which tends to produce underestimates of windspeed. Even when the wind directions at adjacent anemometer sites are within 90° , they still may not represent wind directions far out in the lake when the isobars are highly curved.

Another situation where a well-organized storm can give misleading hindcasts is a storm in which the isobars significantly spread or converge over distances on the order of available fetch lengths. For such storms the windspeeds measured along one side of a lake may not provide satisfactory estimates of windspeeds out in the lake.

Inaccuracies in the hindcast windfield over Lakes Erie and Ontario due to curvature and spreading of the isobars are expected to be very small during major storms. However, these inaccuracies may be a concern

during major storms in a large lake such as Lake Superior. A recent detailed study of wind-driven circulations in Lake Michigan found that wind fields over the lake are sufficiently inhomogeneous for the computed wind field to be quite sensitive to the interpolation techniques used (Allender, 1977). The circulation study also found that an interpolation technique which preserves spatial gradients yet avoids over-smoothing is preferable to a simple weighted averaging technique. The study did not consider an unweighted averaging technique of the type used in the WES model.

b. Waves. In a discussion of how wave estimates from the WES model are affected by the schemes for wave generation and propagation, it is useful to distinguish between a wind blowing predominantly perpendicular to shore (onshore or offshore) and a wind blowing predominantly parallel to shore. During shore-perpendicular winds, the fetch is usually reasonably well defined. During shore-parallel winds the fetch is often ambiguous and highly sensitive to the precise wind direction. Shore-perpendicular winds which have been reasonably constant for about 6 hours or longer provide a good basis for discussing the wave-generation schemes in the WES model. Onshore winds are generally more instructive than offshore winds because they are associated with longer fetches and higher waves.

Spectra representing simple wave generation situations in response to onshore winds extracted from Figure 16 and Appendix C are compared in Figure 26. In all cases the hindcast spectra are very good approximations to the gage spectra. There is a hint that the hindcast spectra tend to contain slightly more energy than the gage spectra and hence, lead to slightly higher estimates of significant wave height. For the simple case of onshore winds, the WES model appears to have a tendency for slight overestimates of the width of the spectral peak. Spectral comparisons by WES show similar differences between measurements and hindcasts. The single comparison in Resio and Vincent (1976a) shows a hindcast spectrum in Lake Erie which is in good agreement with the measured spectrum except that the width of the hindcast spectral peak is clearly greater than the width of the spectral peak from measurements (Fig. 27). The single comparison in Resio and Vincent (1976d) for Lake Michigan shows, to a lesser extent, a similar tendency (Fig. 28).

This tendency is not too surprising since the wave-generation schemes used in the WES model were developed mainly for ocean situations. There is strong evidence (Liu, 1976) that fetch-limited developing spectra in the Great Lakes tend to have narrower and lower peaks than some more widely accepted spectral forms such as the JONSWAP (Hasselmann, et al., 1973) and Mitsuyasu (1971) spectra, both of which are similar to spectral shapes produced by the WES model. As would be expected from Liu's study, the spectra in this study computed from Great Lakes gage data tend to have narrower and perhaps lower peaks than spectra hindcast by the WES model.

Liu (1976) also indicated that the JONSWAP and Mitsuyasu formulas are appropriate in the Great Lakes for the special case of fully developed

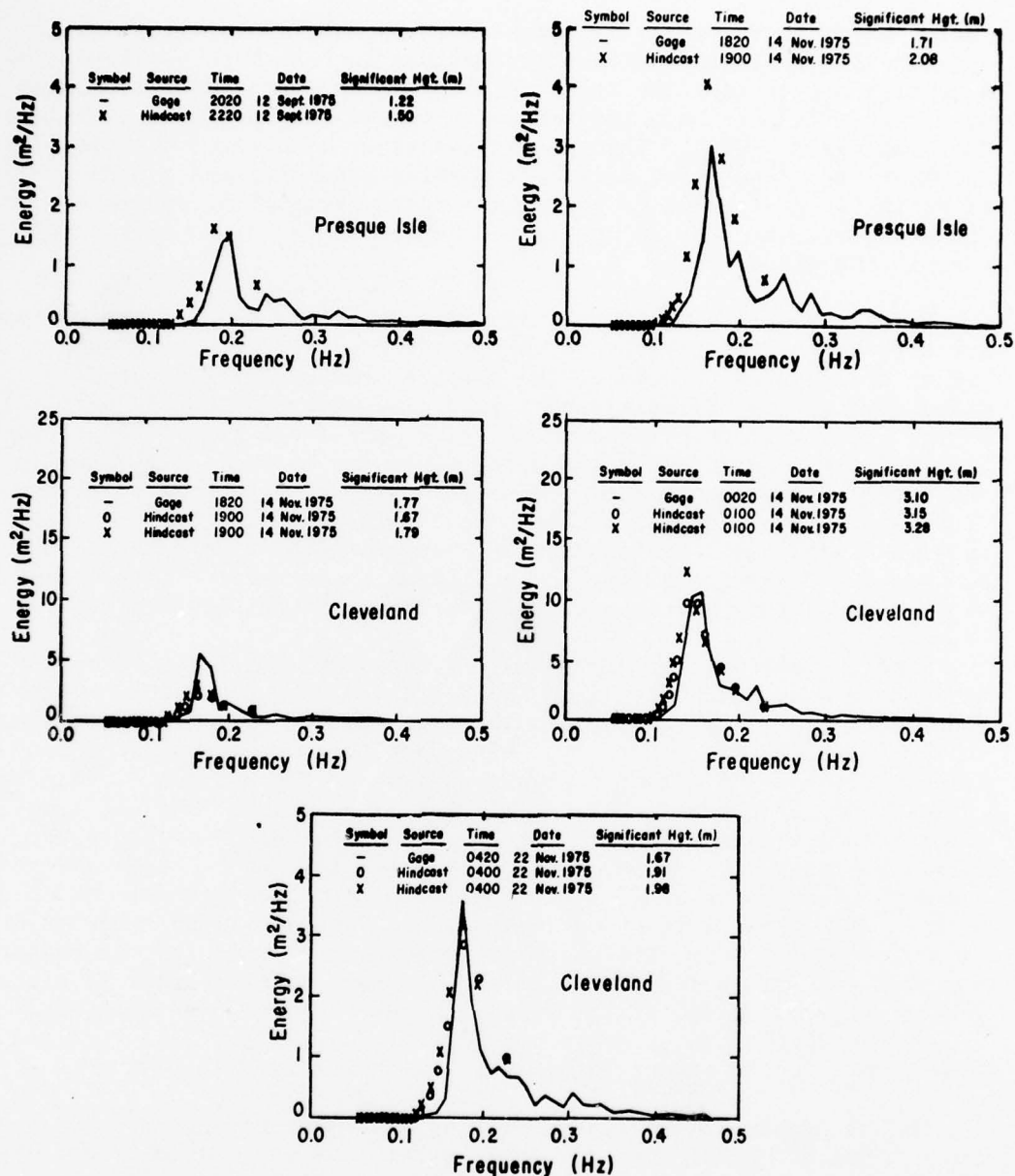


Figure 26. Comparisons of WES hindcast and gage spectra in Lake Erie for situations in which the wind was approximately perpendicular to shore and fetches are well defined.

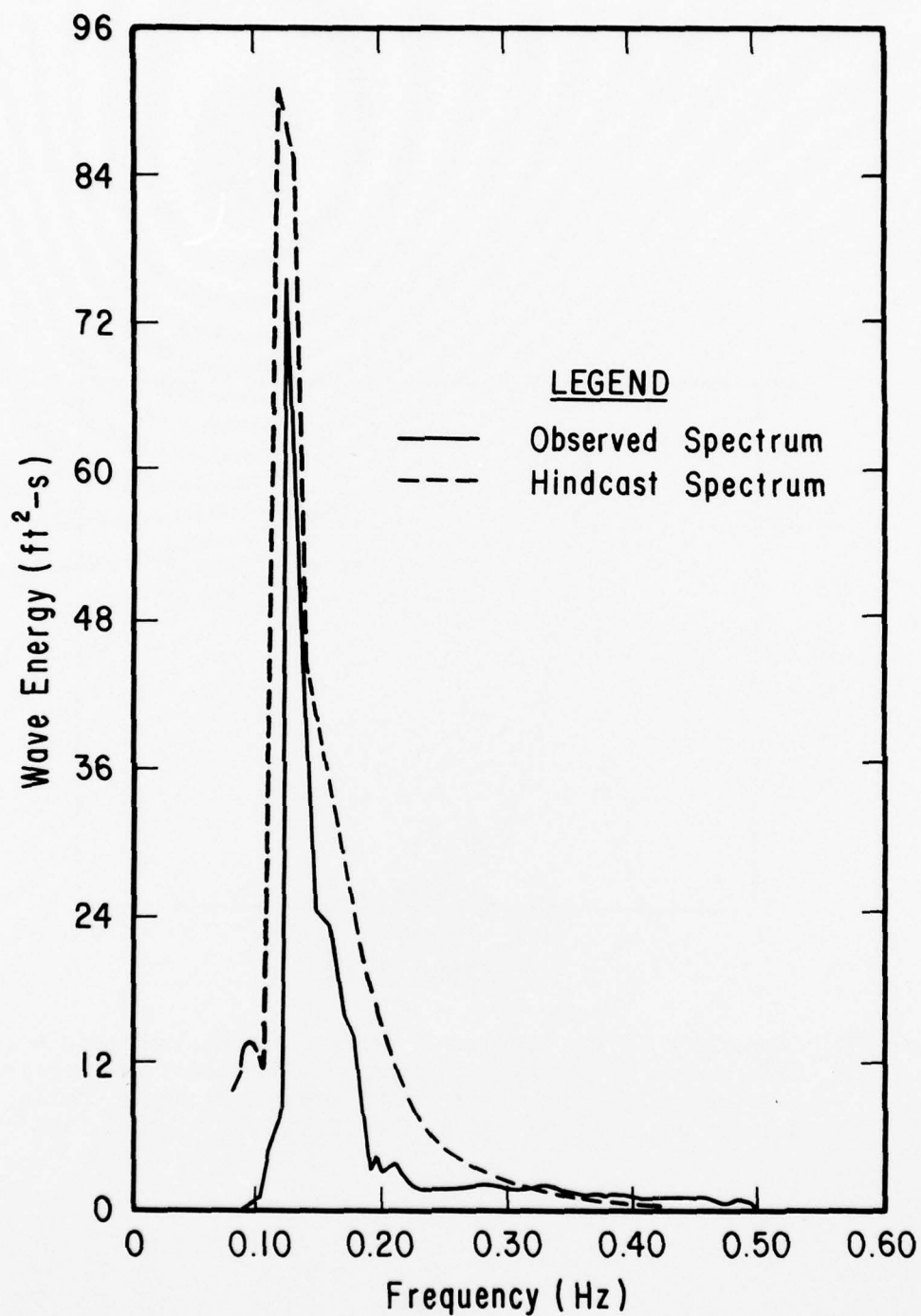


Figure 27. Comparison of WES hindcast spectrum and spectrum obtained from a Canadian Waverider buoy record taken near Point Pelee, Lake Erie, during a storm on 7 April 1973 (from Resio and Vincent, 1976a).

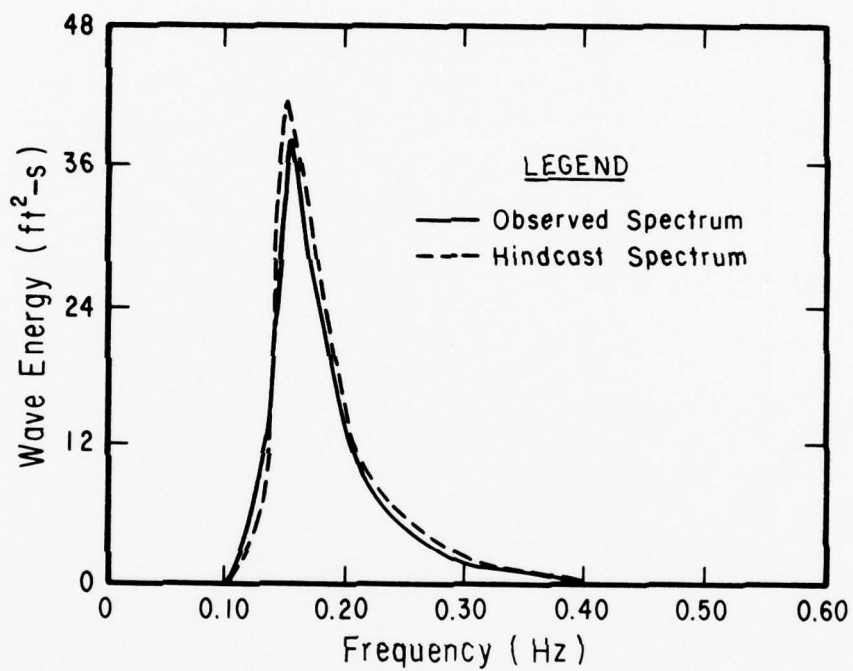


Figure 28. Comparison of WES hindcast spectrum and spectrum obtained from a NOAA Great Lakes Environmental Research Laboratory gage on an offshore tower near Muskegon, Michigan, during a storm on 29 October 1965 (from Resio and Vincent, 1976d).

waves. Thus, the WES model should be unbiased for fully developed waves in the lakes. It is difficult to check the model behavior for fully developed waves in this study because the situation rarely occurs for moderate and high windspeeds in Lake Erie.

There is evidence that the wave energy growth rate in the WES model during moderately high windspeeds (15 meters per second or 35 miles per hour) is slightly higher than even the Mitsuyasu (1968) and JONSWAP growth rates (Fig. 29). The higher windspeeds represented in the fall 1975 data are about 10 to 15 meters per second (20 to 35 miles per hour). It is also evident that for very high windspeeds (30 meters per second) the WES model growth rates are more compatible with the others.

Another factor which may contribute to the small tendency for the WES wave-generation spectra to be too high and too wide is the neglect of energy dissipation due to bottom friction in the WES model.

Wave hindcasting at Cleveland and Presque Isle is considerably more difficult when the winds are blowing approximately parallel to the long northeast-southwest axis of Lake Erie. For these cases, slight uncertainties in the true wind direction can lead to large uncertainties in the fetch length. However, since these wind conditions sometimes generate very high waves, they are an important consideration.

The WES model is fairly effective in estimating spectra for northeast-southwest winds in Lake Erie as evidenced by the spectra shown in Figure 30 (extracted from Fig. 16). In the second and third Presque Isle examples and in the Cleveland examples in the figure, the wind was from the northeast; in the first and fourth Presque Isle examples, the wind was from the southwest.

Although the agreement between gage and hindcast spectra is generally good, there is one fairly consistent difference. In all but the second Presque Isle example, the gage spectrum has a distinct low-frequency peak which is not visible in the hindcast spectrum. This feature is most evident in the example for Cleveland at 1900, 18 October 1975. The corresponding hindcast wind field is illustrated in Figure 31. Similar wind fields were hindcast for at least the preceding 12 hours. The correct fetch to use in estimating waves at both the Cleveland and Presque Isle buoys in this example is ambiguous since the wind is blowing nearly parallel to the New York-Pennsylvania-eastern Ohio shoreline.

For the example in which the low-frequency peak in the gage spectrum was absent (Presque Isle at 1300, 24 September 1975), the hindcast wind field was very similar to the one shown in Figure 31. The hindcast spectra for these two examples are also similar. The secondary peak which appears in the Presque Isle gage spectrum at 1900, 18 October 1975, is evidently due to waves generated over the fetch between Buffalo and Presque Isle; the highest gage spectral peak and the hindcast spectral peaks appear to be based on wave generation over an effective fetch originating about 50 kilometers (30 miles) southwest of Buffalo. The

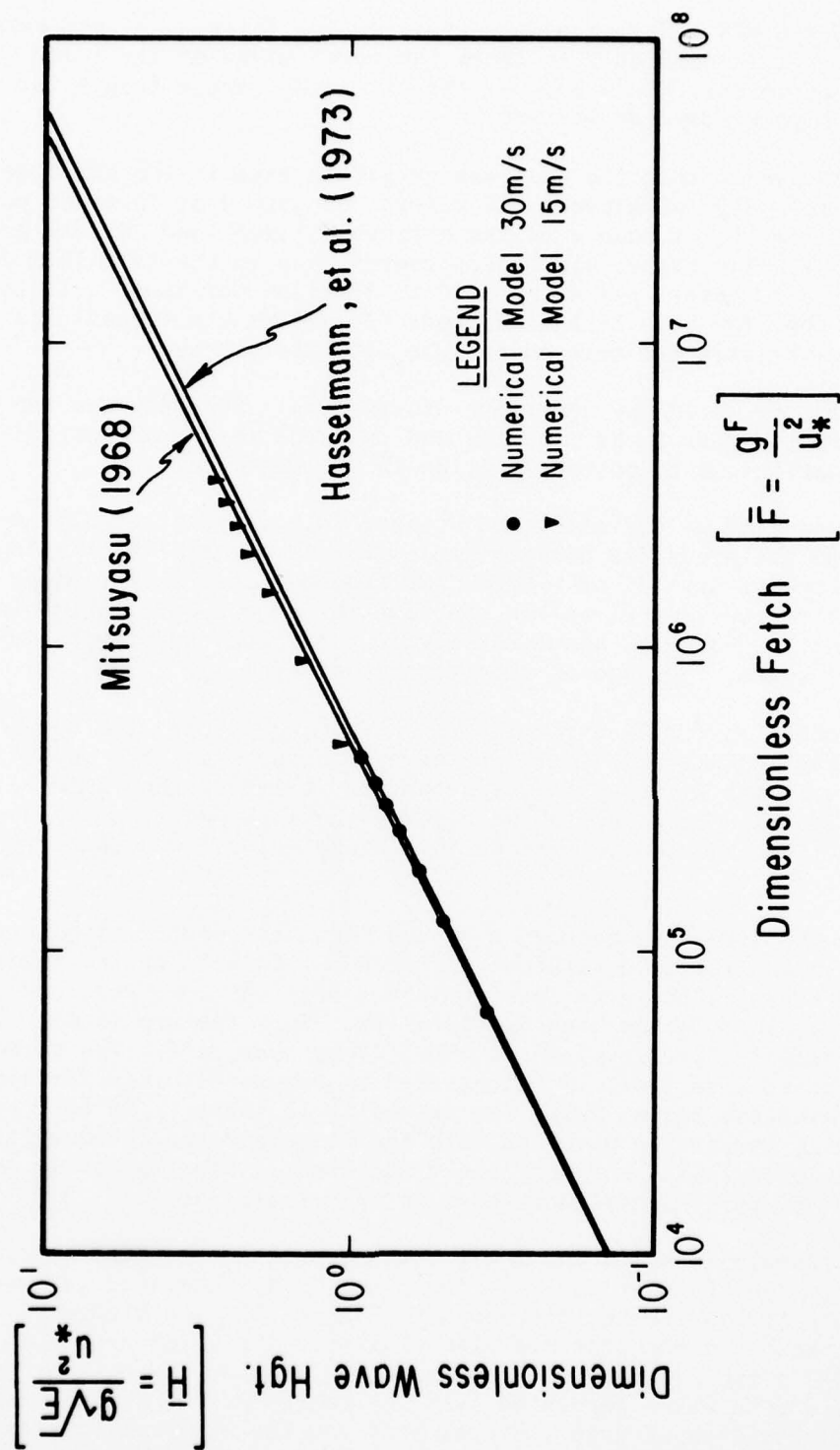


Figure 29. Comparison of the rate of change of dimensionless wave height with dimensionless fetch in the WES numerical model with rates of change observed by Mitsuyasu (1968) and Hasselmann, et al. (1973) (from Resio and Vincent 1976d). \bar{H} and \bar{F} are the dimensionless height and fetch, respectively; g the acceleration due to gravity; E the total wave energy; and u_* the friction velocity.

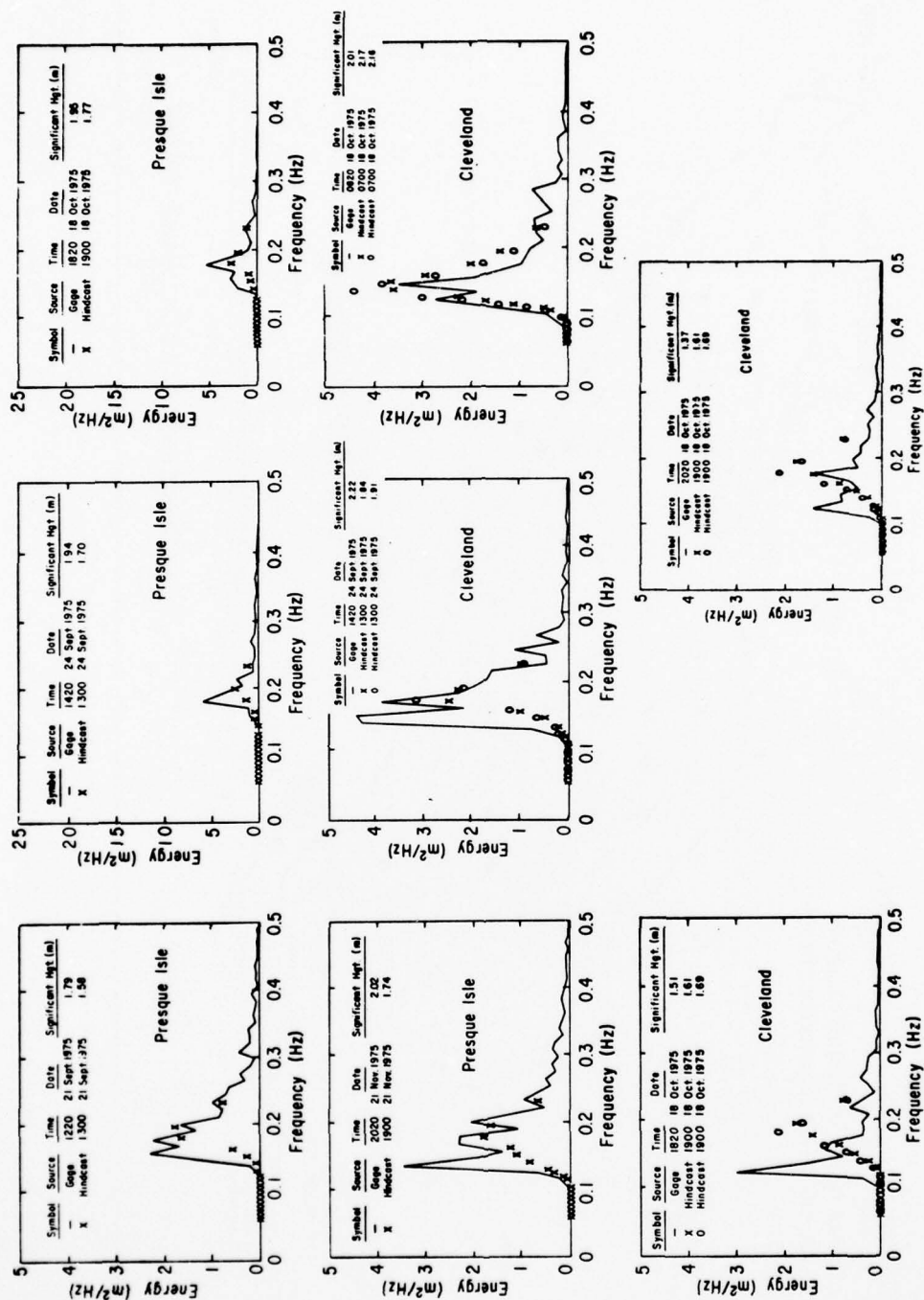


Figure 30. Comparisons of WES hindcast and gage spectra in Lake Erie for situations in which the wind was approximately parallel to shore and fetches are poorly defined.

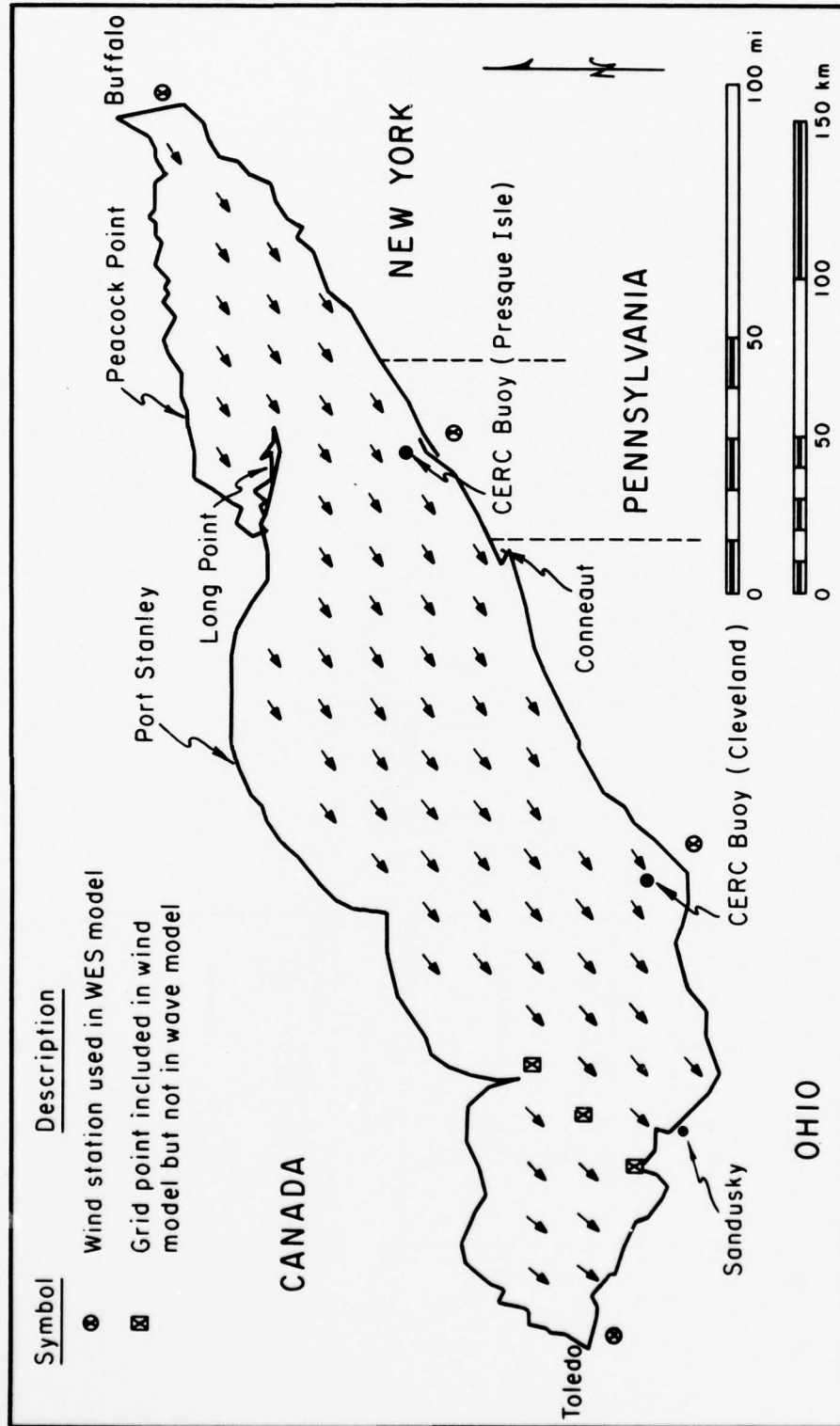


Figure 31. WES hindcast wind field over Lake Erie at 1900 e.s.t., 18 October 1975.

lack of a secondary low-frequency peak in the Presque Isle gage spectrum at 1420, 24 September 1975, indicates that the true wind had a slightly larger component toward the north or south and was effective at generating waves arriving at Presque Isle along only one fetch.

The gage spectrum at Cleveland corresponding to the wind field illustrated in Figure 31 shows a very distinct low-frequency peak which is not present in the hindcast spectrum. The fetch over which waves arriving at Cleveland are being generated in this example is ambiguous. The fetch delineated by a line through the Cleveland buoy site parallel to the wind direction would pass several kilometers east of Long Point and extend nearly to Buffalo. This fetch is laterally constricted to the northwest by Long Point and to the southeast by the Ohio shoreline bulge between Cleveland and Conneaut. The constrictions in fetch width are expected to reduce the height and energy of waves generated along this fetch.

Since wave energy generated by the wind can propagate at small angles to the wind direction as well as in the wind direction, wave energy generated over the relatively wide fetch between the Long Point-Port Stanley shoreline and the area offshore of Cleveland would be expected to appear at the Cleveland buoy site in both measurements and WES hindcasts. Thus, the higher frequency peaks (between 0.15 and 0.23 hertz or 4.4 and 6.7 seconds) in the gage spectra at 1820 and 2020, 18 October 1975, probably represent wave generation along the short fetch between Long Point and Cleveland. The hindcast spectra at 1900, 18 October 1975, which have peaks at 0.18 and 0.20 hertz or 5.1 and 5.6 seconds, probably represent wave generation over the same fetch. In comparison, the fetch-limited estimate of significant period generated along the fetch between Long Point and Cleveland is roughly 5.8 seconds according to Bretschneider's deepwater wave forecasting curves (U.S. Army, Corps of Engineers, Coastal Engineering Research Center, 1977).

The low-frequency peaks (0.12 hertz or 8.1 seconds) in the gage spectra, which do not appear in the hindcast spectra, may represent wave generation over the long fetch between Cleveland and the Canadian shore west of Buffalo. The fetch-limited estimate of significant period generated along the fetch between Buffalo and Cleveland is roughly 6.4 seconds according to Bretschneider's curves. It is not evident why this estimate, based on the longest available fetch, differs from the wave period corresponding to the lowest frequency peak in the gage spectrum.

Another illustration of the same phenomenon is the spectra at 1300, 24 September 1975, when the wind was again from the northeast. At Cleveland the gage spectrum has a prominent peak at low frequency (0.16 hertz or 6.4 seconds) and another prominent peak at intermediate frequency (0.18 hertz or 5.6 seconds). The hindcast spectra have only one prominent peak and it closely matches the intermediate frequency gage spectral peak. In this case, omission of the low-frequency energy caused the hindcasts to underpredict significant wave height by 0.3 to 0.4 meter (1.0 to 1.3 feet). At Presque Isle, where the fetch was more clearly defined, the gage and hindcast spectra are reasonably similar.

The above examples indicate that for winds from the northeast in Lake Erie such that the fetches to Cleveland and Presque Isle are poorly defined, there is a tendency for the WES model to lose wave energy generated over the longer more constricted fetches. Another example, during which the wind was from the opposite direction, further documents the difficulties in ambiguous fetch situations. The hindcast wind field at 1900, 21 November 1975, is shown in Figure 32. At the southwest end of the lake, the wind was blowing nearly parallel to the long axis of the lake. The wind direction shifted over the lake such that near Presque Isle and Long Point the wind was from the southwest at about a 30° angle to the lake axis. The fetch length over which waves arriving at the Presque Isle buoy could have been generated ranged from about 50 kilometers (30 miles) (from Conneaut, Ohio) to 210 kilometers (130 miles) (from Sandusky, Ohio). The fetch lengths in this example were clearly sensitive to the wind direction, which can never be specified exactly.

The gage spectrum for Presque Isle at 2020, 21 November 1975, has at least three prominent peaks: at 0.13 hertz (7.4 seconds), at 0.17 hertz (6.0 seconds), and at 0.20 hertz (5.0 seconds). The hindcast spectrum has only one peak, at 0.18 hertz (5.6 seconds), which nearly coincides with the middle peak in the gage spectrum. The biggest failing of the hindcast spectrum is omission of the large low-frequency peak. This omission leads to an underprediction of significant height by 0.3 meter.

The observed tendency for the WES hindcast spectra to miss low-frequency spectral peaks during ambiguous or multiple fetch situations is in part a consequence of the wave propagation scheme. The scheme is based on the assumption that variations in energy at each frequency are linear along a path perpendicular to the direction of wave propagation. In open water far from shorelines, the variations are small and this assumption is reasonably good. Near a shoreline, the assumption may often be poor. In a small lake such as Lake Erie, wave generation and propagation nearshore is an important factor in many situations.

A qualitative discussion of wave generation and propagation in the Presque Isle-Long Point area will help to illustrate difficulties encountered in ambiguous fetch situations. A larger scale representation of the area with an assumed wind direction is shown in Figure 33. Only wave energy moving in the wind direction will be considered in the following discussion.

Wave generation and propagation in the wind direction is presumed to be relatively straight forward up to the grid points G and H. The energy at each frequency at G is updated in each time step by interpolation between grid points A and G and between C and D as discussed in Section III,1. The assumption of small variations in energy lateral to the propagation direction (between C and D) is reasonably good. Similarly, the assumption of small lateral variations in energy between D and E, which must be invoked to estimate the energy at H, is reasonably good.

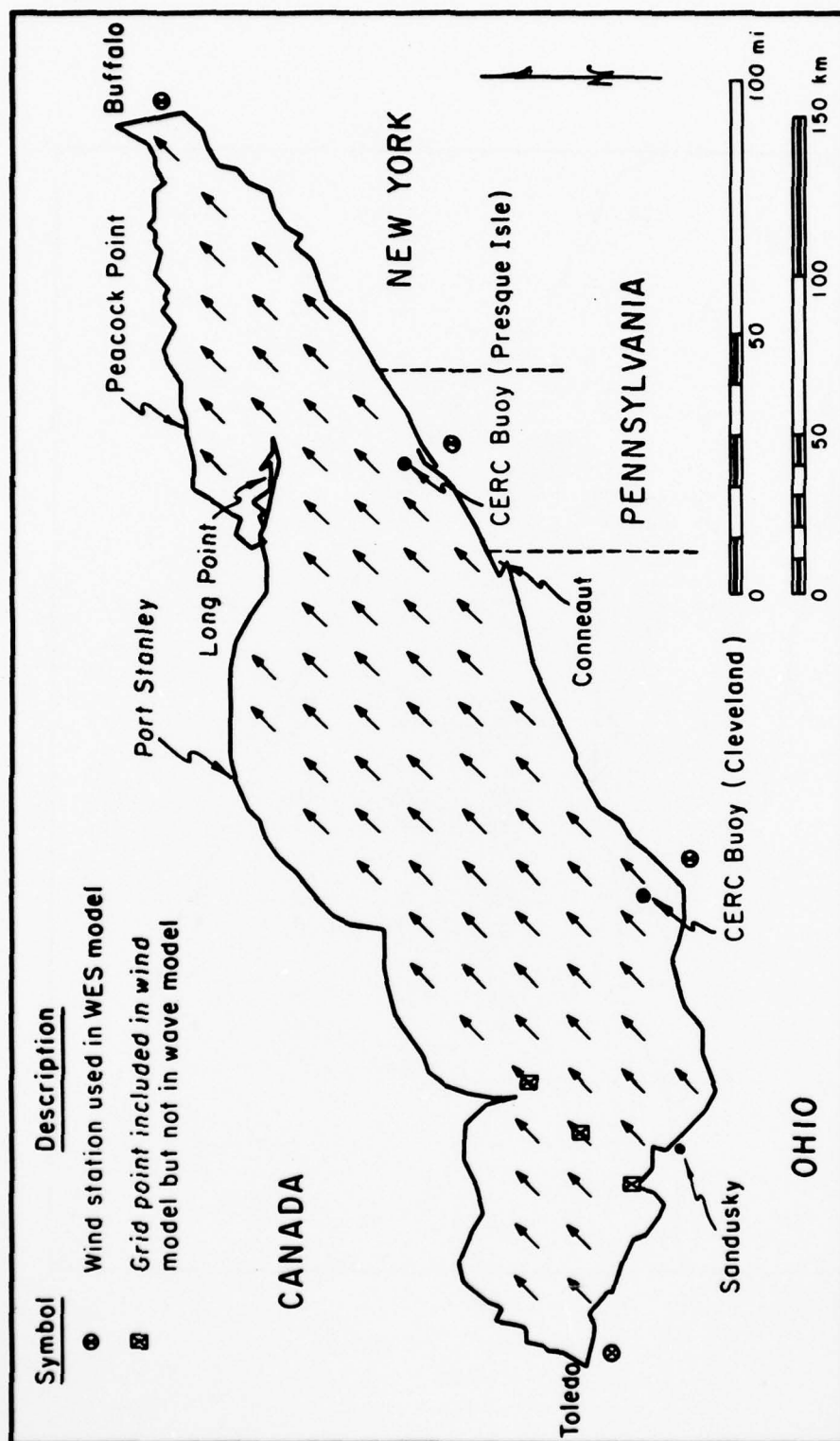


Figure 32. WES hindcast wind field over Lake Erie at 1900 e.s.t., 21 November 1975.

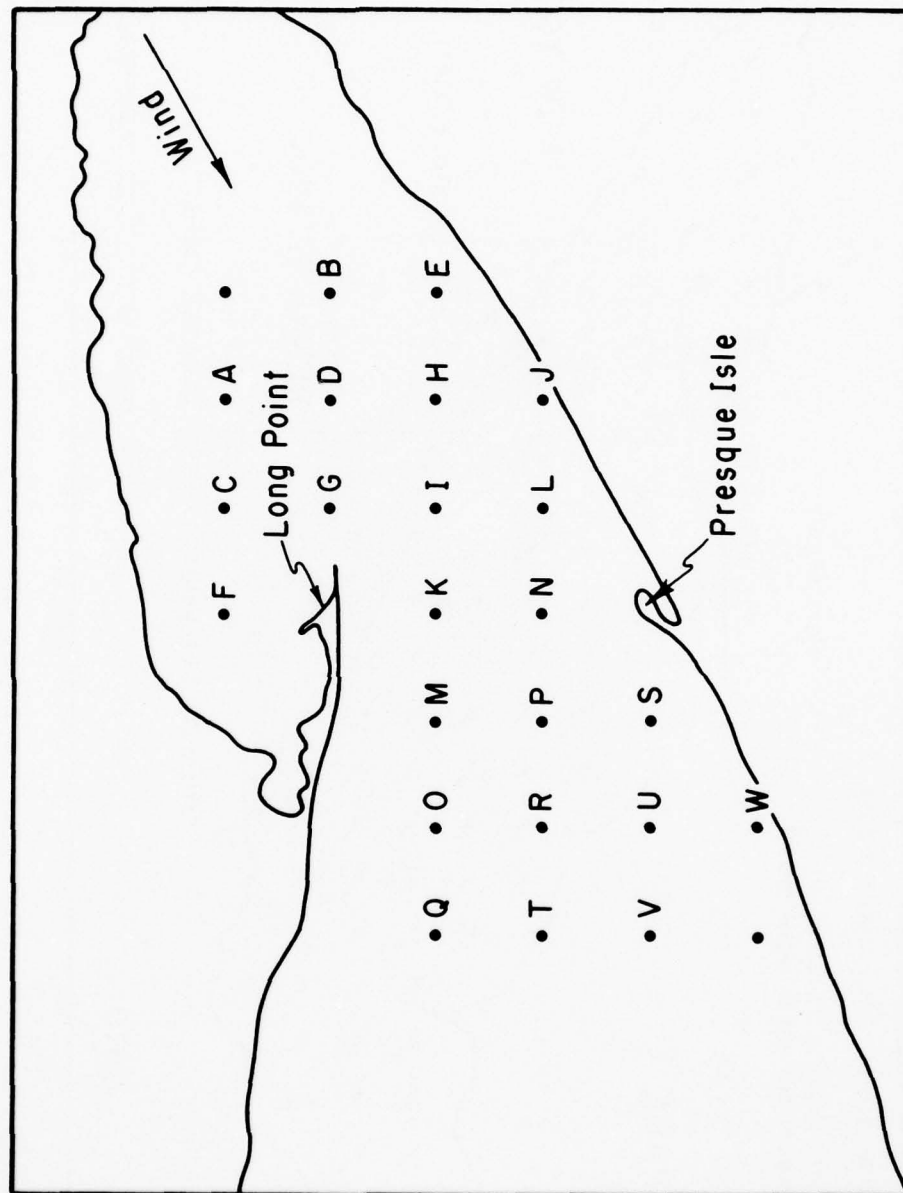


Figure 33. WES wave model grid points in the vicinity of Long Point and Presque Isle in Lake Erie.

To estimate the energy at grid point I, it is assumed that lateral variations in energy between G and H are small. Again, the assumption is reasonable. However, at J the energy is updated by interpolation between E and J and between H and an imaginary zero-energy grid point on land. The assumption of small lateral variations in energy may be grossly violated. Thus, the updated energy actually appearing at J is somewhat less than the energy interpolated between E and J. The reduction is greater for low-frequency energy than for high-frequency energy.

Difficulties with the assumption of small lateral variations in energy also arise at K. The energy at K is obtained by interpolation between G and K with an adjustment to account for the lateral energy gradient between I and a zero-energy grid point on land. In this case, the adjustment for lateral gradients acts to increase the energy at K for waves moving in the wind direction. However, the energy in spectral bands which are already saturated is not permitted to increase. Hence, the effect of lateral gradients on the spectrum at K is expected to be very small for waves moving in the wind direction.

Wave energy losses at grid points along the southeast shore of Lake Erie continue as waves propagate in the wind direction. Energy is lost during propagation between N and S and between S and W in the same way it is lost between E and J. The energy losses continually affect low-frequency energy more than high-frequency energy.

In the absence of further wave generation by the wind, the energy at W would continue to dissipate as it propagates toward Cleveland. However, in this example, new energy is continually being added at each grid point to account for further wave generation. The new energy, which is normally added near the spectral peak, would also go toward reestablishing a fully developed high-frequency spectral tail at grid points along the southeast shore where the fractionating effects of the propagation scheme have caused high-frequency energy levels to fall below saturation.

To reach the Cleveland buoy site, the energy must propagate through an additional six lines of grid points. As it propagates, energy originally generated in the eastern basin of Lake Erie will continue to be diluted at grid points near the southeast shore. Meanwhile, energy input from the wind acting between the Presque Isle-Long Point area and Cleveland will begin to dominate the spectrum. Eventually, the new energy obliterates in the hindcast (but not in nature) all trace of the spectral peak originally generated in the eastern basin.

The above reasoning seems to explain the total absence of the lowest frequency peaks in hindcast spectra for Cleveland during winds from the northeast. Similar reasoning might be used to explain some of the observed shortcomings in hindcast spectra for other ambiguous fetch situations. The absence of secondary peaks in all of the hindcast spectra contained in this report appears to result from the inability of the general computation scheme to precisely simulate the effects of complex boundaries.

One of the largest discrepancies between hindcast and measured significant height in this study occurred at Cleveland during the afternoon and evening of 10 November 1975. The hindcast wind field at 1600 is shown in Figure 34. The wind field at 1900 showed similar directions but reduced speeds. Although it is doubtful that the islands in western Lake Erie had much effect on the waves at Cleveland for this wind field, the fetch to Cleveland is ambiguous because it is nearly parallel to part of the southern shore of the lake. A tendency for the hindcasts to be low would be expected. However, the hindcast significant height at Cleveland (at 1800, 10 November 1975) is 1.7 meters (5.6 feet) higher than the measured significant height. The large difference in significant heights may be indicative of excessive directional spreading of wave energy in the hindcasting model.

The previous discussion has dealt primarily with several specific examples of spectral comparisons between hindcasts and gage data during particular wind conditions. The WES model produces spectra which more nearly match gage spectra during simple fetch rather than ambiguous fetch situations. In terms of significant heights, the hindcasts would be expected to show less scatter in comparison to gage data for simple fetch than for ambiguous fetch situations.

To check this hypothesis using all the data gathered in this study, a simple method for classifying each wind condition at each buoy site was developed. Sectors were marked around each buoy site such that winds from anywhere in the sector would be blowing over either relatively well-defined fetches (case 1) or ambiguous fetches (case 2). By necessity, the sector boundaries (shown in Fig. 35) are subjectively located. It should be reemphasized that the string of islands north of Sandusky, Ohio, forms a virtually complete barrier between the western and central basins of Lake Erie in the model and, presumably, in nature.

Each hindcast significant wave height and peak spectral period was classified as either case 1 or case 2 according to the wind direction at hindcast time. Then, statistical summaries were prepared for each case at each location. Scatter plots of hindcast significant height versus gage significant height are shown in Figures 36 and 37. Contrary to expectations, the scatter in the simple fetch data at Presque Isle (Fig. 36a) is actually greater than in the ambiguous fetch data (Fig. 36b), particularly to the right of the 45° line, where the hindcast heights exceed gage heights. Wind fields which generated the five highest significant heights measured at Presque Isle during fall 1975 fell in the ambiguous fetch classification. In all five cases, the winds were from the southwest and blowing parallel to the long axis of Lake Erie. The WES hindcasts corresponding to the two highest of these were 1.0 and 1.2 meters (3.3 and 3.9 feet) higher than the gage heights. When the gage significant heights are less than 2 meters, the hindcasts for ambiguous fetches have a clear tendency to be too low and the hindcasts for simple fetches a tendency to be too high.

At Cleveland, the scatter is slightly greater for the ambiguous fetch data (Fig. 37b) than for the simple fetch data (Fig. 37a). Two points in

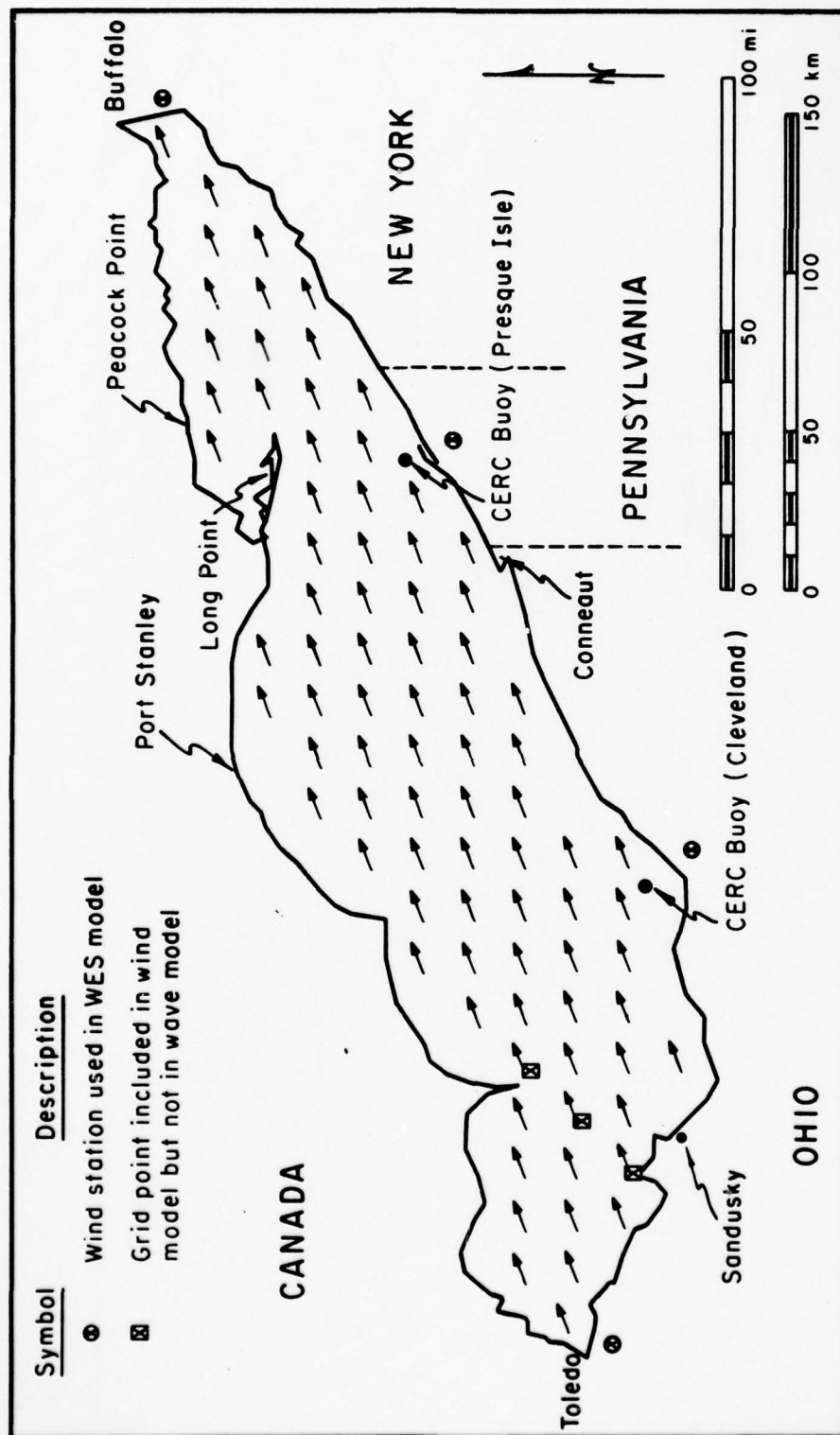


Figure 34. WES hindcast wind field over Lake Erie at 1600 e.s.t., 10 November 1975.

AD-A063 935

COASTAL ENGINEERING RESEARCH CENTER FORT BELVOIR VA
AN EVALUATION OF TWO GREAT LAKES WAVE MODELS.(U)

F/G 8/8

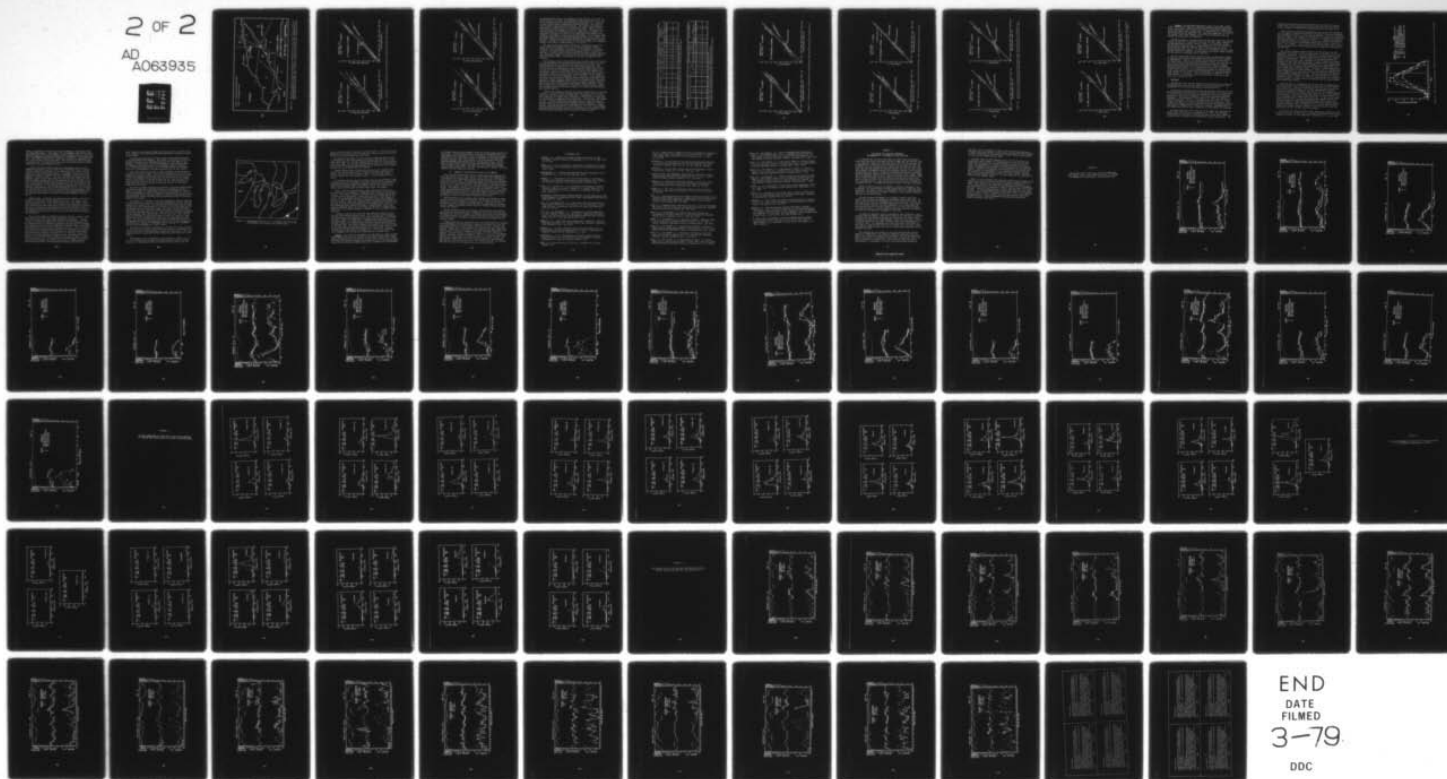
UNCLASSIFIED

OCT 78 E F THOMPSON
CERC-TR-78-1

NL

2 OF 2

AD
A063935



END
DATE
FILMED
3-79
DDC

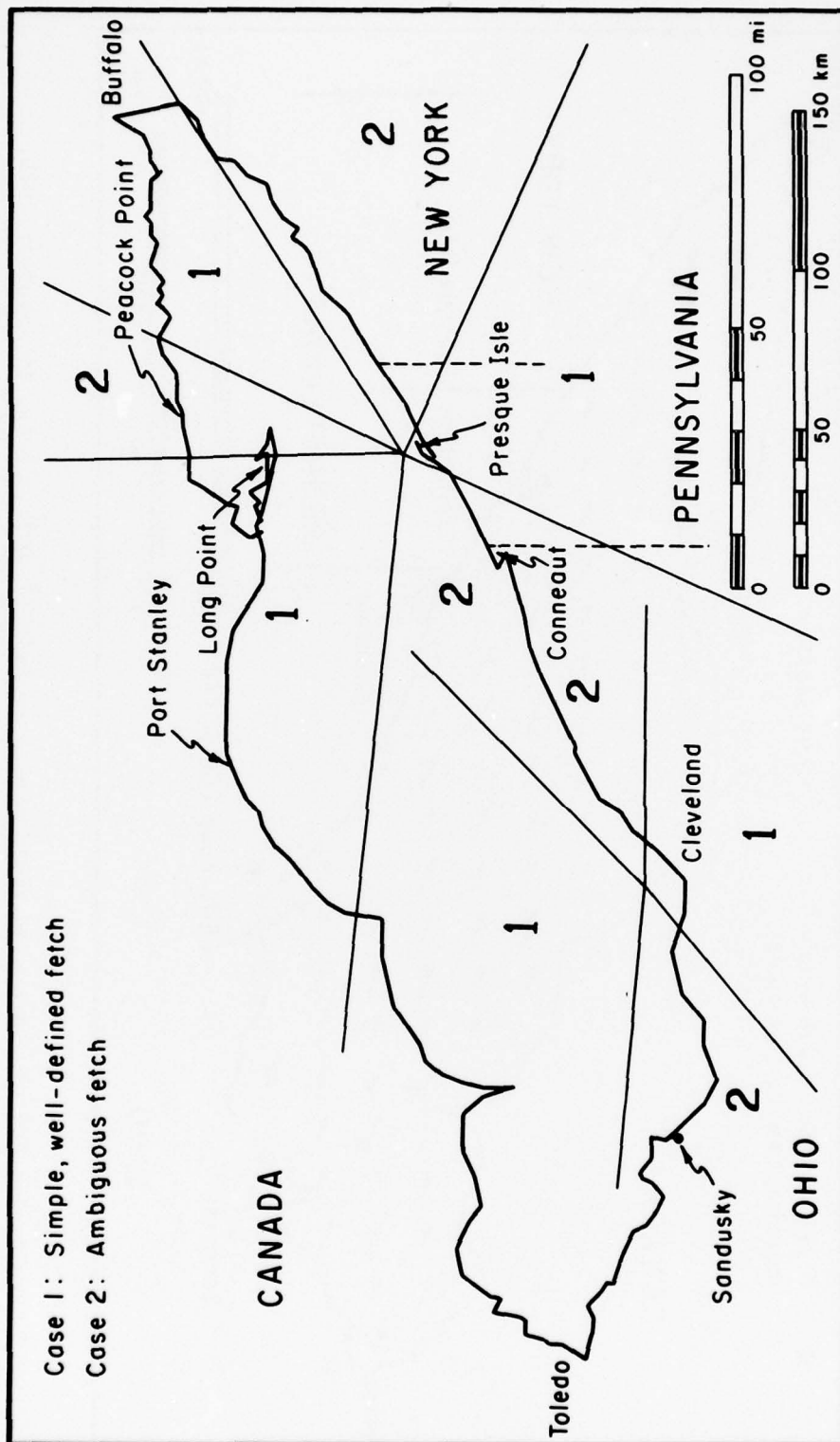


Figure 35. Definition sketch for sectors around Cleveland and Presque Isle gage sites in Lake Erie. Winds approaching the gage sites from case 1 sectors are blowing over reasonably well-defined fetches; winds from case 2 sectors are generally blowing over ambiguous fetches.

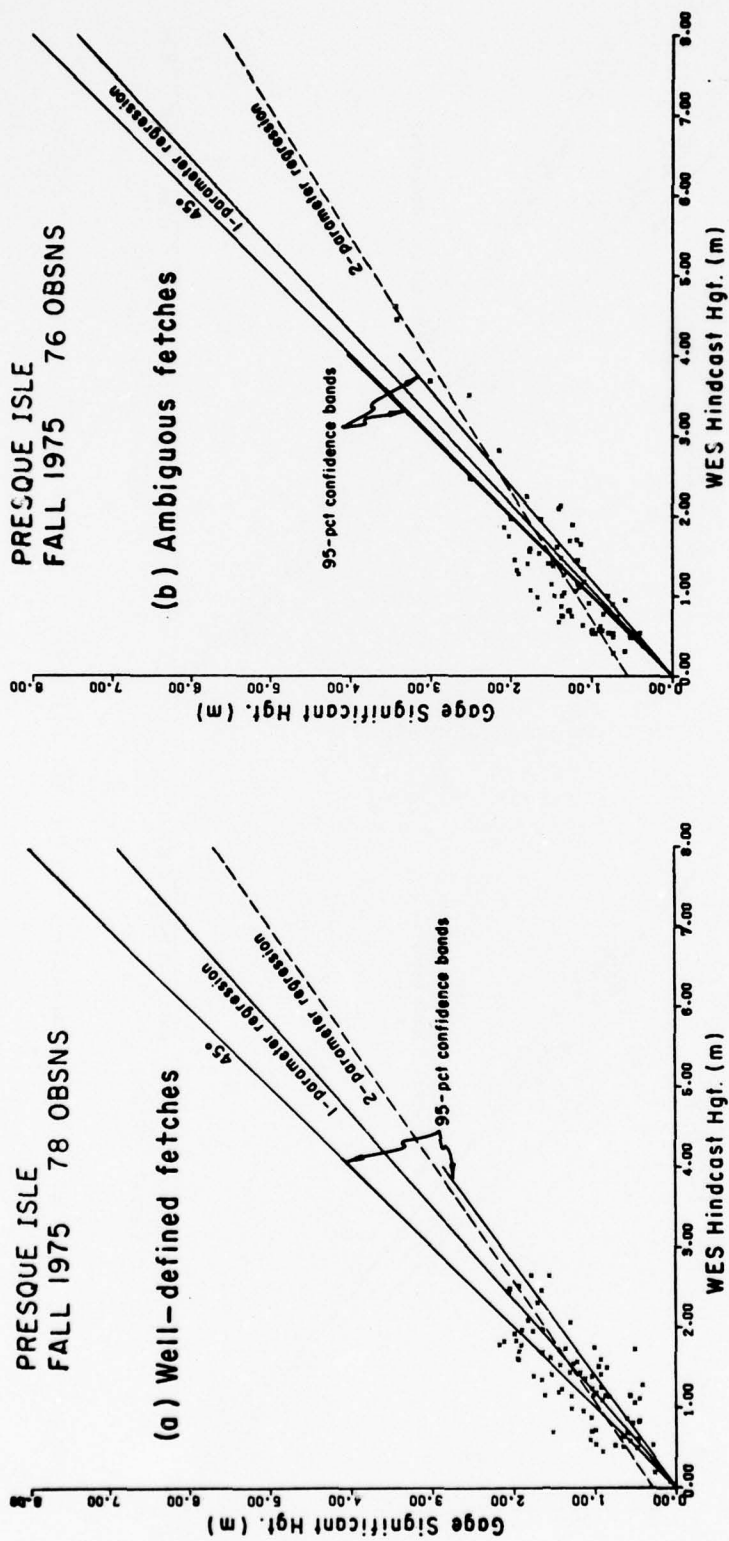


Figure 36. Scatter plots of measured versus WES hindcast significant height near Presque Isle.

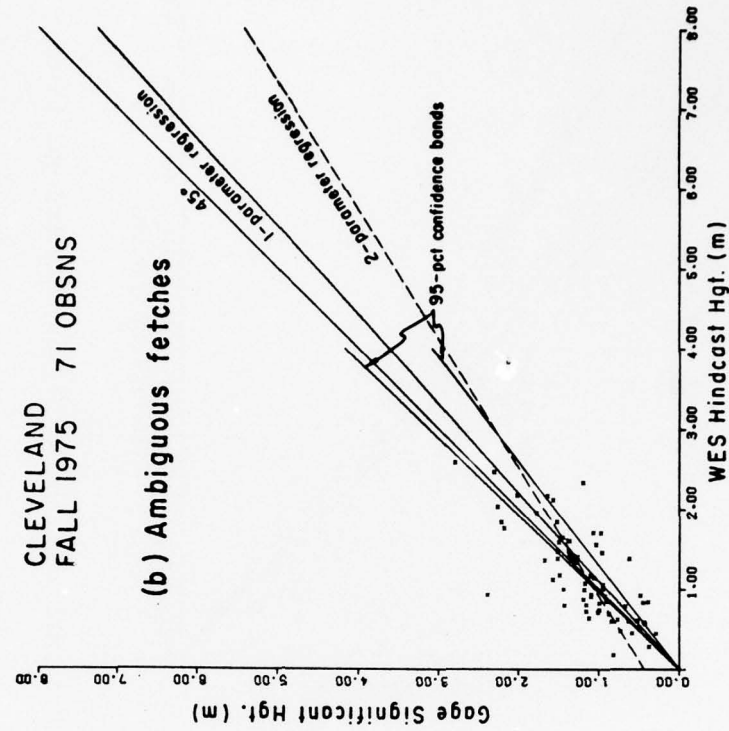
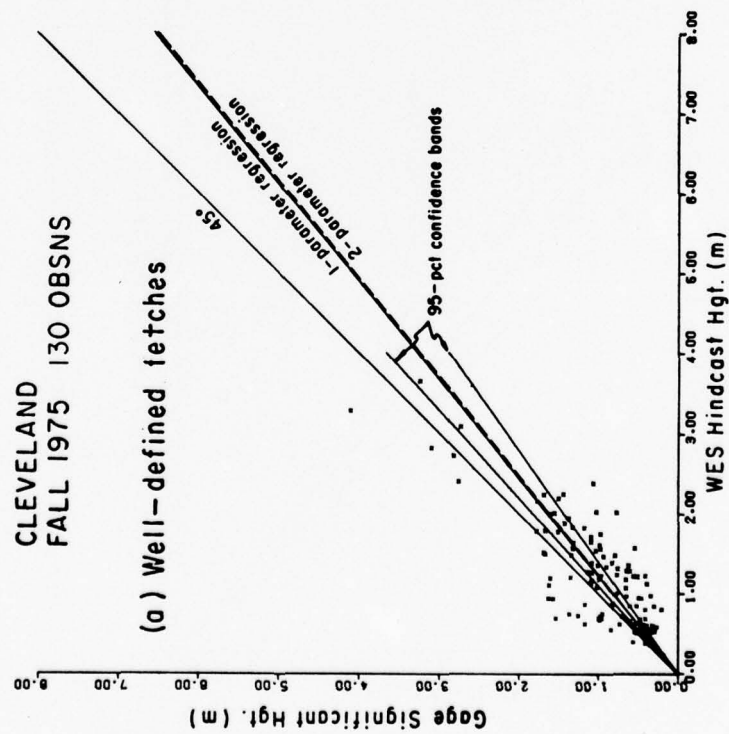


Figure 37. Scatter plots of measured versus WES hindcast significant height near Cleveland.

the ambiguous fetch data, corresponding to gage heights of 2.1 and 2.4 meters (6.9 and 7.9 feet), are particularly far from the 45° line. One of the points indicates a gage significant height which is 1.5 meters (5 feet) greater than the hindcast significant height. The winds for this case were coming from the northeast. The other point indicates a gage height 1.7 meters less than the hindcast height. Winds for this case were from the southwest, as shown in Figure 34. The highest significant heights at Cleveland were in the simple fetch category; all were within 0.8 meter (2.6 feet) of the gage height and showed no clear tendency to be higher or lower than the gage height. As at Presque Isle, the simple fetch data for Cleveland gage heights less than 2 meters show an overall tendency for the hindcast heights to be higher than the gage heights. Contrary to Presque Isle, the Cleveland hindcasts for ambiguous fetches do not show a strong tendency to be too low.

The correlation between gage and hindcast significant heights for simple fetches at Presque Isle is lower than for ambiguous fetches (Table 8). This difference is puzzling. At Cleveland the correlation is higher for simple fetches than for ambiguous fetches, as would be expected. At both Presque Isle and Cleveland the means of gage and hindcast significant heights are more nearly the same for ambiguous fetches than for simple fetches. The reverse is true for variances at both locations.

Scatter plots of gage versus hindcast peak spectral period at Presque Isle show tendencies for the hindcast periods to be too short for long measured periods and too long for short measured periods (Fig. 38). Scatter plots for Cleveland (Fig. 39) show similar tendencies. When only the periods corresponding to gage significant heights greater than or equal to 1 meter are considered (Figs. 40 and 41) the tendency for the hindcast period to be too long for short measured periods is greatly diminished. There is evidence of an overall tendency for the hindcast periods to be too short in ambiguous fetch situations. This tendency is consistent with the earlier finding that the WES hindcasting model tends to miss the lowest frequency spectral peak in ambiguous fetch situations. Apparently in many ambiguous fetch cases, the lowest frequency spectral peak is also the tallest (contains the highest energy density). Hence, the reciprocal of its frequency is reported as the peak spectral period for the gage record and this period tends to be longer than the hindcast peak spectral period.

A statistical comparison of gage and hindcast peak periods is provided in Table 9. Cases for which the gage significant height was less than 1 meter have been omitted from the comparison. Surprisingly, the correlation of periods for simple fetch situations at Presque Isle is lower than the correlation for ambiguous fetch situations. At Cleveland, the reverse is true. At both locations the mean gage period is closer to the mean hindcast period for simple fetch situations than for ambiguous fetch situations. The mean gage period for ambiguous fetch situations is longer than the mean hindcast period at both locations. The rms error between gage and hindcast periods is about 0.2 second greater for ambiguous fetch situations than for simple fetch situations at both locations.

Table 8. Comparison of measured and WES hindcast significant heights for well-defined and ambiguous fetch situations.

Location	Case ¹	Obsns. (No.)	Correlation	$H_G = A + B H_{WES}^2$		Mean significant hgt. (m)		Variance of significant hgt. (m ²)		Rms error in significant hgt. (m)	
				A	B	WES	Gage	WES	Gage	Gage vs. hindcast	Gage vs. corrected hindcast
Presque Isle	1	78	0.74	0.86		1.34	1.19	0.33	0.28	0.43	0.38
	2	76	0.87	0.93		1.28	1.36	0.72	0.37	0.45	0.43
Cleveland	1	130	0.82	0.82		1.14	0.93	0.43	0.42	0.44	0.37
	2	71	0.74	0.91		1.23	1.20	0.39	0.28	0.43	0.36

¹Case 1 indicates simple fetch situations; case 2 indicates ambiguous fetch situations.

² H_G = significant height from Waverider buoy gage; H_{WES} = significant height from WES hindcast.

Table 9. Comparison of measured and WES hindcast peak spectral periods for well-defined and ambiguous fetch situations.¹

Location	Case ²	Obsns. (No.)	Correlation	$T_G = A + B T_{WES}^3$			Mean period (s)		Variance of period (s ²)		Rms error in period (s)	
				A (s)	B		WES	Gage	WES	Gage	Gage vs. hindcast	Gage vs. corrected hindcast
Presque Isle	1	46	0.45	2.79	0.48		5.46	5.38	0.51	0.56	0.78	0.68
	2	54	0.56	3.76	0.38		5.47	5.83	1.25	0.56	1.01	0.62
Cleveland	1	46	0.53	3.13	0.41		5.49	5.35	0.83	0.48	0.82	0.59
	2	45	0.50	2.37	0.62		5.35	5.69	0.69	1.06	1.02	0.90

¹Cases for which the gage significant height was less than 1 meter are omitted.

²Case 1 indicates simple fetch situations; case 2 indicates ambiguous fetch situations.

³ T_G = peak spectral period from Waverider buoy gage; T_{WES} = peak spectral period from WES hindcast.

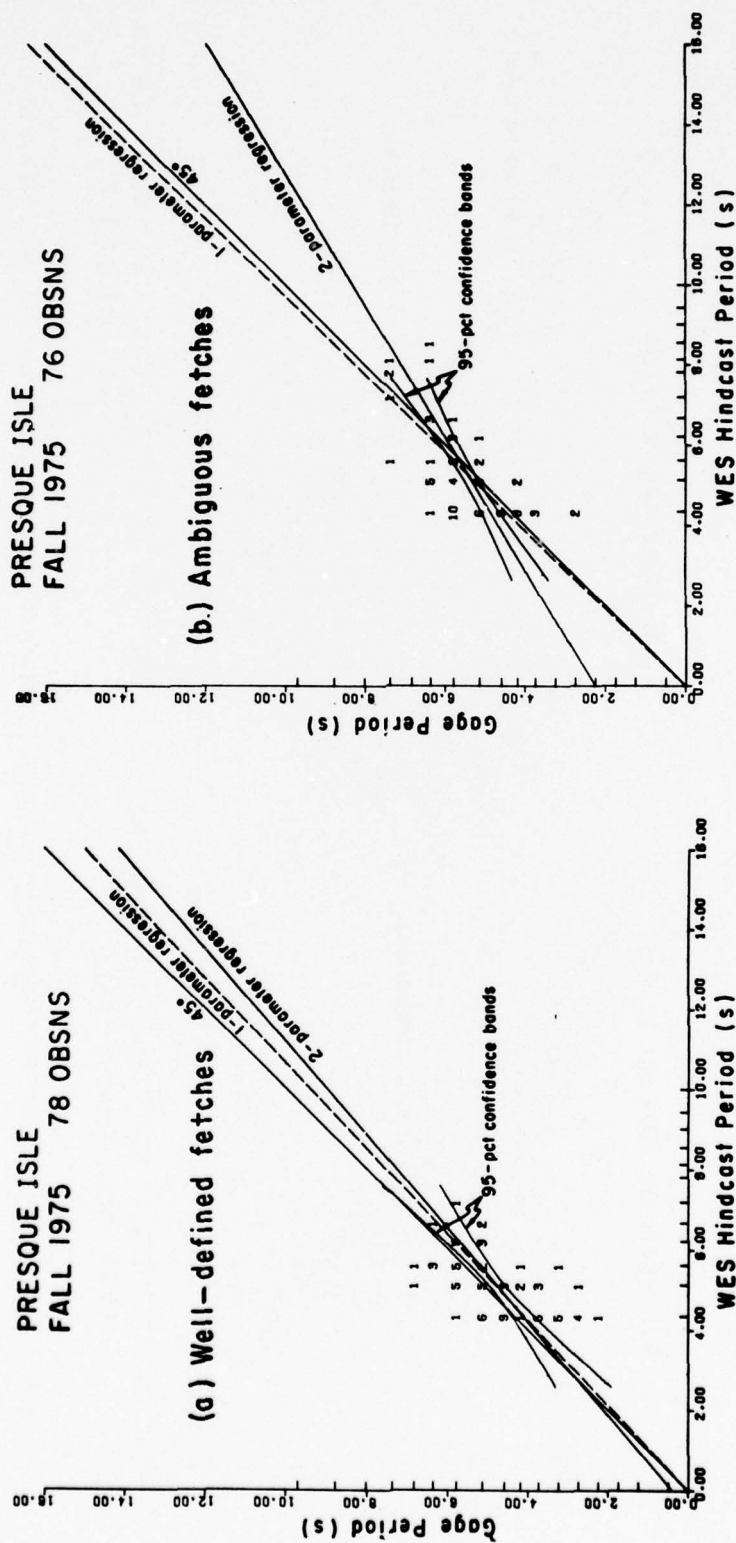


Figure 38. Scatter plots of measured versus WES hindcast peak spectral period near Presque Isle.

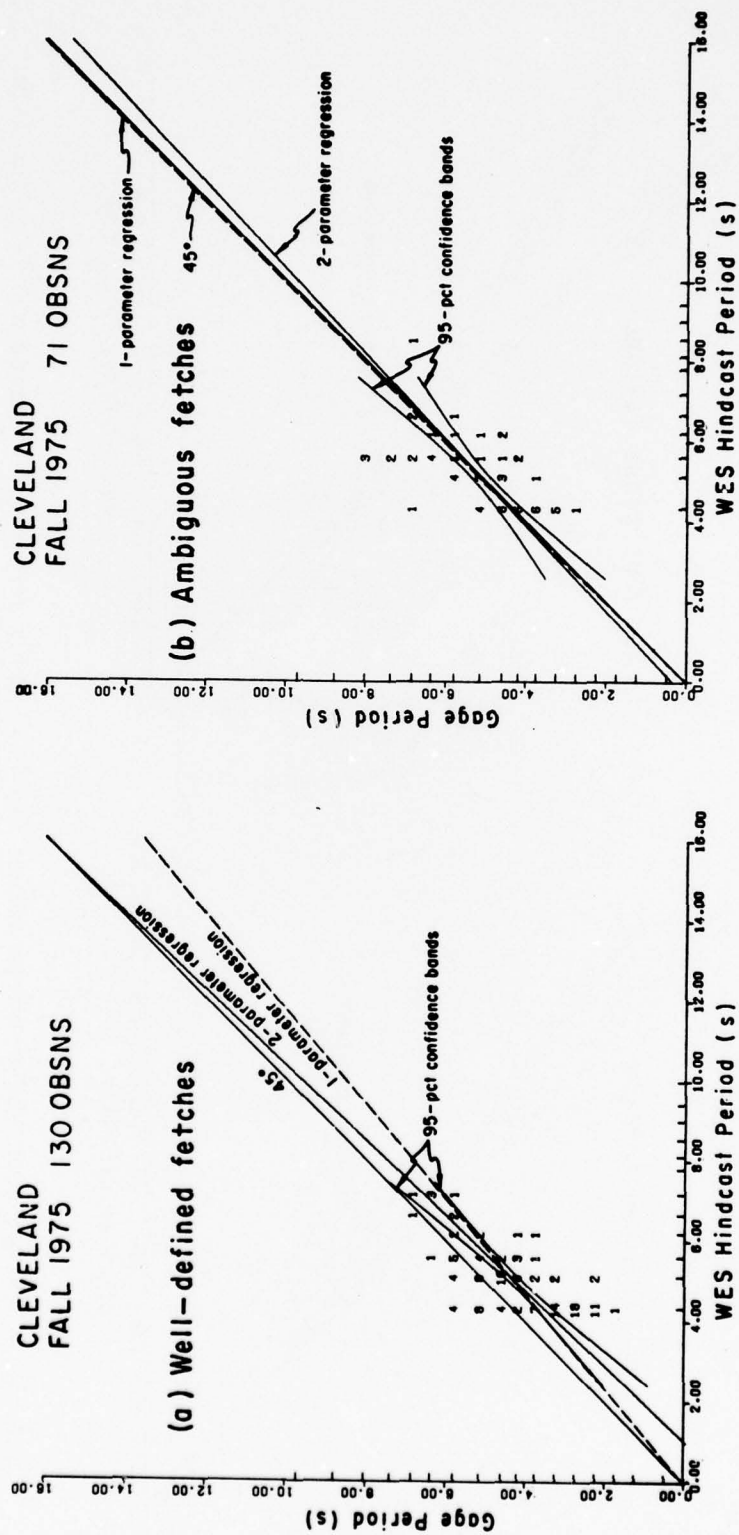


Figure 39. Scatter plots of measured versus WES hindcast peak spectral period near Cleveland.

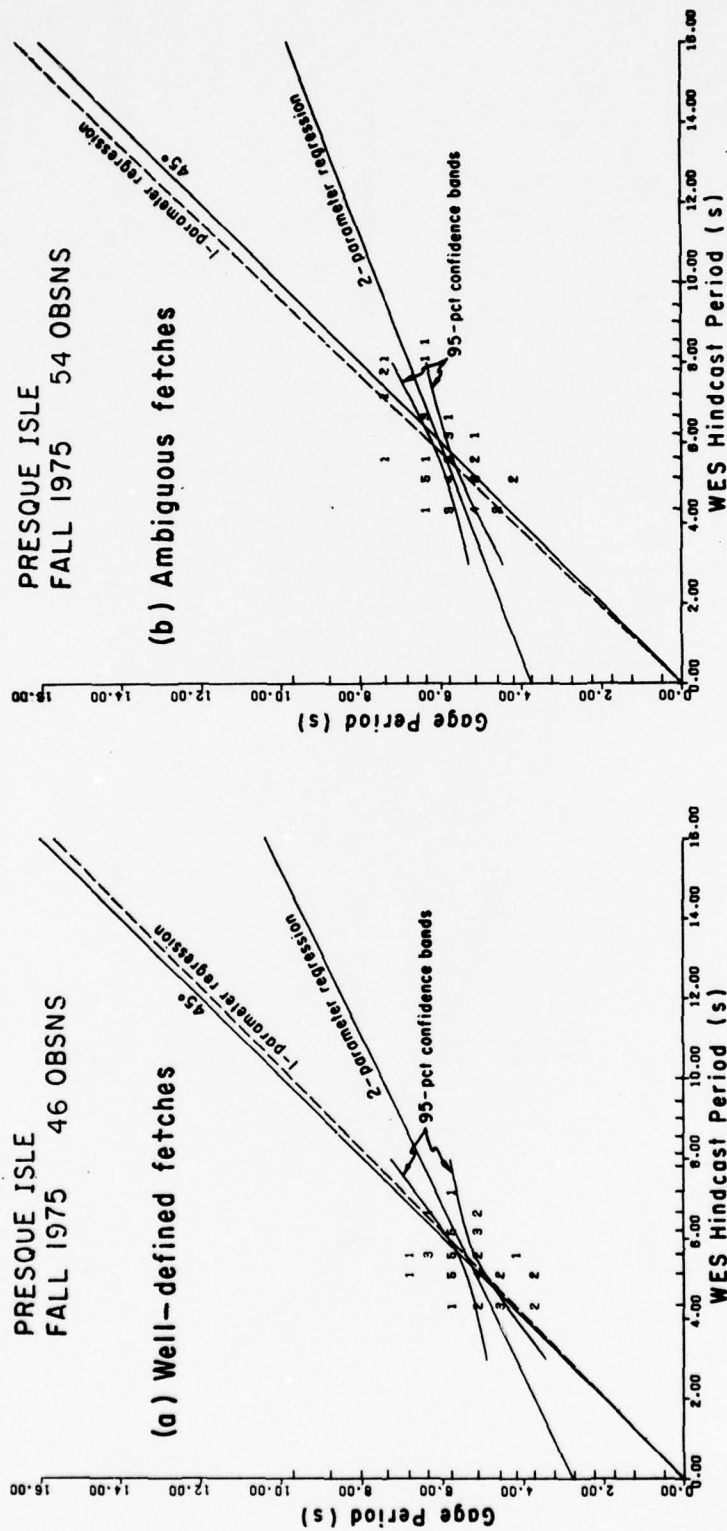


Figure 40. Scatter plots of measured versus WES hindcast peak spectral period near Presque Isle for cases in which the measured significant height is greater than or equal to 1 meter.

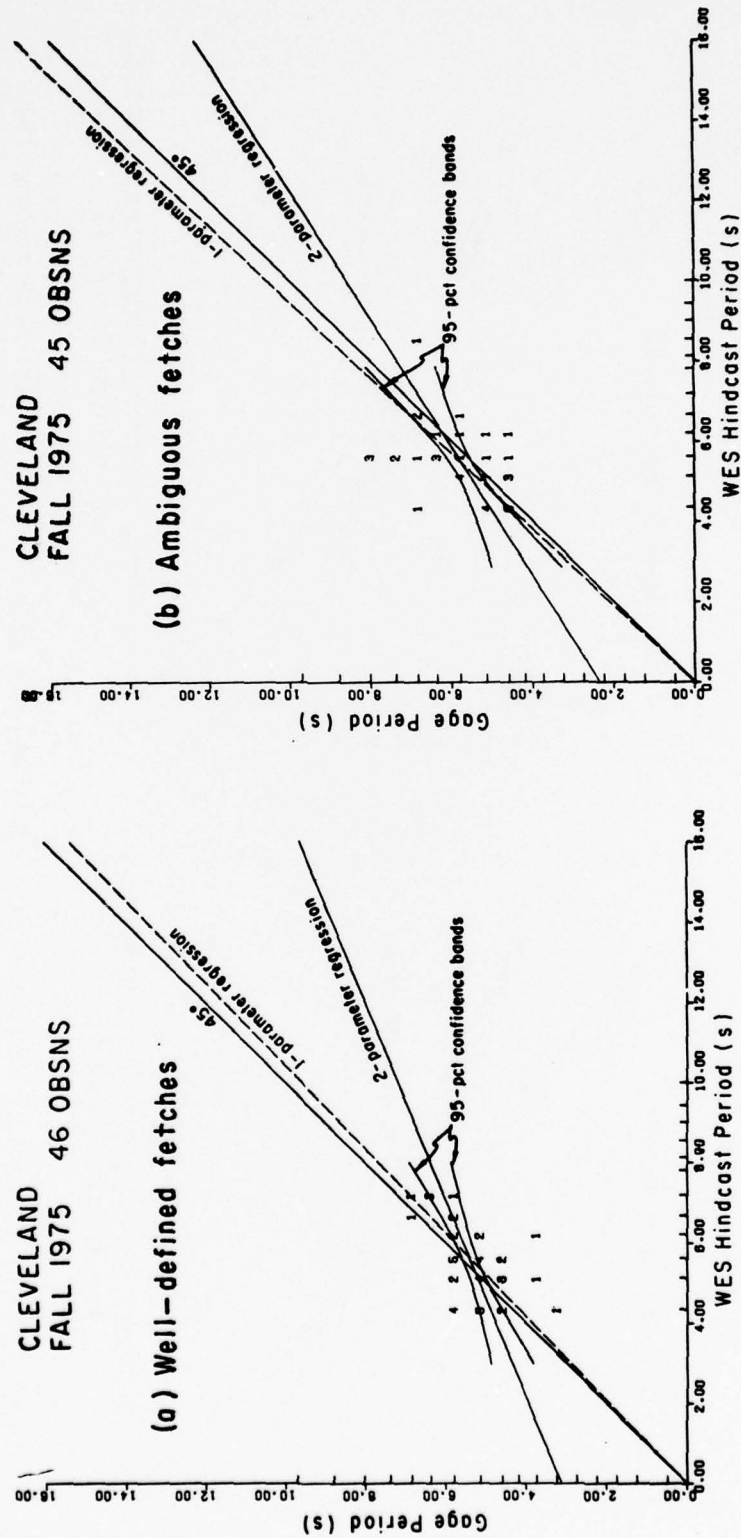


Figure 41. Scatter plots of measured versus WES hindcast peak spectral period near Cleveland for cases in which the measured significant height is greater than or equal to 1 meter.

c. Summary. The WES model developed by Resio and Vincentt (1976c, 1976d, 1977a, 1977b, 1978a) has difficulty properly representing weather fronts and weather situations characterized by significant spreading or curving of isobars over a single lake. In hindcasting for severe storms, these difficulties are expected to be relatively unimportant, at least in the smaller Great Lakes; however in day-to-day hindcasting, they can degrade the accuracy of the hindcasts.

The WES procedure for computing wave growth along simple well-defined fetches in Lake Erie is generally excellent, but has a small tendency to overestimate spectral width, spectral energy, and significant height. The WES hindcasting model has a strong tendency to omit the lowest frequency spectral peak for ambiguous fetch situations giving rise to multiple-peaked gage spectra. By omitting a low-frequency spectral peak, the WES model has a tendency to underestimate significant height and peak spectral period in ambiguous fetch situations.

The two shortcomings tend to balance so that an unstratified sample of hindcast significant heights seems relatively unbiased when compared to measurements. However, in dealing with extreme wave conditions in the Great Lakes with return periods measured in years, the winds may not be a mix of onshore winds with easily determined although irregular fetch lengths and winds along the long axis of the lake with highly ambiguous fetch lengths. It is expected that the extreme coastal waves at most Great Lakes sites will be generated primarily by onshore winds, since refraction will severely reduce the heights of waves generated by winds parallel to the coast. Thus, the WES model is expected to have a small tendency to overpredict the most severe wave conditions at most sites over a period of years.

2. TDL Model.

Although the wave forecasts produced by the TDL model are useful for NWS applications, they are less accurate than the WES hindcasts. The limitations of the existing TDL model are discussed below.

In deriving the surface wind forecasting equations, TDL used only the maximum shipboard observed wind for each day and time in each lake sector. It is likely that this procedure has inherently biased the forecasting equations to overpredict windspeeds in the range of normally observed windspeeds. This procedure is also expected to reduce the variance of forecast windspeeds. For low or moderate winds, more ships are likely to be on the lakes with many of them taking marine observations. Thus, a number of "chances" are often available to select an unrepresentatively high observed windspeed due to spatial and temporal inhomogeneities in the surface wind field or due to anomalies in measurement and recording.

For very high winds, fewer ships are on the open lakes and those in transit often tend to follow the upwind shore. Thus, few windspeed observations are available to choose from, and for the worst storms in a typical year, there may be no observations in many lake sectors. The

shortage of observations during high winds and the statistical method used by TDL to derive equations for the surface wind may give the TDL model a tendency to underestimate windspeed during very strong winds.

Thus, the TDL wind forecasting equations are expected to overpredict low and moderate windspeeds and perhaps underpredict very high windspeeds. These tendencies would act to decrease the variance of forecast windspeeds and wave heights. The tendency to overpredict wave heights during low and moderate conditions is illustrated in Figure 17. A tendency to underpredict during very high wave conditions can also be inferred from Figure 17 for Lake Erie sites for significant heights greater than 2.5 meters (8 feet). This tendency is not evident for the Lake Michigan sites, possibly because no very severe storms occurred while the gages were operating in Lake Michigan.

The surface windspeed estimate used in the TDL model is derived empirically to include a coarse consideration of the effect of air-lake temperature difference. The gross effects of air-lake temperature difference during April to September and October to December are treated separately in the model. This treatment is reasonable because the greatest cooling of the lakes, and hence the most frequent and intense unstable air-lake temperature differences normally occur during October to December (Fig. 42). The 1921-50 average surface water temperatures in the figure were computed using monthly mean air temperatures and a heat storage function (Snyder, 1960). The 1966-74 surface temperatures were estimated from Feit and Goldenberg's (1976) plots of average daily surface temperature for each day of the year derived from Canadian airborne radiometer temperature surveys. The 1975 averages were obtained from nearshore measurements at a depth of 3 meters below the surface (Grumblatt, 1976). January 1975 data have been plotted out of sequence next to December 1975 data to show the tendency for decreasing temperature between these months.

Some inaccuracy is introduced into the TDL surface windspeed estimates due to the use of climatological seasonal mean air-lake temperature differences. Ideally, the estimates would be based, in some way, on near real-time measurements of air-lake temperature difference. Since this procedure is presently impractical, the TDL estimates do not include any consideration of day-to-day variations in air-lake temperature difference. This shortcoming could affect the TDL estimates; e.g., when an unusually cold airmass crosses the lake. If the air were much colder than the lake, it would be exceptionally unstable and the air would be expected to produce exceptionally high surface winds. The unusually severe air-lake temperature difference over Lake Michigan on 24 and 25 September 1975, as evidenced by a 2° Celsius drop in water temperature, almost certainly caused an intensification of winds and waves which the TDL estimate would not include.

If the rate of change in surface water temperature indicated by the slope of the curves in Figure 42 is considered representative of overall average day-to-day air-lake temperature differences, it is clear that

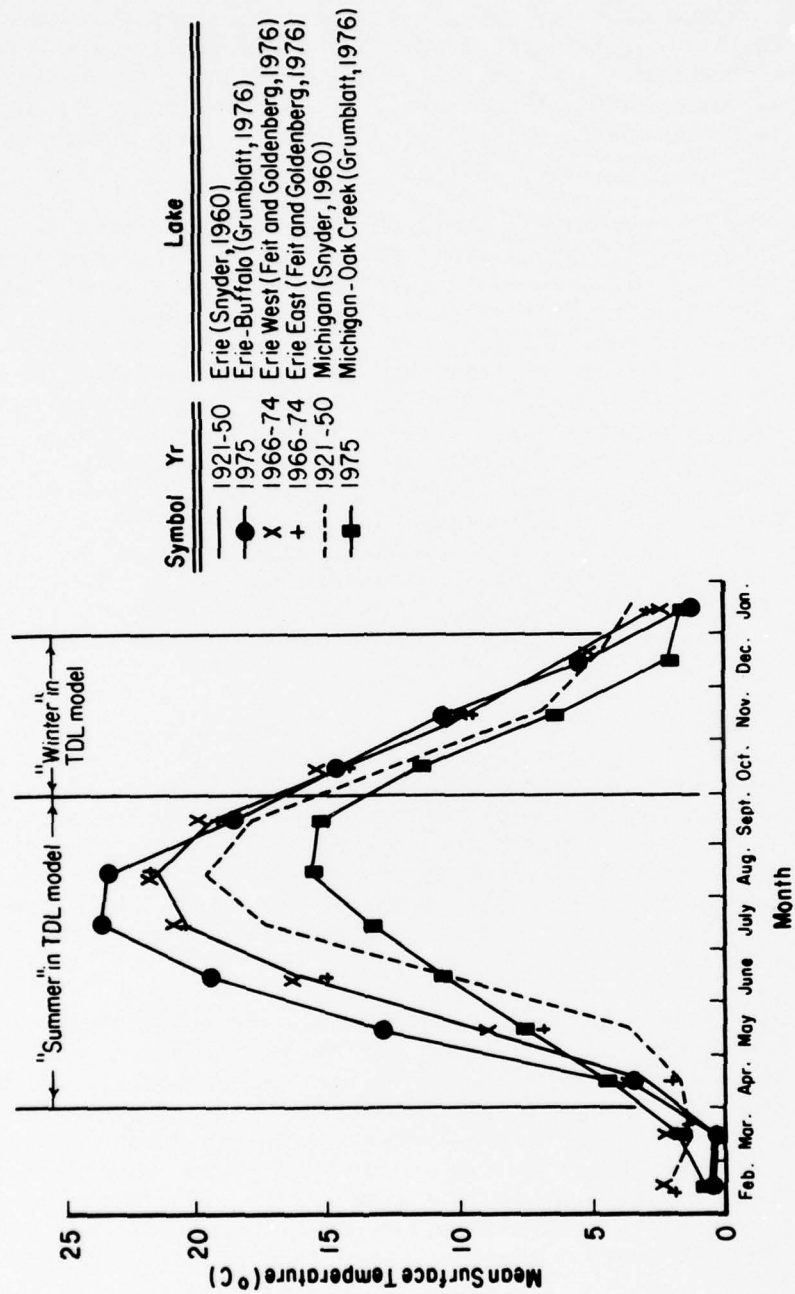


Figure 42. Plot of mean surface water temperature versus month for Lakes Erie and Michigan.

there is considerable variation in air-lake temperature difference within the demarcated seasons. For example, the steep upward slope of the curves marked by square and circular symbols at June indicates that the day-to-day air-lake temperature differences tended to be abnormally stable during June 1975. This effect would give the TDL model a tendency to overpredict surface winds and waves during this month. The cooling rates during October to December 1975, as indicated by the slope of the same curves were fairly uniform in both Lakes Michigan and Erie.

Finally, the TDL estimates, based on climatological mean air-lake temperature differences, have another small uncertainty because the mean air-lake temperature differences in any particular year rarely coincide exactly with the climatological means. For example, data points on the dashline in Figure 42 indicate that the climatological drop in mean lake temperature during December is less than in October and November in Lake Michigan. However, the figure indicates that the drop in mean lake temperature during December 1975 in Lake Michigan was about the same as the drop in October and November and was greater than the climatological drop. Thus, there appears to have been unusually severe cold air-warm lake temperature differences in Lake Michigan during December 1975. The TDL predictions during December 1975 in Lake Michigan may tend to be low. Figure 42 indicates very little cooling in Lake Michigan during September 1975. This may partially account for the relatively good agreement between predictions and measurements at Michigan City during September 1975 (see App. E).

Another factor to consider in evaluating the TDL model is the use of identical surface wind forecast equations in every lake sector. This obscures any systematic local effects on the wind. One effect which is possibly germane to this study can be qualitatively considered. Severe fall storms in the Great Lakes often consist of low-pressure systems from the west or northwest and sweeping across the lakes from west to east. The airmasses are often cold relative to the lake water which results in considerable vertical mixing in the air over the lake and very effective wave generation.

The air-lake temperature difference during such fall storms is often more unstable than the fall average temperature difference. For such storms the actual wave heights tend to exceed TDL forecasts. Although partially accounted for empirically insofar as PE model parameters can be correlated with air-temperature difference during October to December, such variations of the air-lake temperature difference about the seasonal mean produce some of the scatter in Figures 17 and 18. Since an airmass from the west or northwest during fall tends to be warmed as it crosses the westerly lakes (Superior and Michigan), the temperature differences over the easterly lakes may also tend to be less drastic. Hence, the effect of air-lake temperature difference might systematically be more evident in Lake Michigan than in Lake Erie, and more evident in western than eastern Lake Erie. For winds which are inordinately cold relative to the seasonal average for winds of that speed, a tendency might be observed for hindcasts in Lake Michigan and western Lake Erie to be

lower relative to actual wave heights than they would be in eastern Lake Erie. However, this effect has not been identified in the data collected in this study.

A similar mechanism could act when a warm airmass moving from west to east encounters Lake Michigan. The airmass is cooled by the lake and becomes more effective at generating waves in Lake Erie than in Lake Michigan. For such cases, the forecast heights in Lake Michigan might be expected to be higher relative to measurements than in Lake Erie; e.g., the overprediction of the very low measured heights at Michigan City on 27 to 30 September 1975 may be partially due to this effect.

In the TDL surface wind model, a single windspeed and direction are assigned to each lake sector. This wind is considered to be the wind at forecast time along the fetch for every wave forecast point in the sector. If the true windspeed and direction vary in the sector, or more importantly, if the fetch is long and extends into other sectors where windspeeds and directions are likely to vary, the TDL model continues to treat the winds in the sector of the forecast point as if they apply along the entire fetch.

Since this procedure sometimes overestimates, but never underestimates the distance along which the wind direction is reasonably constant, it leads to a tendency to overestimate significant wave height for cases in which the geographical fetch is long and the wind direction is variable. The importance of this limitation should be diminished during major storms associated with large-scale meteorological patterns giving less variable winds over the lakes.

An example of a situation in which the geographical fetch is long and the wind direction is variable is provided by Michigan City data from the morning of 29 October 1975. The TDL model predicted winds from the north for the first three observations on 29 October. The fetch from the north at Michigan City is exceptionally long. The winds over Lake Michigan during this time were caused by circulation around a high-pressure center west of Lake Michigan (see Fig. 43). Wind directions around the perimeter of Lake Michigan varied over nearly a 90° arc (Fig. 43). Thus, the TDL model overestimate of significant height by about 0.75 meter (2.5 feet) for each of the three observations may be due to overestimation of the fetch. Two similar examples also associated with winds from the north at Michigan City due to a high-pressure center west of Lake Michigan, are provided by the evening of 25 September and the morning of 26 September and by the evening-morning of 1 and 2 October.

The effect of ignoring ice formation in the TDL model leads to potential overestimates of fetch length from early January to late March, which in turn, may lead to overestimates of significant wave height. This consideration does not appreciably affect comparisons with gage data in this study.

Wind duration time is estimated in the TDL model as either 3, 9, 15, 21, 27, or 33 hours on the basis of PE model forecasts made at 6-hour intervals. Storm duration times are never precisely correct, but the

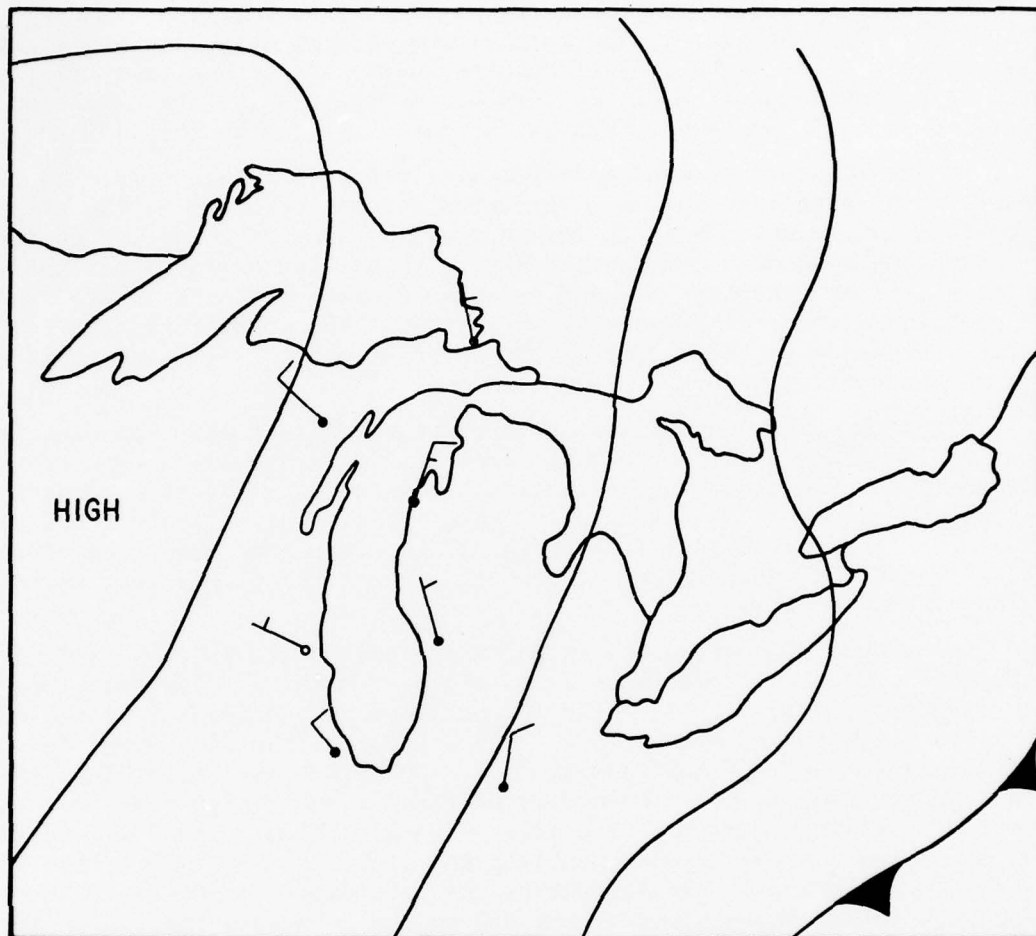


Figure 43. Weather map for 0700 e.s.t., 29 October 1975 (from NOAA Environmental Data Service daily weather maps).

error in duration time is normally less than 6 hours. The errors are not expected to be systematic and are expected to merely increase the scatter of TDL wave forecasts about the true values.

An example of the effect of a TDL error in estimating duration time is offered by the data from Presque Isle between 0700 and 1300, 13 September 1975 (App. B). At 0700, measured wave heights were rising rapidly until about 1300. The TDL model identified the trend for increasing wave heights but underestimated the magnitude of the increase by half a meter, possibly due to an underestimate of duration.

Another example may be obtained from the record for Cleveland from 0100 to 0700 on 14 November 1975. Between these times, measured wave heights rose and then fell by about 1 meter. The TDL model almost entirely missed this rapid change because it occurred between forecast times.

As mentioned earlier, there is evidence that the Bretschneider (1970) technique used in the TDL model to forecast significant wave heights and periods overestimates significant heights by as much as 20 percent in short fetch situations (Resio and Hiipakka, 1976). This effect could further bias the TDL height estimates toward high wave heights.

Finally, the TDL wave model deals rather poorly with swell waves, which may give it a tendency to underpredict wave height in some circumstances. For example, consider a situation where a strong, uniform wind is blowing over a long fetch. Large waves will exist along much of the fetch. If the windspeed decreases considerably with little change in direction, the TDL model will heavily weight the diminished windspeed at the next forecast time, even though previously generated large waves will continue to arrive at forecast points in the downwind part of the fetch. This mechanism might lead the TDL model to underestimate significant height at downwind points on long fetches during decay of large storms. The effect is not readily apparent in Appendix E, and is probably rarely important.

A related situation can occur when wind direction changes of more than 45° occur between forecast times. The TDL model has no provision for recognizing waves generated by previous winds blowing in a different direction. Hence, the model tends to underestimate wave height in circumstances where it is important to consider waves previously generated by winds blowing in a direction much different from the wind direction at forecast time. This effect should be most apparent for the first one or two observations following an abrupt wind shift of more than 45° after the wind has been blowing long and hard over a long fetch. Possible illustrations of this effect at Michigan City are the last observation on 13 September 1975 and the last observation on 2 October 1975.

Summary. Wave forecasts produced by the TDL model are useful for NWS applications, but are not as accurate as hindcasts generated by the WES model developed by Resio and Vincent (1976c, 1976d, 1977a, 1977b, 1978a). One factor limiting the accuracy of the forecasts is the statistical derivation of the surface wind model which gives a tendency for overestimates

of windspeed during low and moderate winds and underestimates during very high winds. Other limiting factors are the gross consideration of air-lake temperature differences, the use of identical surface wind forecast equations in every lake sector, lack of refinement in estimating fetch and wind duration, basic shortcomings of the Bretschneider wave forecasting technique, and difficulties in treating swell waves. The TDL model could be modified to treat these limiting factors more satisfactorily; however, the computer run time for a more sophisticated model could increase dramatically. For TDL's applications, a greatly increased computer run time cannot be tolerated.

VII. SUMMARY OF THE EVALUATION OF WES AND TDL MODELS

Wave estimates from the WES spectral hindcasting model developed by Resio and Vincent (1976c, 1976d, 1977a, 1977b, 1978a) were compared with accelerometer buoy measurements obtained at two Lake Erie sites during nine storms in fall 1975. The hindcast significant heights are generally within 0.5 meter of the gage significant heights, but occasional differences of over 1 meter are observed. The mean hindcast significant height at both sites differs by only 0.1 meter from the mean gage significant height. The hindcast peak spectral periods are generally within 1 second of the gage peak spectral periods. For high wave conditions (significant height greater than or equal to 1 meter) the hindcast peak periods have a tendency to be shorter than the gage peak periods, although the mean peak periods differ by less than 0.2 second at both sites.

The WES hindcasts for situations where fetches are reasonably simple and well defined are generally excellent. The hindcast spectra for such situations are very similar to the gage spectra. However, they have a tendency to contain slightly more energy than the gage spectra and hence lead to hindcast significant heights which are slightly higher than gage significant heights.

The WES hindcast spectra for situations where fetches are ambiguous and change significantly with small changes in wind direction do not have multiple peaks, which often appear in the gage spectra for such situations. The hindcast spectra are usually missing the lowest frequency peak, which gives the hindcasts a tendency to underestimate spectral energy and significant height.

Estimates from the TDL significant wave forecasting model were compared with accelerometer buoy measurements obtained at two Lake Erie sites and three Lake Michigan sites during fall 1975 and fall 1976. Forecast significant heights show a clear tendency to be higher than gage significant heights. At two sites, the forecast significant heights during very high wave conditions indicate a tendency to be lower than gage significant heights. The mean forecast significant height is 0.1 to 0.5 meter greater than the mean gage significant height at each site. Forecast significant periods are usually within 2 seconds of gage peak spectral periods. The mean forecast significant period is within 0.3 second of the mean gage peak period at four of the five sites. The forecast periods are considerably less variable than the gage periods at all but one site.

LITERATURE CITED

- ALLENDER, J.H., "Comparison of Model and Observed Currents in Lake Michigan," *Journal of Physical Oceanography*, Vol. 7, No. 5, Sept. 1977, pp. 711-718.
- BARNETT, T.P., "On the Generation, Dissipation, and Prediction of Ocean Wind Waves," Ph.D. Dissertation, University of California, San Diego, Calif., 1966.
- BRETSCHNEIDER, C.L., "Forecasting Relations for Wave Generation," *Look Lab Hawaii*, Vol. 1, No. 3, July 1970, pp. 31-34.
- CARDONE, V.J., "Specification of the Wind Distribution in the Marine Boundary Layer for Wave Forecasting," Technical Report 69-1, Geophysical Sciences Laboratory, New York University, New York, 1969.
- ELDER, F.C., and SOO, H.K., "An Investigation of Atmospheric Turbulent Transfer Processes Over Water," Report No. 4, Special Report No. 29, Great Lakes Research Division, University of Michigan, Ann Arbor, Mich., May 1967.
- ENVIRONMENTAL SCIENCE SERVICES ADMINISTRATION, "Local Climatological Data Annual Summary with Comparative Data, 1966," Environmental Data Service, Asheville, N.C., 1967.
- FEIT, D.M., and BARRIENTOS, C.S., "Great Lakes Wind Forecasts Based on Model Output Statistics," *Proceedings of the 17th Conference on Great Lakes Research*, International Association for Great Lakes Research, 1974, pp. 725-732.
- FEIT, D.M., and GOLDENBERG, D.S., "Climatology of Surface Temperatures of Lakes Superior, Huron, Erie, and Ontario," unpublished TDL Office Note 76-16, National Oceanic and Atmospheric Administration, National Weather Service, Silver Spring, Md., Nov. 1976.
- GRUMLATT, J.L., "Great Lakes Water Temperatures, 1966-1975," Technical Memorandum ERL-GLERL-11-1, National Oceanic and Atmospheric Administration, Ann Arbor, Mich., Aug. 1976.
- HARRISON, L.P., "History of Weather Bureau Wind Measurements," Key to Meteorological Records Documentation No. 3.151, U.S. Department of Commerce, Weather Bureau, Washington, D.C., 1963.
- HASSELMANN, K., et al., "Measurements of Wind-Wave Growth and Swell Decay During the Joint North Sea Wave Project JONSWAP," Deutsches Hydrographisches Institut, Hamburg, Germany, 1973.
- KRAUS, E.B., *Atmosphere-Ocean Interaction*, Clarendon Press, Oxford, England, 1972.

LIU, P.C., "Applications of Empirical Fetch-Limited Spectral Formulas to Great Lakes Waves," *Proceedings of the 15th Conference on Coastal Engineering*, American Society of Civil Engineers, Vol. 1, 1976, pp. 113-128.

MITSUYASU, H., "On the Growth of the Spectrum of Wind-Generated Waves (I)," *Reports of Research Institute for Applied Mechanics*, Kyushu University, Fukuoka, Japan, Vol. 16, No. 55, 1968, pp. 459-482.

MITSUYASU, H., "On the Form of Fetch-Limited Wave Spectrum," *Coastal Engineering in Japan*, Vol. 14, Dec. 1971, pp. 7-14.

NATIONAL OCEANIC AND ATMOSPHERIC ADMINISTRATION, "Summary of Synoptic Meteorological Observations for Great Lakes Areas," Vols. 1 and 3, National Climatic Center, Asheville, N.C., Jan. 1975.

PEACOCK, H.G., "CERC Field Wave Gaging Program," *Proceedings of the International Symposium on Ocean Wave Measurement and Analysis*, American Society of Civil Engineers, Sept. 1974, pp. 170-185.

PIERSON, W.J., "The Loss of Two British Trawlers--A Study in Wave Refraction," *The Journal of Navigation*, Vol. 25, No. 3, July 1972, pp. 291-304.

PORE, N.A., "Operational Marine Environmental Prediction Programs of the Techniques Development Laboratory," unpublished TDL Office Note 76-10, National Oceanic and Atmospheric Administration, National Weather Service, Silver Spring, Md., June 1976.

PORE, N.A., "Automated Great Lakes Wave Forecasts," Technical Memorandum NWS TDL-63, National Oceanic and Atmospheric Administration, National Weather Service, Silver Spring, Md., Feb. 1977.

RESIO, D.T., and HIIPAKKA, L.W., "Great Lakes Wave Information," *Proceedings of the 15th Conference on Coastal Engineering*, American Society of Civil Engineers, Vol. 1, 1976, pp. 92-112.

RESIO, D.T., and VINCENT, C.L., "Lake Erie," Report 1, Technical Report H-76-1, *Design Wave Information for the Great Lakes*, U.S. Army Engineer Waterways Experiment Station, Vicksburg, Miss., Jan. 1976a.

RESIO, D.T., and VINCENT, C.L., "Lake Ontario," Report 2, Technical Report H-76-1, *Design Wave Information for the Great Lakes*, U.S. Army Engineer Waterways Experiment Station, Vicksburg, Miss., Mar. 1976b.

RESIO, D.T., and VINCENT, C.L., "Estimation of Winds Over the Great Lakes," Miscellaneous Paper H-76-12, U.S. Army Engineer Waterways Experiment Station, Vicksburg, Miss., June 1976c.

RESIO, D.T., AND VINCENT, C.L., "Lake Michigan," Report 3, Technical Report H-76-1, *Design Wave Information for the Great Lakes*, U.S. Army Engineer Waterways Experiment Station, Vicksburg, Miss., Nov. 1976d.

- RESIO, D.T., and VINCENT, C.L., "Test of Nondimensional Growth Rates," Report 1, Miscellaneous Paper H-77-9, *A Numerical Hindcast Model for Wave Spectra on Water Bodies with Irregular Shoreline Geometry*, U.S. Army Engineer Waterways Experiment Station, Vicksburg, Miss., Aug. 1977a.
- RESIO, D.T., and VINCENT, C.L., "Lake Huron," Report 4, Technical Report H-76-1, *Design Wave Information for the Great Lakes*, U.S. Army Engineer Waterways Experiment Station, Vicksburg, Miss., Sept. 1977b.
- RESIO, D.T., and VINCENT, C.L., "Lake Superior," Report 5, Technical Report H-76-1, *Design Wave Information for the Great Lakes*, U.S. Army Engineer Waterways Experiment Station, Vicksburg, Miss., 1978a.
- RESIO, D.T., and VINCENT, C.L., "Model Verification with Observed Data," Report 2, Miscellaneous Paper H-77-9, *A Numerical Hindcast Model for Wave Spectra on Water Bodies with Irregular Shoreline Geometry*, U.S. Army Engineer Waterways Experiment Station, Vicksburg, Miss., 1978b.
- SAVILLE, T., Jr., "The Effect of Fetch Width on Wave Generation," TM-70, U.S. Army, Corps of Engineers, Beach Erosion Board, Washington, D.C., Dec. 1954.
- SNYDER, F.F., "Evaporation on the Great Lakes," Extract of Publication No. 53, International Association of Scientific Hydrology, Commission of Land Erosion, Belgium, 1960, pp. 364-376.
- THOMPSON, E.F., "Wave Climate at Selected Locations Along U.S. Coasts," TR 77-1, U.S. Army, Corps of Engineers, Coastal Engineering Research Center, Fort Belvoir, Va., Jan. 1977.
- THOMPSON, E.F., "Results from the CERC Wave Measurement Program," *Proceedings of the International Symposium on Ocean Wave Measurement and Analysis*, American Society of Civil Engineers, 1974, pp. 836-855 (also Reprint 7-74, U.S. Army, Corps of Engineers, Coastal Engineering Research Center, Fort Belvoir, Va., NTIS AD A002 114).
- U.S. ARMY, CORPS OF ENGINEERS, COASTAL ENGINEERING RESEARCH CENTER, *Shore Protection Manual*, 3d ed., Vols. I, II, and III, Stock No. 008-022-00113-1, U.S. Government Printing Office, Washington, D.C., 1977, 1,262 pp.

APPENDIX A

WES METHOD FOR ADJUSTING ANEMOMETER MEASUREMENTS TO A STANDARD SITE AND ELEVATION

To simulate the low level wind field over water from wind observations over land, Resio and Vincent (1976c) assumed that the free-air wind is the same over nearby land and water areas, that the free-air wind can be expressed as a function of the measured wind over land, and that the overwater wind can be expressed as a function of the free-air wind. However, the relation between the measured wind and the free-air wind varies with changes in anemometer design and instrument location, which occurred during the 69-year period covered by the published design wave estimates. The most important aspects of location are elevation, local surface roughness, and distance from the lake. Resio and Vincent (1976a, 1976b, 1976d, 1977b, 1978a) developed useful procedures, based partly on theory and partly on empirical data, for correcting all wind data from each station to a standard location. They did not consider the effects of changes in anemometer design. A standard elevation of 6 meters (20 feet) was chosen.

Harrison (1963) discussed the changes in design of anemometers used by the NWS. He indicated that the NWS stations have been reporting true windspeeds since 1932. However, an anemometer design in common use before 1932 led to overestimates of roughly 20 percent in the higher windspeeds reported by some NWS stations.

To adjust measured windspeeds to a standard location, Resio and Vincent used an empirical method for measurements taken after 1948. For every season and every NWS anemometer site and elevation considered, the data were used to obtain a windspeed distribution function. By adjusting the distribution function from each anemometer site to approximate the distribution function from the standard local site and at the standard elevation (6 meters), a linear equation expressing standardized windspeed as a function of anemometer windspeed was obtained.

The empirical approach requires considerable data processing. Since overland wind measurements taken before 1948 are not available in computer-readable form, the empirical approach was impractical for establishing adjustment factors for pre-1948 anemometer sites and elevations. Instead, a theoretical approach was used to relate overland wind measurements to overwater winds. For anemometer sites more than about 8 kilometers inland from the lake, neutral stability was assumed over land and a simple logarithmic windspeed profile was used to adjust wind measurements to the standard elevation.

This approach was also tested on some post-1948 wind data and was found to be comparable to the empirical approach except where the anemometer was located more than several kilometers from the standard site. Spatial relocations of anemometers before 1948 were generally small; however, relocations as large as five city blocks near Lake Erie (Erie, Pennsylvania), 6 kilometers (3.7 miles) near Lake Ontario (Rochester,

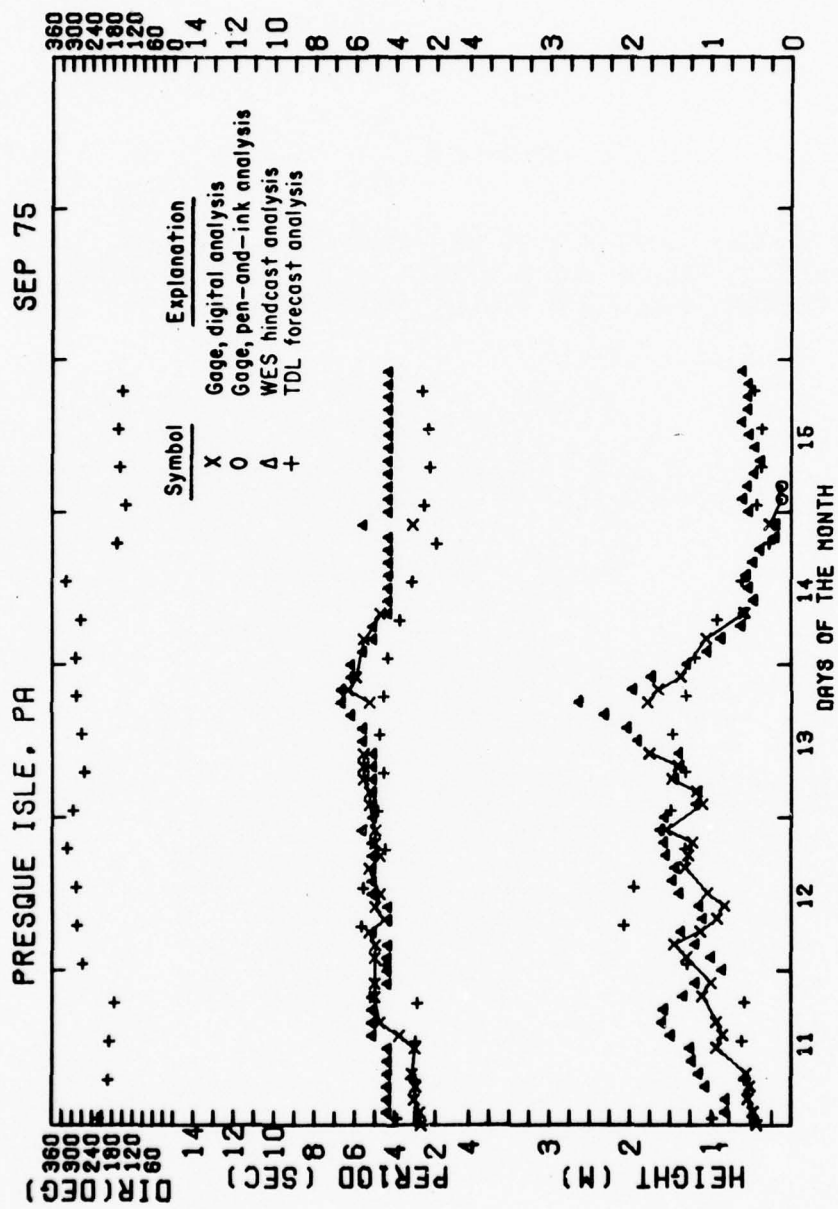
New York), and 11 kilometers (7 miles) near Lake Michigan (Muskegon, Michigan) have been reported in the station location histories included in Local Climatological Data summaries for NWS stations (Environmental Science Services Administration, 1967).

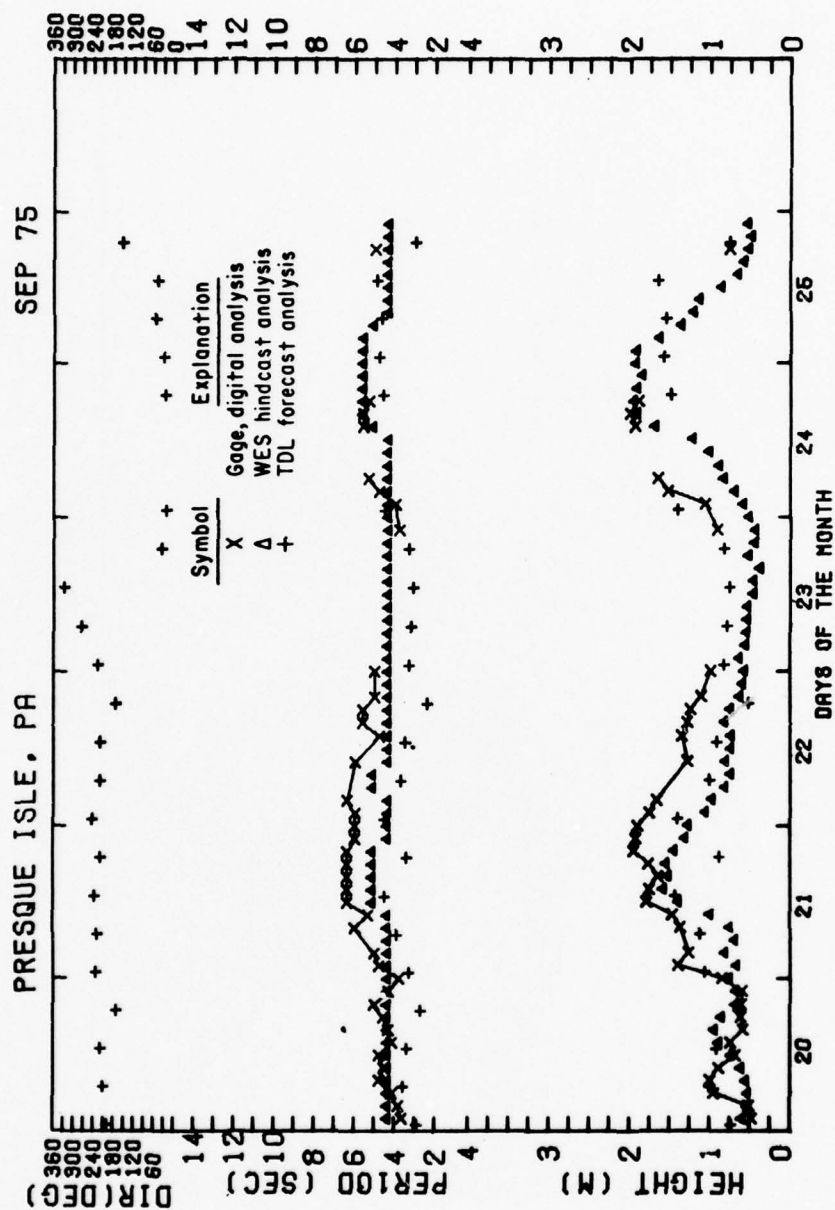
For data from pre-1948 anemometer sites close to the lake, the measurements were assumed to be representative of the overland wind profile for offshore winds and the logarithmic profile was used to adjust the measurements to standard overland elevations; for onshore winds, measurements were assumed to be representative of the overwater profile. Theoretical expressions for the overwater wind profile were used to adjust the measurements to the standard overwater elevation. The expressions are developed in Resio and Vincent (1976c), although much of the development and all of the final equations are identical to those given by Cardone (1969).

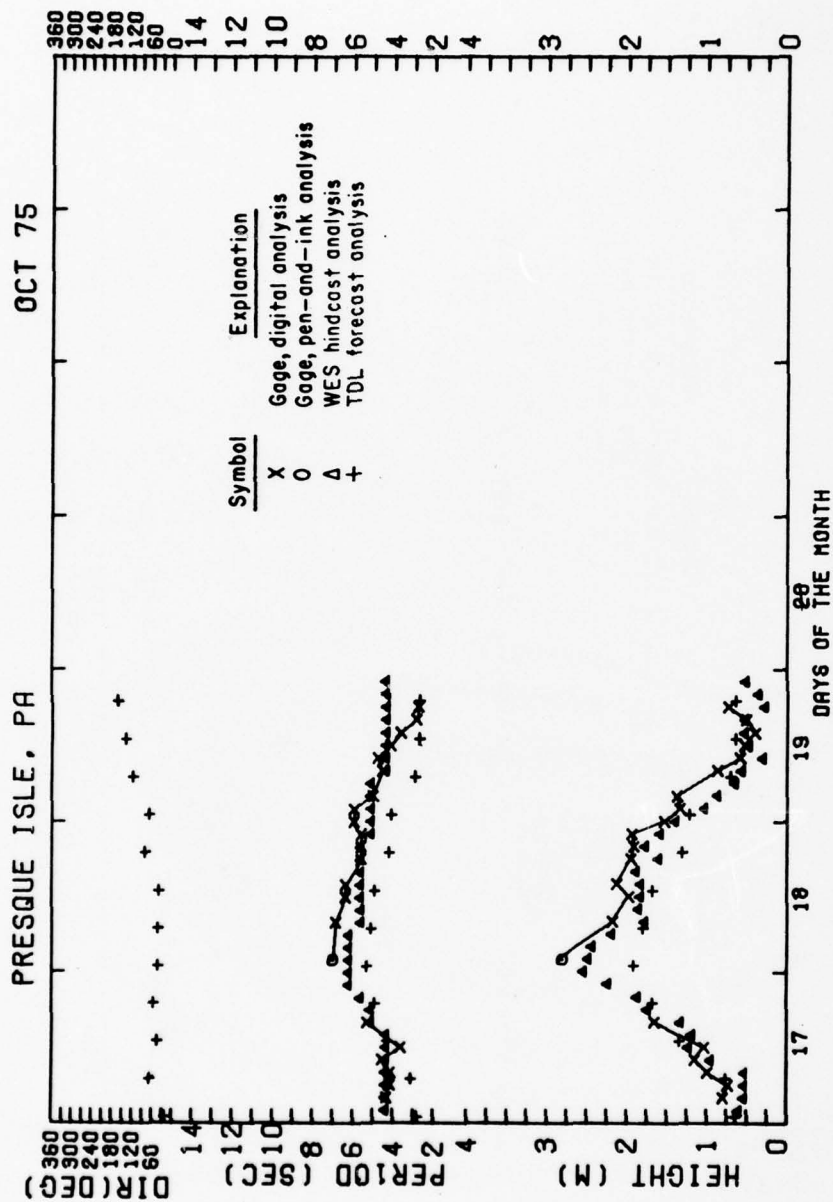
Thus, in all of the post-1948 cases the overland wind estimate at the standard site and elevation was calculated from the measured wind by a simple linear equation with empirically determined coefficients. A linear relationship was also used for pre-1948 data when the anemometer was located more than 8 kilometers inland or when the winds were blowing offshore. The only situation where a linear relationship was not used was when: (a) the measurements were taken before 1948, (b) the anemometer was located within 8 kilometers of the lake, and (c) the winds were blowing onshore. In this special situation the overwater winds were estimated directly from the anemometer measurements using the WES planetary boundary layer model.

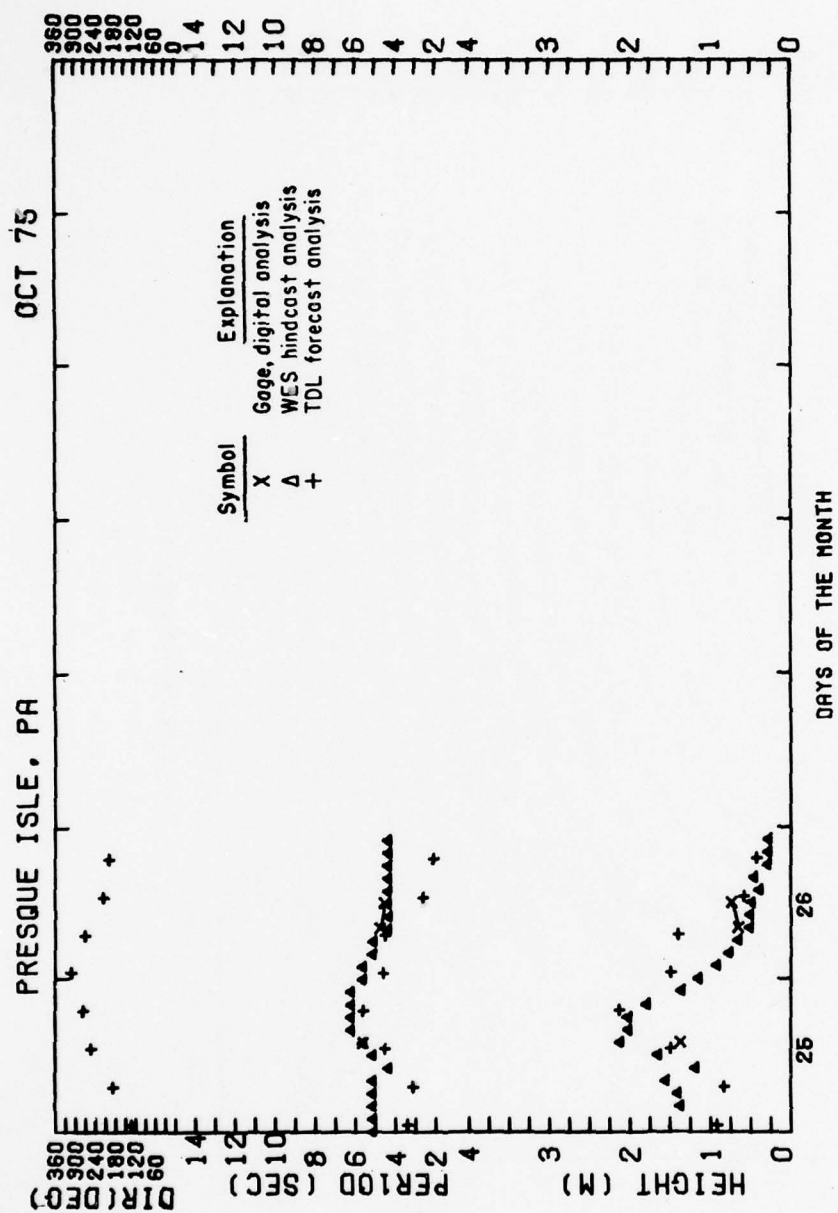
APPENDIX B

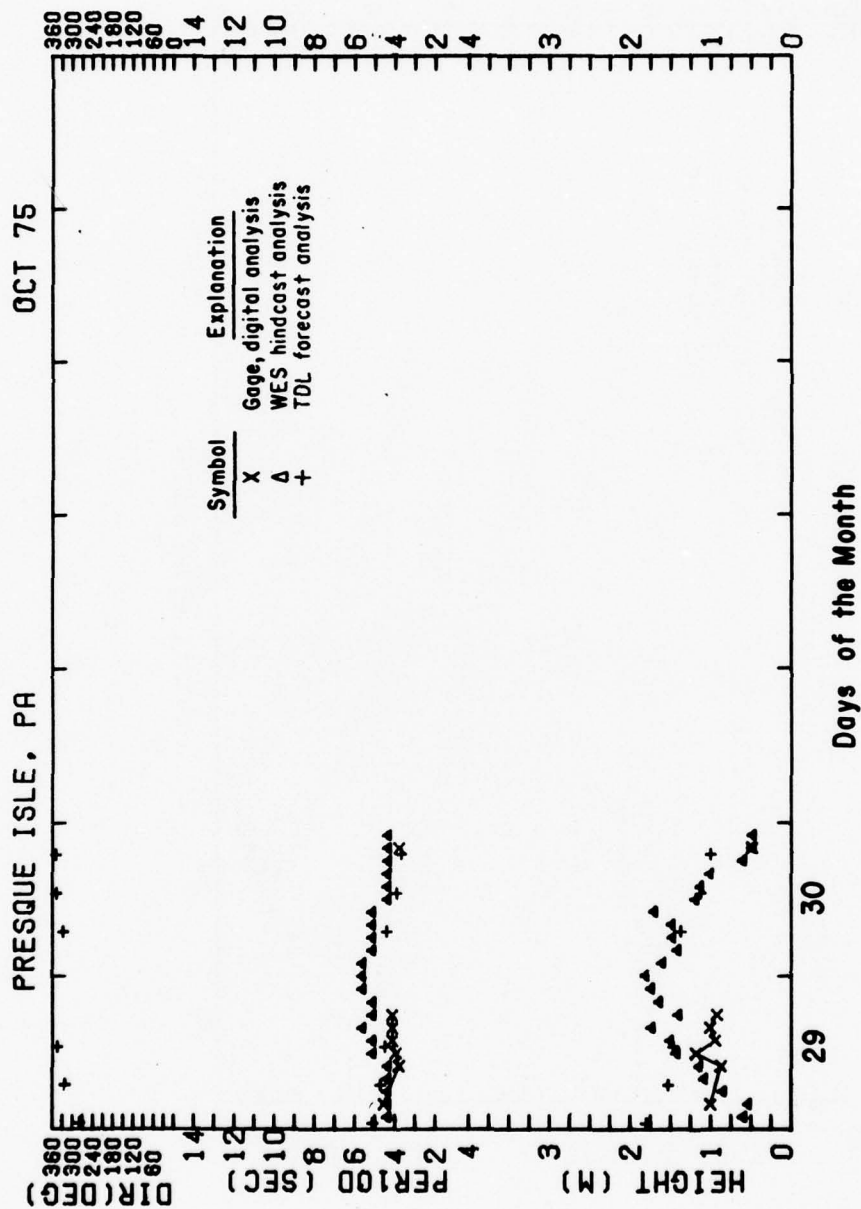
TIME-HISTORY PLOTS OF WES, TDL, AND GAGE SIGNIFICANT
WAVE HEIGHT, PERIOD, AND DIRECTION FOR FALL 1975 STORMS
AT PRESQUE ISLE, PENNSYLVANIA, AND CLEVELAND, OHIO

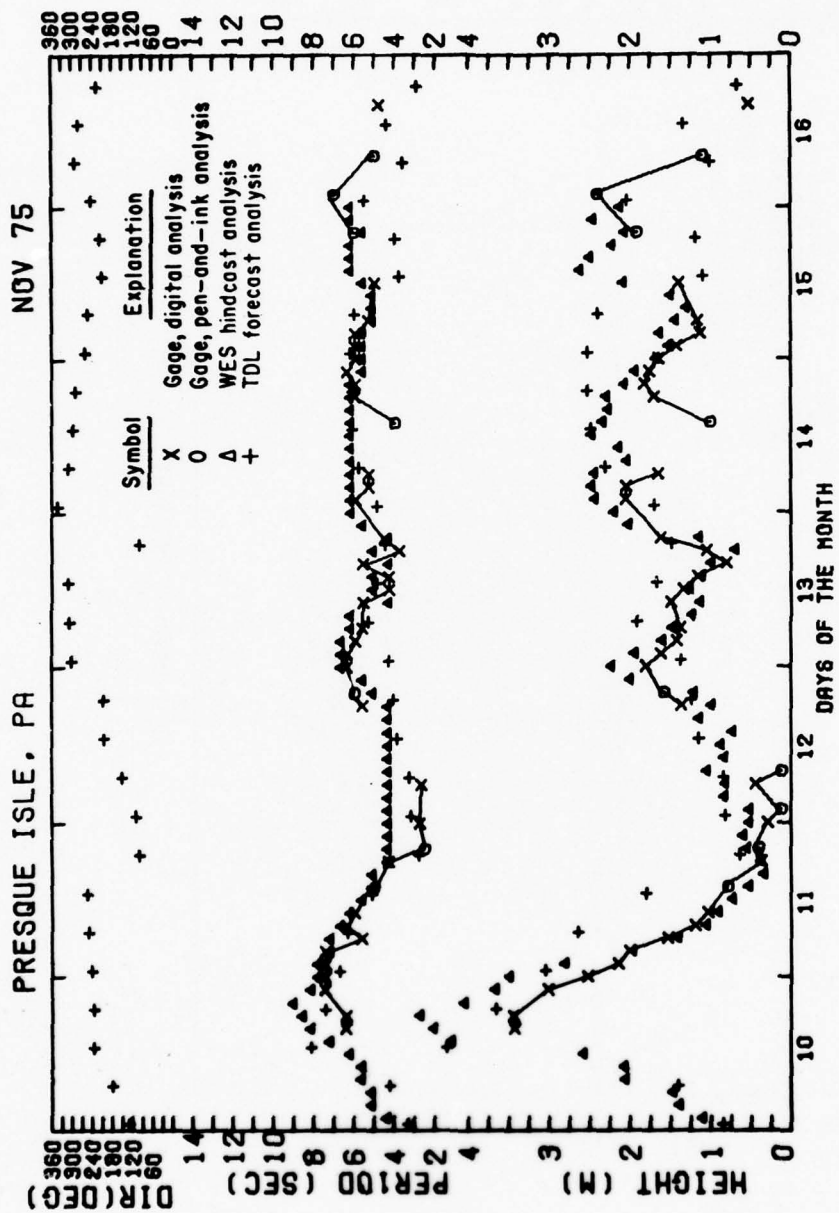


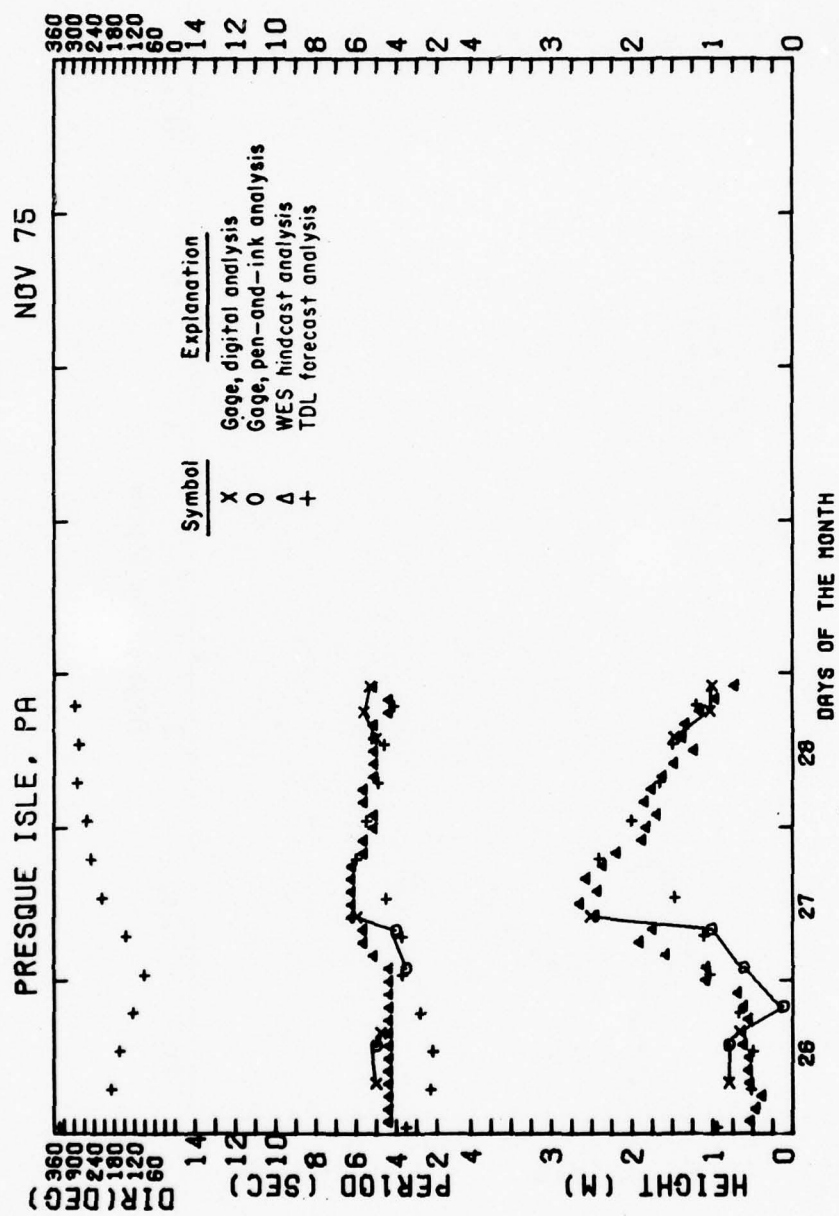


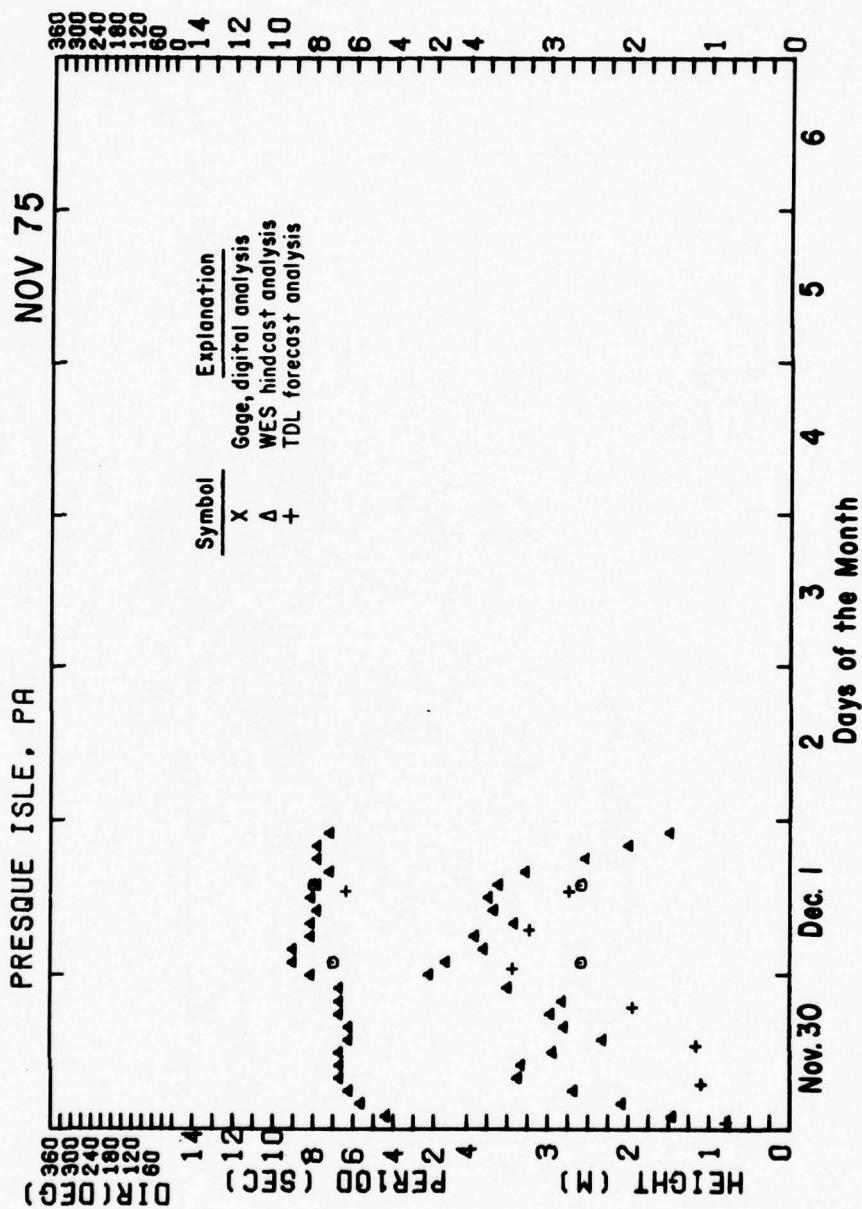


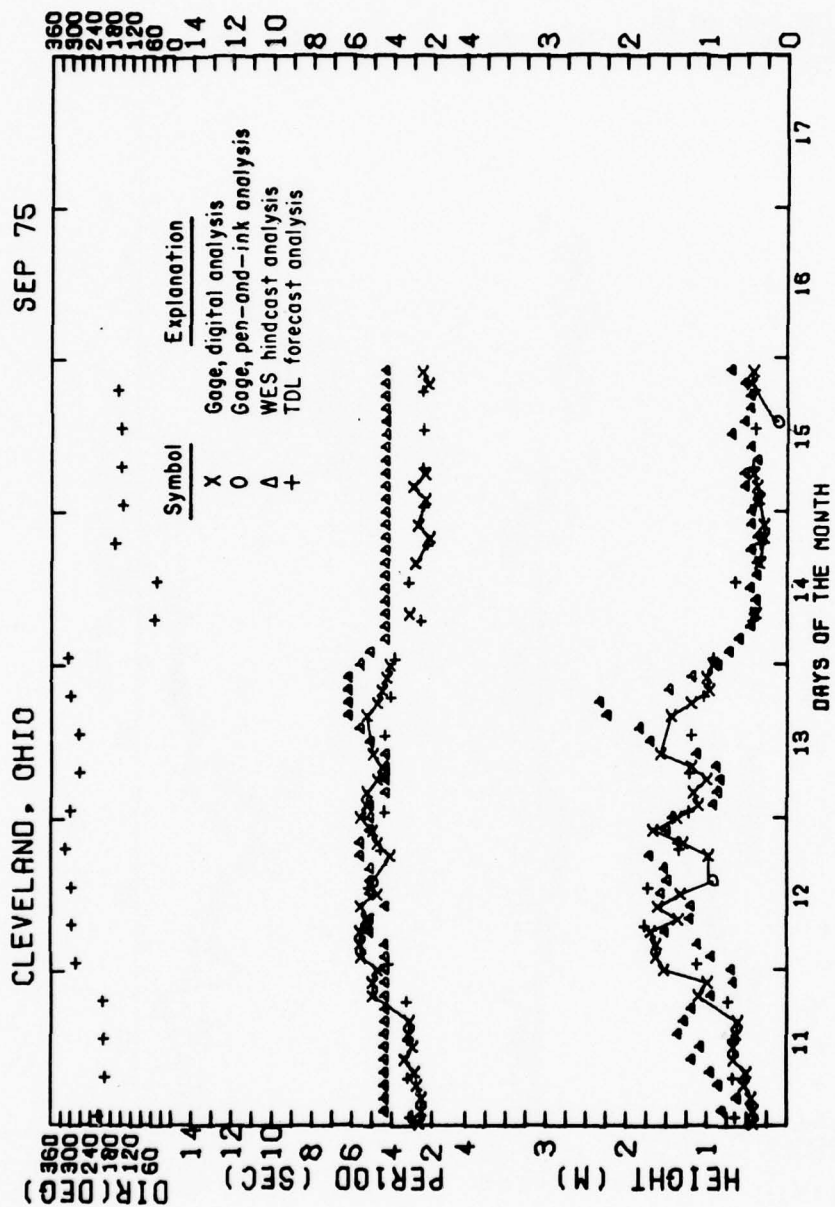


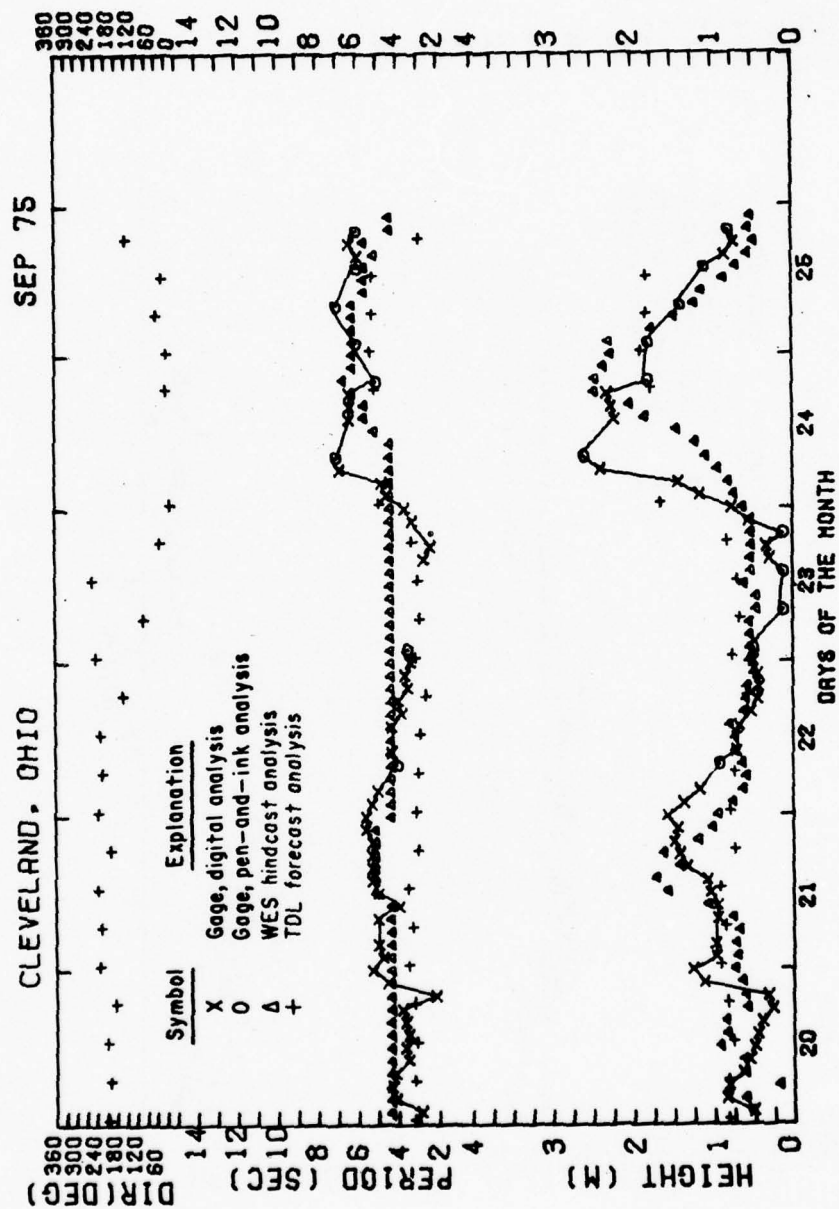


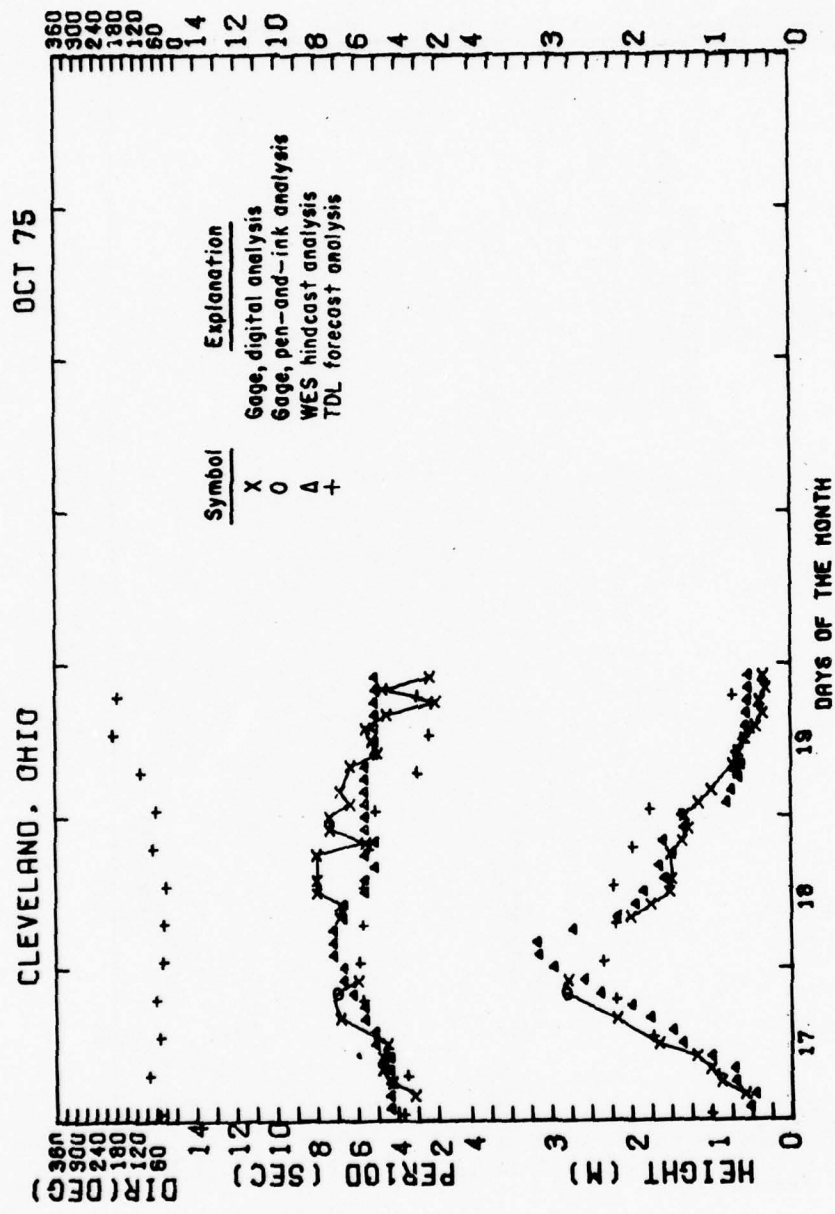


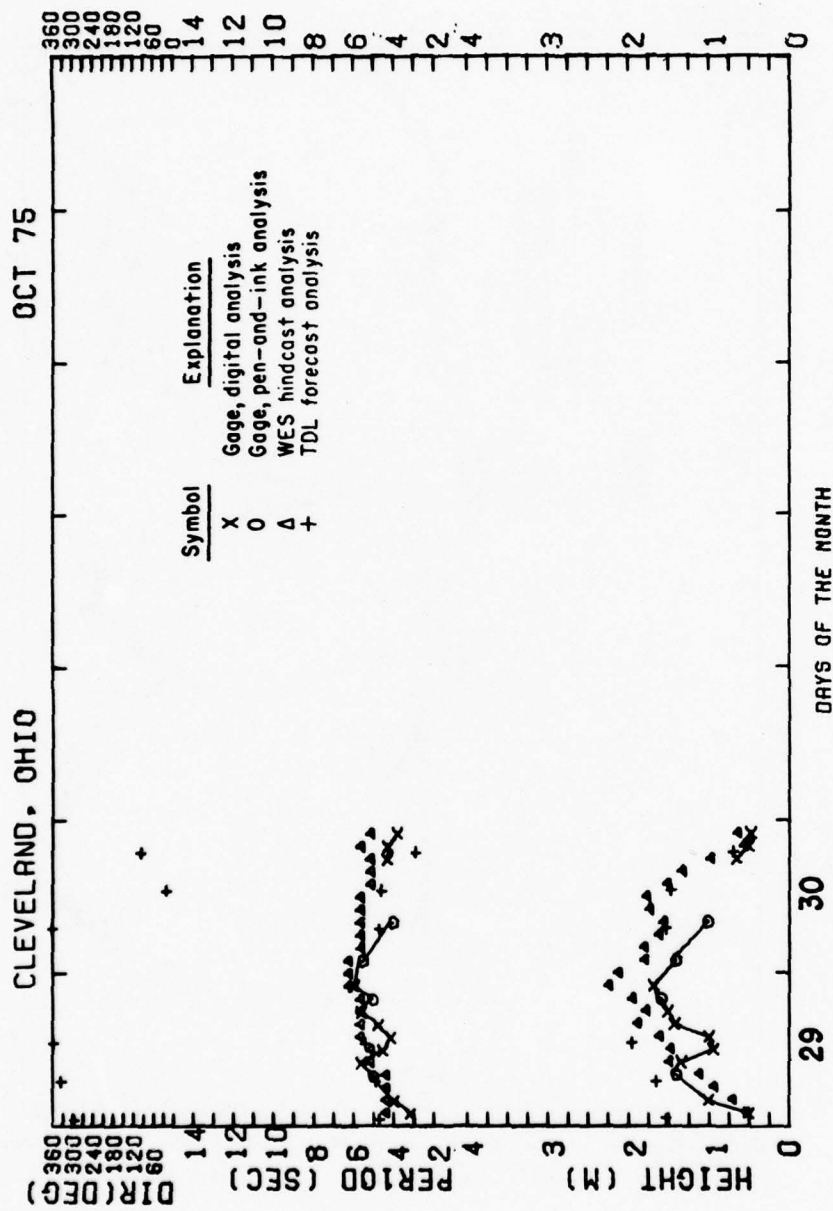


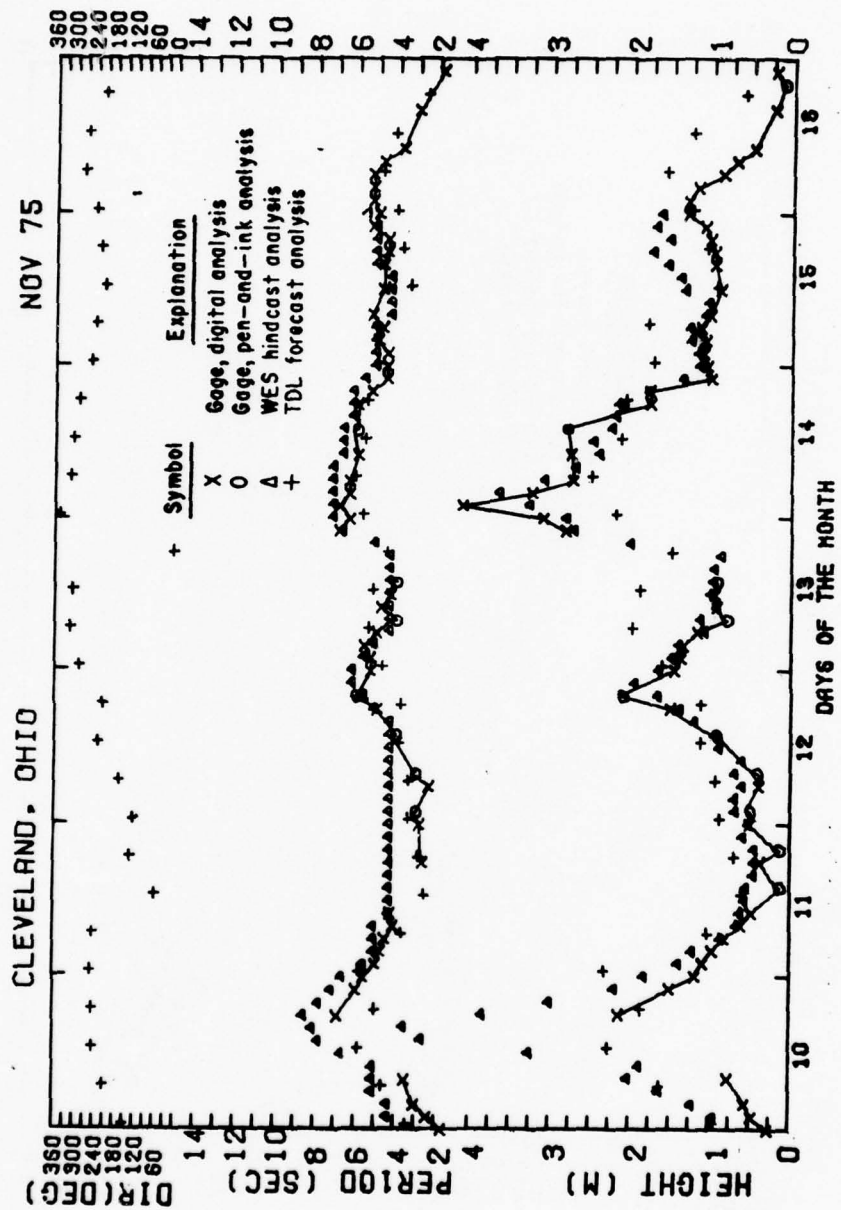


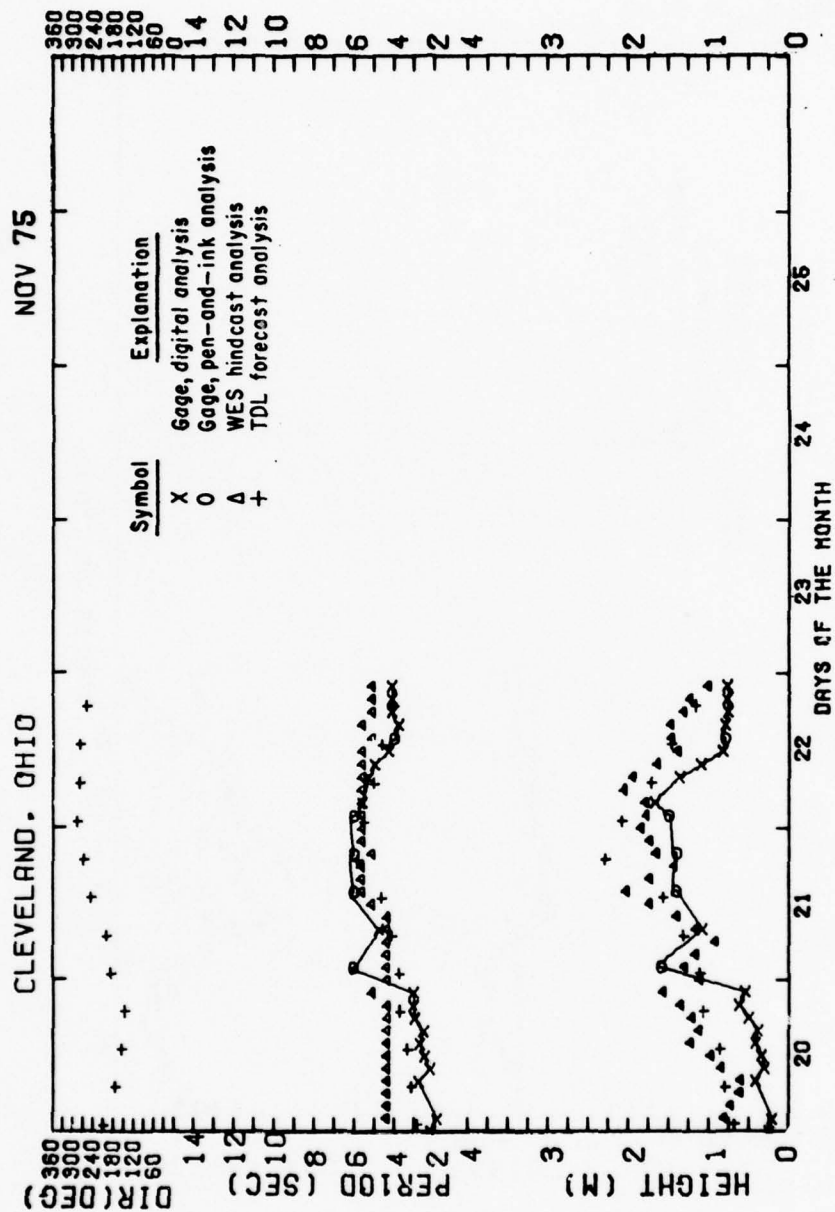


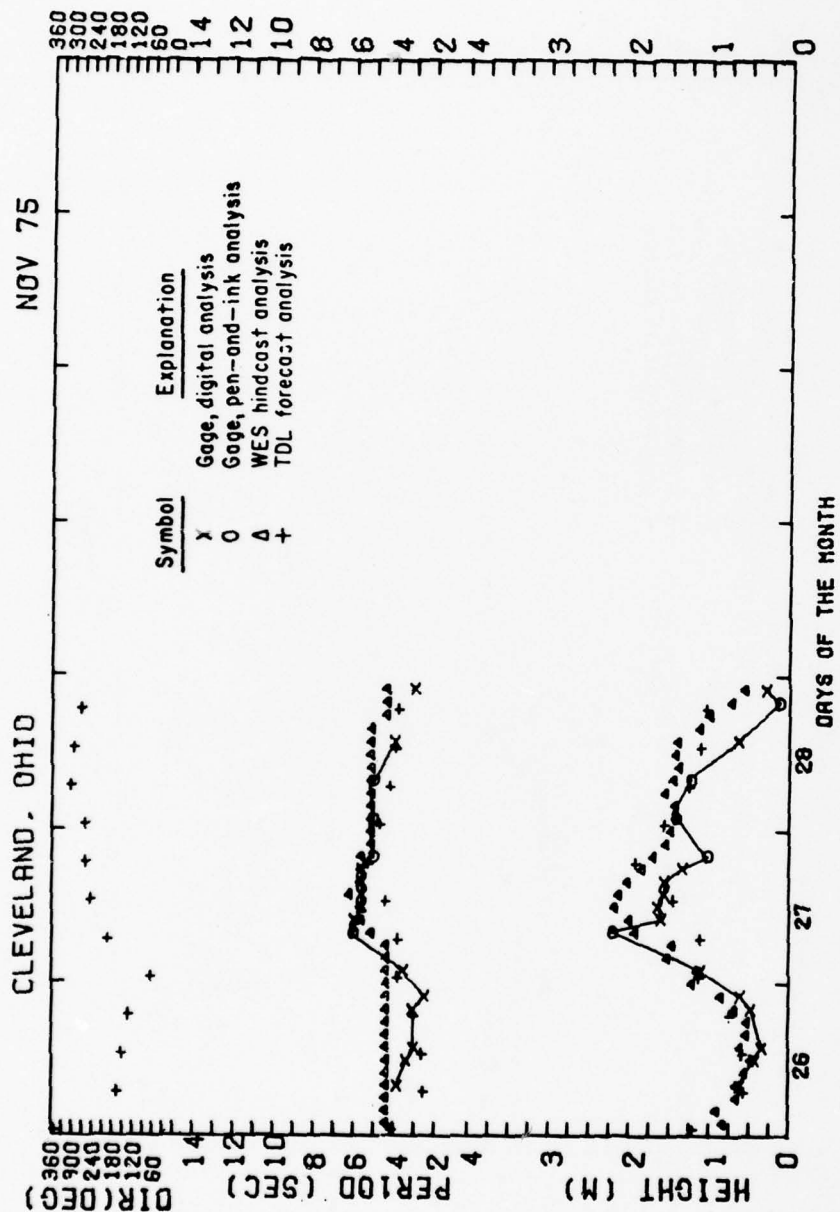


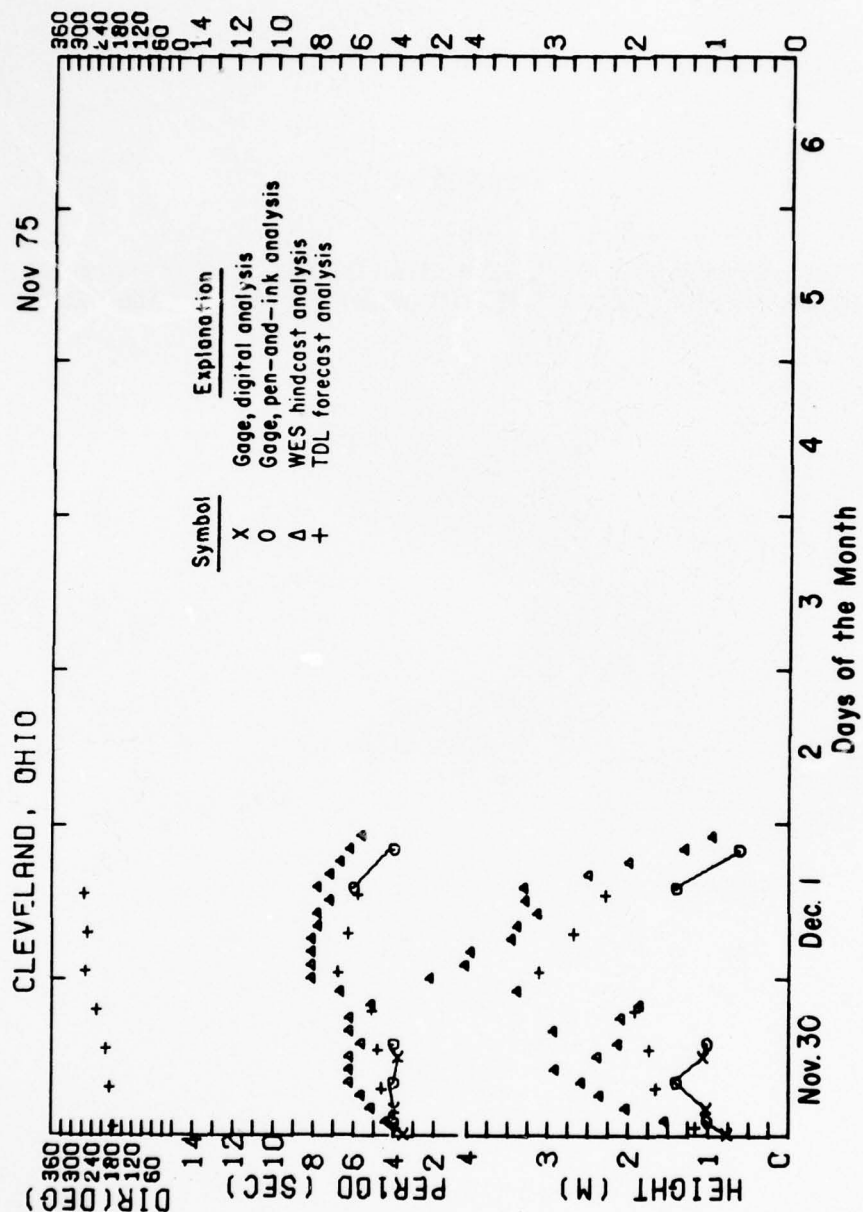






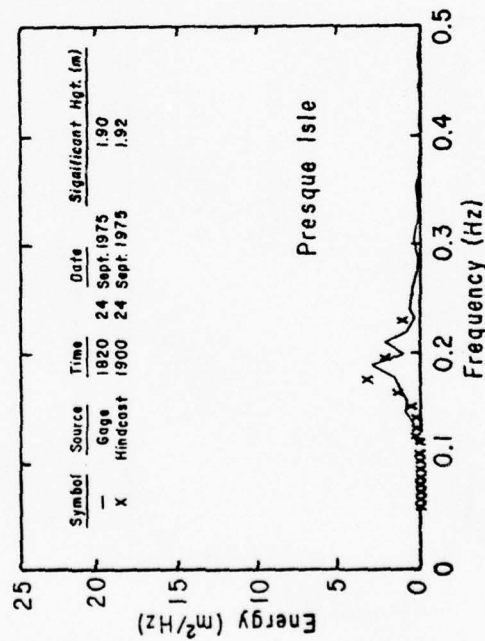
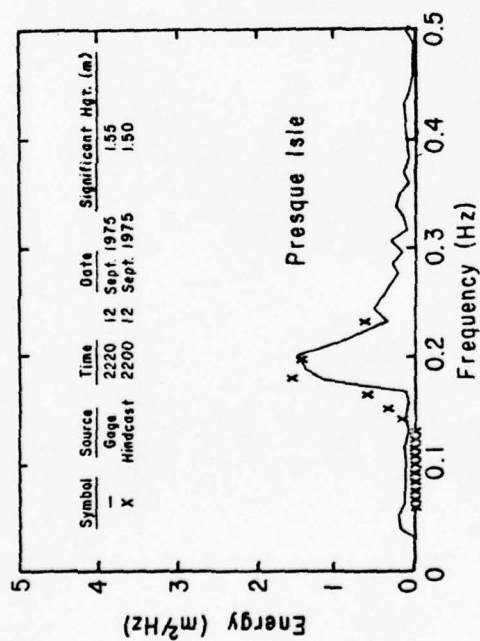
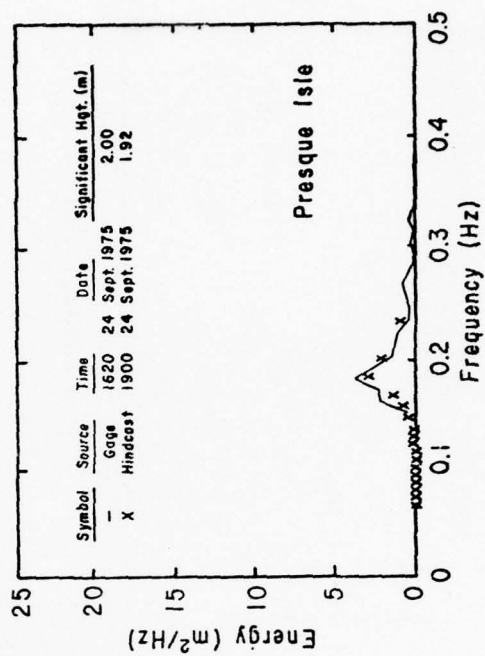
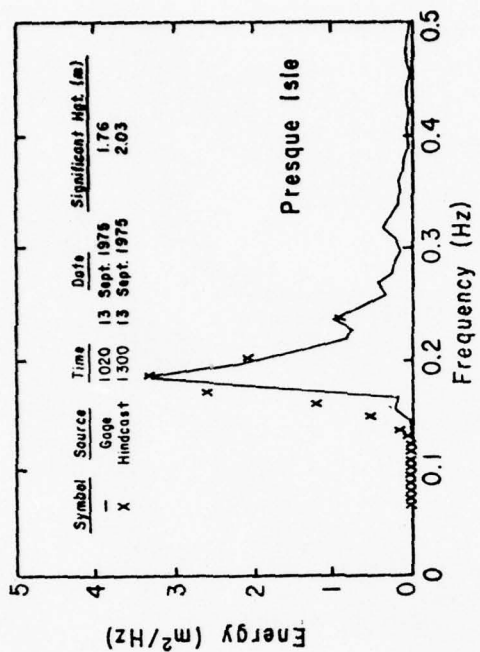


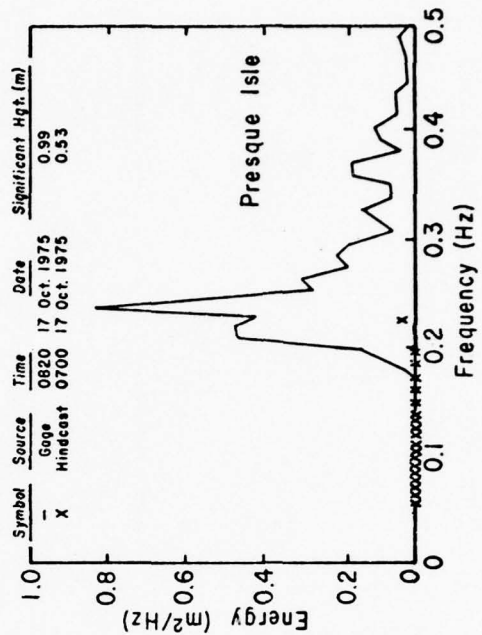
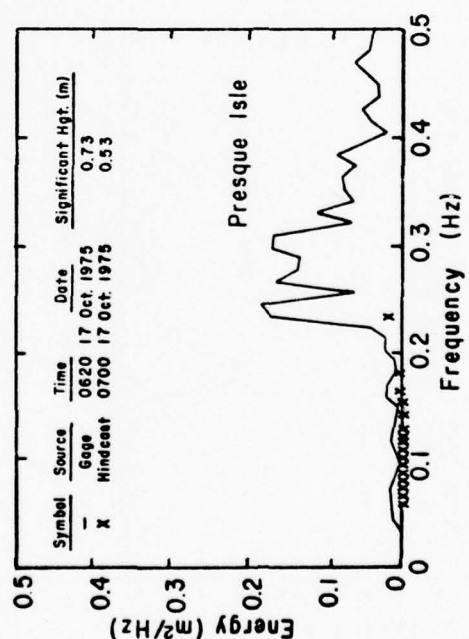
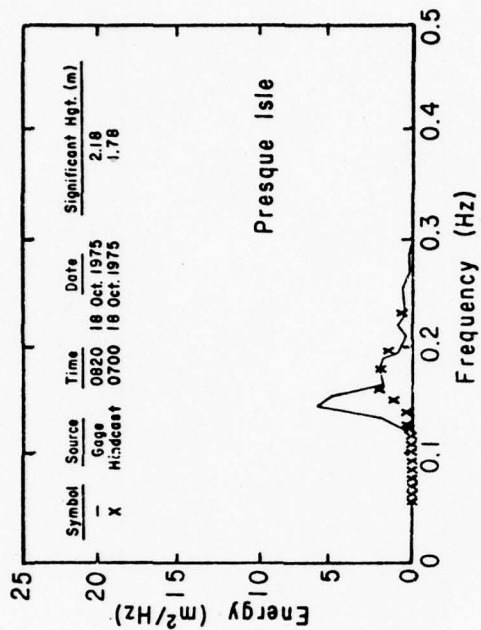
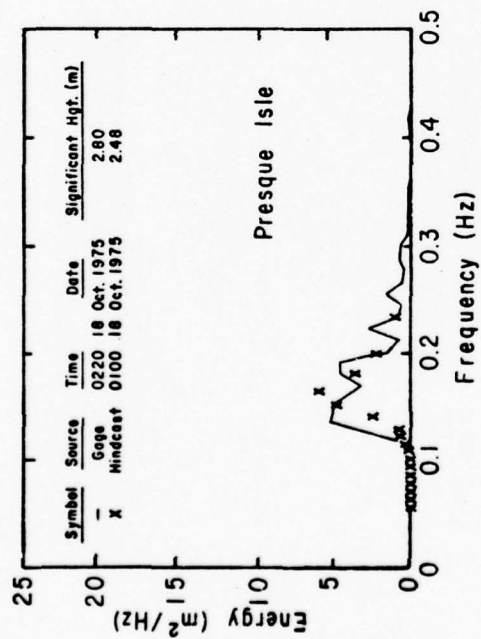


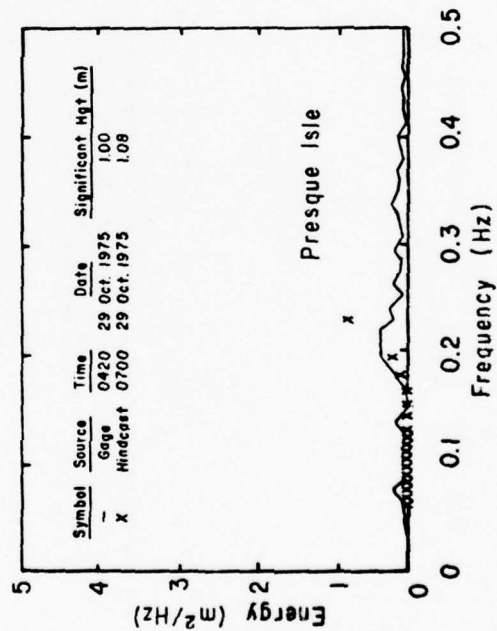
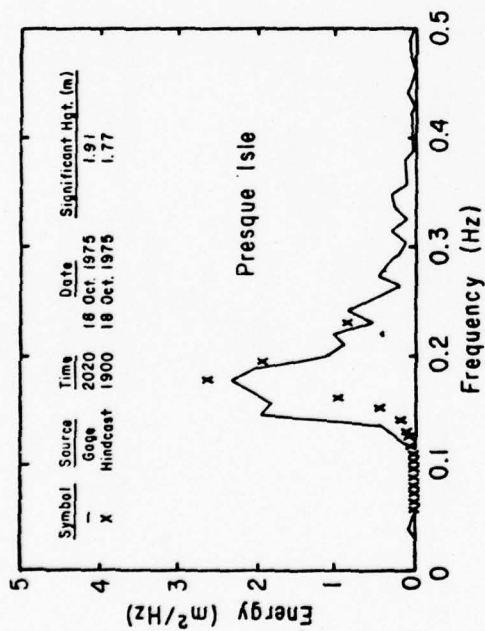
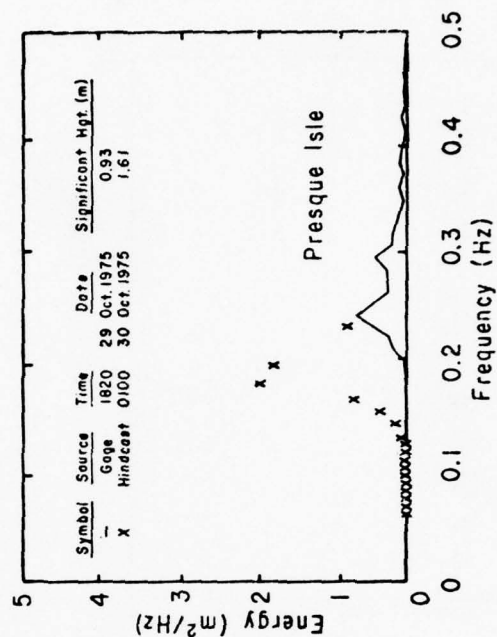
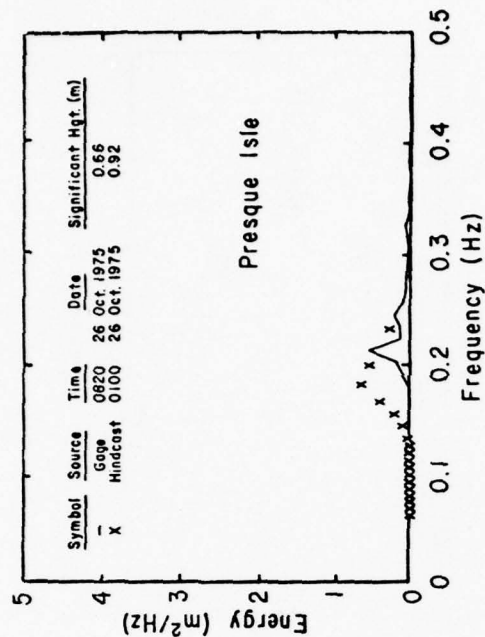


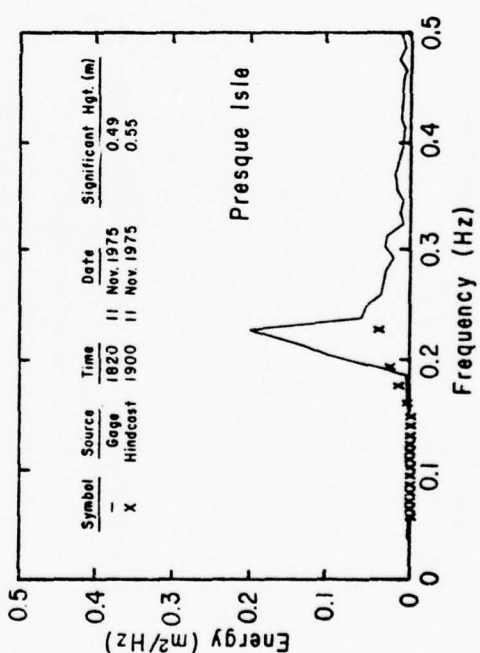
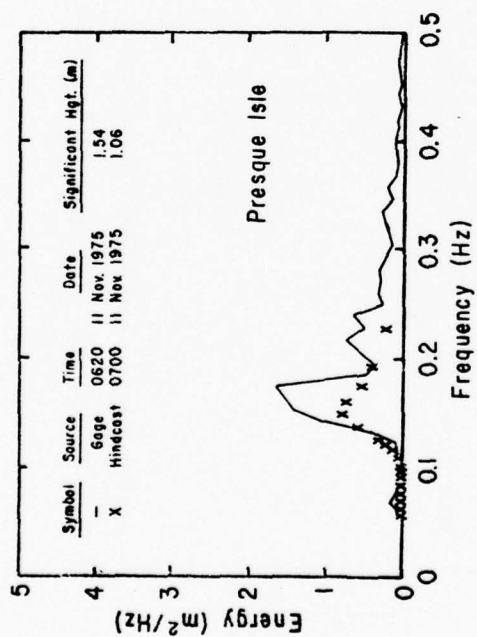
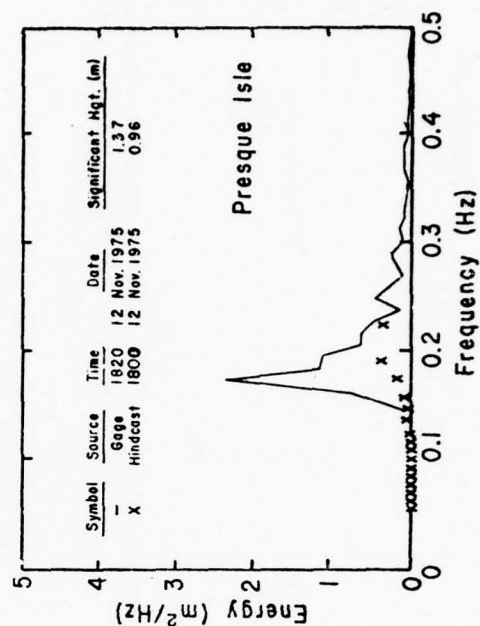
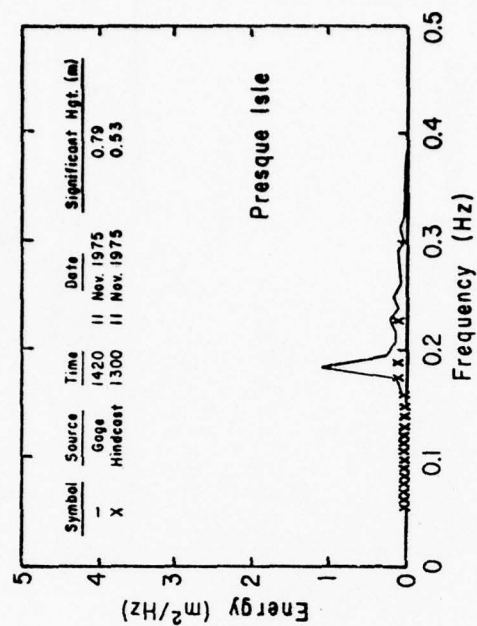
APPENDIX C

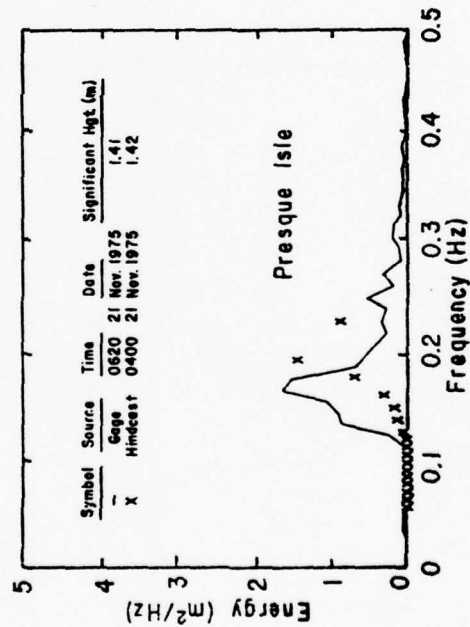
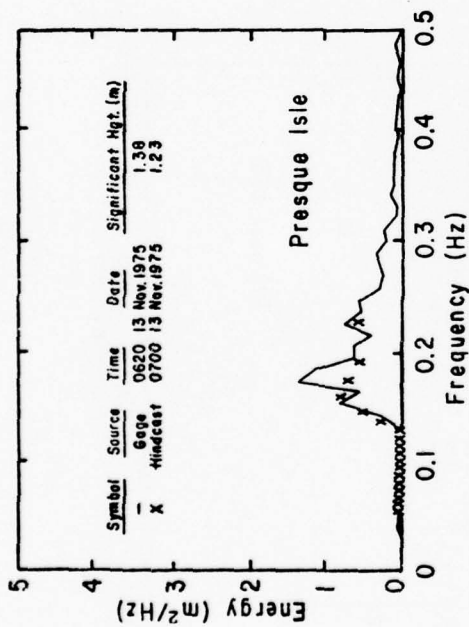
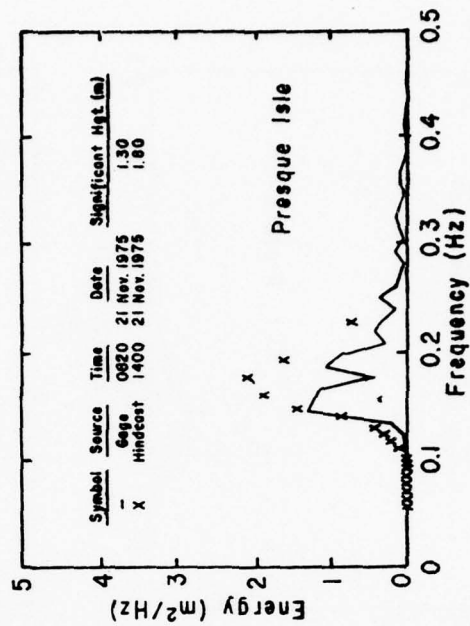
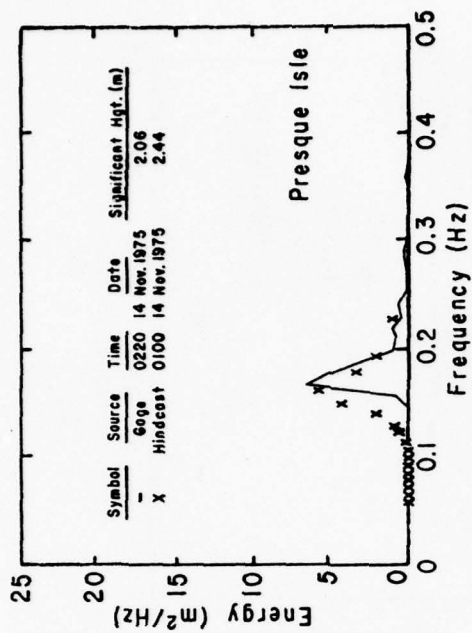
SPECTRAL COMPARISONS OF LESSER QUALITY DUE TO POOR MATCHING
OF HINDCAST-GAGE RECORD TIMES OR TO NOISE IN THE GAGE RECORD

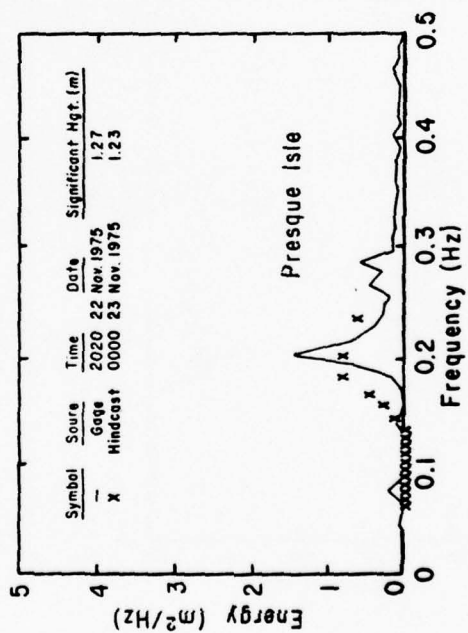
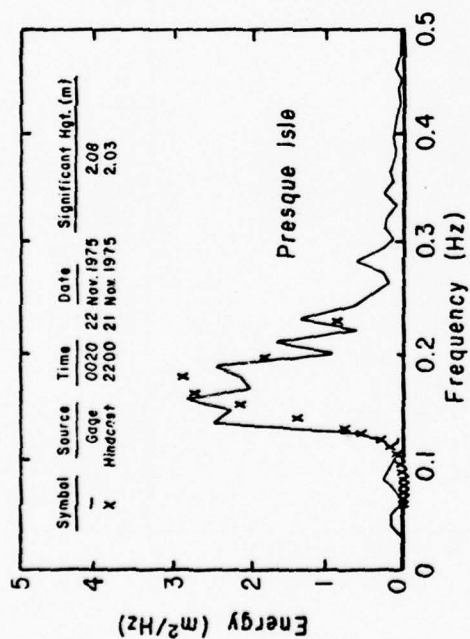
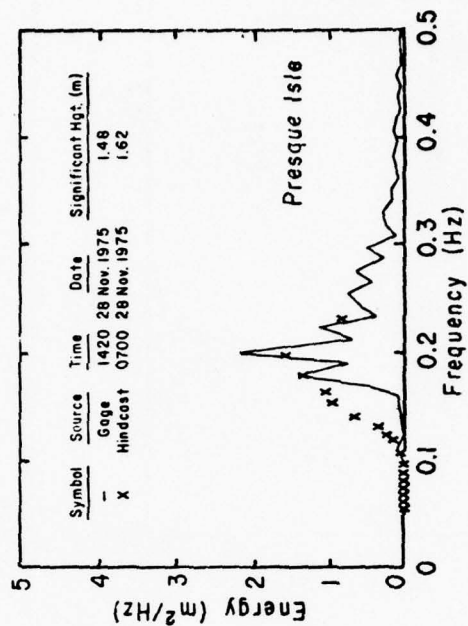
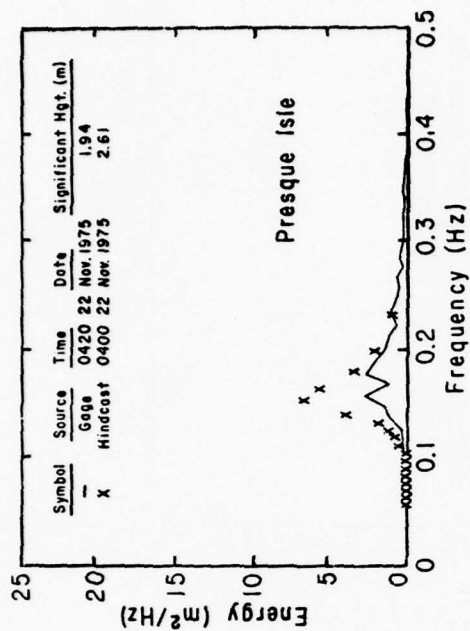


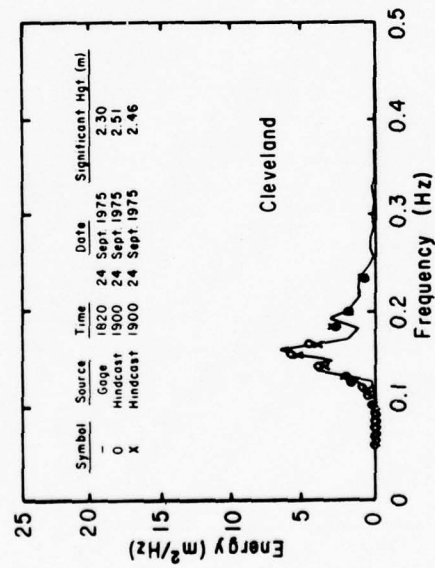
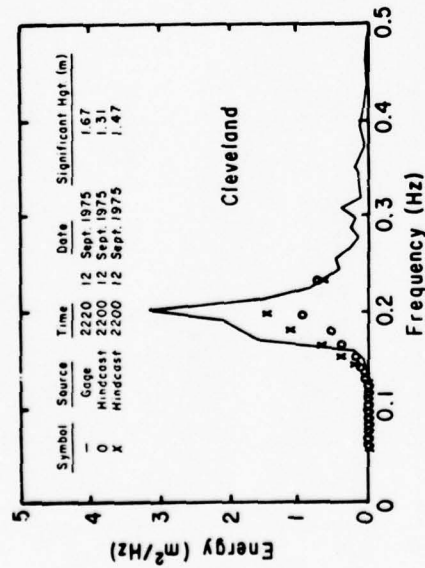
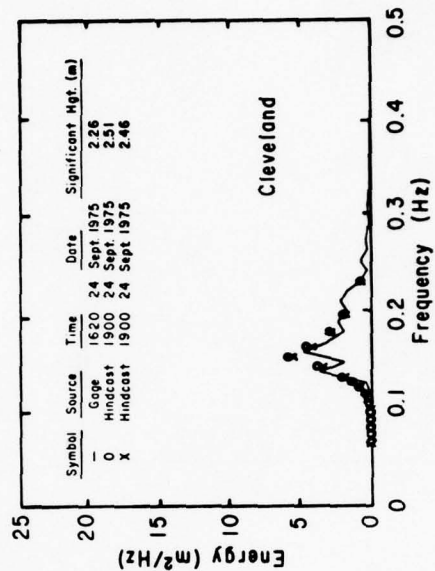
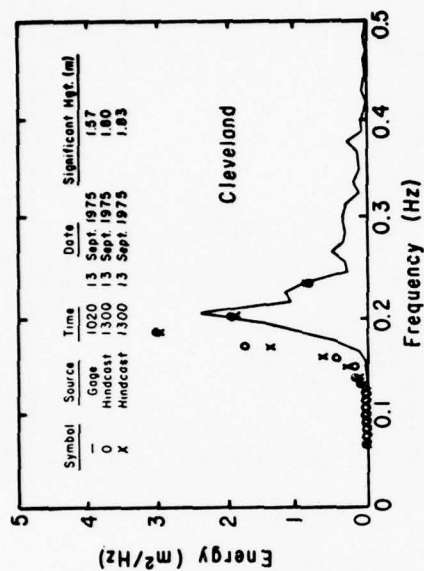


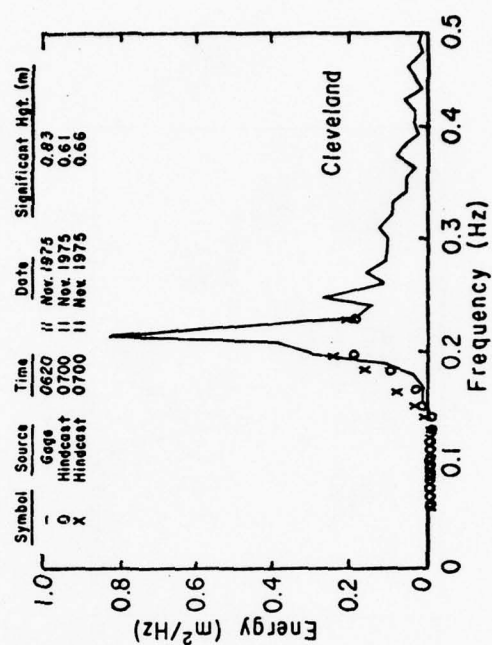
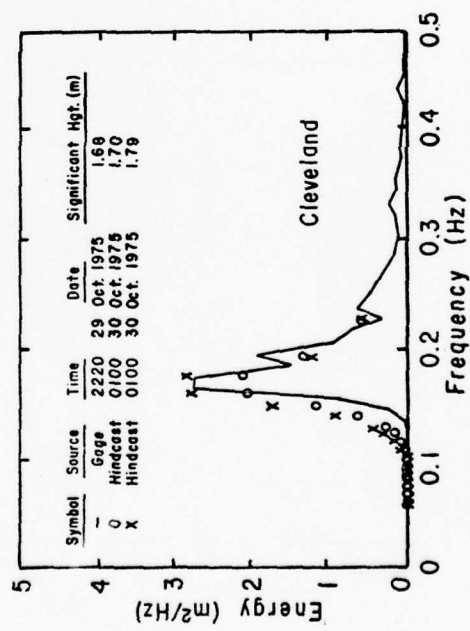
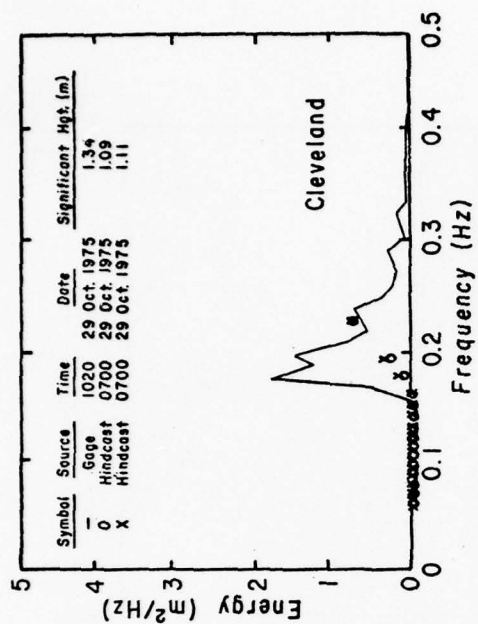
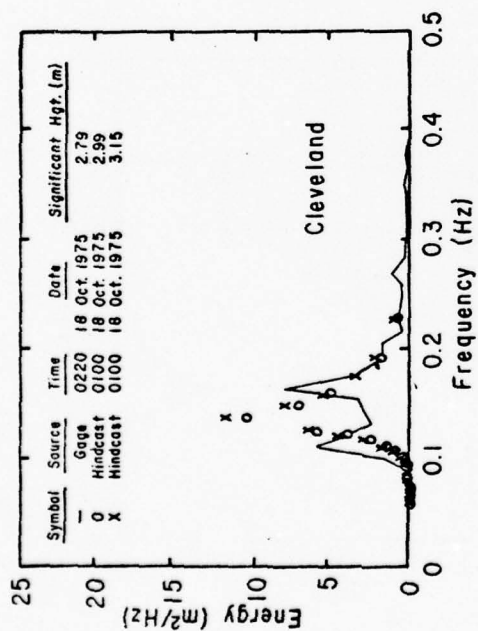


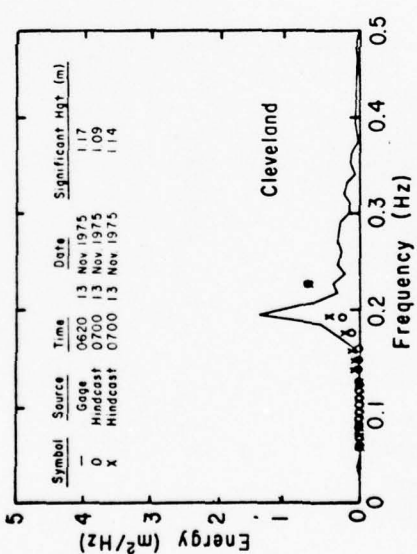
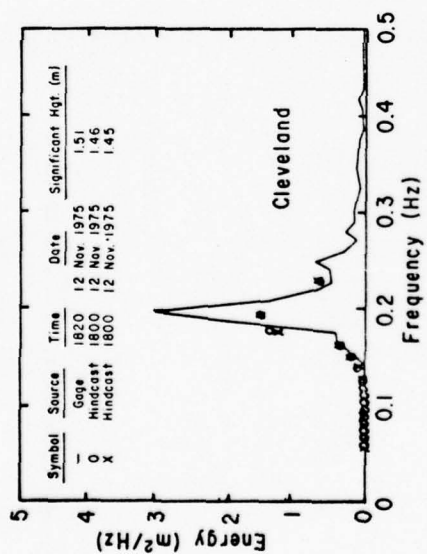
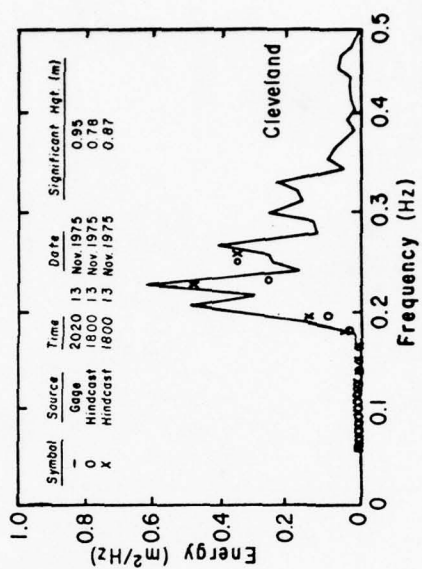
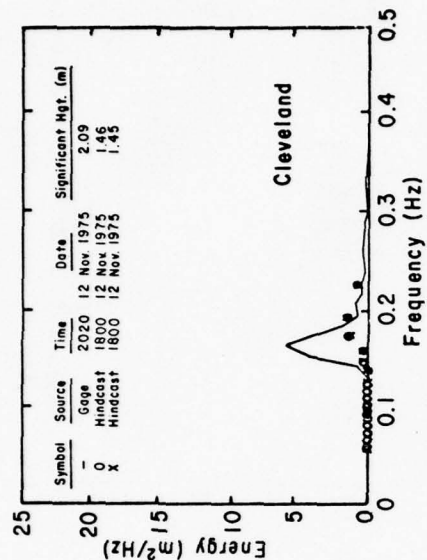


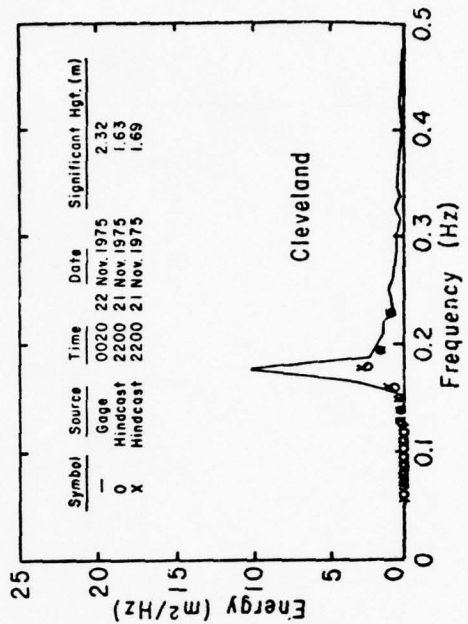
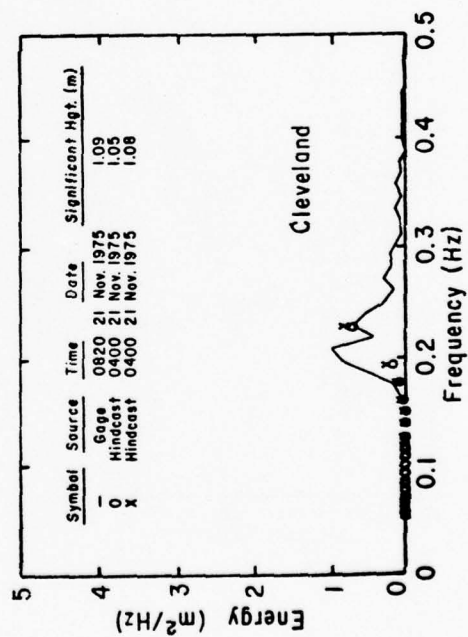
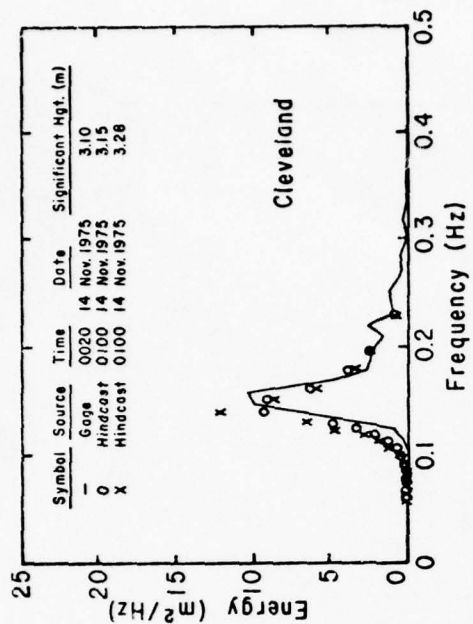
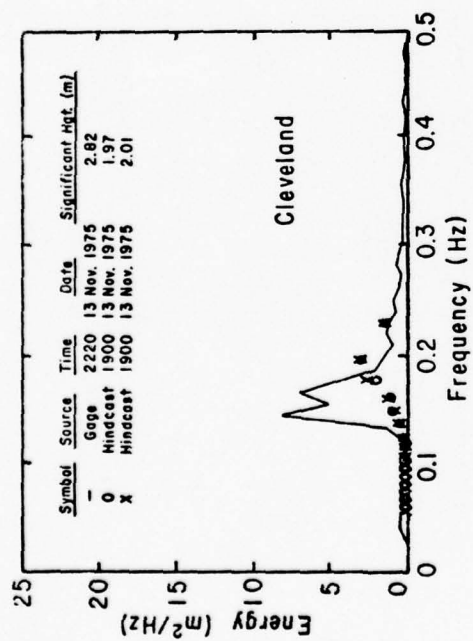


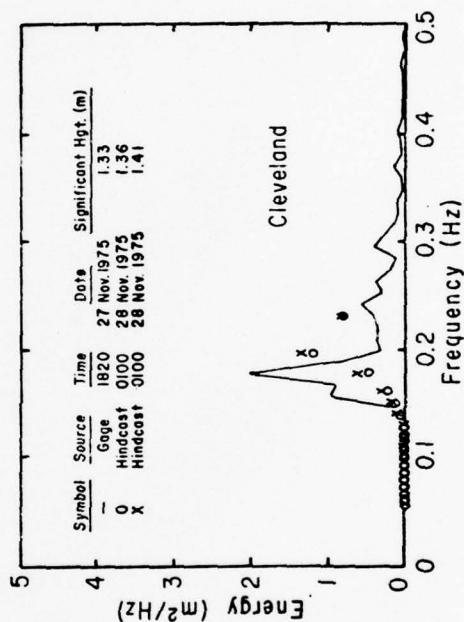
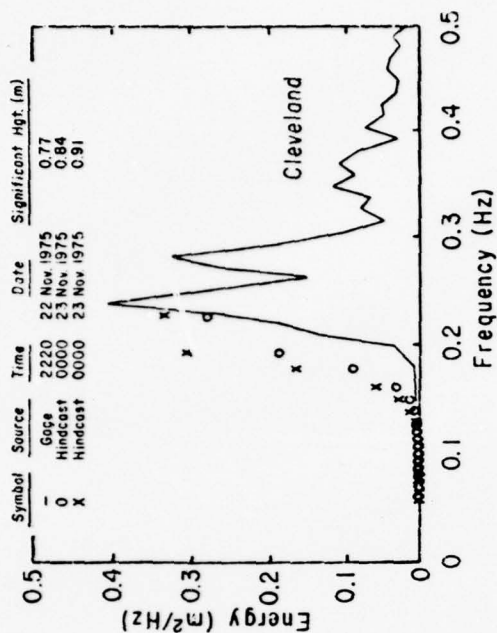
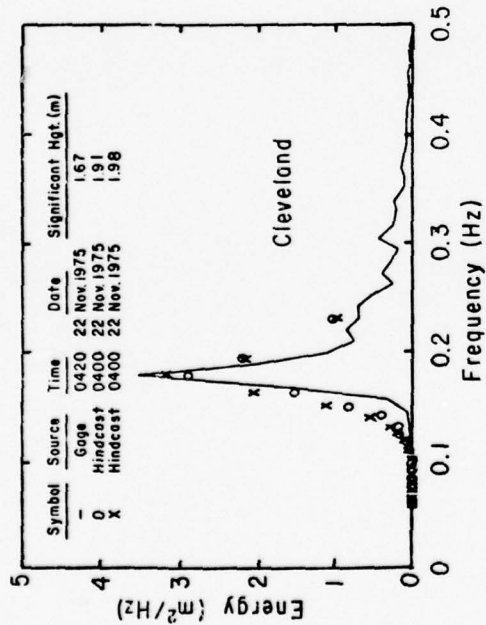






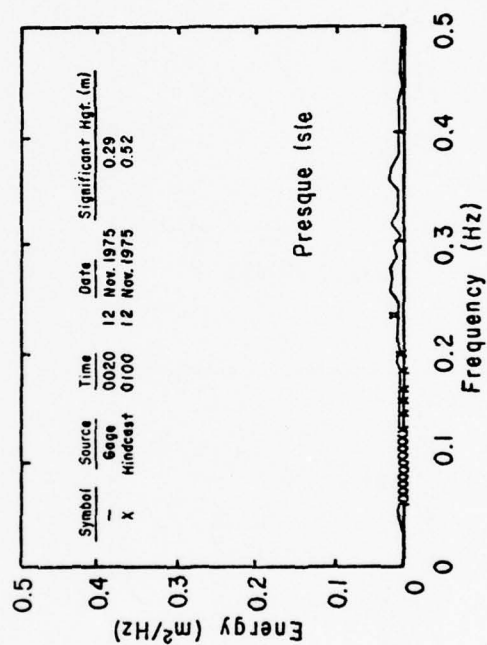
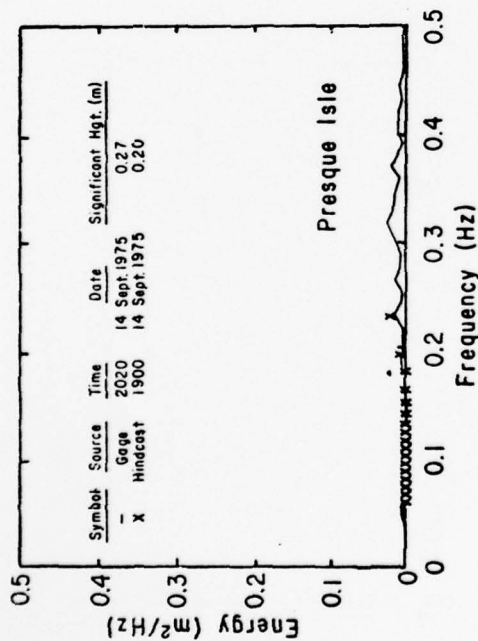
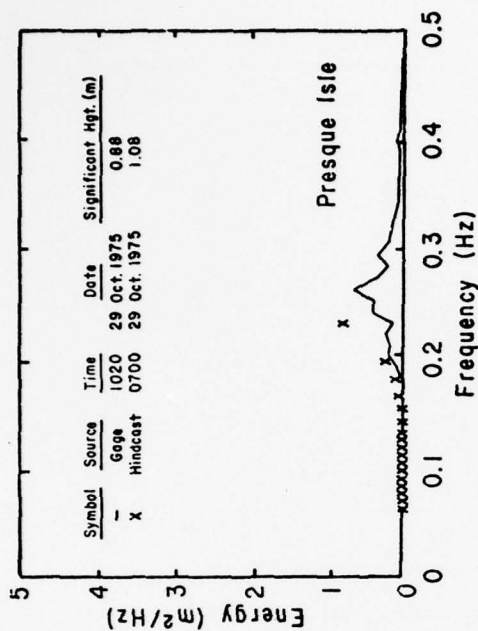


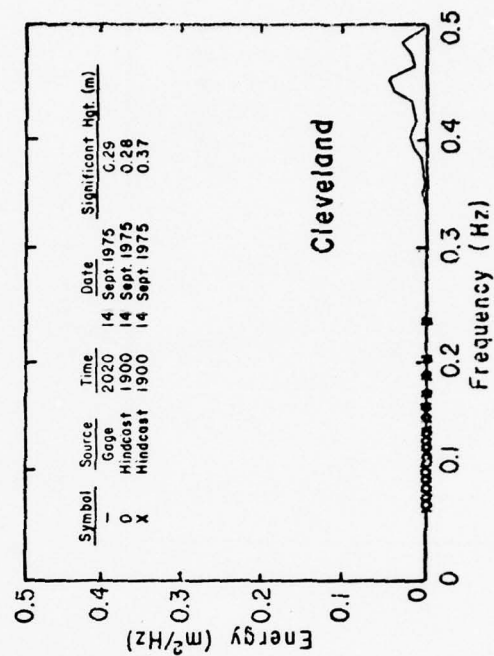
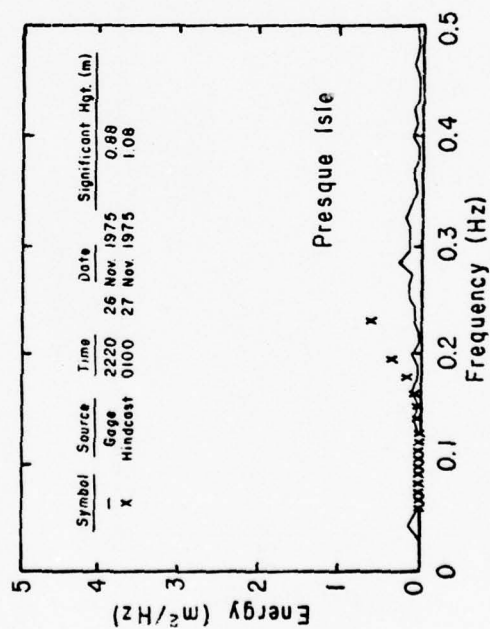
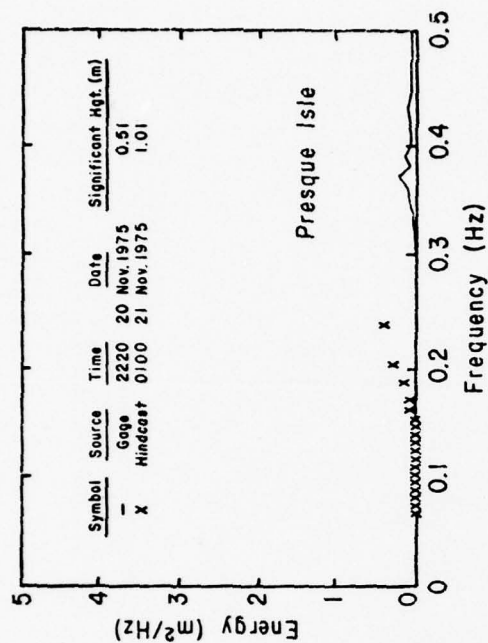
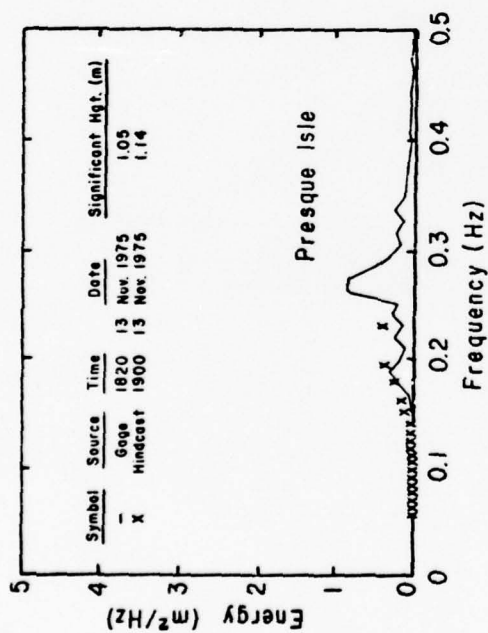


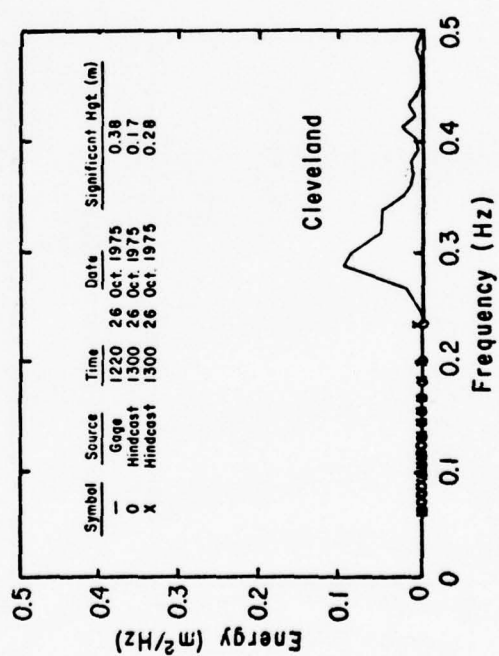
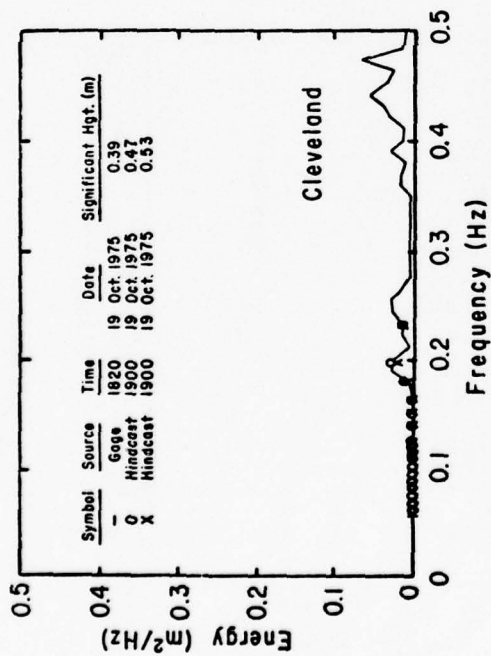
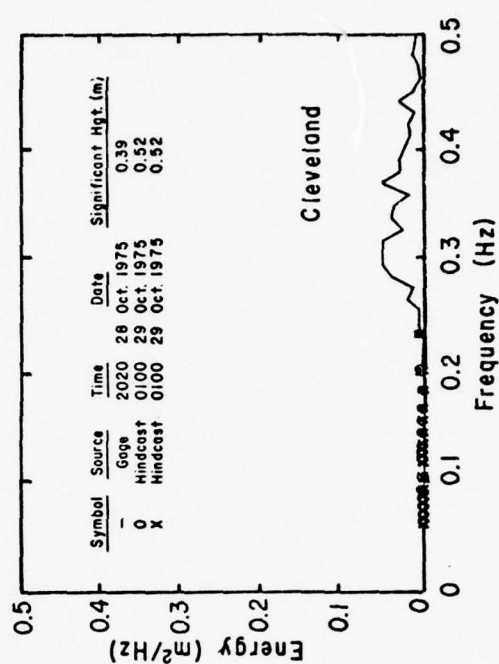
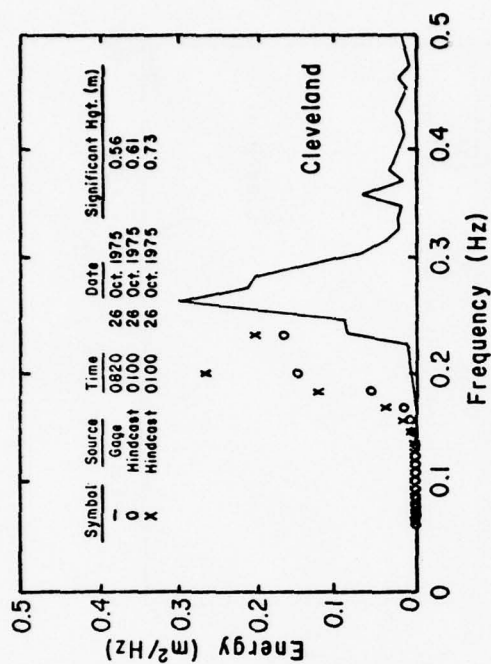


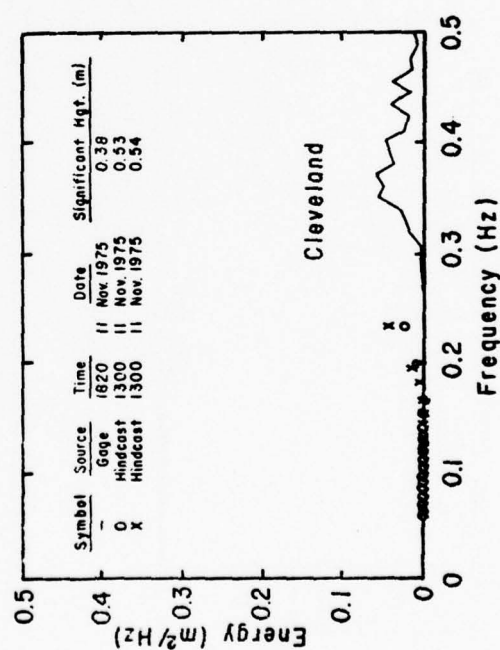
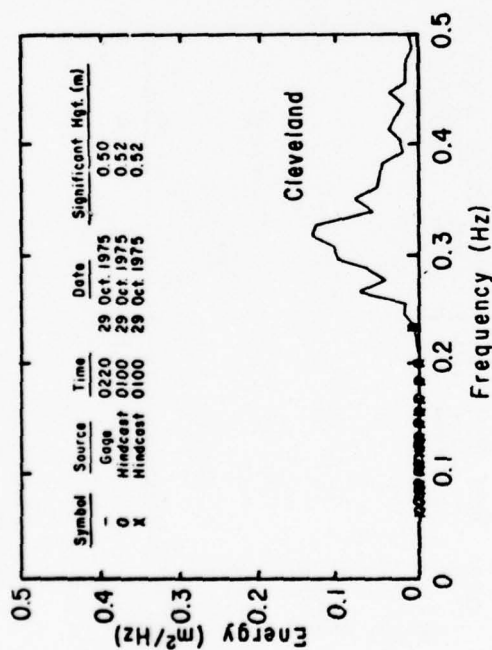
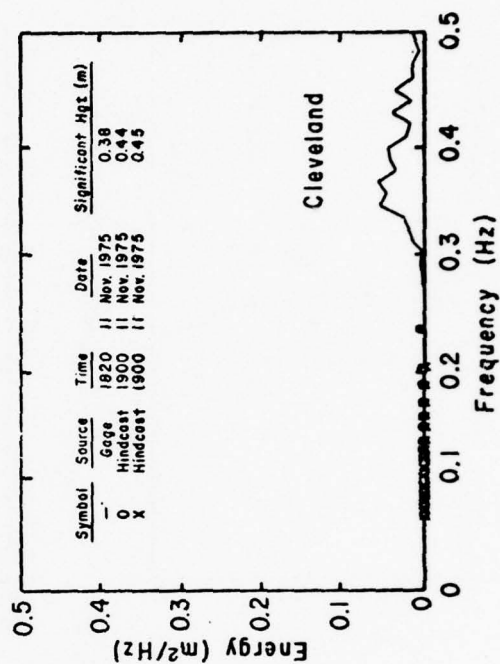
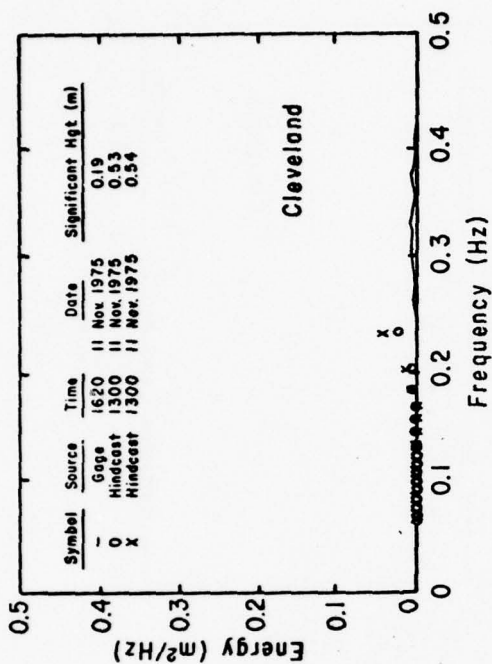
APPENDIX D

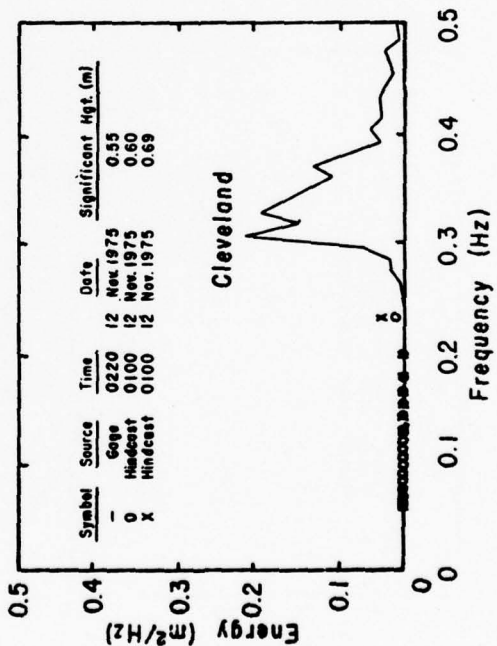
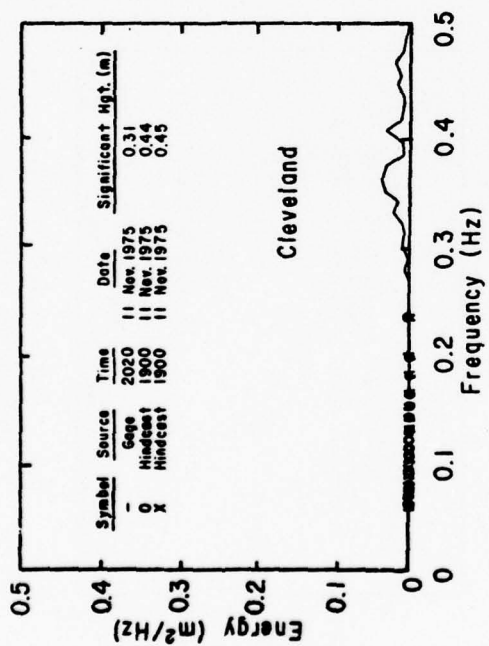
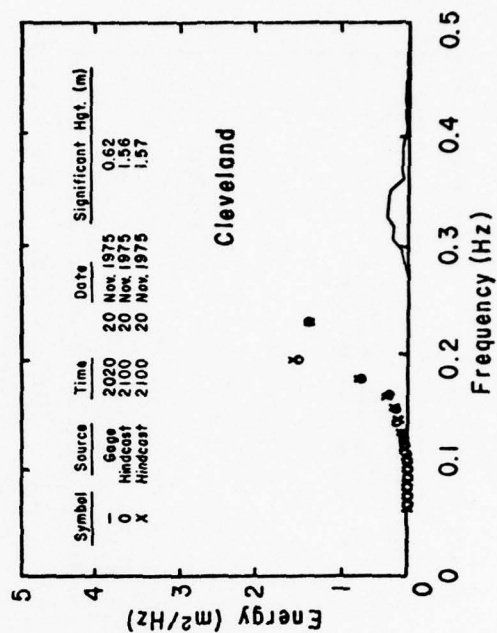
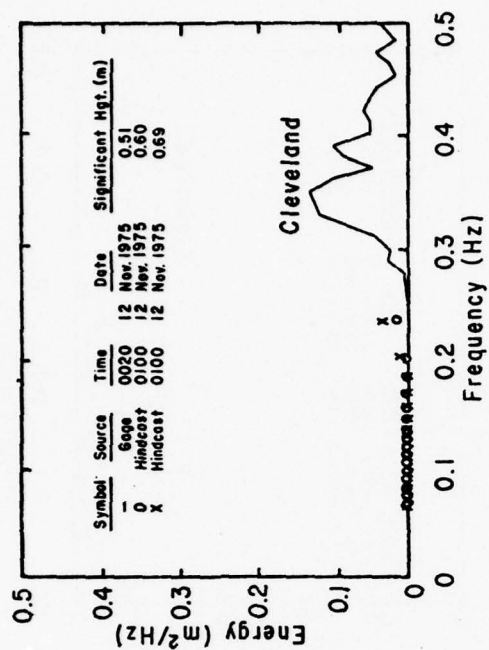
SPECTRAL COMPARISONS IN WHICH MOST OF THE GAGE SPECTRUM
IS AT FREQUENCIES HIGHER THAN 0.23 HERTZ

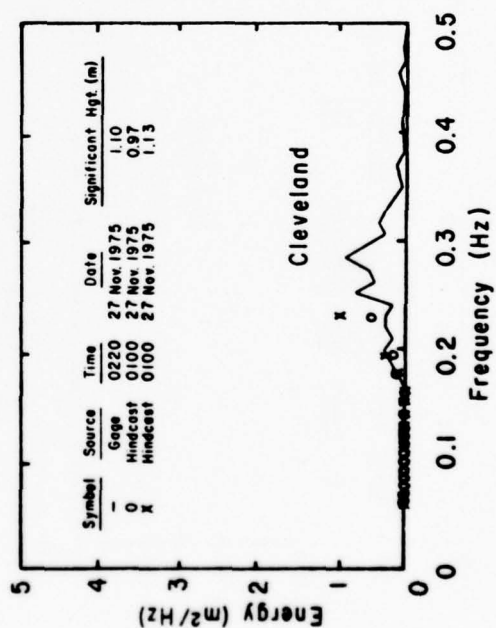
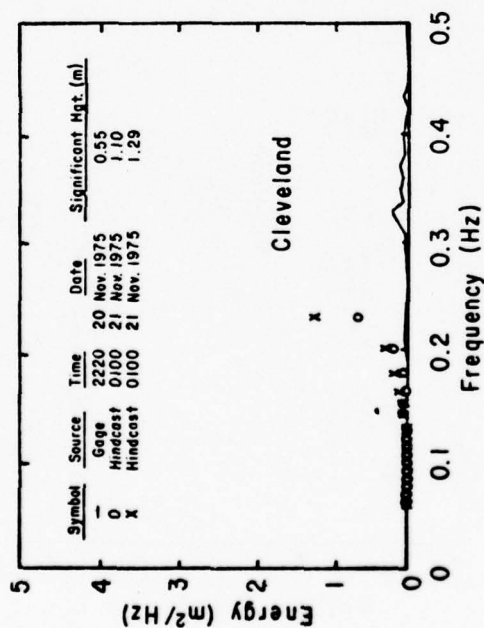
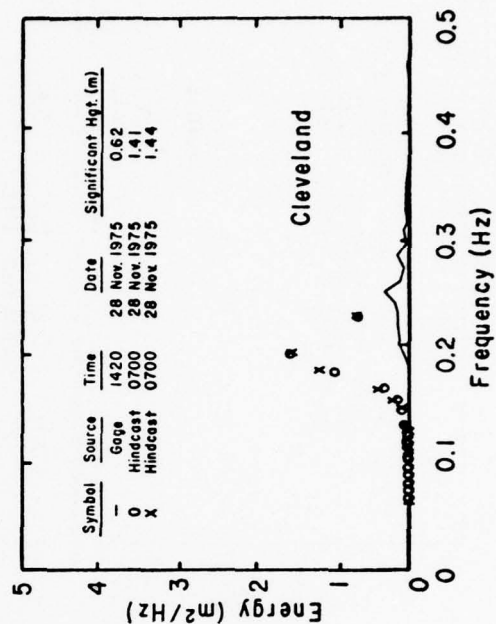
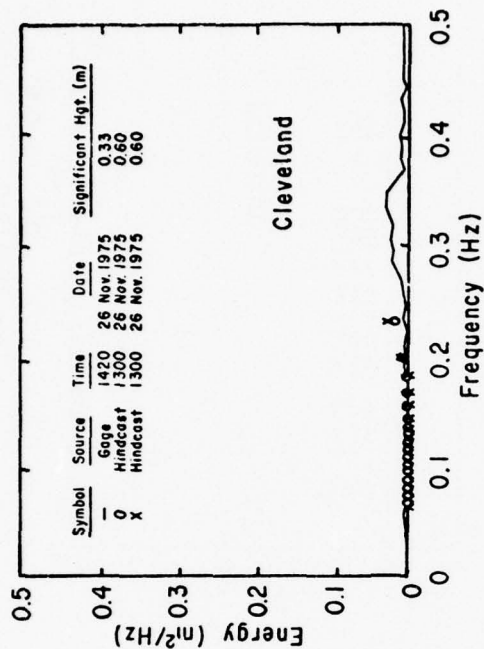






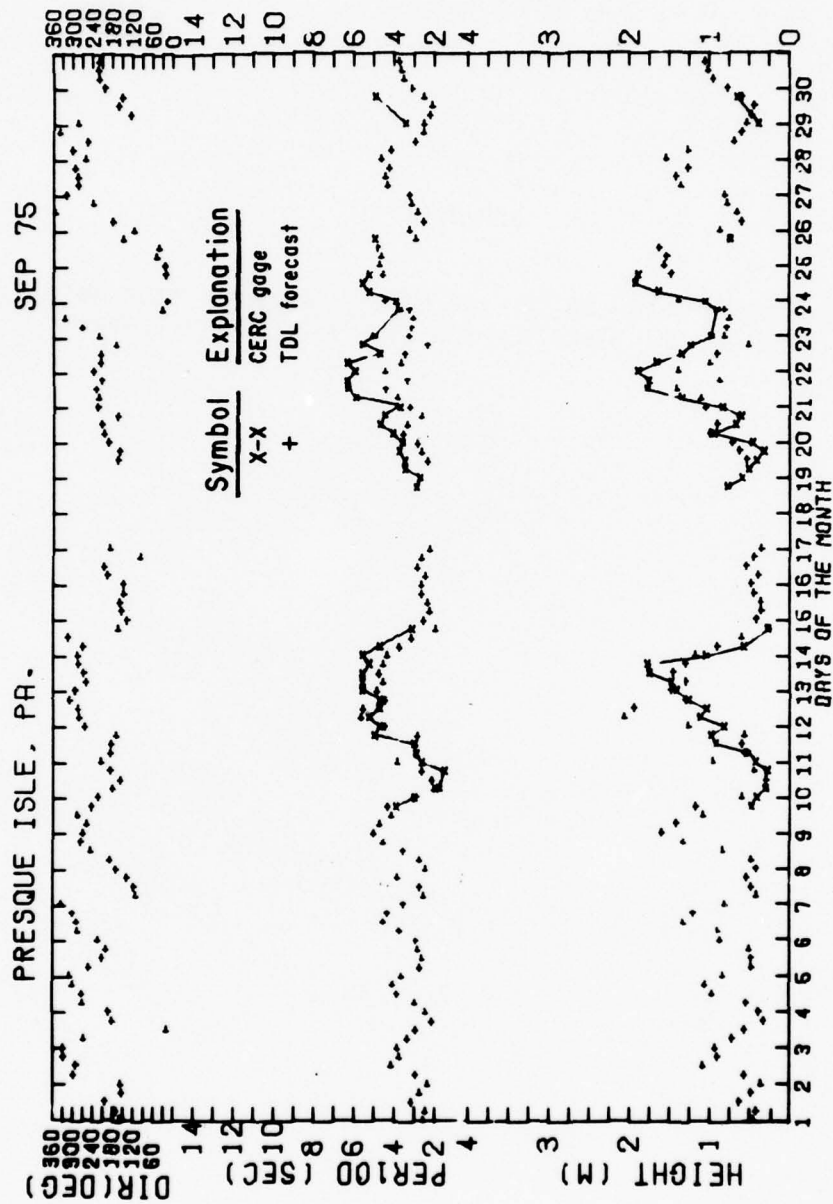


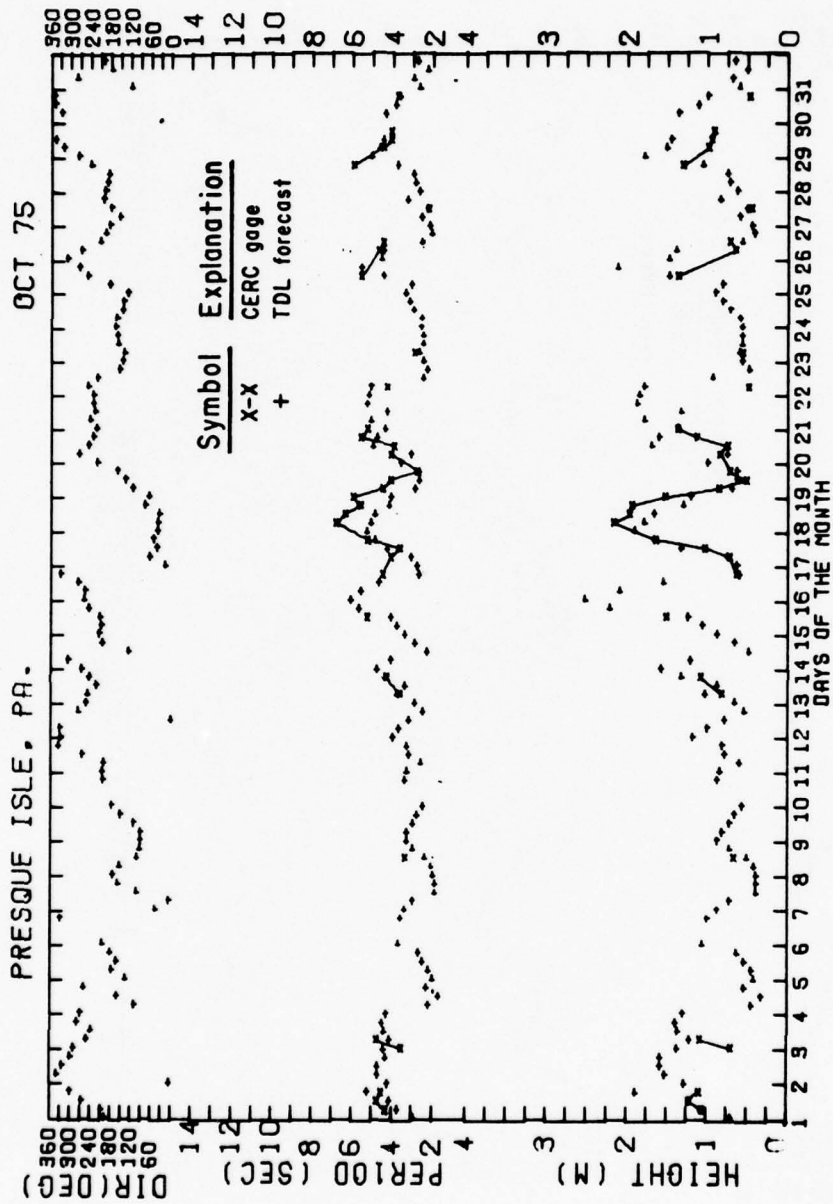


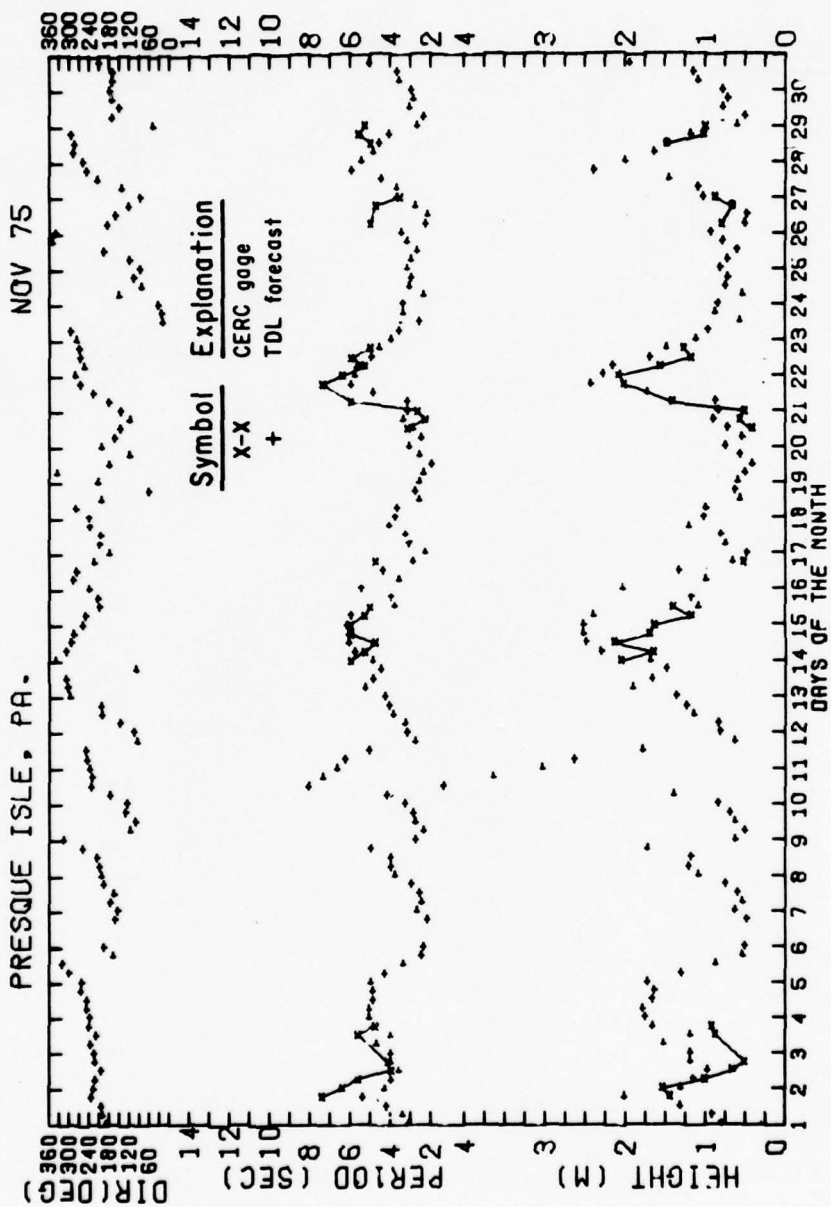


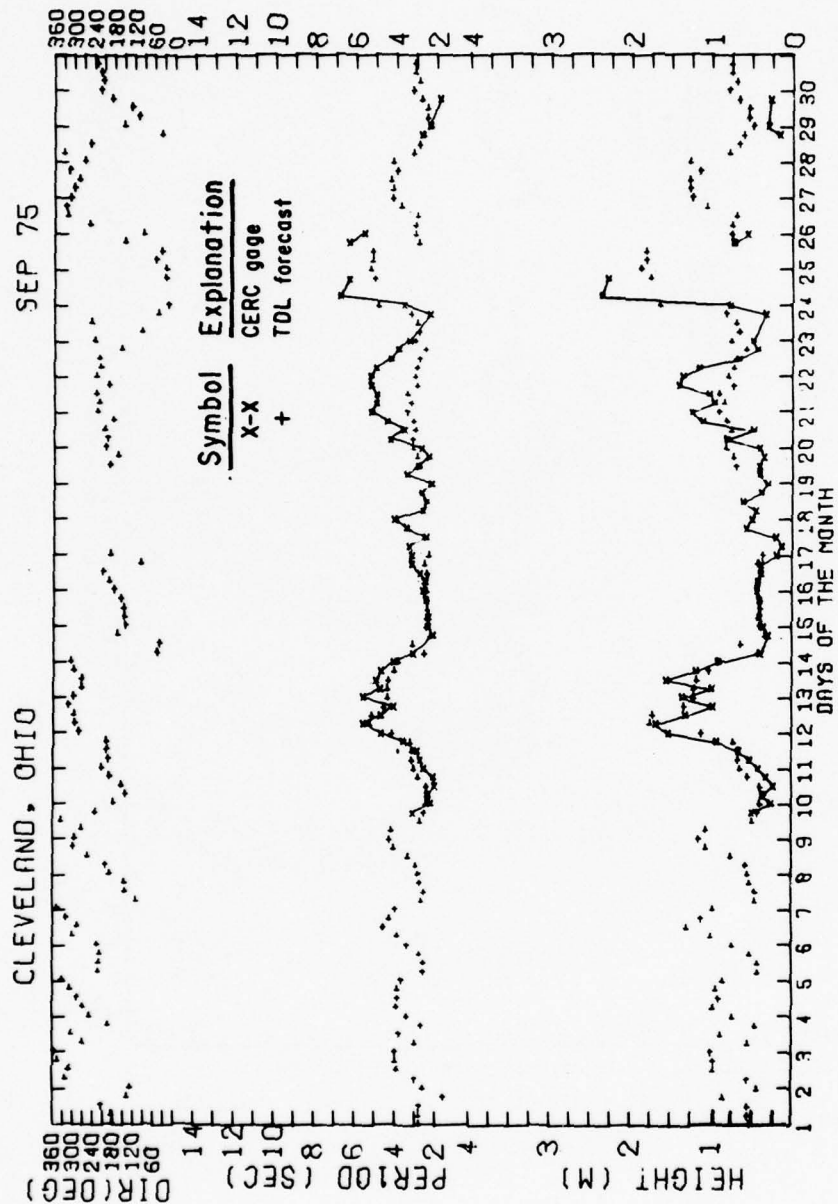
APPENDIX E

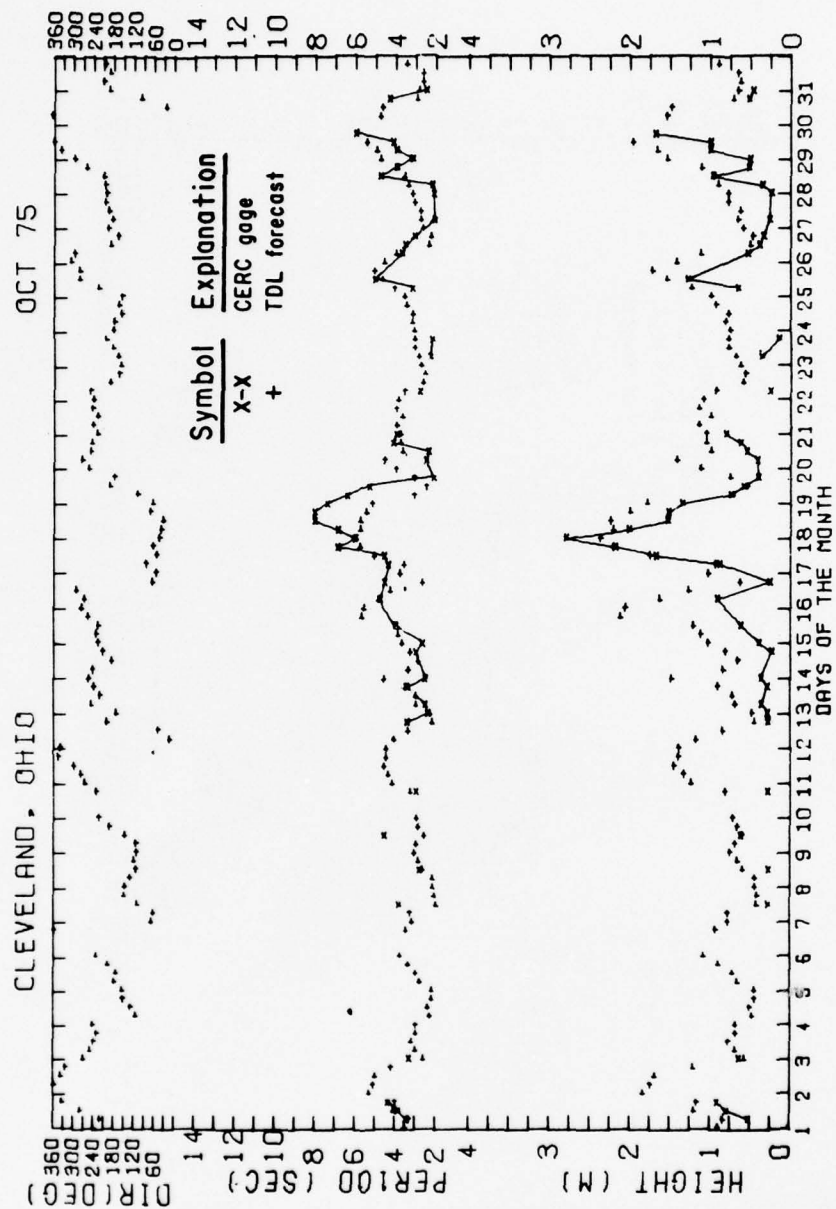
TIME-HISTORY PLOTS OF TDL AND GAGE SIGNIFICANT WAVE HEIGHT,
PERIOD, AND DIRECTION FOR FALL 1975 AND FALL 1976

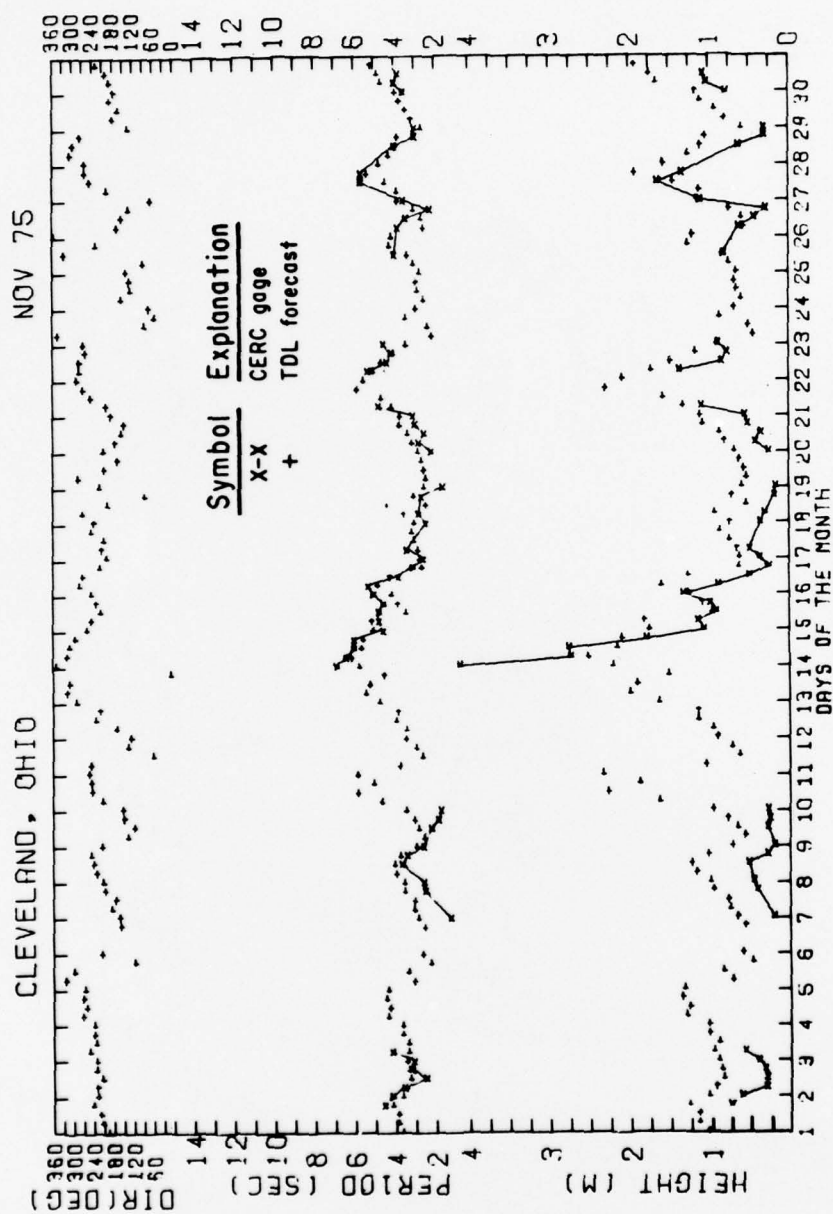


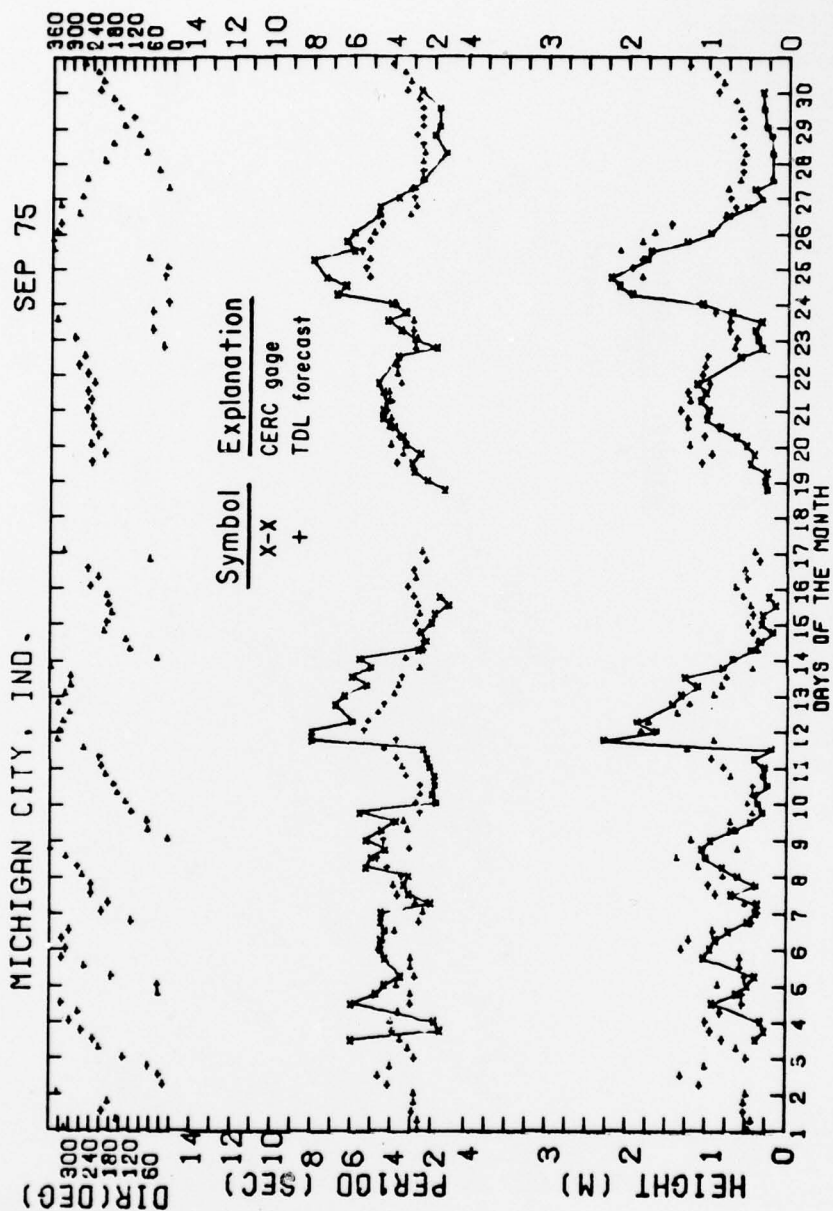


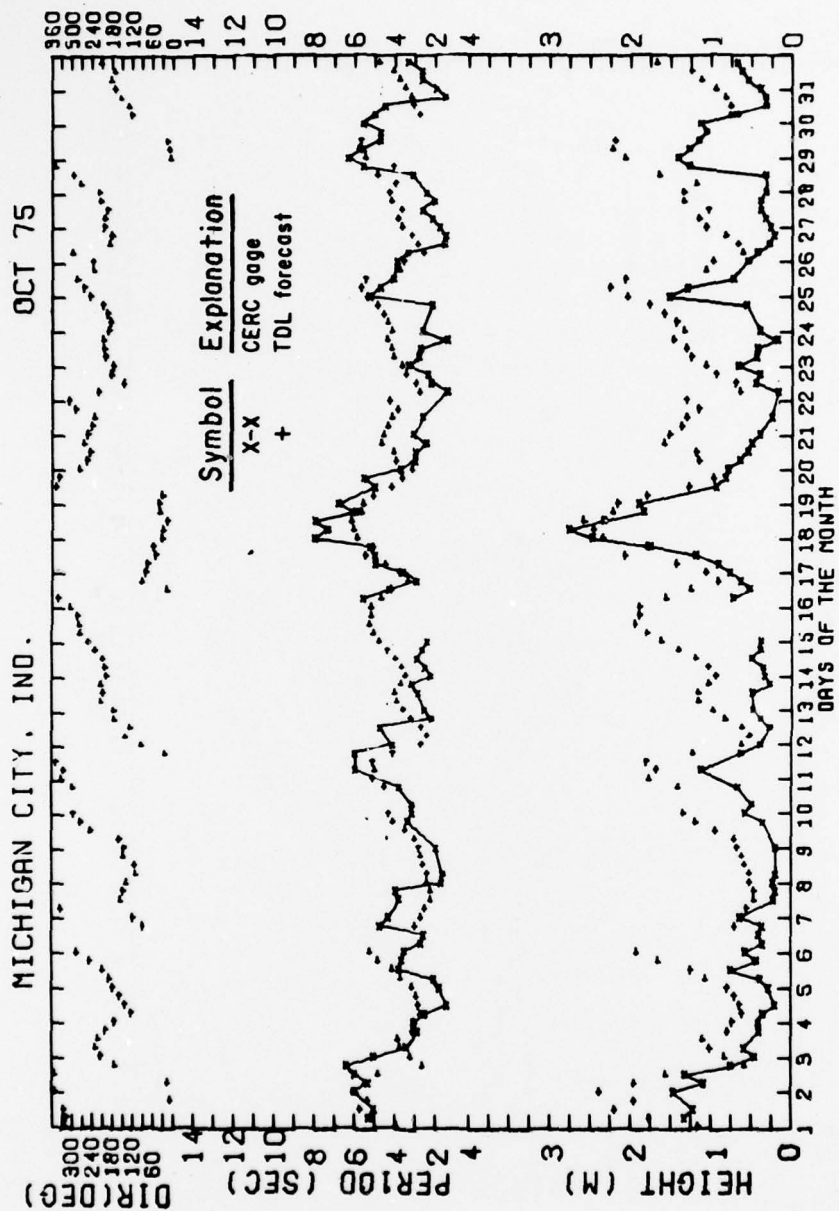


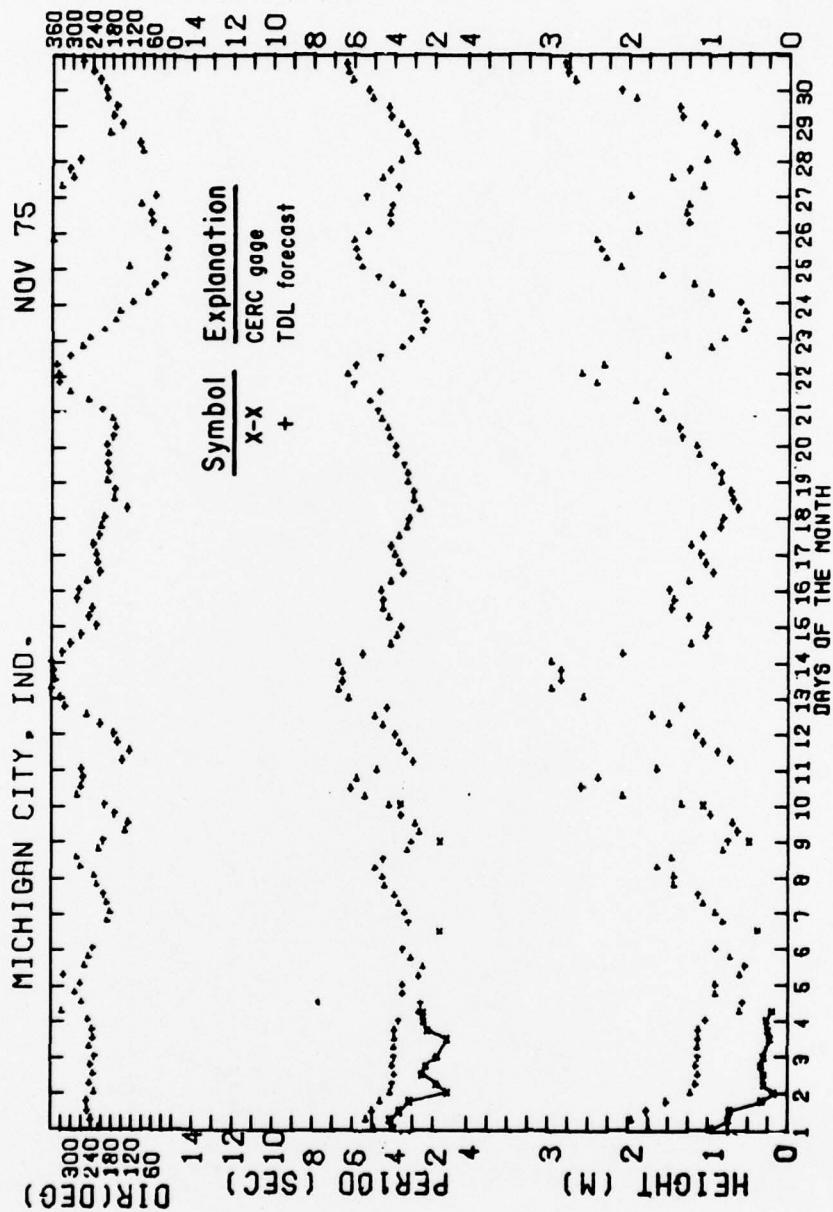


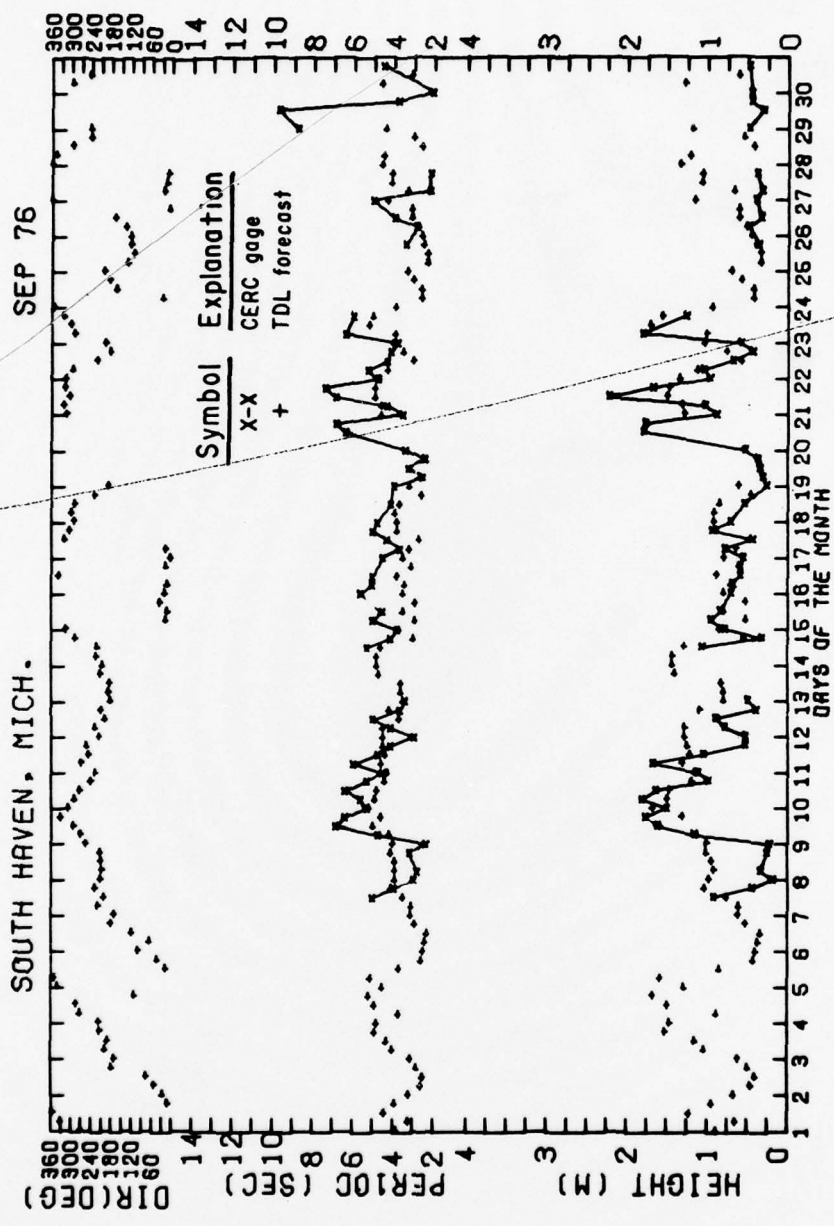


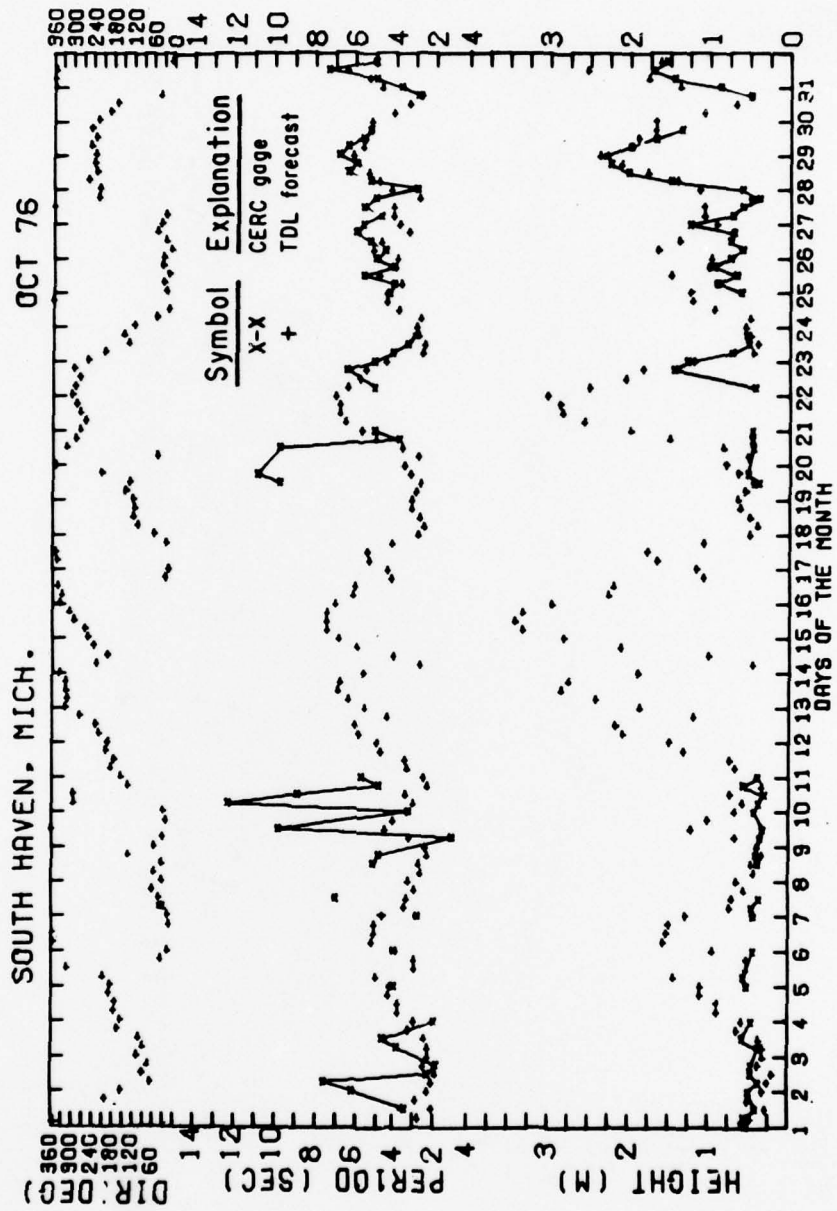


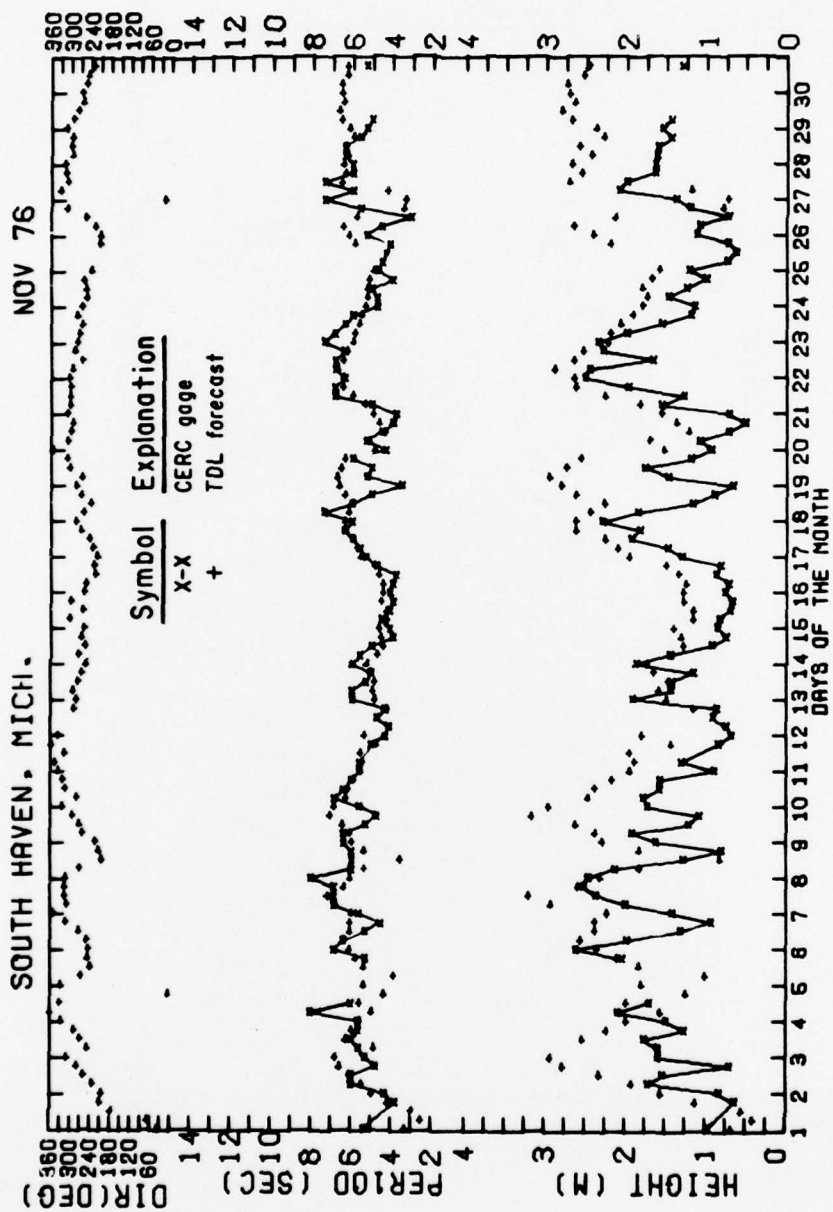


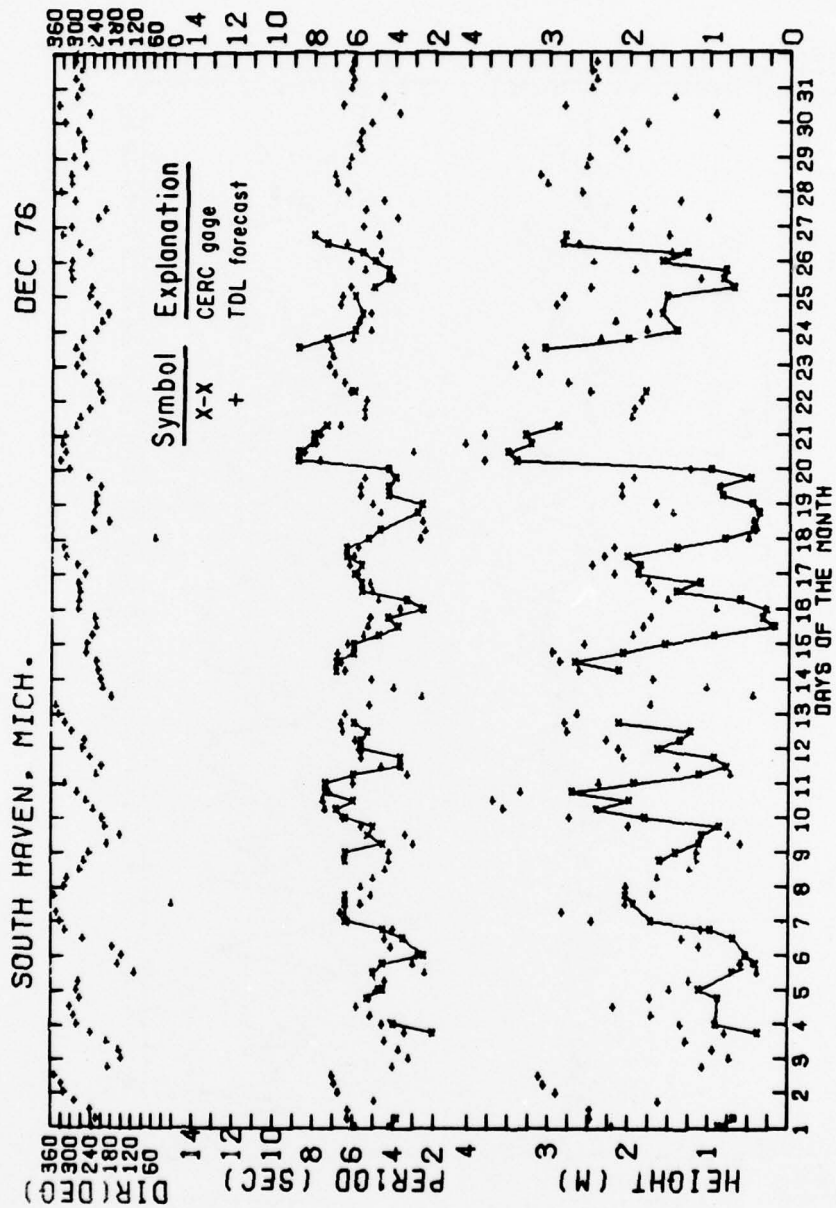


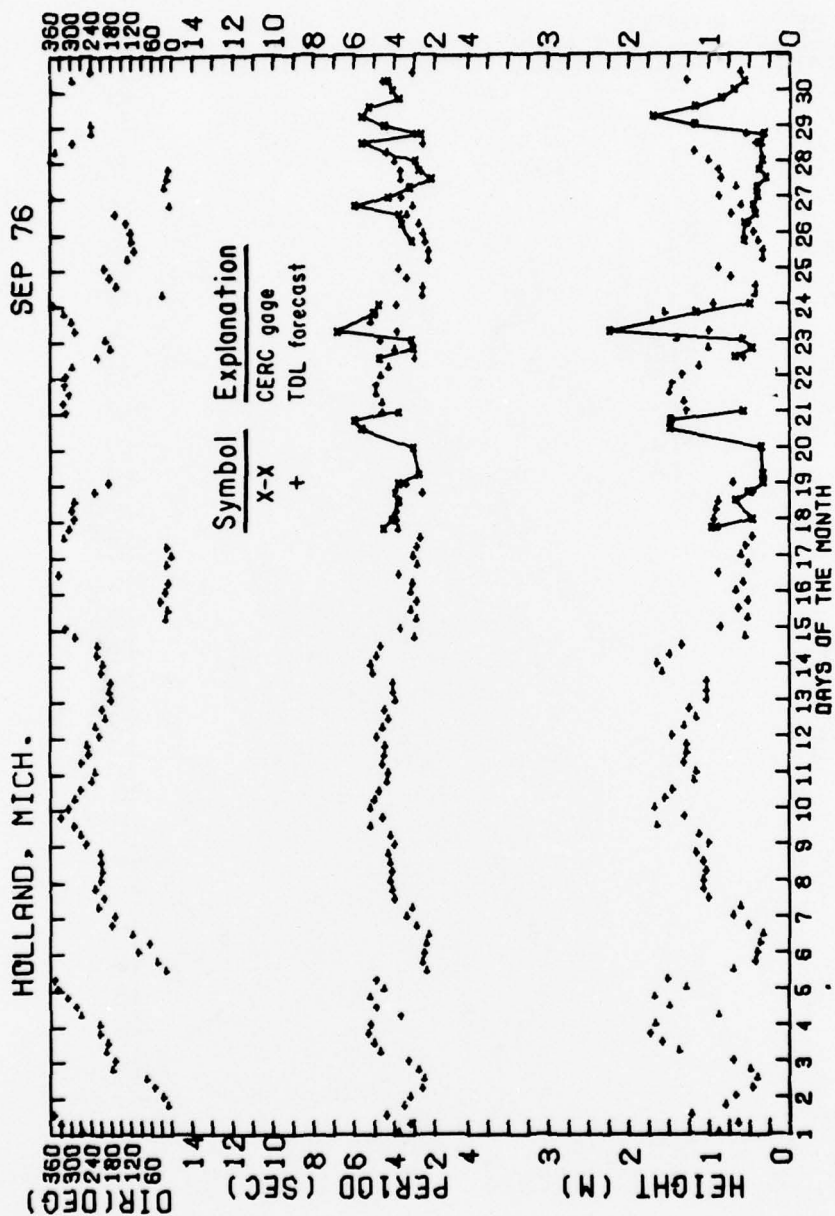


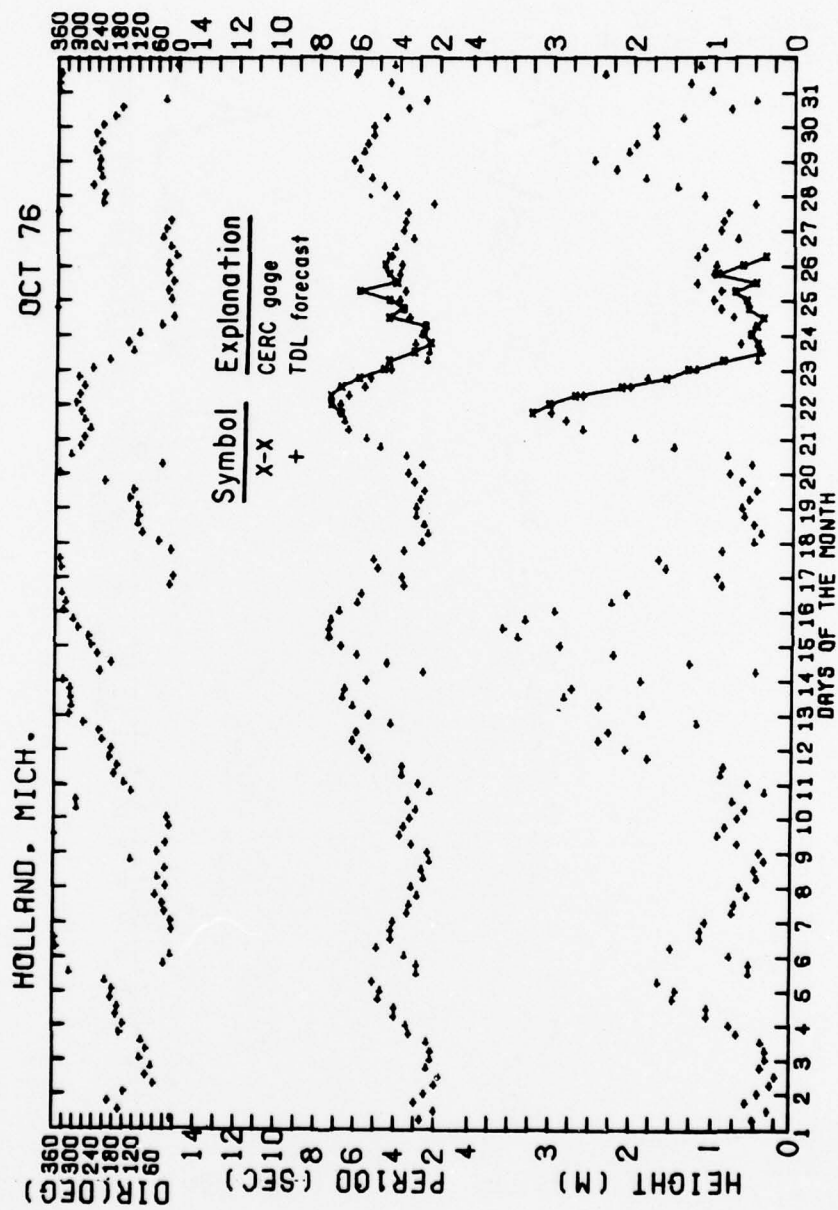


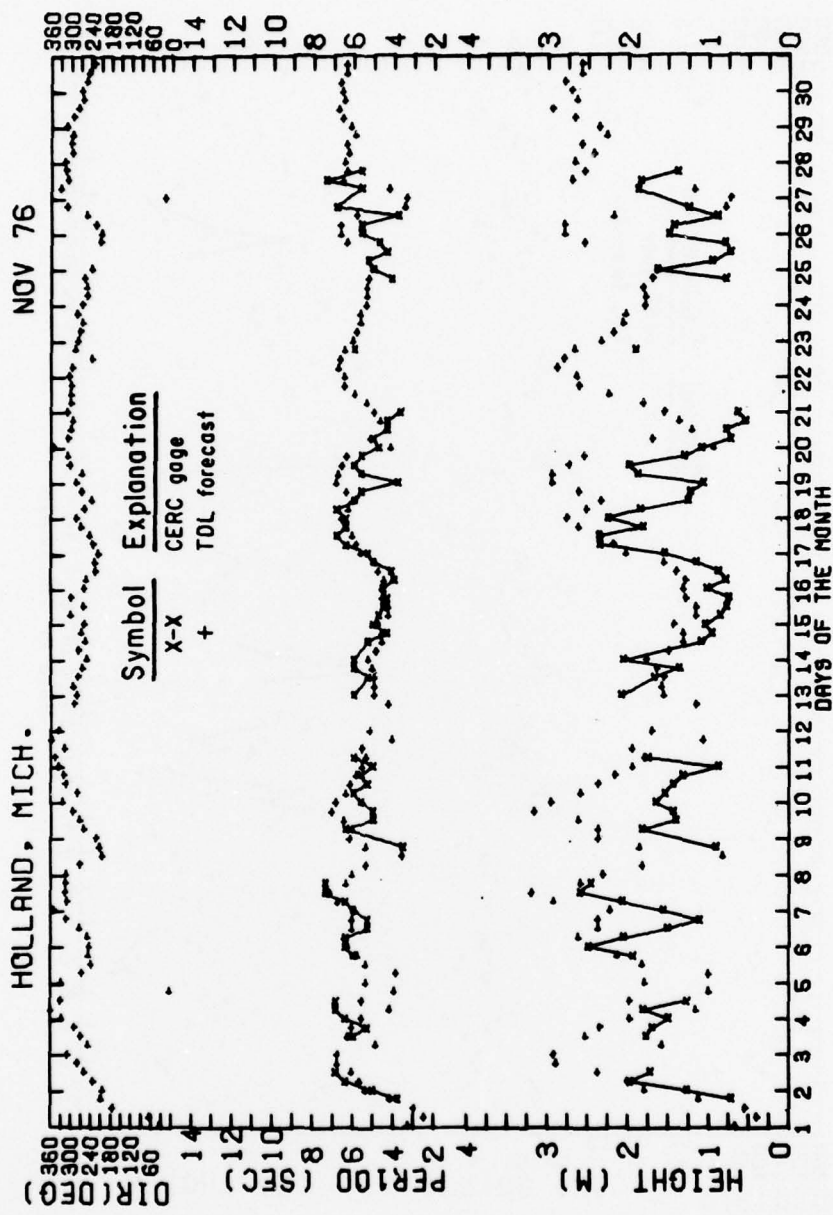


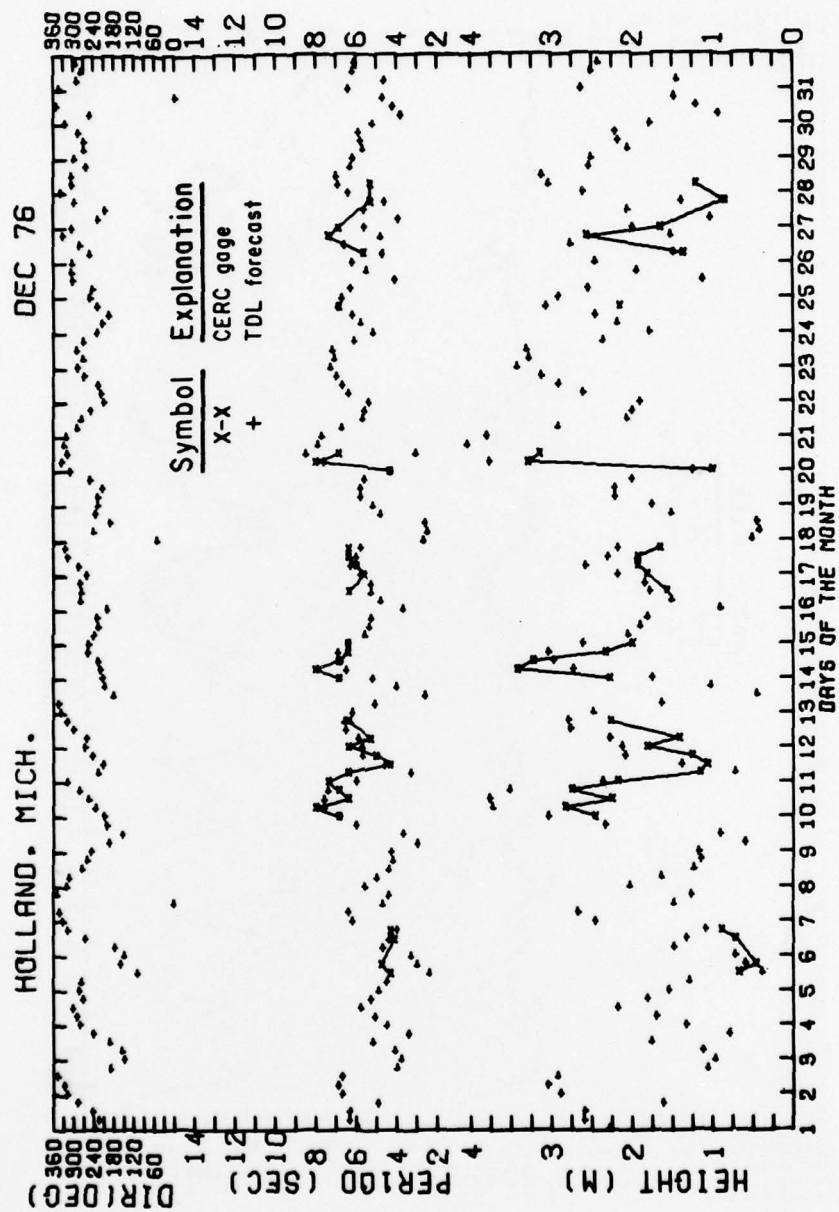












Thompson, Edward F.

An evaluation of two Great Lakes wave models / by Edward F. Thompson. - Ft. Belvoir, Va. : U.S. Coastal Engineering Research Center ; Springfield, Va. : available from National Technical Information Service, 1978.
174 p. : ill. (Technical report - U.S. Coastal Engineering Research Center ; no. 78-1)

Bibliography : p. 113.

Two operational numerical Great Lakes wave models are described in detail and evaluated. Evaluation of one model developed by WES compared wave hindcasts for nine storms in Lake Erie during fall 1975; evaluation of the other model developed by TDL compared forecasts during fall 1975 and fall 1976 in Lake Erie and Lake Michigan.

1. Waves. 2. Models. 3. Wave height. 4. Wave hindcasting.
5. Wave period. 6. Great Lakes. I. Title. II. Series: U.S. Coastal Engineering Research Center. Technical report no. 78-1.

TC203

.U581tr

no. 78-1

627

Thompson, Edward F.

An evaluation of two Great Lakes wave models / by Edward F. Thompson. - Ft. Belvoir, Va. : U.S. Coastal Engineering Research Center ; Springfield, Va. : available from National Technical Information Service, 1978.
174 p. : ill. (Technical report - U.S. Coastal Engineering Research Center ; no. 78-1)

Bibliography : p. 113.

Two operational numerical Great Lakes wave models are described in detail and evaluated. Evaluation of one model developed by WES compared wave hindcasts for nine storms in Lake Erie during fall 1975; evaluation of the other model developed by TDL compared forecasts during fall 1975 and fall 1976 in Lake Erie and Lake Michigan.

1. Waves. 2. Models. 3. Wave height. 4. Wave hindcasting.
5. Wave period. 6. Great Lakes. I. Title. II. Series: U.S. Coastal Engineering Research Center. Technical report no. 78-1.

TC203

.U581tr

no. 78-1

627

Thompson, Edward F.

An evaluation of two Great Lakes wave models / by Edward F. Thompson. - Ft. Belvoir, Va. : U.S. Coastal Engineering Research Center ; Springfield, Va. : available from National Technical Information Service, 1978.
174 p. : ill. (Technical report - U.S. Coastal Engineering Research Center ; no. 78-1)

Bibliography : p. 113.

Two operational numerical Great Lakes wave models are described in detail and evaluated. Evaluation of one model developed by WES compared wave hindcasts for nine storms in Lake Erie during fall 1975; evaluation of the other model developed by TDL compared forecasts during fall 1975 and fall 1976 in Lake Erie and Lake Michigan.

1. Waves. 2. Models. 3. Wave height. 4. Wave hindcasting.
5. Wave period. 6. Great Lakes. I. Title. II. Series: U.S. Coastal Engineering Research Center. Technical report no. 78-1.

TC203

.U581tr

no. 78-1

627

Thompson, Edward F.

An evaluation of two Great Lakes wave models / by Edward F. Thompson. - Ft. Belvoir, Va. : U.S. Coastal Engineering Research Center ; Springfield, Va. : available from National Technical Information Service, 1978.
174 p. : ill. (Technical report - U.S. Coastal Engineering Research Center ; no. 78-1)

Bibliography : p. 113.

Two operational numerical Great Lakes wave models are described in detail and evaluated. Evaluation of one model developed by WES compared wave hindcasts for nine storms in Lake Erie during fall 1975; evaluation of the other model developed by TDL compared forecasts during fall 1975 and fall 1976 in Lake Erie and Lake Michigan.

1. Waves. 2. Models. 3. Wave height. 4. Wave hindcasting.
5. Wave period. 6. Great Lakes. I. Title. II. Series: U.S. Coastal Engineering Research Center. Technical report no. 78-1.

TC203

.U581tr

no. 78-1

627

Thompson, Edward F.

An evaluation of two Great Lakes wave models / by Edward F. Thompson. - Ft. Belvoir, Va. : U.S. Coastal Engineering Research Center ; Springfield, Va. : available from National Technical Information Service, 1978.

174 p. : ill. (Technical report - U.S. Coastal Engineering Research Center ; no. 78-1)

Bibliography : p. 113.

Two operational numerical Great Lakes wave models are described in detail and evaluated. Evaluation of one model developed by WES compared wave hindcasts for nine storms in Lake Erie during fall 1975; evaluation of the other model developed by TDL compared forecasts during fall 1975 and fall 1976 in Lake Erie and Lake Michigan.

1. Waves. 2. Models. 3. Wave height. 4. Wave hindcasting. 5. Wave period. 6. Great Lakes. I. Title. II. Series: U.S. Coastal Engineering Research Center. Technical report no. 78-1.

TC203

.U581tr

no. 78-1

627

Thompson, Edward F.

An evaluation of two Great Lakes wave models / by Edward F. Thompson. - Ft. Belvoir, Va. : U.S. Coastal Engineering Research Center ; Springfield, Va. : available from National Technical Information Service, 1978.

174 p. : ill. (Technical report - U.S. Coastal Engineering Research Center ; no. 78-1)

Bibliography : p. 113.

Two operational numerical Great Lakes wave models are described in detail and evaluated. Evaluation of one model developed by WES compared wave hindcasts for nine storms in Lake Erie during fall 1975; evaluation of the other model developed by TDL compared forecasts during fall 1975 and fall 1976 in Lake Erie and Lake Michigan.

1. Waves. 2. Models. 3. Wave height. 4. Wave hindcasting. 5. Wave period. 6. Great Lakes. I. Title. II. Series: U.S. Coastal Engineering Research Center. Technical report no. 78-1.

TC203

.U581tr

no. 78-1

627

Thompson, Edward F.

An evaluation of two Great Lakes wave models / by Edward F. Thompson. - Ft. Belvoir, Va. : U.S. Coastal Engineering Research Center ; Springfield, Va. : available from National Technical Information Service, 1978.

174 p. : ill. (Technical report - U.S. Coastal Engineering Research Center ; no. 78-1)

Bibliography : p. 113.

Two operational numerical Great Lakes wave models are described in detail and evaluated. Evaluation of one model developed by WES compared wave hindcasts for nine storms in Lake Erie during fall 1975; evaluation of the other model developed by TDL compared forecasts during fall 1975 and fall 1976 in Lake Erie and Lake Michigan.

1. Waves. 2. Models. 3. Wave height. 4. Wave hindcasting. 5. Wave period. 6. Great Lakes. I. Title. II. Series: U.S. Coastal Engineering Research Center. Technical report no. 78-1.

TC203

.U581tr

no. 78-1

627

Thompson, Edward F.

An evaluation of two Great Lakes wave models / by Edward F. Thompson. - Ft. Belvoir, Va. : U.S. Coastal Engineering Research Center ; Springfield, Va. : available from National Technical Information Service, 1978.

174 p. : ill. (Technical report - U.S. Coastal Engineering Research Center ; no. 78-1)

Bibliography : p. 113.

Two operational numerical Great Lakes wave models are described in detail and evaluated. Evaluation of one model developed by WES compared wave hindcasts for nine storms in Lake Erie during fall 1975; evaluation of the other model developed by TDL compared forecasts during fall 1975 and fall 1976 in Lake Erie and Lake Michigan.

1. Waves. 2. Models. 3. Wave height. 4. Wave hindcasting. 5. Wave period. 6. Great Lakes. I. Title. II. Series: U.S. Coastal Engineering Research Center. Technical report no. 78-1.

TC203

.U581tr

no. 78-1

627